TECHNISCHE UNIVERSITÄT MÜNCHEN
Advanced Technologies in Radiation Therapy

Optimization of efficiency and dosimetric quality in treatment planning of intensity modulated radiotherapy with photon and proton beams

Birgit Sabine Müller

Vollständiger Abdruck der von der Fakultät für Physik der Technischen Universität München zur Erlangung des akademischen Grades eines

Doktors der Naturwissenschaften (Dr. rer. nat.)

genehmigten Dissertation.

Vorsitzender:	Univ.-Prof. Dr. Martin Zacharias
Prüfer der Dissertation:	1. Univ.-Prof. Dr. Jan J. Wilkens
	2. Univ.-Prof. Dr. Franz Pfeiffer

Die Dissertation wurde am 26.04.2016 bei der Technischen Universität München eingereicht und durch die Fakultät für Physik am 06.06.2016 angenommen.

PHYSIK-DEPARTMENT

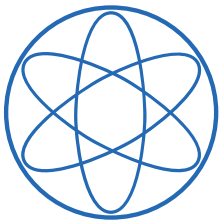

Optimization of efficiency and dosimetric quality in treatment planning of intensity modulated radiotherapy with photon and proton beams

Dissertation
von

Birgit Sabine Müller

-2016-

TECHNISCHE UNIVERSITÄT MÜNCHEN

Abstract

Advanced radiotherapy (RT) techniques, such as intensity modulated RT and image guided RT, achieve high dosimetric quality in terms of superior dose distributions and more accurate deliveries compared to previous techniques. They are, however, accompanied by greater staff involvement and longer treatment times, and may moreover not always be fully exploited.

This thesis suggests and evaluates methods to improve dosimetric quality and efficiency in intensity modulated radiotherapy (IMRT) with photons (IMXT) and protons (IMPT) by analyzing main components of RT treatment. IMRT planning determines both interdependent objectives dosimetric quality and efficiency, where the latter comprises both planning and treatment time. Treatment planning involves multiobjective dose optimization, on the basis of computed tomography (CT) images, with the intention to cover tumors with sufficient dose and simultaneously spare organs at risk (OAR). This work is based on different projects, which investigate and discuss the planning process and resulting RT plan delivery times.

Planning efficiency and dosimetric quality are analyzed by the utilized optimization algorithm and the clinical planning procedure. Plan optimization typically faces a trial-and-error process of selecting optimization parameters. This inefficient process is eliminated by multicriteria optimization (MCO). This thesis demonstrates the superiority of MCO in dose distributions and planning times by a comparison to non-MCO generated plans. To further improve planning efficiency and quality, an alternated planning procedure is proposed, which standardizes the process by utilizing templates of optimization parameters, and individualizes treatments by allowing physicians to find the best dosimetric compromise for every patient. The feasibility of this approach is demonstrated by a planning study.

To maintain dosimetric quality throughout the treatment period, despite of variations in set-up and anatomy, image guided and adaptive RT are part of clinical practice. Due to the increased workload, it is of interest to reduce the number of plan adaptions and study their relevance. The impact of geometric variations on IMPT and IMXT dose distributions was investigated on the basis of clinical control CT images. Results show large dose changes, non-monotonically decreasing plan quality and interpatient variations, which illustrate the importance of both techniques. Frequent image controls and plan adaptions are therefore recommended to prevent over- and underdosage, even if accompanied by additional expenses.

Delivery efficiency is determined by plan parameters, assigned during optimization, and is correlated to dose quality. Typically plans are calculated without incorporating delivery times into the optimization process. To improve IMPT delivery efficiency, an algorithm was developed which integrates delivery efficiency into the treatment plan optimization. Based on prioritized optimization, plan quality is optimized first, and treatment time is reduced in a consecutive step while maintaining prior achievements. The prioritized efficiency optimization algorithm (PrEfOpt) further allows the exploration of inevitable trade-offs between treatment time and dosimetric quality. Its application to clinical cases achieved considerable time reductions at similar plan qualities. Therefore, efficiency optimization as part of treatment planning is of great potential in clinical practice.

In conclusion, this work demonstrates the feasibility of optimizing efficiency and dosimetric quality in IMRT planning by use of different methods and at diverse stages of radiotherapy and the associated workflow. The benefit of each suggested method will certainly depend on the individual patient case and institute.

Zusammenfassung

Heutige Bestrahlungstechniken, wie intensitätsmodulierte Strahlentherapie (RT), erzielen eine hohe dosimetrische Qualität mittels hochkonformaler, d.h. den Tumor eng umschließender, Dosisverteilungen und präzisen Bestrahlungen. Im Vergleich zu früheren Techniken ist deren Anwendung jedoch häufig mit höherem personellen Aufwand und längeren Bestrahlungszeiten verbunden. Zudem werden sie nicht optimal genutzt: einerseits hinsichtlich der Effizienz in der Bestrahlungsplanung und der entstehenden Behandlungsdauer, und andererseits bezüglich der bestrahlten Dosis an den Patienten.

Diese Dissertation schlägt Methoden zur Verbesserung der dosimetrischen Qualität und Effizienz in intensitätsmodulierter Strahlentherapie (IMRT) mit Photonen (IMXT) und Protonen (IMPT) vor und analysiert diese. IMRT-Planung beinhaltet eine multikriterielle - auf Computertomographieaufnahmen (CT) basierende - Dosisoptimierung mit dem Ziel, Tumore ausreichend mit Dosis abzudecken und gleichzeitig Risikostrukturen zu schonen. Die Bestrahlungsplanung bestimmt die voneinander abhängigen Ziele der dosimetrischen Qualität und der Effizienz von Planung (benötigte Planungszeit) und Bestrahlungsdauer. Diese Arbeit basiert auf Projekten, die den Planungsprozess und die sich daraus ergebende Bestrahlungszeiten untersuchen und diskutieren.

Planungseffizienz und Qualität der Dosisverteilung werden anhand von den verwendeten Optimierungsalgorithmen und dem klinischen Planungsablauf behandelt. Die Optimierung von Bestrahlungsplänen mit herkömmlichen Algorithmen beruht typischerweise auf der sukzessiven Veränderung und Überprüfung von Optimierungsparametern. Dieser ineffiziente Prozess wird durch Multikriterielle Optimierung (MCO) eliminiert. Diese Dissertation zeigt die Überlegenheit von MCO hinsichtlich Planungsdauer und Planqualität durch einen Vergleich mit nicht-MCO erzeugten Plänen. Zur weiteren Verbesserung von Planungseffizienz und Qualität wird ein alternativer klinischer Planungsablauf vorgeschlagen. Dieser standardisiert die Planung durch die Verwendung von Optimierungsparameter-Templates und ermöglicht zugleich eine Individualisierung der Therapie, in dem der Strahlentherapeut die Dosisverteilung an die jeweilige Patientensituation anpassen kann. Die Umsetzbarkeit dieser Alternative wird in einer Planungsstudie demonstriert.
Bildgeführte und adaptive Strahlentherapie ermöglichen es, die dosimetrische Qualität über den gesamten Behandlungsverlauf trotz variierender Patientenlagerung und anatomischer Veränderungen, z.B. Gewichtsabnahme, zu erhalten. Aufgrund des erhöhten Arbeitsaufwands ist es von Interesse die Anzahl der Planadaptionen (Neuplanungen) zu reduzieren und die Relevanz dieses Verfahrens zu analysieren. Der Einfluss geometrischer Veränderungen auf IMXT- und IMPT-Dosisverteilungen wurde auf der Basis klinischer Kontroll-CT-Aufnahmen untersucht. Die Ergebnisse zeigen deutliche Dosisänderungen, eine nicht-kontinuierliche Verschlechterung der Planqualitäten und individuelle Unterschiede zwischen Patienten. Sie verdeutlichen die Bedeutung beider Techniken. Die regelmäßige Durchführung von Bildkontrollen und Planadaptionen wird daher trotz des zusätzlichen Aufwands empfohlen, um Über- und Unterdosierungen zu verhindern.
Die Bestrahlungseffizienz ist gekoppelt an die Planqualität und wird durch Planparameter beeinflusst, die während der Optimierung bestimmt werden. Üblicherweise werden Bestrahlungspläne erstellt, ohne die Bestrahlungsdauer direkt in die Optimierung einzubeziehen. Um IMPT-Bestrahlungsdauern zu reduzieren, wurde ein Algorithmus entwickelt, der die Bestrahlungseffizienz in die Planoptimierung integriert.

Basierend auf priorisierter Optimierung, wird zunächst die Planqualität optimiert und darauffolgend, unter Erhaltung vorheriger Errungenschaften, die Bestrahlungszeit reduziert. Der „prioritized efficiency opimization“ Algorithmus (PrEfOpt) ermöglicht zudem, unvermeidliche „Trade-offs“ zwischen dosimetrischer Qualität und Bestrahlungszeit zu untersuchen. Angewandt auf klinische Patientenfälle wurden deutliche Zeitersparungen bei gleichbleibender Qualität erzielt. Die Implementierung effizienz-optimierender Schritte in die RT-Planung hat daher großes Potential für die klinische Praxis.

Abschließend zeigt diese Arbeit Möglichkeiten auf, wie Effizienz und dosimetrische Qualität in IMRT Planung an verschiedenen Stellen der Therapie und im Behandlungsablauf verbessert werden können. Der Nutzen jeder vorgeschlagenen Methode ist vom individuellen Patientenfall sowie vom jeweiligen Institut (und verfügbaren Techniken) abhängig.

Contents

1 An introduction to efficiency and quality in radiotherapy

1.1 Context

Over the last decades great progress in cancer treatment was achieved improving the prognosis of patients diagnosed with cancer. As cancer is a leading cause of death worldwide, in developed and developing countries [61, 25], and as the number of cancer diagnosis is expected to rise continuously, partly due to an ageing society, cancer treatment will remain a challenge in the future.

1.1.1 Rationale

Radiotherapy (RT) is a constituent component in approximately 50% of tumor treatments [24, 137]. Its therapeutic effect is based on the irradiation with ionizing particles in order to kill tumor cells by breaking chemical bonds in their deoxyribonucleic acid (DNA) and by the consequent loss of cell reproducibility [50]. Cell death efficacy increases with dose, the deposited energy per mass[1]. The required dose for a succesful tumor treatment mainly depends on the biological properties and on the size of the tumor [49]. As radiation does not only affect tumor cells, but also cells of healthy tissue, the dose given to the tumor is limited; tolerance doses of organs at risk (OARs) are mostly based on clinical experiences (e.g. [45]). The major intention and challenge of radiotherapy treatment planning is to cover the tumor with sufficient dose to kill all tumor cells and simultaneously preserve the functionality of surrounding OARs. Radiotherapy planning requires an inevitable compromise between tumor coverage and sparing of healthy tissue, for which it is generally desirable to limit dose to a minimum in order to reduce the risk of radiation induced secondary cancer and acute/late side effects.
The dose distributions and opportunities to spare adjacent organs are determined by the applied radiation type and technique; a variety of radiation types[2] are employed in external radiotherapy[3]. Besides the most commonly applied photon therapy (high energetic X-rays), produced and delivered by linear accelerators (linac), proton therapy is an increasingly utilized treatment modality [19, 104].

[1] $D = \frac{\Delta E}{\Delta m}$ [Gy]
[2] Utilized radiation are e.g. photons, electrons, protons, neutrons, heavy ions.
[3] The source of radiation is outside the patient - in contrast to brachytherapy (short distance) where the source is brought into the patient.

1.1.2 Photon and proton radiotherapy

The application of proton therapy and the number of facilities increased steadily over last years[4]; its availibility compared to photon therapy is however still limited [50, 19]. Proton therapy requires spacious facility components, such as accelerators (synchrotons or cyclotrons), beam lines and heavy gantries, and is therefore entangled to higher therapy costs [85, 107, 113]. With the intention to increase the accessibility of particle therapy in the future, more compact proton machines are developed (e.g. one room facilities), and novel accelerating techniques are under investigation - such as laser accelerated proton therapy [116, 56, 19].
The utilization of proton therapy is encouraged by the favorable physical properties of protons, which allow the generation of superior dose distributions compared to photons (figures 1.1 and 1.2) [122, 34]. While the deposited dose of photon beams posesses its maximum shortly behind the skin (dose build-up effect [49]) and decreases nearly exponentially, proton dose depth curves are characterized by the Bragg Peak. The Bragg Peak and the finite proton range allow for very precise dose deposition by energy modulation, and can reduce integral doses to normal tissue up to a factor between two and four [82, 30], which makes it particularly eligable for children [90].

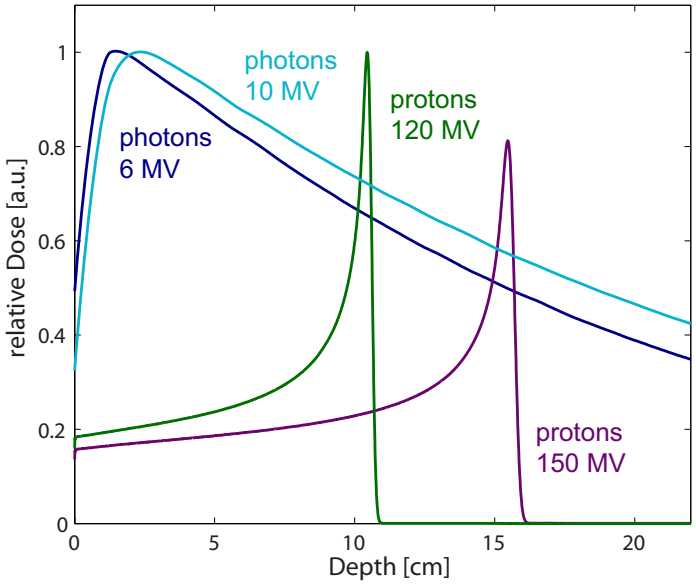

Figure 1.1: Depth dose curves of photons (6 MV and 10 MV) and protons (120 MV and 150 MV). Photon curves differ hardly by their initial energies; the dose yields its maximum shortly behind the entrance and decreases continuously in matter. The finitie range of protons, determined by their energies, allows for precise radiotherapy treatments and reduces doses to normal tissue, especially for deep seated tumors.

[4]Particle Therapy Co-Operative Group, http://ptcog.web.psi.ch.

For various diagnosis, proton therapy is undouptly preferable while the benefit for others is controversially discussed [46, 139]. Yet data supporting the clinical evidence is lacking for numerous entities [85, 114, 89]. Due to the correlated costs and the limited availability, it is important to identify the patients who benefit from this high precission therapy [85, 74, 57]; randomized trials[5], comparing the outcome of photon and proton therapy, are ongoing in order to answer these questions in the future. Besides the comparably higher costs, proton therapy comes along with one major challenge: range uncertainties. This term comprises uncertainties in computational dose calculations/range predictions and in dose delivery due to the sensitivity of the Bragg peak to changes of traversed tissue densities [86, 104]; the latter is analyzed in detail in chapter 4.

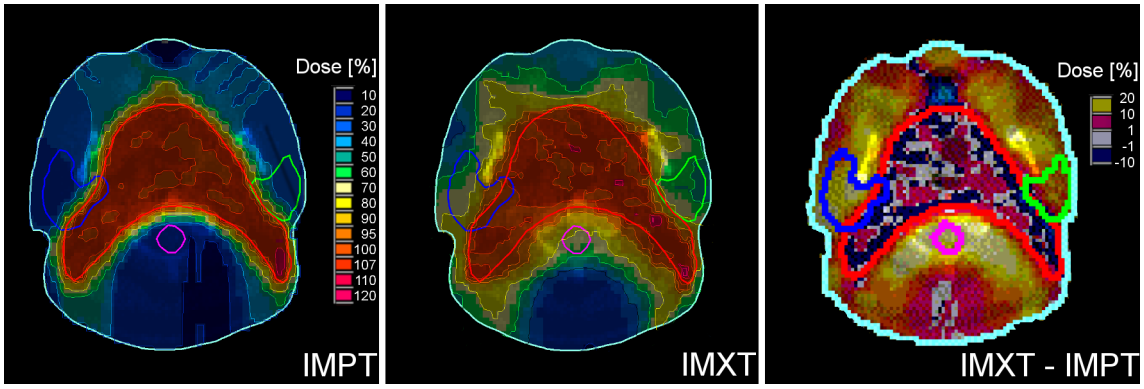

Figure 1.2: Dose distributions of intensity modulated proton (IMPT) (left) and photon therapy (IMXT) (center) and their dosimetric differences (IMXT - IMPT) for an exemplary head and neck cancer case. Contoured structures: planning target volume (red), spinal cord (magenta), left and right parotid glands (green and blue).

1.1.3 Progress in radiotherapy: state of the art and main objectives of radiotherapy treatment planning

The times of James Ewing (pathologist 1866-1943) who once prescribed radiotherapy treatment of a hodgkin lymphoma patient with the words "all you could really do was to place the patient underneath the machine and hope for the best" are long of the past [8]. Radiotherapy offers a large variety of sophisticated high precision techniques, which allow the generation of high quality dose distributions and their accurate deliveries. Major accomplishments within the last decades certainly were intensity modulated radiotherapy (IMRT) (see section 2.2) and with it computer based inverse planning - which are both established as clinical standards. Stereotactic radiosurgery, image guided RT (IGRT), adaptive RT and

[5] e.g. https://clinicaltrials.gov or https://www.mdanderson.org/patients-family/diagnosis-treatment/care-centers-clinics/proton-therapy-center/clinical-trials.html

particle therapy are further examples in the spectra of modern RT technologies. The clinical benefit of these techniques is notable by improved overall survival and reduced toxicities [147, 126, 1, 105]. Its applications, however, come along with longer treatment times, increased quality assurance procedures and greater staff involvement, which leads to higher overall treatment expenses [132, 19, 24, 137]. Previous investigations demonstrated that IMRT remarkably prolongs treatment times and medical staff workload, compared to the previous state of the art technique, 3D conformal RT (see section 2.2) [38, 132, 137]; Budach et al. quantified an average increase of both concerns by a factor of 1.5 for head and neck RTs [24]; similar RT time comparison results were obtained by an earlier study [132]. The additional utilization of IGRT further extends room occupancy times and staff involvement, as presented by [137]. Finally, proton therapy comprises a well suitable example for a highly precise but expensive treatment technique (see above); diverse cost-effectiveness analysis are performed to clarify whether the treatment outcome justifies the higher treatment costs [85, 113, 57].
Besides the objective of high treatment qualities, economic aspects become continuously more of interest [132, 19, 133, 113]; efficiency in daily work processes, as treatment planning, and clinical routine are gaining in importance. The objective of radiotherapy treatment planning can therefore be formulated as to improve efficiency but simultaneously make use of developed advanced techniques and their potential to obtain high dosimetric qualities as best as possible.

1.2 The relation of efficiency and quality in radiotherapy

Radiotherapy treatment, enclosing the overall time of a patient in the radiation oncology department, consists of different phases undergone by the patient, and tasks performed by diverse medical staff (figure 1.3). The clinical RT workflow includes the treatment preparation, i.e. the **treatment planning** phase (approx. one week) and the **irradiation period**, which is typically spread over several weeks in fractionated radiotherapy[6]. Each part comprises "efficiency" and "quality" in different contexts, which are related and connected to treatment planning, the core procedure of the presented interrelations. "Efficiency" may refer to planning efficiency with respect to the treatment planning procedure itself, and to an efficient dose delivery, which is determined by plan properties, attributed by treatment planning. "Quality" in radiotherapy treatment planning corresponds to dosimetric quality, and is typically assessed by dose criteria like tumor coverage and OAR sparing (see section 2.3.2).

[6] typically five RT fractions per week

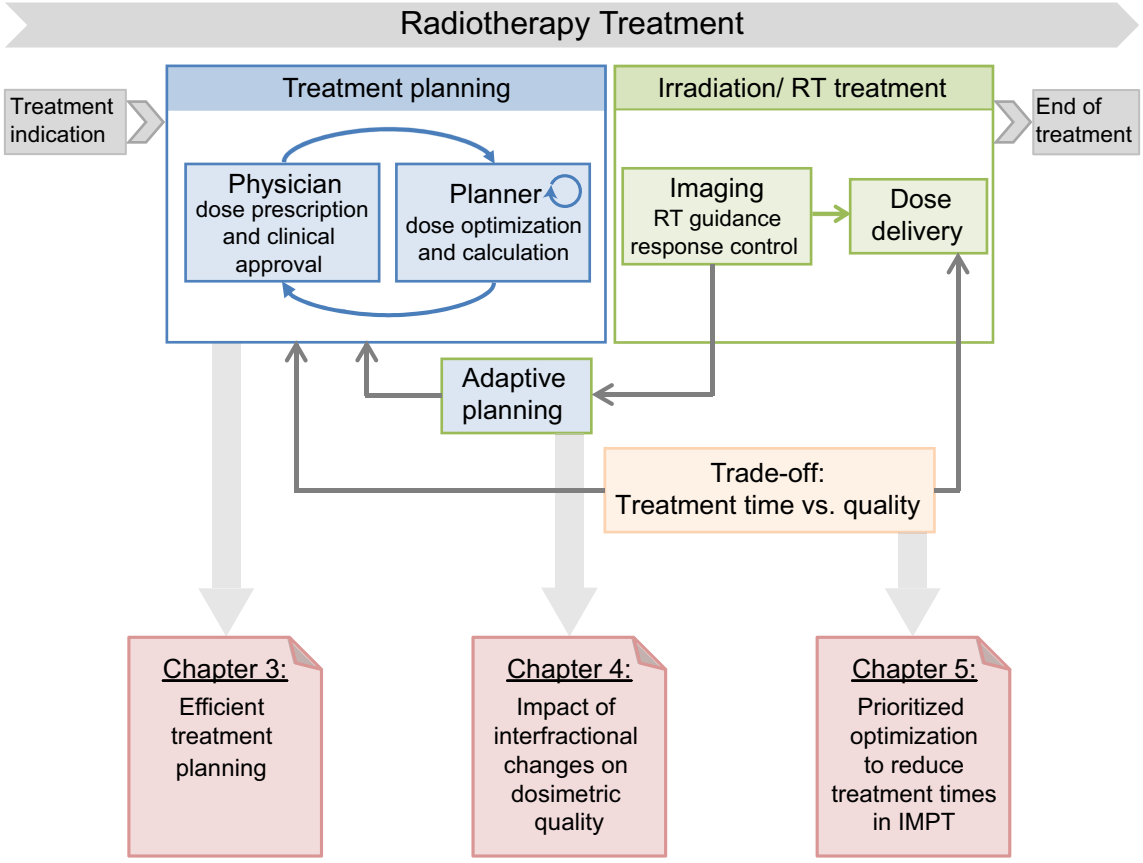

Figure 1.3: The relation of efficiency and quality in radiotherapy. Three components were identified and investigated by different projects within the scope of this thesis: chapter 3 analyzes the treatment planning process and suggests methods to improve planning efficiency and quality; chapter 4 examines the relevance of adaptive planning; chapter 5 presents an optimization algorithm to improve delivery efficiency.

The process of radiotherapy treatment

Starting at the patients' indication for radiotherapy treatment, **treatment planning** is initiated with the acquisition of the planning computed tomography image (p-CT), the basis for computational dose optimization and calculation. RT planning is an iterative and interactive process between physicians, who define the target and anatomical structures as well as the dose prescription, and planners[7] who conduct the actual planning, according to physicians' prescription. Due to the multiobjective optimization problem of different interdependent dosimetric goals, i.e. tumor coverage and simultaneous preservation of healthy tissue, the search for

[7]Planning personnel varies between countries and clinics: in Germany planning is generally performed by medical physicists while in other countries (e.g. the US) specialised professions ("dosimetrists") exist for this purpose; in some clinics, planning is (partly) executed by physicians.

the "best plan" for every patient is a complex task. The dose optimization occurs by iterative adaption of optimization parameters until the plan is acceptable for clinical treatment approval. This **optimization process** is often inefficient and commonly known as a "trial-and-error" process with the planning efficiency and resulting plan quality frequently depending on the planners' experience.
Tumor coverage and specified dose limitations of OARs are not always achievable at the same time, and may require compromises. The communication between physicians who possess the medical background knowlegde and the planner, who translates the clinical demands into the treatment plan, plays a fundamental role in the process of obtaining a satisfactory plan result for every individual.
The derived and treatment approved plan is typically irradiated in daily fractions over several weeks - the **RT treatment period**. In order to maintain dosimetric quality over the whole treatment cycle, IGRT and adaptive radiotherapy became part of clinical practice. IGRT accounts for variations in daily set-up by correcting patients' position according to control images in the treatment position prior to irradiation. In case of severe anatomical changes, adaptive planning is performed, which prescribes the generation of a new treatment plan on the current anatomy (new p-CT). Due to the correlated workload and expenses in clinical practice, plan adaptions are often reduced to a minimum, although dosimetric quality has the highest clinical priority. The decision whether a plan requires adaption is not trivial, and neither is the preliminary estimation of dosimetric consequences, if treatment is continued with the original plan despite of anatomical changes. Yet there are no clear indicators to identify patients and timings for plan adaptions; such indicators would certainly improve planning efficiency. The impact of changing geometries and the relevance of IGRT and plan adaptions presumably varies with the tumor location, applied RT type and technique.
Short treatment times are a major concern, not only for economical reasons, but also to increase patients' comfort and treatment quality (by reduction of dosimetric uncertainties and improved biological response) [103, 11, 123, 91, 130]. The duration of each RT session (treatment room occupancy) consists of the required time for patient set-up (incl. IGRT) and of the **dose delivery time**. The latter is determined by machine parameters (dose rate, currents, etc.) and by the plan complexity, i.e. by geometrical settings, as the number of fields, and by the degree of intensity modulation (see section 2.2). Typically treatment plan optimization prescribes the optimization of the dose distribution based on specified dose criteria, and does not incorporate delivery efficiency. The objectives to obtain a high dosimetric quality and short RT times are conflicting goals (see section 2.3.3): intensity modulation achieves highly conformal dose distributions, with the generated fluence pattern being correlated to the application time, since it is delivered by moving multi-leaf collimators (MLCs) which follow the optimized pattern (see section 2.2).

The introduced components of radiotherapy treatment indicate the potential for the optimization of efficiency and dosimetric quality, the content of this thesis.

1.3 Outline and structure

This thesis addresses the above illustrated main components of radiotherapy treatment and especially the conflicting goals of obtaining high treatment qualities and efficiency in and by treatment planning. It suggests and analyzes diverse possibilities to optimize the interdependent radiotherapy objectives "efficiency" and "dosimetric quality". In this context figure 1.3 identified three main topics which were investigated by different independent projects and are presented in **chapters 3-5**. Each chapter consists of separate specific material and methods, results, discussion and conclusion sections.

After the general introduction to the context of radiotherapy and its main treatment (planning) goals presented in **chapter 1**, an overview of fundamental principles of IMRT planning is given in **chapter 2**, where moreover general concepts of dose optimization and plan quality evaluation are introduced.

Chapter 3 analyzes the treatment planning process by two core components: the actual "dose optimization" and the clinical treatment planning workflow. Both projects were conducted at Massachusetts General Hospital (MGH).
First, the impact of the utilized computational optimization software on planning efficiency and resulting dosimetric quality is investigated. The potential of multicriteria optimization (MCO) to approach the multiobjective optimization problem of treatment planning is demonstrated by comparing MCO to non-MCO generated plans for non-small cell lung cancer patients, which resulted in superior dose distributions (better OAR sparing) at shorter planning times for MCO. This study was published by Kamran, Müller et al. [66].
The second project questioned the current practice of task splitting and communication between physicans and physicists in RT planning. With the intention to improve planning efficiency and the plan quality for every individual patient, physician driven planning in IMRT with MCO is proposed as an alternative planning routine. The suggested planning approach standardizes the planning process by utilizing site specific templates and integrates physicians more tightly into treatment planning. Its feasibility is demonstrated by a comparison of clinical plans, generated by dosimetrists, and physician driven plans in terms of dose criteria and physician preferences, for brain and prostate cases. This work was in parts submitted for publication and is currently in revision.

Chapter 4 presents a retrospective treatment planning study to investigate the relevance of adaptive planning for head and neck cancer patients, who are subject to severe anatomical changes throughout the treatment period. Dosimetric consequences of interfractional geometrical changes intensity modulated proton therapy (IMPT) versus photon therapy (IMXT) were analyzed on the basis of clinically acquired control images in the actual treatment position. The results demonstrated for both modalities the importance of frequent control images and

recalculations of treatment plans on control CTs, in order to answer the question, if plan adaption is necessary to avoid any underdosage of the tumor (most relevant for IMPT) or overdosage of OARs (more critical in IMXT). Parts of this chapter were published by the author [95]; the publication was featured on MedicalPhysicsWeb [42].

Chapter 5 investigates the potential of treatment time reductions for IMPT plans and analyzes ineviatable trade-offs between delivery efficiency and dosimetric quality. On the basis of prioritized optimization, an algorithm was developed which allows to reduce IMPT delivery times while maintaining plan quality, and to study potential trade-offs of those two interdependent objectives. IMPT times strongly depend on facility features, such as energy switch times and proton currents. The implemented routine offers distinctive alternative methods to improve efficiency whose potential was analyzed by achieved time savings and dosimetric quality for two proton facility types, i.e. of constant and variable proton current. Remarkable delivery time reductions were achieved at similar plan qualities; the magnitude of time reductions depended on the patient case, facility type and applied optimization method. Parts of this work were submitted for publication.

Chapter 6 summarizes the results of the presented work and discusses their relevance towards clinical realizations. An outlook on future radiotherapy regarding challenges in efficiency and quality is given.

2 Fundamentals of intensity modulated radiotherapy treatment planning with photons and protons

2.1 Dose deposition by photons and protons

The merits of proton therapy compared to photon therapy are found in their favorable physical properties and the hereby achievable superior dose distributions (see section 1.1.2, figures 1.1 and 1.2); corresponding dose depositions occur by distinctive interactions with matter. Protons, being charged particles, are directly ionizing radiation and lose most of their energy by ionization and excitation of the traversed matter while electrically neutral photons are indirectly ionizing particles. Photons interact primarily by secondary particle production (mainly electrons) to which energy is transferred and in a second step deposited to the patient.

Interactions of photon beams

Primary photon interactions by the photon effect, the Compton effect and pair productions, with a dominating ocurrance in the order of increasing energy, reduce the initial photon fluence. The photon absorption is prescribed exponentially, dependent on the mass absorption coefficient $\mu(E)$ (exponent) of the traversed matter (density ρ). In radiotherapy, with typical energies between 6 MV and 15 MV, the Compton effect is the dominant primary effect whose produced electrons deposit the largest fraction of dose to the patient by secondary ionizations and excitations. The build-up effect of photon dose depth curves is explained by the comparably large energy transfer and the finite range of electrons which leads to an increased dose deposition at a short distance to the electrons' origin. The delivered dose depends on the photon fluence distribution $\Phi_E(E) = \frac{d\Phi}{dE}$ with $\Phi = \frac{dN}{dA}$ $[\frac{photons}{cm^2}]$, the initial energy spectrum $[E_{min}, E_{max}]$ and on material/absorption properties (equation 2.1). The weighting factor $\frac{<E_{ab}(E)>}{E}$ incorporates the averaged locally deposited energy fraction, dependent on the photon energy E.

$$D = \int_{E_{min}}^{E_{max}} \frac{1}{\rho} \cdot \Phi_E(E) \cdot (1 - e^{-\mu(E)\cdot\Delta x}) \cdot E \cdot dE \cdot \frac{< E_{ab}(E) >}{E} \qquad (2.1)$$

For a monoenergetic photon beam, the dose is well approximated by equation 2.2, with the energy mass absorption coefficient $\frac{\mu_{en}}{\rho}(E)$:

$$D \approx \frac{\mu_{en}(E)}{\rho} \cdot \Phi(E) \cdot E \tag{2.2}$$

Interactions of proton beams

Protons interact directly with the traversed matter, mainly by electromagnetic interactions with atomic electrons, i.e. by collisions and multiple Coulomb scattering, and to a smaller extent by nuclear interactions (relatively infrequent). The charged particles loose their energy primarily due to collisions with outer electrons which is captured by the linear stopping power $S(E)$ (equation 2.3).

$$S(E) = -\frac{dE}{dx} \quad [\frac{MeV}{cm}] \tag{2.3}$$

The rate of energy loss increases as protons slow down in matter, which is mathematically approximated by the Bethe-Bloch formula, and expressed by the indirect proportionality to velocity squared (equation 2.4), with density ρ, atomic number Z and mass number A of the absorber.

$$\frac{dE}{dx} \propto \rho \cdot \frac{Z}{A \cdot v^2} \tag{2.4}$$

The stopping power S(E) is commonly normalized by the density to the mass stopping power, measured in $\frac{MeVcm^2}{g}$. The delivered dose by protons of energy E is calculated by the product of the proton fluence $\Phi = \frac{dN}{dA}$ $[\frac{protons}{cm^2}]$ and mass stopping power (equation 2.5).

$$D = \Phi \frac{S(E)}{\rho} \tag{2.5}$$

Radiobiological effectiveness

Based on the physical interactions of photons and protons, biological damage is produced by different mechanisms. The radiobiological effect of photon radiation is based on secondary processes, mainly by radicals which are produced through the radiolysis of water and attack the DNA. DNA damage by protons occurs directly by ionizations and excitations. Proton and photon RT differ in their radiological effectiveness, expressed by the relative biological effectiveness (RBE) with the reference dose D_X of photons (Co-60) and the proton dose D_p, which causes the same biological damage (e.g. measured cell survival).

$$RBE = \frac{D_X}{D_p} \tag{2.6}$$

Proton doses are often presented as RBE-weighted doses, with a constant value[1] of $RBE = 1.1$.

2.2 Intensity modulated radiotherapy

The concept of intensity modulated radiotherapy (IMRT) was initially suggested for photon therapy (also referred to as IMXT) and was later introduced for proton therapy (IMPT). The following introduction to the basic principles of this technique is based on photon therapy. An overview of the main components of IMPT and spot scanning proton therapy as a prerequisite for IMPT is presented in subsection 2.2.2.

2.2.1 Intensity modulated radiotherapy with photons

The invention of IMRT was one of the major milestones in radiotherapy. IMRT improves the conformity of dose distributions remarkably compared to 3D conformal radiotherapy (3D-CRT)[14]. Even though IMRT became a standard technique in most clinics, 3D-CRT is still widely applied - dependent on the individual situation and available techniques - and may well compete with IMRT in some cases. Dose distributions of 3D-CRT are formed by fitting the aperture of each field, restrained by multileaf collimators (MLC)[2], to the shape of the target of each beam perspective (figure 2.1(a)).

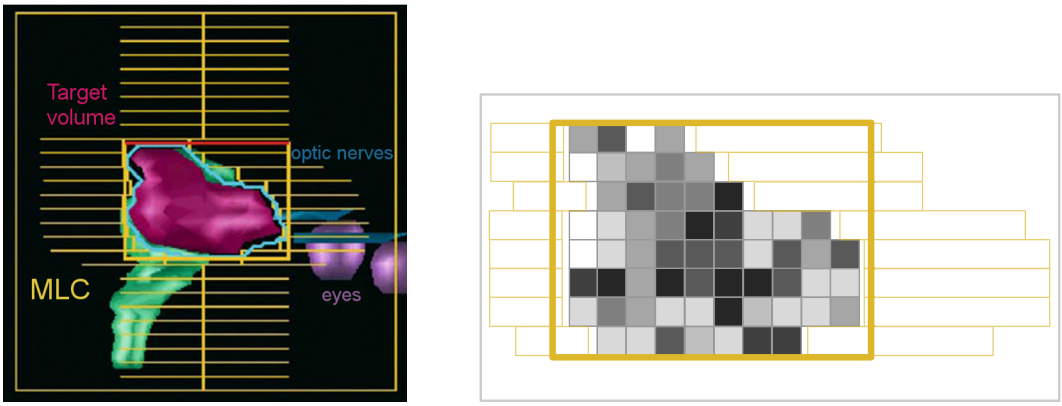

(a) Beam-eye-view (BEV), adapted from [117].

(b) Potential IMRT fluence map for the beam geometry of figure 2.1(a).

Figure 2.1: Treatment planning in 3D conformal RT and IMRT: BEV for conformal RT and corresponding schematic presentation of a potential fluence map (grey values refer to different beamlet intensities).

[1] The RBE depends on the linear energy transfer; the constant value of 1.1 is an approximation.
[2] MLCs are state of the art; earlier, apertures were produced individually for every patient and beam direction.

The superposition of several fields achieves an increased dose in the target region. Contrary to IMRT, the photon fluence is homogeneously distributed over the size of the field, i.e. beams deliver uniform dose distributions[3] (figure 2.2(a)). IMRT-fields are partitioned into segments of different intensities (distinctive beam-on times), delivering non-uniform dose distributions to the target (figure 2.1(b)) whose superposition results in the desired dose distribution (figure 2.2(b)).

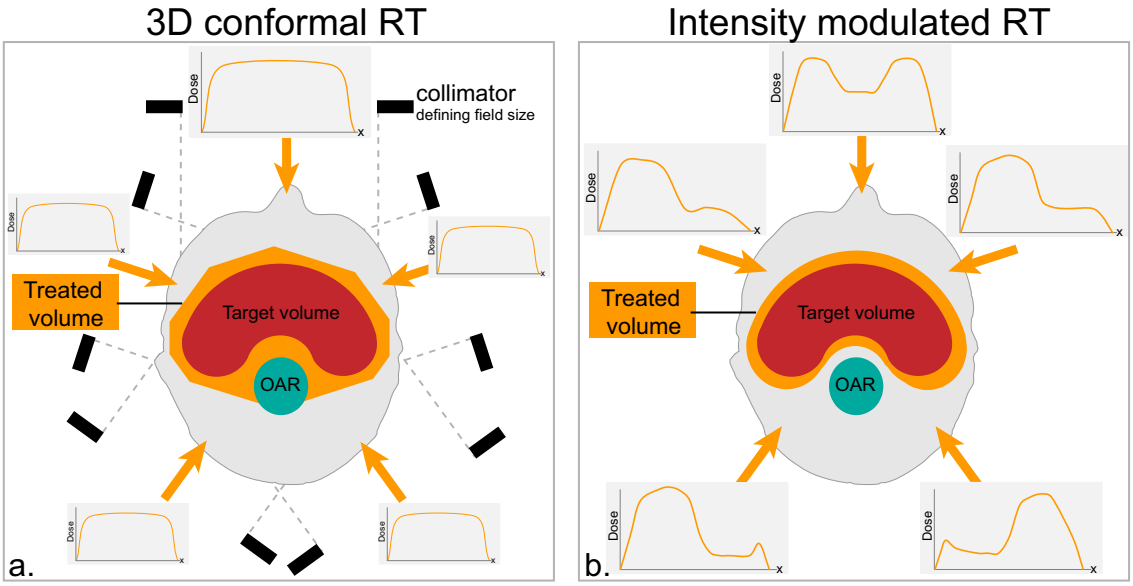

Figure 2.2: Basic concepts and differences of 3D-CRT and IMRT, based on [21]: 3D-CRT achieves conformity by superposition of several homogeneous dose distributions of different beam directions while IMRT delivers fluence patterns of non-uniform dose distributions whose superposition result in superior target dose conformity.

The delivery of the calculated fluence segments is executed by MLC tracing of a sequence of small apertures either by multiple static fields or continuous MLC-motion and irradiation [17, 121, 15].
The realization of IMRT requires inverse planning and was enabled by the development of corresponding computational optimization algorithms (see subsection 2.3.1) [23, 18, 32]. By defining dose parameters for the given structures, an ideal fluence map is calculated - idealized in the sense that fluence segments of the beams are assumed to be infinitesimaly small such that the calculated dose distribution is not applicable in reality. A sequencing process translates the idealized intensities into the pattern of small segments of different fluences; it can be performed as a subsequent step to the optimization or be included in the optimization, which eliminates potentially resulting undesired dose changes caused by the sequencer.

[3]except for dose gradients in specific directions, generated by the introduction of wedges;

The quality of the dose distributions is determined by the size of the MLC leaves and to the correlated number of segments the fluence map is split into: the larger the number of segments, the smaller the rectangular fluence segments, and the closer the deliverable dose will be to the ideal distribution. The assigned intensities are typically limited to a discrete number of available levels, which is a premise for "step and shoot" delivery [14]. Fluence intensities are quantified by monitor units (MU), a measure of machine output which is detected by ionization chambers in the head of the linac. Typically MUs are calibrated to a certain dose for specific beam parameters[4]. The number of utilized beam angles in IMRT varies typically between 5 and 9 angles, e.g. with the complexity of the case.
By delivering complex patterns of spatially varying fluences, IMRT achieves highly conformal dose distributions [140, 18, 32] and sparing of OARS, even in close proximity to the target (see figure 2.2), which enables dose escalations to increase tumor control. The superiority of IMRT dose distributions versus 3D-CRT was supported by studies, which documented less OAR toxicity and improved tumor control [147, 126, 1, 105].

Special intensity modulated radiotherapy techniques

"Volumetric modulated arc therapy" (VMAT) [100] - also known as rotational arc technique - prescribes a special IMRT technique, which achieves great dose conformity by delivering intensity modulated dose distributions while the source rotates around the patient. The main advantage of VMAT compared to regular IMRT is the shorter treatment time [22, 101, 16]. With respect to the comparability of corresponding dose distribution, controversial discussions are ongoing [22, 101].
Another special variant of IMRT is realized by the tomotherapy unit[5], which combines CT-technique components with radiotherapy.

2.2.2 Intensity modulated radiotherapy with protons

Proton therapy is delivered by two beam delivery techniques: "scattering" and "spot scanning" [50]. Within this work, proton therapy exclusively addresses the latter, which is a prerequisite to perform IMPT [80]; in clinical practice, IMPT additionally requires precise steering of the narrow pencil beam in order to achieve accurate dose applications.
Spot scanning proton therapy planning can be performed by single field uniform dose optimization (SFUD) or simultaneous optimization of several fields (multifield optimization), commonly known as IMPT and is analogous to the above prescribed IMXT [112]. SFUD optimizes each field separately to a homogeneous target dose such that each field contributes a uniform fraction of the total dose (similar to 3D-CRT). Technically, plans of one field or several SFUD-optimized fields are not

[4]Parameters: field size, measured depth, source skin distance (SSD); typical callibration: 1 Gy refers to 100 MU at depth of dose maximum, 10 cm x 10 cm field size, SSD = 1 m, [110].
[5]Accuray Inc., Madison, WI

considered to be IMPT. The planning of spot scanning proton therapy however consists of the same components and only differs in the number of included fields in the (simultaneous) beamlet optimization. In IMPT, fluence patterns are optimized; the beamlet segments correspond to spots, which refer to specific beam positions. Planning is initialized by defining the spot grid, i.e. the spacing over the target volume[6] (figure 2.3, left). The definition of optimal grid parameters is a complex task, which involves a variety of interdependent quantities such as target volume, beam widths (spot size), treatment and optimization times. Spots can be distributed within a regular and non-regular grid. While lateral spot distances $\Delta x/\Delta y$ are commonly selected equally (e.g. between 0.3 and 0.6 cm), the distances in depth Δz are often adapted to the width of the Bragg peak of the corresponding energy, which in deep seated tumors especially reduces the number of spots and therefore delivery efficiency [67]. Recently, statistical and iteratively generated spot placement (during optimization) was proposed [131]. The assigned spot intensities by the subsequent optimization correlate directly to the number of particles, and are translated into beam on times for delivery (figure 2.3, right).

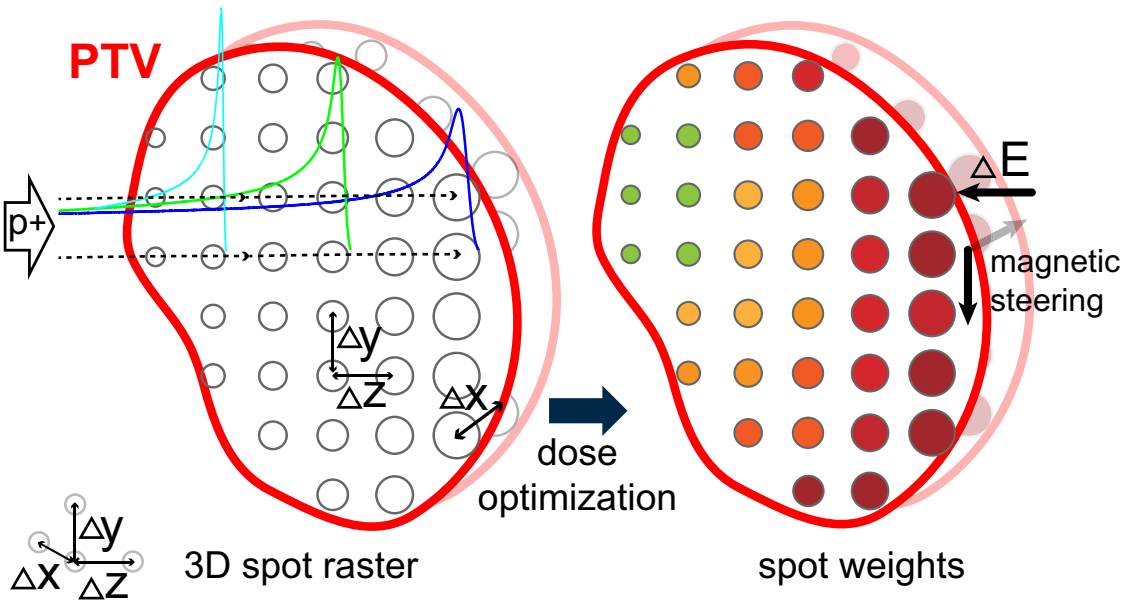

Figure 2.3: Basic components of spot scanning proton therapy planning and delivery. Spot grids are specified prior to optimization (left). Different spot intensities are assigned in the optimization process (illustrated by different colors: from green, the lowest intensity, to dark red, the highest intensity) (right). Delivery occurs by iterative energy adjustment ΔE and magnetic beam steering between lateral spot positions within each energy layer.

[6]To improve coverage spots are often placed within a volume of target plus an additional margin.

Treatment plans consist of differently weighted spots, each of which belongs to one so-called energy layer (spots of equal energy), and are delivered by sequential adjustment of proton energies (start at highest energy layer) and subsequent magnetic beam steering. Radiation can be continuous or with breaks between different spot positions depending on the facility and spot distances.
Proton plans generally feature less fields compared to IMXT.

2.3 Intensity modulated radiotherapy treatment planning

The main goal of treatment planning is to achieve a homogeneous coverage of the target volume with the prescribed dose and simultaneously to stay below tolerance doses of surrounding OARs. IMXT and IMPT treatment planning follow the same principles of inverse planning which is executed in treatment planning systems (TPS), i.e. software to optimize and calculate dose distributions, on the basis of planning CTs (p-CTs).

Volume definitions and dose prescriptions - a preliminary planning step

Volumes of interest (VOIs) are delineated on p-CTs which are frequently registered to magnetic resonance images (MRI) and/or positron emission tomography (PET) images for improved spatial resolution. Doses are typically prescribed to the planning target volume (PTV); including the solid tumor (gross tumor volume (GTV)), potentially infiltrated surrounding tissue (clinical target volume (CTV)[7]) and a safety margin for variations in the daily set-up and motion [59]. To account for range uncertainties, specific to IMPT, additional margins are added in beam directions resulting in distinctive targets for each field; for simultaneous IMPT optimization these structures are commonly unified to one planning target (PTV range).

Choice of geometrical plan settings

Prior to optimization, geometrical settings and certain beam parameters are defined, e.g. beam energies and collimator angles for IMXT, spot grids for IMPT, and beam angles for both[8]. The choice of beam directions is primarily determined by the tumor location and critical structures nearby. Specific to proton therapy and associated range uncertainties, directions are avoided, which position the Bragg peak shortly in front of critical organs. More than in IMXT, IMPT demands the avoidance of traversing matter of extremely inhomogeneous densities, regions, which include large day to day variations (paranasal or intestinal regions), implants and resulting regions of artefacts. The dependency of proton doses on the traversed matter leads

[7]The GTV is typically part of the CTV which may for instance include adjacent lymph nodes.
[8]Beam angle optimization is an ongoing research topic; for more information see e.g. [10].

to a greater sensitivity to interfield and intrafield changes for IMPT compared to IMXT which demands additional considerations, i.e. robustness analysis; treatment plans are created such that geometrical variations affect the dose distribution as little as possible.

2.3.1 Treatment plan optimization

Inverse IMRT planning prescribes the optimization of beamlet (segments in IMXT, spots in IMPT) intensities according to dose restrictions and objectives specified in one or several objective functions (OF). Various biological and physical dose criteria can be translated into OFs, the most common ones being physical dose-volume criteria (see section 2.3.2) such as minimum, mean or maximum doses[9] [14, 97].

Problem formulation

Mathematically the beamlet intensities ω_j with $j \in \{1, ..., n\}$ are optimized such that the dose $D_i(\omega) = \sum_j D_{i,j} \cdot \omega_j$ to voxel i approaches the specified goals as well as possible, with the voxel i being a volumetric fraction of the structure "VOI", i.e. $i \in VOI = \{1, ..., N_{VOI}\}$. The dose-influence matrix $D_{i,j}$ is generated before optimization, and comprises the physical information of the deposited dose by unit beamlet fluence ω_j to i [98].
A typical optimization problem is given by the minimization of the standard quadratic objective function (least squares optimization) which optimizes $D_i(\underline{\omega})$ to the precribed dose D^{prescr} (equation 2.7) [14]:

$$F(\underline{\omega}) = \sum_i (D_i(\underline{\omega}) - D^{prescr})^2 = min \quad \text{subject to:} \quad \omega_j > 0 \quad \forall\, j \tag{2.7}$$

The so-called **weighted-sum approach** combines multiple objectives of different structures in one OF, each assigned with a penalty factor to specify the relative importance of the corresponding goal (see equation 2.8). This approach is implemented in various commercial and research TPSs.

$$OF = \sum_{\nu=1}^{n_{OF}} p_\nu \cdot OF_\nu \tag{2.8}$$

Penalty factors are initially guessed and then iteratively adjusted. It is up to the planner to find suitable weighting factors, which achieve the desired dose distribution.
Both, IMXT and IMPT optimization problem formulations, yield degenerate solutions [141, 5], i.e. different fluence patterns can be found, which fulfill the same objectives/criteria; as IMPT offers more degrees of freedom, the degeneracy of IMPT is greater than of IMXT.

[9] Biological criteria are e.g. the equivalent uniform dose (EUD), tumor control probability (TCP) and normal tissue complication propability (NTCP).

What is an optimal plan? - Treatment planning: a multiobjective problem

The question of what the "optimal" plan looks like is challenging and cannot be answered in general as it may differ between tumor sites and patients. The theoretical ideal solution of a high dose in the tumor and zero dose in all other tissue is obviously physically not achievable. Even though the ideal plan may not exist a number of acceptable solutions, which fulfill the clinical demands of PTV coverage and dose limits to OARs might be found; in case of conflicting dosimetric goals, the final plan typically yields a compromise rather than being "optimal". The preferred dose distribution and selected trade-offs vary between physicians and physicists. In order to compare dose distributions and to assess their dosimetric qualities standardized criteria were established (see section 2.3.2).
A slightly different approach to answer the question is that not one optimal solution but various optimal solutions exist - however not simultaneously in all specified goals - which presents the basic idea of multicriteria optimization (see below, and section 3.2). Radiotherapy objectives are often interdependent and cannot be optimal simultaneously, i.e. feasible solutions accompany inevitable compromises (figure 2.4). The collectivity of optimal plans generate the so-called Pareto front, comprising all plans, which cannot be improved in one criterion without worsening another (dashed line, figure 2.4) [37].

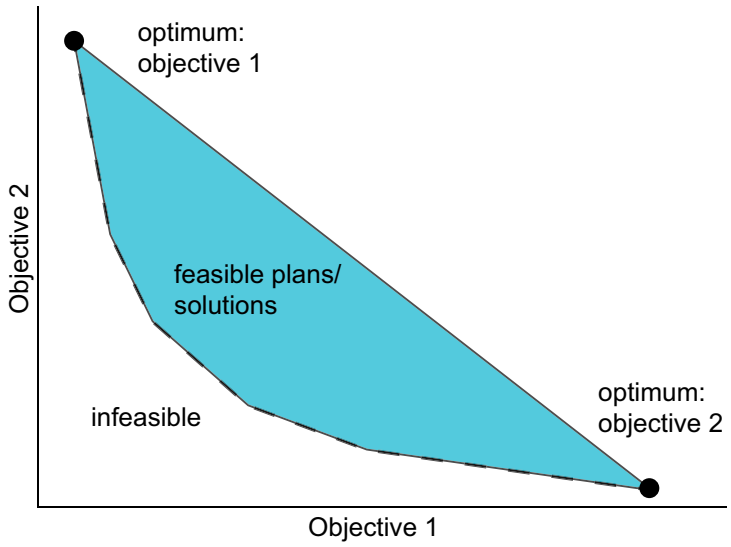

Figure 2.4: Illustration of plan optimization with two interdependent objectives: the simultaneous optimization of objective 1 and 2 requires compromises; all "optimal compromises" generate the Pareto surface (dashed line); adapted from [37].

Finding the "optimal" plan by varying penalty factors in the weighted-sum approach is a trial-and-error process and obtained plans are not necessarily optimal in their objectives (highlighted area, figure 2.4). The choice of suitable parameters and the resulting plan strongly depend on the planner's experience and provided planning time [14]. Different optimization strategies were suggested in order to eliminate this trial-and-error process and to improve planning efficiency - prioritized and multicriteria optimization (MCO) being examples.

Prioritized optimization

Prioritized optimization describes a stepwise approach of clinical goals [143]. In contrast to the weighted sum approach (one objective function of several objectives), prioritized optimization splits the optimization process into several optimization runs of variable objective functions which are executed sequentially. The achievements of each optimization are turned into constraints such that the successive step cannot degrade prior achievements. The introduction of a so-called slip factor allows for minor violations and thereby enlarges the solution space.
By defining a hierarchy of clinical objectives, dosimetric goals are approached in a systematic manner (for more details see subsection 5.2.1). Prioritized optimization yields the basis for a developed algorithm to reduce delivery time in IMPT, in chapter 5.

Multicriteria optimization (MCO)

Radiotherapy treatment planning is a multiobjective problem (figure 2.4), which motivates the application of multicriteria optimization. Instead of one objective function, MCO optimizes several objective functions simultaneously whose plan solutions combined with a variety of corresponding linear combinations create a plan database of exclusively optimal plans [37]. MCO eliminates the search of penalty factors in the weighted sum approach by supplying a navigation tool which visualizes the inevitable dose trade-offs of correlated goals in real time. By comparing different alternative solutions in the TPS interface the user selects the final dose distribution [125] (further details on MCO see section 3.2).
The merits of MCO were demonstrated in terms of shorter planning times and superior plan quality for a number of entities in the past [39] and are further motivated by an executed planning study on lung cancer comparing MCO to non-MCO planning in section 3.3.

Optimization algorithms

IMRT treatment plan optimization is conducted by deterministic optimization algorithms, i.e. gradient based methods, or stochastic algorithms such as simulated annealing and genetic algorithms. For details, refer to e.g. [14, 21].

Dose calculation in photon and proton RT

CT Hounsfield units (HU) represent the physical properties of the traversed matter, which determine the dose deposition. Dose calculation algorithms utilize so-called look-up tables (LUT), conversion tables, which assign each voxel the underlying electron density (photons) or relative stopping power (protons), as the basic input for the dose calculation [115, 118] (see section 2.1). Different dose algorithms are implented in TPSs, pencil beam algorithms and Monte Carlo simulations representing widely applied examples (see literature for details, e.g. [7, 20, 3]).

2.3.2 Plan evaluation by DVH criteria

Dose volume histograms (DVH) present an effective and widely used tool to quantitatively assess plan quality [43]. Cumulative DVHs[10] depict the absolute or fractional integral volume of a selective structure which receives at least a certain dose (see figure 2.5). All curves of the DVH start at 100% of the volume receiving at least 0 Gy and end in their maximum doses.

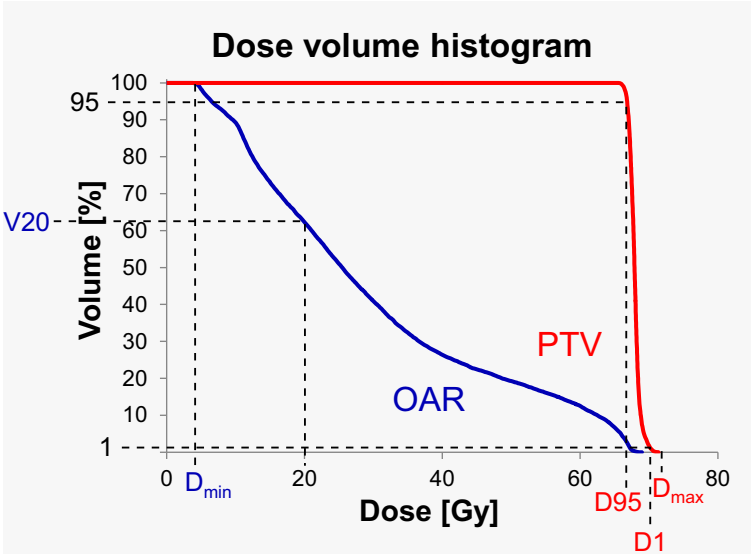

Figure 2.5: Exemplary dose volume histograms of one PTV (red) and one OAR (blue); typical utilized dose points to characterize the corresponding 3D dose distributions are illustrated.

Treatment plans are evaluated by PTV-coverage and dose homogeneity within the PTV, by normal tissue sparing and PTV-conformity (dose fall-off outside the PTV), and by dose criteria to OARs which are driven by associated tolerance doses. The limiting OAR criteria are determined by the tissue functionality; typically serial

[10]Dose volume relations can also be visualized by differential DVHs for which column heights represent the volume receiving the corresponding dose; differential DVH are less established in clinical practice.

and parallel working organs are distinguished, the spinal cord and lung being corresponding examples[11] [70]. For the first one maximum doses are the most critical, for the latter mean doses or other DVH points are of relevance.
Instead of absolute dose maxima and minima, which may refer to a single voxel and be less important in real clinical settings (due to variations in set-up and motion etc.), doses to larger volume fractions are analyzed, e.g. to 1% (D1: maximum to 1% of the volume) or to 1 cm^3 of the structure; minimum dose can be specified e.g. by D99, minimal dose received by 99% of the volume. Criteria can also be expressed by volumes such as V20, i.e. the volume, which receives at least/more than 20 Gy, a relevant measure for the functionality of the lung. Different indices quantify the plan qualities with regards to PTV coverage, homogeneity and conformity; a variety of definitions were previously suggested [83, 52]. Within this work, the following indices were utilized (with V95, the absolute volume in cm^3 receiving 95% of the prescribed dose and normal tissue referring to the patient contour excluding the PTV):

Coverage index:

$$CovI = \frac{V95(PTV)}{V(PTV)} \tag{2.9}$$

Conformity index:

$$ConI = 1 + \frac{V95(normal\ tissue)}{V95(PTV)} \tag{2.10}$$

The values of ConI should be interpreted carefully, and only in combination with PTV coverage to prevent from any false positive conclusions as ConI receives the best value if the PTV is not completely covered. The homogeneity within the PTV can be assessed by the standard deviation σ(PTV) (equation 2.11). Compared to most homogeneity indices, which typically measure the deviation of D_{max} and D_{min} to D_{mean}, σ(PTV) includes every voxel i of the PTV and therefore allows for a better evaluation of the spatial 3D dose distribution.

$$\sigma = \sqrt{\frac{1}{N_{PTV}} \sum_{i=1}^{N_{PTV}} (D_i - D_{mean})^2} \tag{2.11}$$

DVHs and the presented criteria, however, do not capture the whole 3D dose distribution completely and particularly do not yield any information on corresponding localizations. In clinical settings a visual analysis of the 3D dose distribution is inevitable and is typically visualized by isodose lines (lines of the same dose levels).

[11] Due to organs' complexity combinations of both types exist.

2.3.3 The trade-off between dosimetric quality and delivery time

IMRT generates improved dose distributions compared to 3D-CRT but at the same time IMRT plans require a larger number of monitor units leading to increased delivery times [92, 33, 38]. The complexity of the fluence maps frequently determines the plan quality but simultaneously impacts delivery times due to the required MLC motion to deliver the pattern [92, 75, 40]. Treatment plans of especially, highly modulated intensity, e.g. of complex cases, result in long treatment times [38, 144]. Similar issues are observed in IMPT however entangled to specific facility properties (see chapter 5).
The correlation between plan quality, its complexity and treatment time can be illustrated on a simpler level by regarding the number of beams. The application of more beam directions can improve dose conformity in 3D-CRT as well as in IMRT (with an upper limit for additional benefits [16]), while each additional field prolongs the treatment.

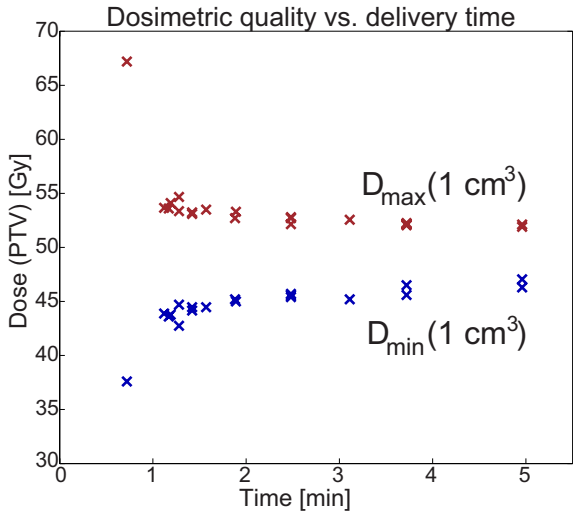

Figure 2.6: Trade-off between treatment time and dosimetric quality: presented are $D_{min}(1\ cm^3)$ and $D_{max}(1\ cm^3)$ of the PTV, at a constant $\overline{D}_{max} = 19.9$ Gy $\pm$ 0.2 Gy, dependent on the treatment time for VMAT plans (realized by varying the number of available arcs for the optimization).

Figure 2.6 demonstrates the correlation between plan quality and delivery time on the basis of VMAT plans, which were calculated in the Eclipse TPS[12] for an exemplary head and neck cancer patient. 20 plans of different "time-quality-trade-offs" were optimized with varying number of rotations (and partial rotations) - all other variable geometry settings (e.g. collimator angle) were identical. For the given machines[13], which featured a constant gantry rotation speed the delivery time was

[12]Varian Medical Systems Inc., Palo Alto, CA
[13]Linear accelerator, Varian Medical Systems

exclusively determined by the number of arcs. Keeping the maximum dose to the spinal cord at a constant level ($\overline{D}_{\max}$= 19.9 Gy ± 0.2 Gy), the plan quality mainly varried in obtained PTV criteria. The derived DVH points demonstrate the decreasing plan quality with reduced delivery time and moreover the tendency to saturation above a certain number of arcs. With respect to this example it should be noted that the utilized optimization algorithm is based on a weighted sum approach and does not necessarily result in optimal plans which explains the presence of different plan qualities with the same RT times.

3 Improving efficiency and dosimetric quality of treatment planning

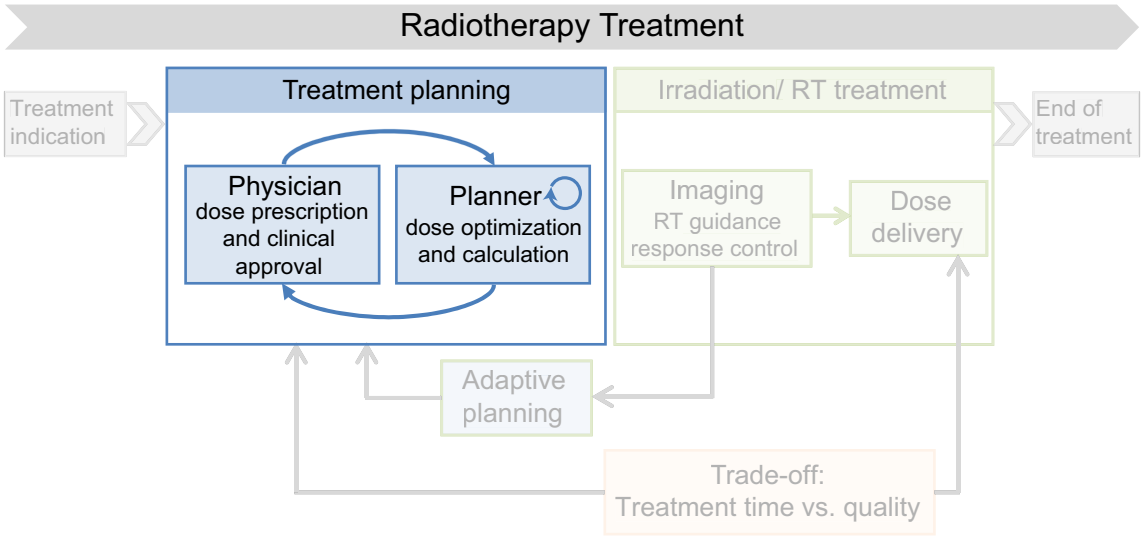

Figure 3.1: Efficiency and quality in radiotherapy, focusing on treatment planning.

The creation of radiotherapy (RT) treatment plans prescribes the process of finding the best plan for every individual patient. Physicians formulate dose prescriptions and potential limitations to OARs, and planners define optimization parameters in the treatment planning system (TPS) in order to achieve a dose distribution which fulfills physicians' prescriptions. The planning routine should be efficient, consistent between planners, reproducible for similar cases, and yield optimal dose distributions tailored to every individual situation.

This chapter breaks the treatment planning process down into two core components: (1) the actual optimization process and (2) the communication between planners and physicians (figure 3.1). Both are frequently not efficient and do not always lead to the best plan for every individual patient.
The first part of the chapter demonstrates the potential of multi criteria optimization (MCO) plannning as an alternative to regular IMRT planning in a treatment planning study (already published by Kamran, Müller et al. [66], see section 3.3). The second part of the chapter (section 3.4) suggests a novel planning approach, referred to as "physician driven planning", with template-based MCO planning as a fundamental part of the process. Its feasibility is demonstrated in a pilot study.

Parts of this work were submitted for publication by the author. Both presented studies were conducted at Massachusetts General Hospital (MGH).
The concept of MCO, as the essential optimizaton technique, utilized in both studies is introduced beforehand after a more precise explanation of the above concerns in the clinical practice of treatment planning.
The prescribed MCO-TPS refers to the MCO module of RayStation[1].

3.1 Concerns of clinical planning practice

The creation of a radiotherapy treatment plan is a stepwise process involving a diverse mix of staff. In clinical practice treatment plans are usually calculated by dosimetrists or medical physicists, translating written clinical prescriptions into dose distributions. The generation of "the best plan" is a subjective process: different planners may come up with different dose distributions to suggest to physicians for treatment approval, and the preferred dosimetric trade-offs vary between physicians. When plans are presented to physicians, they are either accepted as they fulfill all specified criteria or rejected in case the physician wishes for a different dosimetric trade-off. Both scenarios may be sub-optimal: in case of an acceptable plan it will remain unclear if a different dose distribution may have existed, which still fulfilled all requirements and may be preferred by the clinician; the second scenario can lead to an inefficient iterative adjustment of optimization settings according to physicians' instructions - at a certain point this might result in the first scenario.

The adjustment of optimization parameters in conventional inverse planning additionally faces the difficulty of finding penalty factors for each objective, the summands of a single objective function, in order to steer the dose distribution in the intended direction (see subsection 2.3.1). Planners do not know whether an additional change of parameters might further improve the distributions or not. Plans are frequently accepted even though they may not be optimal.

A general concern in the current planning practice is the dependency of the resulting plan quality and planning time on planners' experiences and the inconsistency in utilized helper structures and optimization parameters between planners. Attempts to standardize the process by automatic planning and finding class solutions have been reported before [146, 94, 93, 136, 145, 87, 64]; As the clinical realization is challenging, especially in conventional IMRT planning, standardized planning has not found the way to clinical practice yet.

In the search for the best treatment plan, the choice of TPS plays an essential role. MCO avoids the prescribed trial-and-error process by visualizing inherent trade-offs via an integrated interactive navigation tool. The superiority of MCO compared to regular inverse planning was demonstrated before in both planning time and

[1]RaySearch Laboratories, Stockholm, Sweden, version 4.0

plan quality for a number of tumor sites [69, 138, 39]. But also in MCO planning, concerns like the influence of planning experience and correlated inconsistency as well as the challenges in communication between physicians and planners remain in clinical practice.

3.2 Multicriteria optimization treatment planning

The basic concept and advantages of MCO

Multi criteria optimization (MCO) generally describes a method used to approach optimization problems of interdependent objectives, i.e. of problems which do not have a single solution but require compromises. These compromises are described mathematically on so-called Pareto fronts, i.e. multidimensional surfaces of obtained objectives. Radiotherapy treatment plan optimization is a multiobjective problem which leads to inevitable dosimetric trade-offs. MCO treatment planning avoids the trial-and-error process of regular inverse planning by optimizing all specified objectives seperately to their optimums. It allows the user to experience dosimetric trade-offs between specified objectives by interactive surface navigation [37]. The planner can change objectives, similarly explore the resulting expenses to other objectives and to search the preferred compromise. The selected plan is guaranteed to be optimal such that no objective can be improved without worsening another.

MCO-planning and optimization formulations

MCO-planning comprises three steps: the database generation, subsequent plan navigation and the final plan creation. The database is calculated by optimizing various weighted sums of treatment objectives according to prior defined optimization parameters (constraints and objectives). While constraints are fulfilled in all plans, objectives are negotiable and are the basis for consecutive plan navigation. The database consists of anchor plans, i.e. plans which are fully optimized in one objective function, and of auxiliary plans, i.e. random linear combinations of anchor plans. For n objectives at least n+1 plans are calculated [39]. The surface approximated by these plans is known as the above mentioned Pareto surface of optimal plans.

Each treatment objective is represented by a slider in the interface of the TPS (figure 3.2). It improves the corresponding objective function and updates the dose distribution in real time when moved by interpolating between pre-computed database plans. Sliders can be locked by checking the box beside them such that subsequent navigations occur without worsening the locked sliders/objectives.
After navigation, plans are finalized by aperture creation (MLC sequencing) and the final dose calculation. The sequencing process may lead to undesired dose differences between the navigated plan choice and the final deliverable plan. The MCO plans presented here were exclusively calculated in RayStation TPSs at MGH.

In the clinically implemented and commercial TPS version[2] surface navigation was performed on fluence maps. Additionally planning was performed in a research software version, which allowed navigation on a surface of deliverable plans and potentially reduces dose deviations between navigated and final plan [47].

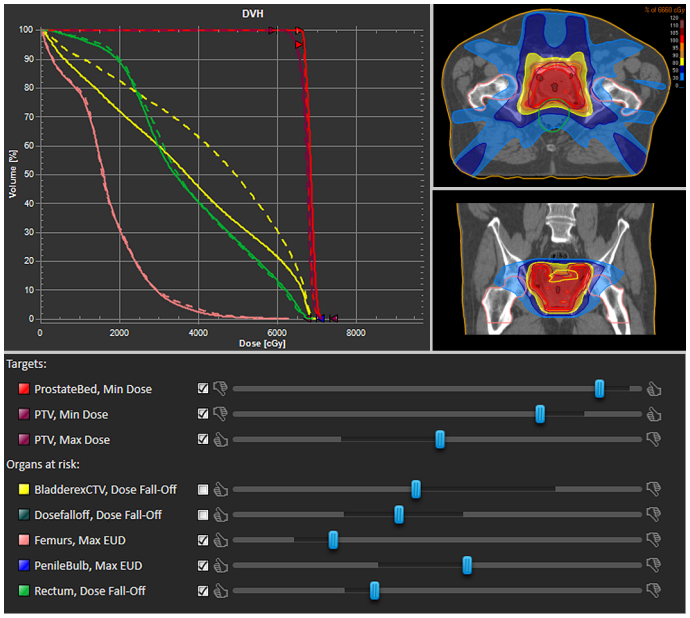

Figure 3.2: Interface components of MCO-plan navigation: dose distributions are adjusted in real time by moving the sliders of different structures. The dosimetric changes are also visualized in the dose volume histogram: current (straight line) and previous (dashed line) dose.

Choice of MCO parameters

The choice of optimization parameters requires some considerations. The **number of database plans** determines the accuracy of the Pareto surface approximation. The more objectives are defined, the greater the number of required plans for an accurate approximation (exponential increase) [36]. A larger database however comes with an increased computational expense, which demands a compromise between accuracy and computational effort. Craft and Bortfeld [36, 35] analyzed the approximation accuracy, dependent on the number of database plans in previous studies.
With regards to **optimization criteria**, a larger number of **objectives** allows the user to steer the dose more precisely but may lead to a less clear interface. **Constraints** are utilized for non-negotiable criteria. They facilitate the process by forbidding certain solutions and guarantee that the calculated plans present realistic solutions. Similarly, constraints reduce the space of solutions.

[2]during the conduction of the studies, fall 2014

3.3 Multicriteria optimization for non-small cell lung cancer

3.3.1 Intention of the MCO vs. non-MCO planning study

The efficiency of MCO in both planning time and quality was demonstrated in previos studies for distinctive entities; the benefit for non-small cell lung cancer (NSCLC) however was not investigated before. As thoracic cancer patients are often subject to severe toxicities, even in highly conformal IMRT treatments [73, 63, 9], patients presumably profit from reduced doses to OARs; especially to the esophagus; esophagitis being a severe problem in chemoradiation therapy.
The performed planning study analyzed the benefit of MCO for NSCLC by comparing MCO-IMRT to non-MCO-IMRT plans with respect to dosimetric quality, in particularly with regards to esophagus sparing, and required planning time.
The plans were optimized according to guideline specified goals. Special focus was set on the contralateral esophagus which was optimized by the recently suggested esophagus sparing technique [4].
Utilizing IMRT with identical machine parameters and beam geometries, identical dose distributions are generally obtainable. The way and effort to achieve satisfactory dose distributions may differ though. MCO planning by Pareto surface navigation shows the planner interactively the space of options, which may guide the planner in a more straightforward manner into the intended direction. Therefore resulting dose distributions may vary and thus not only depend on the applied RT technique and geometries but further on the utilized optimization method.

3.3.2 Material and methods

Patient characteristics and prescription guidelines

Ten locally advanced NSCLC patients were selected out of the clinical database of MGH. Patients were eligible for RTOG 1308 trial[3] and were previously treated with IMRT to a median dose of 70 Gy within chemoradiotherapy.
All patients featured a gross tumor volume (GTV) within 1 cm of the esophagus. The contouring process was performed on the basis of 4D-CT data sets. Structures were delineated according to protocol (see supplements in [66]). The contralateral esophagus (CE) was contoured as an additional supportive planning structure in order to improve esophagus sparing. The prescribed dose was 70 Gy (35 x 2 Gy) to the PTV (CTV + 5 mm); the CTV was an 8 mm expansion of the motion corrected GTV (excluding nearby OARs as esophagus or heart).

[3]RTOG 1308 is an ongoing randomized trial, comparing photon (3D-CRT and IMRT) to proton RT (both: 70 Gy (RBE)) as part of chemoradiation therapy for locally advanced inoparable NSCL patients (www.rtog.org).

Retrospective planning

The retrospective planning was performed by two dosimetrists with the planning system RayStation (RaySearch Laboratories, v4.0.3). The treatment planning system consisted of two alternative optimization modules, a conventional IMRT-approach (non-MCO) and MCO. Each dosimetrist calculated five MCO-optimized and five non-MCO plans for different patients. Identical planning conditions were guaranteed at the initiation of planning for both plans types. Dosimetrists were provided with the CT data and structure set of the anonymized patient, not containing any type of intermediate (supportive planning) structures. All geometrical planning parameters such as five beam directions were agreed upon together before planning.
Treatment objectives were directed by the RTOG guidelines (see supplements in [66]). In MCO planning (see section 3.2), optimization objectives were defined for all target structures and OARs, each of them represented by a slider to steer corresponding trade-offs; constraints were assigned for definite required DVH criteria.
The planning process was finished with the plan approval by two physicians, i.e. all plans had to be acceptable for treatment.

Evaluation criteria

Dosimetric differences were analyzed by several relevant (RTOG-specific) DVH points and statistically evaluated with the Wilcoxon Signed Rank test[4]. RTOG guidelines classify minor and major deviations of DVH criteria from the protocol values. The number of deviations was noted for each plan.
Plans were ranked by physician preference in a blinded plan comparison.
Active planning times were recorded for both optimization types with a maximum planning time of four hours. Time required to calculate the database for MCO planning was noted seperately but was not included. The timer was stopped in case of any planning interruptions. Times of physician involvements, e.g. for assistance and instructions in case of compatible objectives, as well as the required times for plan reviews, were noted.

3.3.3 Results

Dosimetric results

All plans resulted in satisfactory target coverages. While the CTV coverage was similar, the PTV coverage was superior in non-MCO plans (figure 3.3, left). Doses to OARs were smaller in MCO compared to non-MCO plans (selective DVH criteria see figure 3.3, center and right). In particular the irradiated volumes of the heart (V30 and V40) and lung were significantly smaller in MCO-plans. Dose distributions of an exemplary patient visualize these differences in figure 3.4. The maximum dose for

[4]statistical hypothesis test to prove that the medians of two paired samples are (not) equal;

the spinal cord was comparable. With regards to esophagus sparing, the evaluated DVH points of CE and esopohagus showed trends of better sparing in MCO, with significant improvements of V45(CE) and V60(esophagus).
Minor deviations from the protocol were found for both plan types. For five out of the ten patients the non-MCO plans showed a larger number of deviations, for two patients MCO plans resulted in more deviation and for three patients an equal number of deviations was noted.

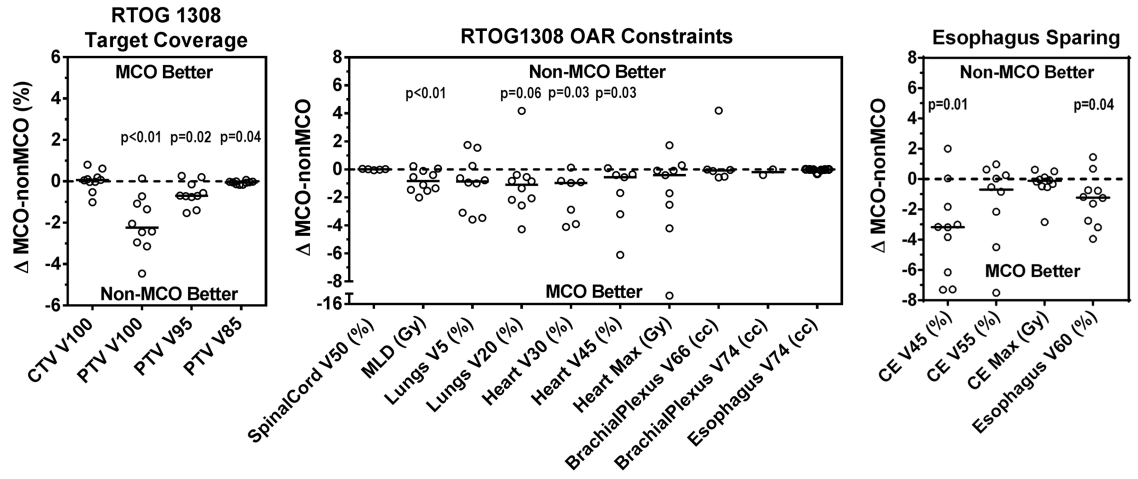

Figure 3.3: DVH criteria of MCO versus non-MCO plans, adapted from [66].

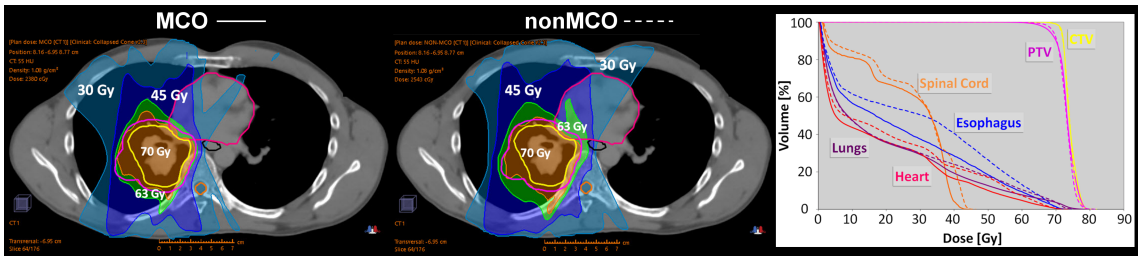

Figure 3.4: Dose distributions of the MCO and non-MCO plan of an examplary patient, adapted from [66].

Physician preference

Physicians rating was eight times in favor of the MCO plans versus two times of the non-MCO versions. These decisions were mainly led by lower doses to OARs. The non-MCO plan selections showed superior esophagus sparing; one of them was additionally superior with respect to skin dose and the other one in the maximum dose to the spinal cord.

Planning times

Active dosimetrist planning times differed significantly between the two optimization methods. The average planning time for MCO was 107 minutes and for non-MCO 193 minutes. Required planning times depended on the cases and varied between 52 to 175 minutes for MCO and 120 to 235 minutes for non-MCO. Times of physician involvement for plan guidance and for plan reviews hardly differed.

3.3.4 Discussion and conclusion

The performed study demonstrated the advantages of MCO-IMRT planning in locally advanced NSCLC with regards to planning time and plan quality. Doses to heart, lung and esophagus were reduced in MCO plans versus non-MCO plans, however, at a compromise in PTV coverage of high doses. CTV coverage was similar for both plan types. The blinded plan comparison results indicated the gain in OAR sparing being greater than the compromise in PTV coverage. Physicians clearly preferred MCO generated to non-MCO plans (8:2).
It should be noted that both optimization techniques achieved high plan qualities; only minor deviations from RTOG 1308 guidelines were noted. Deciding on the preferred plan was challenging in some cases, e.g. when plans differed in dosimetric trade-offs, i.e. each type was superior at different criteria. Decisions were presumably made by weighing associated clinical relevances and the magnitude of differences between corresponding criteria of both plans.

Both plans were generated with the same irradiation technique (IMRT) and beam geometries. Therefore identical dose distributions were generally obtainable. Thus the question of in which time high plan qualities were achieved by each method and presumably if the same qualities were derived in practice was of primary importance. Non-MCO planning is subject to a trial-and-error process of trying different weighting factors for every optimization objective in order to iteratively improve the dose distribution. The planner is not aware of all dosimetric options and accepts the plan at the point when she/he believes no further improvements are obtainable or due to time constraints. This may lead to non-optimal plans, and moreover to strong dependencies of plan qualities and planning times on planners' experience: experienced planner learned to estimate the potential of additional parameter adjustments, while non-experienced planner typically require more time until noticing that dose distributions are not further imrovable or stop trying too early. By Pareto surface navigation, MCO planning shows the planner the inherent dosimetric trade-offs and makes planning more intuitive such that high plan qualities can be achieved faster, which was confirmed by the recorded planning times. MCO planning times were, on average, 88 minutes shorter than non-MCO times. The superiority in planning time was shown for different entitities before, e.g. for glioblastomas, planning times were reduced from 135 to 12 minutes [39] and for head and neck cancers, from 205 to 43 minutes [69].

Potential bias in the plan quality given by different planning experiences with one or the other optimization technique is assumed to be comparably small. The overall planning experience was longer in non-MCO as MCO planning was only introduced a couple of years ago. Currently, clinical planning is however exclusively performed by MCO, which may be of advantage with regards to current practice. Bias due to different dosimetrists' experiences between the two dosimetrist was eliminated by splitting the plan types between both such that each contributed 50% of the plans for each optimization type.
As the DVH differences and number of patients were comparably small, conducting further studies could strengthen the found results and drawn conclusions in the future.

Conclusion on MCO versus non-MCO planning

It was demonstrated that MCO planning was superior to non-MCO for NSCLC in both planning time and OAR sparing. Even though dose differences were rather small, MCO significantly reduced doses to the heart, lung and esophagus. The more intuitive optimization approach made MCO planning remarkably faster compared to regular IMRT planning.

3.4 Physician driven planning with MCO - deriving the best plan for every individual patient

3.4.1 Motivating physician driven planning

In clinical practice treatment plans are typically calculated by dosimetrists or medical physicists, translating written clinical prescriptions into dose distributions. As the treatment plan optimization is a multicriterial problem it leads to inevitable trade-offs between targets and OARs such that not all clinical goals can always be fulfilled [138]. The situation might not be obvious before the initiation of planning and thus might not be addressed in the prescription. Often clinical decisions have to be made during planning as they arise. Planners spend much time trying to find a compromise between the different clinical goals which might not be the trade-offs most preferred by the physician.
When plans are presented to the physicians for clinical approval, it is often the first time the physician has the opportunity to review the dose distribution and many intermediate decision points with minimal or no physician input may have been made. Many physicians accept the initial presented plan that typically fulfills the prescribed dosimetric goals but may not represent the most suitable trade-off between different objectives, and may in fact, be a sub-optimal plan.

MCO planning software visualizes those dosimetric conflicts and allows physicians to interactively investigate the trade-offs (as discussed before). Moreover compared to regular iterative planning it guarantees fully optimized plans (see section 3.2). These advantages make MCO particularly suitable for physician driven planning.
One approach that may improve treatment planning, both in achieving the desired dosimetric goals of the treating doctor and in increasing efficiency, is to involve the physician at an earlier stage of the planning procedure. Physician driven planning by utilizing MCO treatment planning software can avoid the "human iteration loop" between physicians and planners. It gives physicians the control over trade-offs which may reduce planning time and tailor the treatment plans to the individual patient. The overall goal of the following work was to test if MCO actually holds this promise that has been made from the very early stages of MCO development.

In addition to the interaction between physicians and planners for clinical decisions, the actual planning is frequently inefficient. Planning is often a trial and error process, with the quality of the final plan dependent on the skill of the planner. Planners use different helper structures and parameters based on experience and knowledge. Many attempts to standardize treatment planning and improve its consistency by finding class solutions and using knowledge based planning have been reported [146, 94, 93, 136, 145, 87, 64]. Template based planning was additionally tested as suitable basis for MCO planning.

The feasibility of physician driven planning utilizing template based optimization and physician plan navigation as a suitable planning procedure is demonstrated by comparing clinically delivered plans, created by dosimetrists, to plans that physicians interactively navigated (figure 3.5). The long term objective of this approach is to increase planning efficiency and allow physicians to more naturally express their clinical intentions.

3.4.2 Material and methods

The study is based on data of 12 central nervous system (CNS) and 10 prostate cancer patients previously treated with IMRT at MGH and picked randomly out of the clinical database.
For each case, both the clinical and the physician driven plan were formed using the MCO module of the clinical TPS RayStation (version 4.0, Stockholm, Sweden). A systematic scheme of the planning procedure and the main differences in the two different planning processes are summarized in figure 3.5.

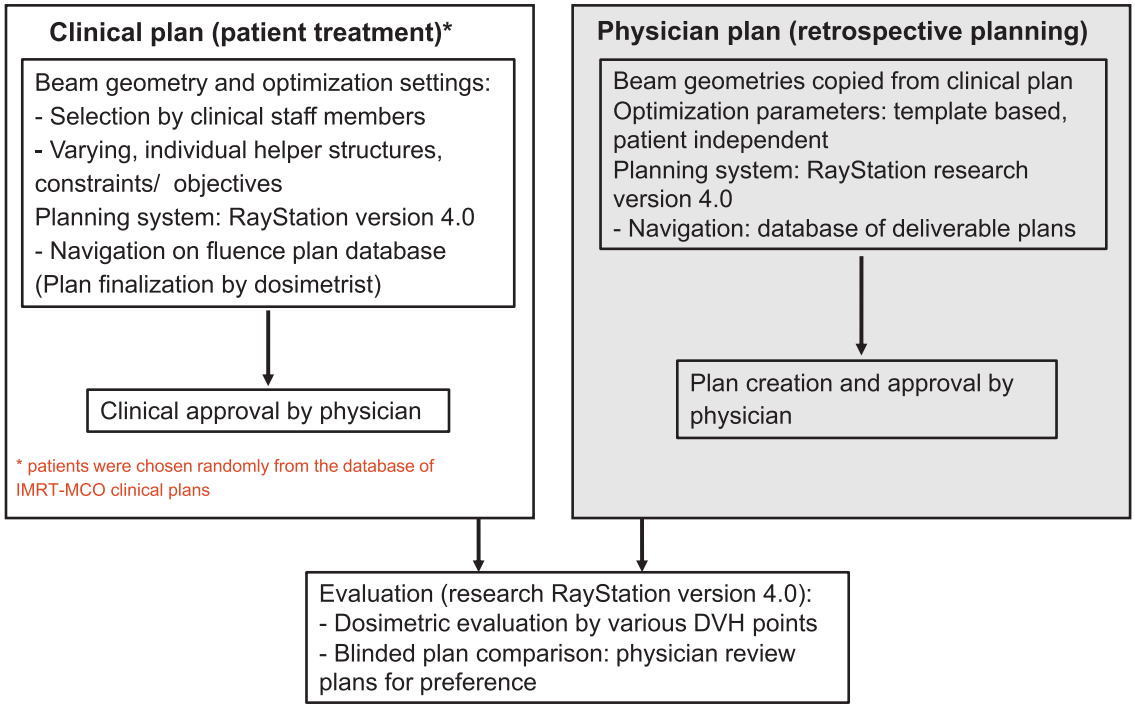

Figure 3.5: Physician driven planning study workflow.

Structure definition

CNS: The patients featured a variety of diagnoses and intracranial anatomical sites (e.g. glioblastoma, meningioma). The gross tumor volume (GTV) was defined based on integrated CT and magnetic resonance imaging from preoperative and postoperative studies. Clinical target volumes (CTV) were created to encompass additional regions of potential microscopic involvement. Prescriptions to the PTV (CTV+3 mm) ranged from 36 Gy (12 x 3 Gy) to 60 Gy (30 x 2 Gy). Standard OARs defined for all cases included the brainstem, chiasm, optic nerves, eyes, lenses, lacrimal glands, and cochleas. The desired dose constraints to each OAR varied depending upon the lowest feasible, reasonable dose based upon the tumor location and necessary dose to be clinically beneficial.
Prostate: All cases had undergone radical prostatectomy and were receiving postoperative radiation therapy. The CTV (prostatic fossa), PTV, rectum, bladder (excluding CTV) and femoral heads were contoured for all patients. Small bowel, sigmoid, residual seminal vessels and penile bulb were added, dependent on individual patients' anatomy and clinical situation. The prescribed dose to the PTV (CTV + 8 mm, posterior: + 4 mm) was 66.6 Gy in 37 fractions.

Treatment planning

Clinical plans were generated in the commercial clinically implemented MCO treatment planning system; retrospective physician driven plans, referred to as "physician plans", were created in a research software version (figure 3.5). Whereas plan navigation in the commercial software is based on fluence maps, the research module allows for navigation on segmented plans which decreases dose differences of the final planning step [47] and is therefore supposed to be more suitable for physician driven planning. A sub-goal of this study was to determine how often, if ever, the dose difference between the navigated plan and the deliverable plan was large enough that the physician deemed it necessary to return to the navigation step. With regards to all other planning and dosimetric parameters, including the dose calculation, the planning systems are identical.
The clinically chosen beam settings were also used for retrospective physician planning to assure that all found dose differences between the clinically created and physician plan were the result of user preferences of plan nuances rather than fundamental factors such as beam direction. The prostate plans featured seven beams, the CNS plans between four and seven beams. The clinical plans that served as our baseline comparison plans were made by the clinical dosimetry treatment planning staff. These planners did not know that their plans would be later used in a retrospective comparison study. Thus these plans represent actual production level clinical treatment plans.
At MGH, treatment site specific optimization templates exist and are recommended for use. As planners often change these as they wish, clinically utilized planning helper structures and optimization parameters varied between planners and patients. For the retrospective planning study a database of Pareto optimal plans was created using mostly patient independent but site specific templates (table A.1) in order to test the idea that a template based Pareto-surface creation technique was suitable for physician based MCO planning.
The prostate plans were created using identical parameters for all patients. The number of objectives and sliders varied with existing structures of patients. For CNS cases constraints were adapted to the prescribed dose by linearly scaling the parameter set based on the prescription dose. CNS target parameters were distinguished by the location of GTV and OARs: if targets overlapped with OARs a slider was provided for the GTV, in order to steer dose more precisely in this area, otherwise a hard minimum dose constraint was used. Generally the set of constraints contained loose minimum and maximum doses to prevent extreme under- and overdosage in the target and uncompromising doses to OARs. Appropriate target coverage was obtained by steering the minimum and maximum dose to the prescribed dose. To minimize dose to normal tissue structures the so-called "dose-fall off-function" and the "equivalent uniform dose function" [97] were used. A detailed explanation of the implemented objective functions can be found in [12]. The number of plans to generate the database for both plan types was approx. four times the number of objectives, the maximum number given by the software.

Physician plan navigation

Each patient case was prepared for physicians by prior database calculation according to the above prescriptions. Physicians were provided with the blinded patients, the plan database and patient information (prescription, constraints and history); no access was given to the prior clinically treated plan. Prostate plan navigation (figure 3.2) was conducted with 9 sliders on average (max. 10), CNS with 15 (max. 16).

Evaluation criteria

The final clinical and physician dose distributions were analyzed by several DVH values and compared by their differences (clinical plan minus corresponding physician plan). The CNS dose differences were normalized to the prescribed doses. A statistical evaluation was performed by paired t-tests[5].
Two weeks after planning physicians were asked for their plan preference, for each patient case, in a blinded comparison. Preferences were rated as slightly or significantly different. The option "no preference" referred to equal plan quality.

3.4.3 Results

Dosimetric results

Selective DVH differences and p-values of the assessed quantities for prostate and CNS are presented in figures 3.6 and 3.7, respectively. The majority of evaluated dose criteria did not show significant differences and did not indicate certain trends but were spread around zero, D_{mean} of the femoral heads (figure 3.6) being a typical example. Physician prostate plans showed a better sparing of high dose regions of bladder and rectum, which was also underlined by the significance of V65(rectum) ($p=0.009$) and V65(bladder) ($p=0.003$). The PTV covered by the 98%-isodose was significantly lower (V65 (PTV)=0.007) while the CTV received higher mean doses. One outlier was noticed which did not oblige the trend of higher clinical plan dose but showed a low D95 of the PTV (due to small bowel sparing). Ignoring this plan in the statistical evaluations, this would lead to significance for D95(PTV) with $p<<0.05$ while the trend of all other criteria would be the same.
Physician derived CNS plans indicated a trend to higher doses in the targets and OARs, with a significantly higher maximum dose to the brainstem (D1(brainstem): $p=0.03$). The physician reported that the increased brainstem dose was intentional in order to allow for improved PTV coverage.
Dose distributions of two examples showing clear dosimetric differences, one CNS and one prostate, are shown in figure 3.8.

[5]hypothesis test to prove the difference of two samples;

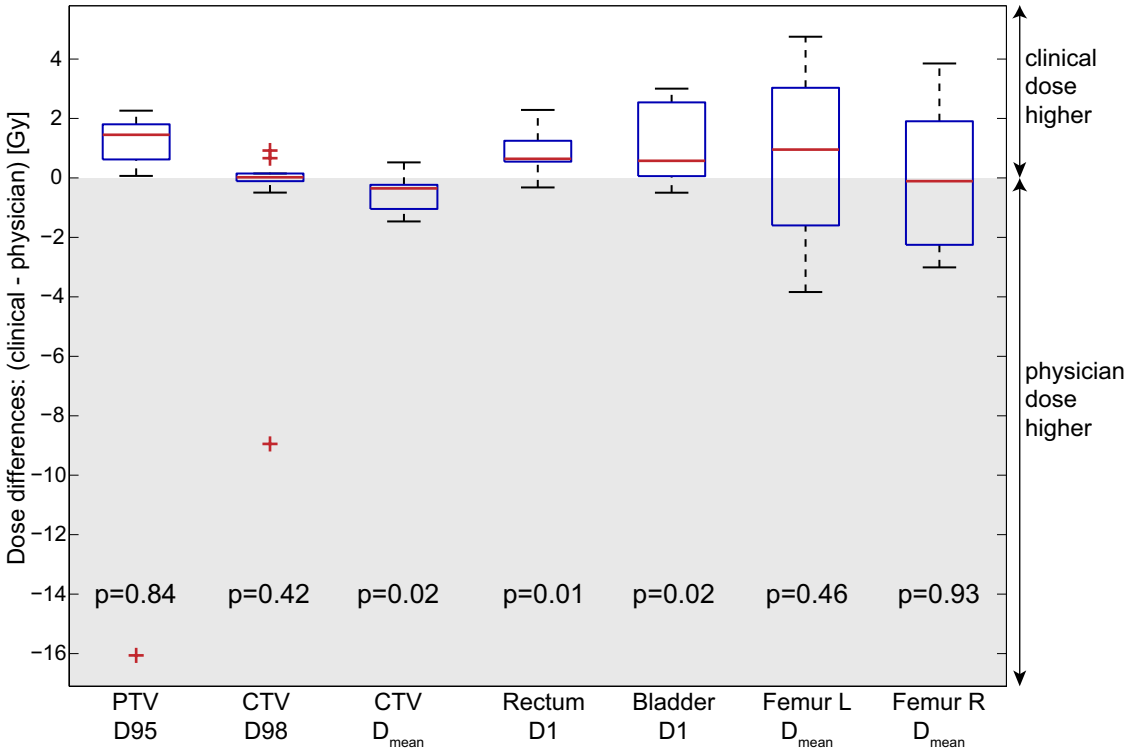

Figure 3.6: Dose differences of prostate plans (clinical minus physician plan), illustrated by boxplots (Box-and-Whisker plots): red marks depict the median differences; edges of the boxes refer to the submedians of corresponding half intervals (25th/75th percentiles). Its height presents the interquartile range, a measure for the spread of middle values. Whiskers (black line intervals) are extended to the most extreme data points, within an interval of 1.5 times the interquartile range; values outside this interval are considered outliers (red crosses). Here (even number of data points), medians are presented by the average of two median values.

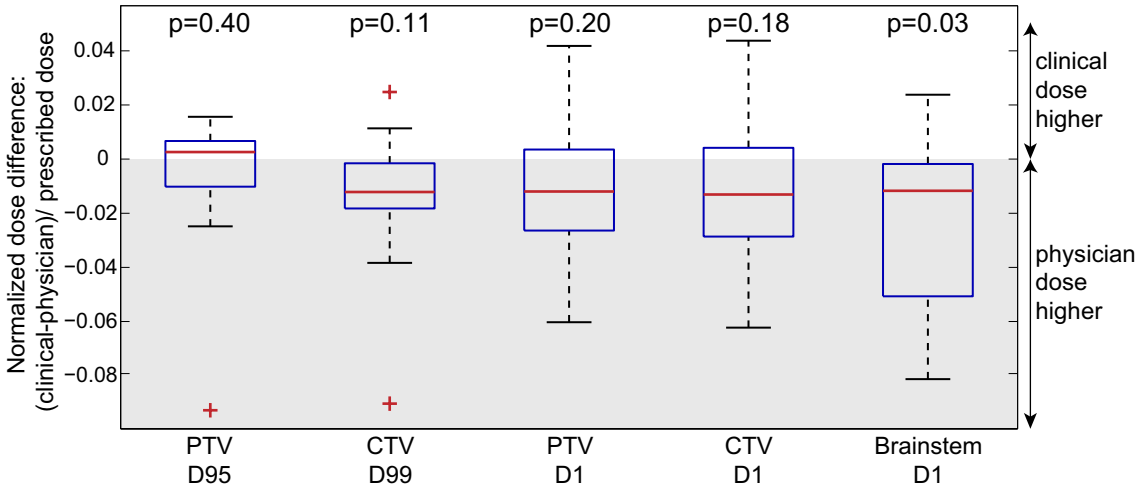

Figure 3.7: Dose differences of CNS plans; DVH values normalized to prescribed doses; remarks: CTV refers to 11 CTVs and one GTV contour; Brainstem statistics based on 11 contours; for further details on boxplots see figure 3.6.

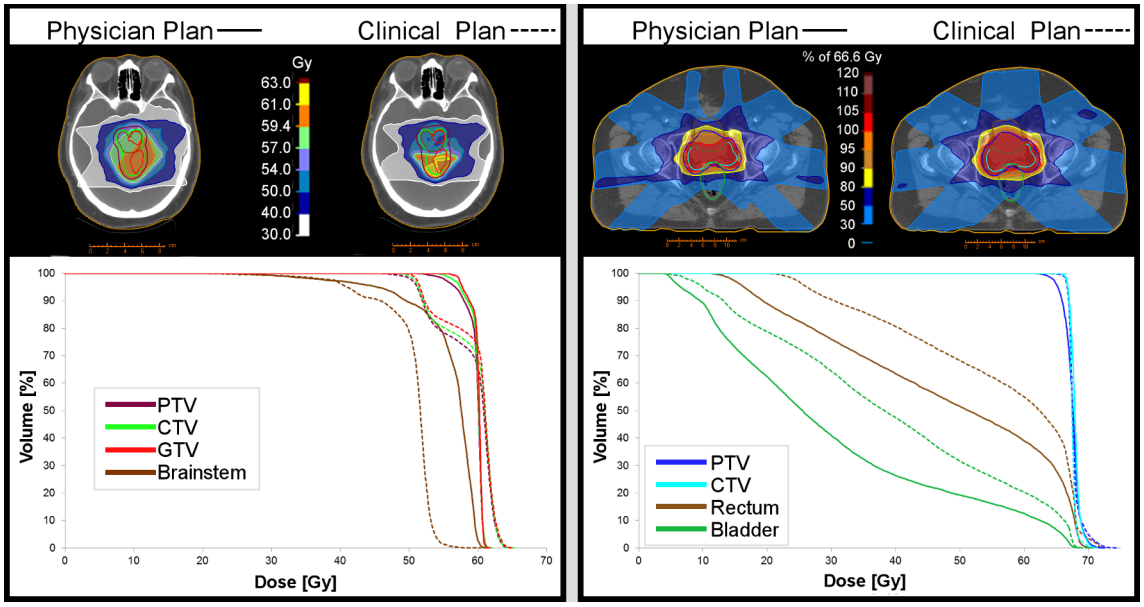

Figure 3.8: Case examples of remarkable differences between clinical and physician planning for CNS and prostate.

Dosimetric trade-offs

The differences between navigated trade-offs of the physician and dosimetrists in prostate plans is emphasized in figure 3.9 (left) by depicting the dependence of V65(bladder and rectum) vs. D95(PTV). The analysis of dosimetric trade-offs for femural heads did not reveal clear compromises to other structures, V40(femural heads) versus V65(rectum) presenting a typical example (figure 3.9, right). While V65(rectum) was lower in physician plans, data points of the femural heads were spread over the whole range for both plan types indicating that no compromise was made at the expense of other OARs but only on PTV coverage (figure 3.9).

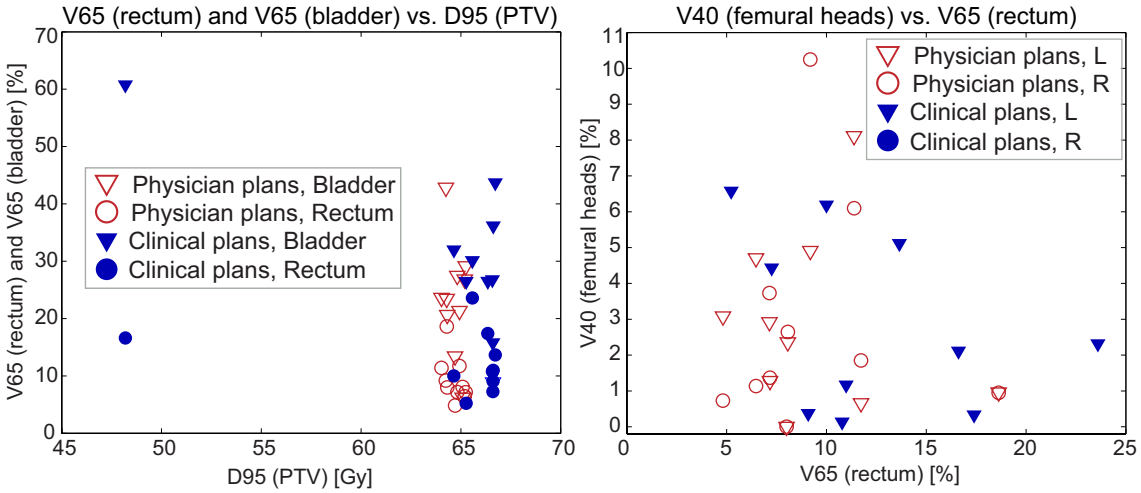

Figure 3.9: Dosimetric trade-offs of selective DVH points (see subfigure titles) for clinical and physician prostate plans; each data point represents the selected trade-off of the corresponding plan; L and R refer to left and right femural heads.

Due to the large number of OARs and different criteria for each of the structures, the search of correlated trade-offs for brain tumor plans was complex. Except for the navigation to higher CTV doses for a cost in increased D1(brainstem), no comprehensive trade-offs over all patients were found but chosen compromises differed between patients (exemplary trade-off plots see figure 3.10). It is notable that although D1(brainstem) was significantly higher in physician plans, D5(brainstem) which was also an important criteria to the physician, did not show any obvious differences to dosimetrists' plans.

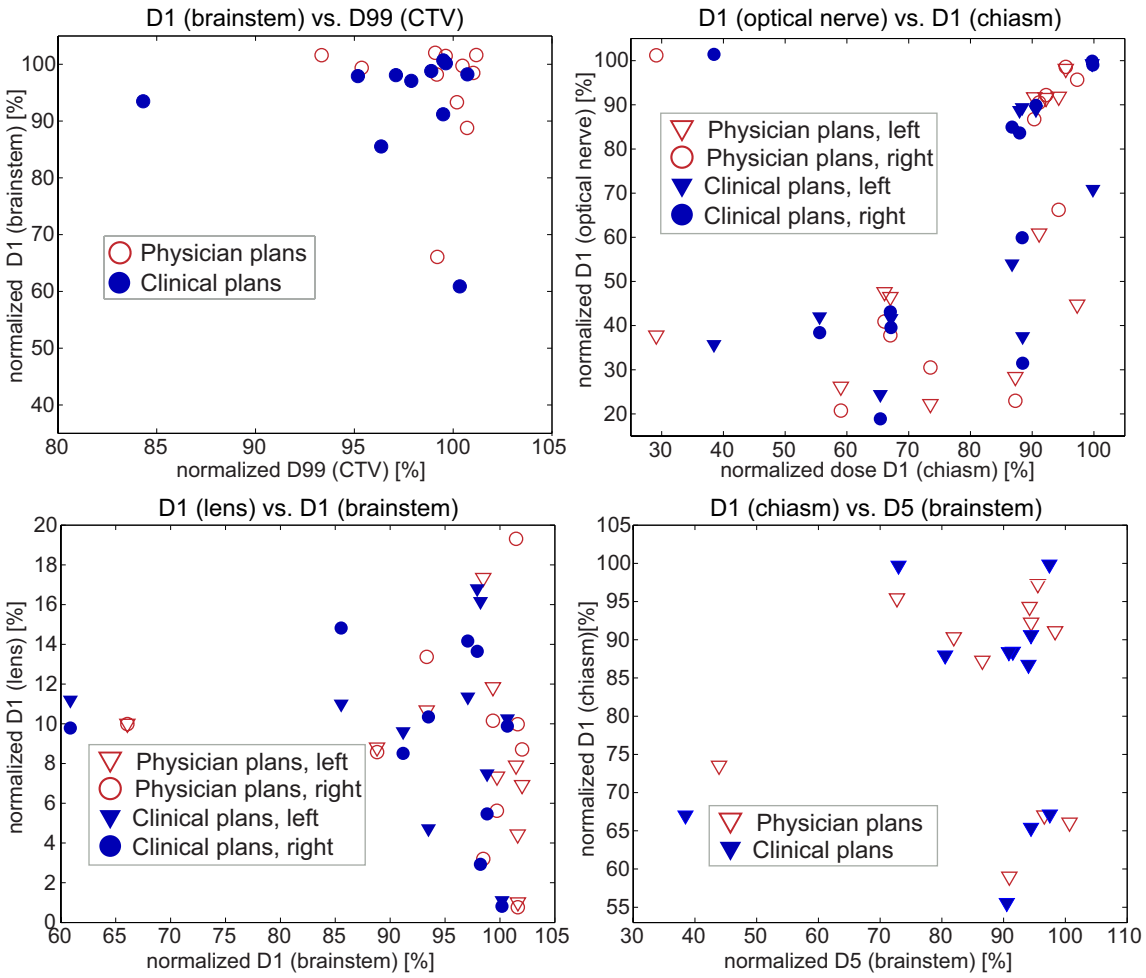

Figure 3.10: Dosimetric trade-offs of selective DVH points (see subfigure titles) for clinical and physician CNS plans; each data point represents the selected trade-off of the corresponding plan. Doses were normalized to the prescribed doses.

Physician preferences

The results of the blinded plan comparisons on physicians' preference are presented in table 3.1. The doctors decided all plans were clinically acceptable but for one CNS case (figure 3.8) the physician would have preferred to go back to planning to try to achieve the average of the presented plans. Prostate plans were rated by two physicians, the actual planner and a non-planning involved doctor. The planner voted 6:2 for the clinical vs the physician plan, the latter 3:5. Both physicians chose equally well twice but on different cases. They had the same preference in five out of ten patients, amongst those, four of the five were rated with the same degree.
An analysis of the dependency of preferences on the time of the plan generation showed that all preferred physician plans were generated in the second half of navigated plans (figure 3.11).

	Brain tumors/ CNS		Prostate planning phys.		Prostate non-planning phys.	
	Preference	Degree	Preference	Degree	Preference	Degree
Physician Plan	3	all slightly	2	1 slightly, 1 significantly	5	3 slightly, 2 significantly
Clinical Plan	6	5 slightly, 1 significantly	6	4 slightly, 2 significantly	3	2 slightly, 1 significantly
None	3	/	2	/	2	/
Total	12	/	10	/	10	/

Table 3.1: Physicians' plan preferences: results of blinded plan comparison

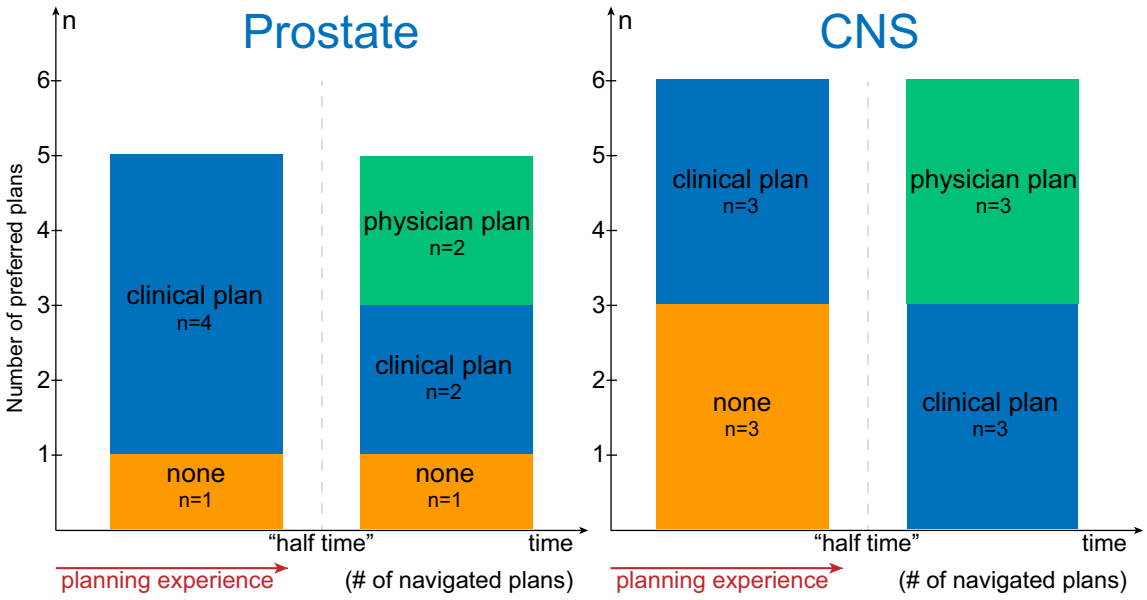

Figure 3.11: Physicians' learning curve: course of preferred plans

Navigation Times

Average physician navigation times were 10 minutes for prostate and 16 minutes for CNS (figure 3.12). Distinguishing average times by the first and second half of navigated plans, times decreased from 13 to 7 minutes (averages over 5 plans) and 17 to 15 minutes (averages over 6 plans) for prostate and CNS respectively, demonstrating that the physicians became more efficient with the software throughout the course of the study.

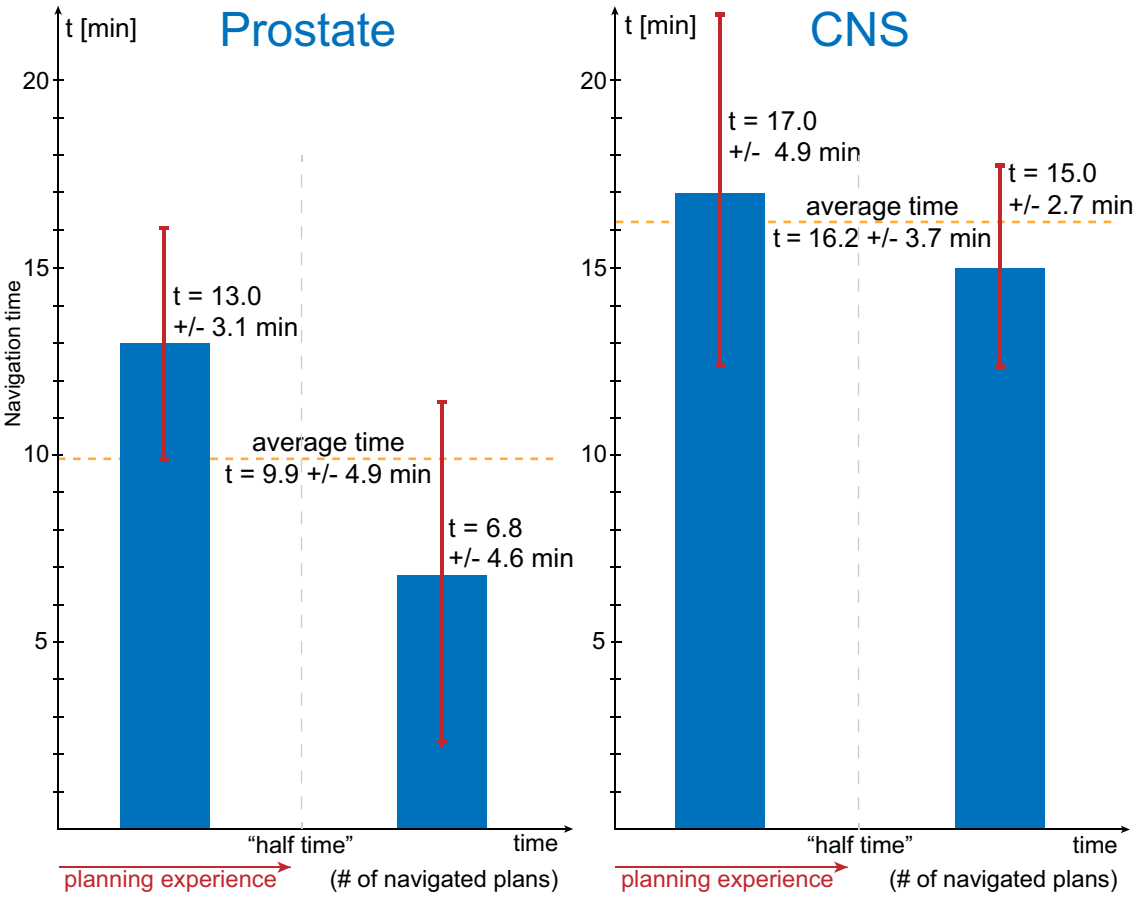

Figure 3.12: Physicians' learning curve: course of navigation times

MCO with deliverable plan navigation

No plans were rejected after the MLC segmentation process, which is attributed to the software improvement of navigating on MLC deliverable plans.

3.4.4 Discussion

Standardization and individualization of RT treatment planning - intention of the study

Our study presented a planning approach with physician navigation as a defining part of the process. While making planning more patient independent by utilizing standardized databases, our approach makes it more individualized for each patient by not following the same standard prescription for everyone but finding the best trade-offs for every individual.
The performed study sought to determine if standardized MCO templates plus physician navigation of the resulting Pareto surfaces could offer a viable alternative to the standard planning process, where tradeoffs are explored by the treatment planners and the physicians are only involved in the final YES/NO decision.

Resulting dosimetric qualities and selected trade-offs

All plans generated by clinicians were of high quality and acceptable for treatment by the physicians, while showing significant differences and trends in some criteria when compared to the physician navigated plans.
Physician prostate plans showed better sparing of high dose bladder and rectum regions for a compromise in PTV coverage. Physicians' CNS plans indicated a trend to be generally hotter, as well in targets as in the brainstem. With regards to all other structures no clear tendencies were observed but trade-offs varried between patients (figures 3.9 and 3.10). It is assumed that trade-offs exhibit randomness when the different alternatives do not make any explicit difference in toxicities or tumor control.

Case dependent benefits

The benefit of physician driven planning regarding plan quality is case dependent and might be greater for more complex cases. Not only in cases of incompatible goals but also when all constraints are achievable simultaneously, physician background knowledge is important in order to decide how best to distribute or escalate the dose. Often plans are approved by physicians if they hit all constraints. However, if aware of the options, different plans might be selected.
Figure 3.8 presents a brain tumor case for which the physician prioritized better target coverage over the hard constraint on the brainstem. This case raises the question of strictness of dose constraint rules, revealing the difference of desired versus compromised trade-offs. While dosimetrists usually respect formulated hard constraints, physicians will not always rigidly adhere to their standard prescriptions when compromises are required. Such trade-offs may be beneficial for some patients and difficult to address in written prescriptions.It should be noted that physician planning might come with an increase in the potential risk of losing sight of a detail or going too high in OAR doses. Planners usually have to justify chosen trade-offs

to the physician which might lead to more conscious/careful planning. In order to prevent any mistakes a second pair of eyes should have to check the plan before treatment[6].

Template based planning: a gain in efficiency

To measure the efficiency gain of this planning process by giving absolute planning times is useful. Times vary with case complexities, planners, and familiarity with the planning system. Here it was not possible to record times for the clinical planning. However by considering the different workflows it is expected that in most cases time can be decreased. Utilizing template (helper) structures and optimization parameters reduced pre-optimization work time. Further, by addressing the clinical trade-off navigations directly to the person who is responsible for these decisions saves time during the planning process: trade-off decisions and plan review can happen in the same session.
The feasibility of template based MCO planning was recently also demonstrated for head and neck cancer planning by Kierkels et al. [69]. Comparing MCO-planning by novice planners to clinical plans (created by trained staff and regular IMRT), it was shown that MCO was superior in efficiency and plan qualities were equivalent. The general high plan quality and the fact that all plans were clinically acceptable leads to the conclusion that template based plan optimization in MCO works.
Compared to non-MCO planning, this is likely due to the MCO concept: variations in patient cases, e.g. of geometry, can be compensated via the sliding process. The overall plan quality did not indicate remarkable difference; plans only differed in the preference of focused structures. Due to MCO treatment planning all plans were fully optimized.

Physicians' experiences, plan preferences and learning processes

Contrary to possible expectations, the blinded comparison showed a preference (not statistically significant) for the clinical plans for both doctors. This may reflect the fact that the treatment planners 1) are very experienced and 2) have had long working relationships with the respective physicians such that they know what each physician desires to see in a plan. In light of these ideas, it is encouraging from the perspectives of increased throughput and increased physician involvement that the plan quality of both treatment planner generated plans and physician generated plans are on par.
Picking a preference between two plan options was difficult. To examine whether the preferences revealed any underlying randomness prostate plans were rated by a second non-planning involved physician. Their plan preferences differed (table 3.1): the planner preferred the clinical plans 6:2 times while the other physician voted 5:3 in favor of the physician plans. Both voted "no preference" twice, however on different cases. The choice of trade-offs was noted to be doctor specific and

[6]Plan control by a second person is obligatory in the US.

depended on personal clinical experiences, i.e. having experienced certain side-effects might lead to a different point of view. This second physician selection experiment highlighted the result from the initial physician selections that the two plans for each patient are generally different but also both perfectly acceptable plans.

In this discussion, it should be considered that dosimetrists were trained on planning for years while each of the participating physicians ended up planning 10 or 12 cases. It is to expect that clinicians will improve their planning abilities with greater experience.
While conducting the study, physicians experienced a learning progress. By observing the physician navigation times, and through informal interviews, it was concluded that doctors will improve their planning abilities over time. After some plans, each physician developed specific strategies of how to approach their preferred trade-offs reflected by an increase in preferred plans in the plan comparison and faster navigations (figures 3.12 and 3.11). Physicians found the use of "clinical goals" (a TPS implementation), which visualize fulfilled and violated dose criteria through different colors, helpful.
Due to the ongoing learning process throughout the study, a final conclusion on physicians' dose preferences might be too early and would require a planning study with more physicians at a later stage of MCO-training. This feasibility study was performed with minimally trained physicians to prove that physicians can quickly learn plan navigation.
Further improvements are expected by adapting objective functions and structures, represented by the sliders, to physicians' needs instead of dictating them.

General difficulties in the selection of (MCO) optimization parameters

Generally the choice of optimization parameters is crucial. To reduce the sliders to a minimal required number, i.e. the reduction of redundant objectives, should be a general MCO-planning goal. First, in order to have a clear interface and second, the more objectives, i.e. number of sliders, the more plans have to be calculated in the database to approximate the Pareto surface accurately. As the maximal number of plans is limited by the TPS, the higher the number of objectives, the less accurate is the approximation. Within the study each structure was presented by only one slider. For tumor sites with a lot of surrounding structures of risks, like CNS, this lead to already 15 sliders on average. The high number of objectives is hard to control and time consuming as the navigation times for CNS compared to prostate demonstrated.

A further challenge is the choice of objective functions and structures: each objective is optimized by a function chosen prior to the Pareto plan calculation. Translating physicians' desires for each organ by one slider is challenging and probably not even possible, given that judging the dose distribution on even a single organ is a multi-dimensional task (discussed in [39]). In general it is difficult to steer three

dimensional dose distributions by using one criterion, e.g. trying to get rid of a hot spot at a certain position might reduce dose of that structure at a different location simultaneously.
One possibility is that for one slider to take on different roles depending on the planners immediate goals (maximum, minimum, some other DVH points) as well as allowing the control of the dose with respect to location. This type of flexible slider is a design and implementation challenge however. Generally there is still room for improvements with regards to objective functions in radiotherapy treatment plan optimization. Objective functions that allow for a more accurate and specific steering and control of the doses could improve any type of planning technique in the future.

Suggestions for a future planning routine

This study may serve as a basis for a discussion to redesign the current planning procedure. But what should the future planning process look like? Which parts should be done by the physicians? Obviously the planning cannot be done by physicians only, as the whole plan creation would be too time consuming for an efficient clinical workflow and best utilization of clinician time. Here physicians were provided with the prepared database, including prior required work steps such as beam angle selections. Physician planning consisted of plan navigation and generation. The whole process is and will stay an interactive process of a mix of professions.
A redesign towards an involvement for certain parts of the process or in case of specific situations or cases would be an option. Possible scenarios where dosimetrists might need clinician's support could be in cases of overlapping targets and OARs or if all constraints are met to decide further structures of improvement. In such scenarios, partial physician involvement should be included prior to the finalization of plans. During plan review meetings with physicians, dosimetrists have the opportunity to present the possibilities or decisions they face. The plan could then be finalized together, which would not be more time-consuming as the regular plan-review for the phycisians.

It could also be promising to combine MCO with knowledge-based planning [146, 94, 93, 87]. The knowledge-based system could provide the templates and beam orientations, as well as the starting point for the interactive navigation. The physician would then be involved in making relatively minor adjustments using only a small number of sliders, without being overwhelmed by too many options.

Whether the proposed planning workflow is more efficient and results in better plans when doctors are more trained in planning is difficult to answer. More studies on different cases and with more clinicians are needed in order to conclude the gain. The involved physicians emphasized the value of dosimetrists as a profession but stressed similarly that they enjoyed being more involved in the planning process.

Physicians' insight and potential of MCO in clinical practice

The physician navigation approach provided insight into the planning process to physicians with which they are often not familiar. Physicians experienced the dosimetric patient-specific trade-offs that they otherwise are not privy to. Statements which were recorded during the physician sliding sessions, such as: "it is interesting how this dose increases while the other one decrease" or "that was a good deal" underline the physicians appreciating having the control over the dose.
Involving physicians is not only feasible but can also be regarded as a gain of knowledge on more levels. Knowing the expense of a certain dosimetric goal like a homogeneous target dose distribution might change the physicians' point of views or expectations of a plan. Even if clinical planning and navigation is not done by the physicians (yet) it is a gain for the physician to understand the process, and experience the trade-offs also for comprehending difficulties planners sometimes face. Planning should not be kept a secret from the physicians.

MCO-treatment planning was proven to be a suitable method to experience dosimetric trade-offs, and the technology could also serve as a tool for educational purposes. Furthermore by utilizing templates and a set of equally spaced beam angles it could be used in clinicians' rounds. Being aware of realizable dose distributions the physician could better specify the prescriptions and clinical goals to each individual case [102]. Clearer formulated prescriptions will shorten the "back and forth" process between planner and doctor and thus make the planning process more efficient.

3.4.5 Conclusion

The performed retrospective planning study demonstrated the feasibility of physician driven planning in MCO treatment planning by Pareto surface navigation on template based optimized plans. The plan quality of physician plans was comparable to the clinical plans with differences being observed due to focusing on different clinical goals. Increasing the involvement of physicians and at an earlier stage into the planning process can lead to gains both in efficiency and planning insight. Physicians' insight into the planning process and evaluation on conflicts is of great value to plan optimization. In particular, MCO planning can be a powerful tool for education and training.

3.5 Conclusion of both studies: improving quality and efficiency of IMRT planning by MCO

Several components influence the resulting quality of a plan. Factors like available planning time and planners' experience play a fundamental role in the outcome of a plan. The influence however of those factors can be reduced by the choice of treatment system.
Both performed planning studies demonstrated the potential of MCO planning with regards to efficiency as plan quality. A recent publication showed that MCO planning reduces the impact of planners knowledge on the plan quality and that in fact also novel planners achieve high plan qualities by MCO [69].
The potential of MCO is found in the visualization of inherent trade-offs due to interdependent objectives. Exploring the different compromises and dependencies of objectives makes MCO planning intuitive and efficient. It enables different staff members as well as less experienced planners to achieve plans of higher quality. Furthermore the attempt to standardize planning in clinical practice seems to be realizable by MCO, and should indeed be feasible, as template based planning proved to be feasible in the physician driven planning study.
Generally the planning system and optimization approach contributes essentially to the resulting plan and planning efficiency-however not all contributing concerns can be solved by the choice of TPS. A main factor of efficiency and quality is found in the utilization and integration of the TPS in the clinical planning workflow. MCO has the potential to improve the workflow but may hardly be of advantage when used similarly to the regular inverse planning routine. The impact of available planning time and planning experience on the final plan quality will always remain to some extent but the degree of impact can be reduced by MCO planning.
The search for the best, i.e. most efficient planning procedure leading to the best plan product, will remain a challenge of future investigations.

4 Relevance of adaptive planning for IMPT and IMXT

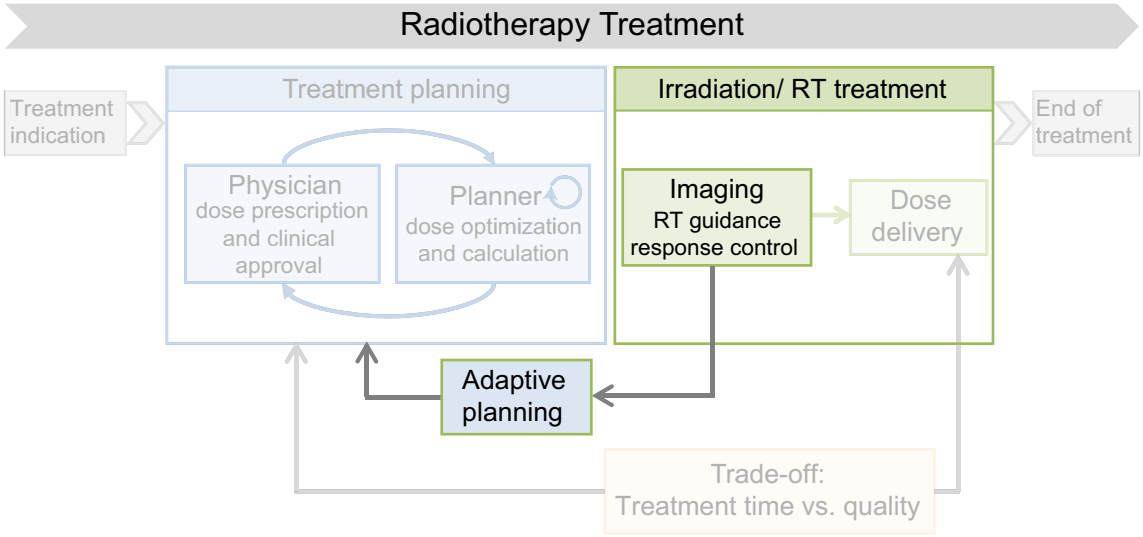

Figure 4.1: Efficiency and quality in radiotherapy, focusing on adaptive planning.

Interfractional changes of patient anatomy, due to weight loss, shrinkage of the tumor and anatomical structures nearby, as well as variations in daily set-up, are of concern in radiotherapy. Image guided radiotherapy (IGRT) and adaptive planning are part of clinical practice to retain dosimetric quality during the treatment phase (figure 4.1). Both techniques come along with additional workload and costs, which motivates investigations on their relevance for more specific indications for their applications. This chapter introduces the current clinical use of both techniques, and analyzes particularly the relevance of adaptive planning on the basis of a treatment planning study with intensity modulated proton therapy (IMPT) and photon therapy (IMXT) in head and neck cancer (HNC) patients. It is an extended version of the publication by the author [95].

4.1 Introduction and motivation for the treatment planning study

4.1.1 IGRT and adaptive planning in clinical practice

Radiotherapy treatment plans are based on planning CTs (p-CT), which determine the patient set-up for subsequent treatment sessions. Any geometrical difference compared to the p-CT influences the dose distribution and leads to deviations from the intended planned treatment. IGRT is a supportive technique to improve positioning and therefore the precision of the dose application. Images are acquired in the treatment position prior to irradiation and registered to the p-CT. The treatment position is then corrected by the derived couch shift. Over a treatment course of typically three to eight weeks, patients often undergo anatomical changes, which make CT registration more difficult and less accurate. In order to maintain dosimetric quality in case of large anatomical changes, plans are adapted to the current anatomy. So far, there are no quantitative measures of anatomical changes to decide when adaptive planning is required. The frequency of adaptive planning depends on the clinic, staff capacities, the responsible physicians and her/his individual assessment of the gravity of the situation.

Both applications are more time consuming in terms of staff involvement and room occupation, compared to the straightforward delivery of the same plan over the whole treatment period without IGRT. Studies demonstrated that the utilization of IGRT, as a supportive tool to position the patient, prolong the treatment considerably [137, 108]. Adaptive planning is even more time consuming. The decision to replan, requires the entire treatment planning procedure to be performed again (see chapter 3) along with an additional workload: tracking the overall delivered dose over the whole treatment period is an important basis for adaptive plan optimization and for documentation purposes. Dose accumulation of different plans (on distinctive CTs) involves the registration of CT data sets, the generation of new structures and the copying of all dose distributions onto one CT. Due to these correlated expenses, it is of interest to reduce the number of plan adaptions to a minimum.
The question arises: how relevant are IGRT and adaptive planning? What are the consequences if plans are not adapted but patient geometry changes? And are there any obvious indications to support physicians in the decision for or against re-planning without extensive work, like the recalculation of plans on new CT data sets and adapted contours?

The impact of geometrical changes and thus the relevance of both techniques presumably varies with the RT technique (3D-CRT or IMRT) and the applied radiation type, i.e. photons or protons. The following planning study investigated the impact of interfractional geometrical changes on IMPT and IMXT dose distributions of HNC patients.

4.1.2 Interfractional changes in IMPT and IMXT for HNC patients

HNC patients are known to be subject to severe anatomical changes throughout their treatment and benefit from frequent image controls [119, 62, 120, 44, 53]. Due to the complexity of anatomy, i.e. the large number of OARs in proximity to the target, their treatment plans are often strongly intensity modulated. Steep dose gradients (within fields) allow for highly conformal dose distributions and sparing of critical structures, but make the plans similarly more sensitive to geometrical changes [120, 53, 55]. Therefore HNC patients are particularly eligible to study the impact of geometrical changes.

Depending on the applied irradiation technique, alterations may have different degrees of impact. Dose distributions of IMPT are often superior compared to IMXT (see subsection 1.1.2)[120, 113, 88, 27, 124, 122, 34]. The Bragg peak and the well-defined range of protons allow better sparing of healthy tissue and higher conformity of the target volume. Nevertheless it is also known that these advantageous physical properties can be a risk in clinical practice [84, 71, 86, 76, 81, 6, 128].

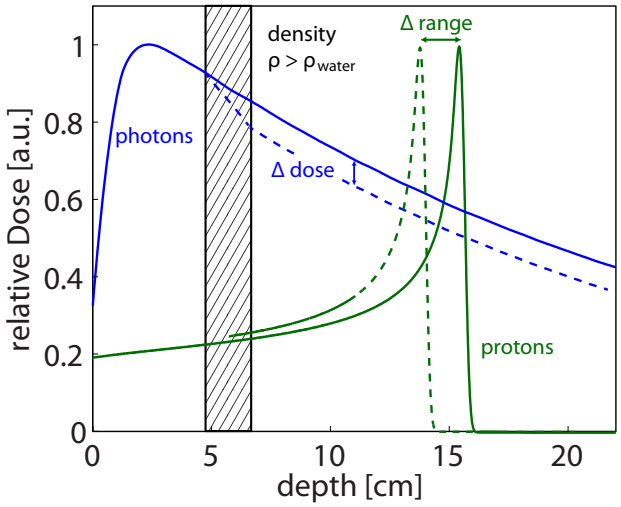

Figure 4.2: Consequences for proton and photon dose depth curves when penetrating more dense material, introduced into the beam direction.

Figure 4.2 is a schematic of the difference in sensitivities of dose depth curves to density changes of traversed matter for protons and photons. The introduction of e.g. denser material leads to greater photon absorption and subsequently a decreased dose behind the obstacle. As proton doses strongly depend on the density of the penetrated matter (see section 2.1), higher densities shorten the proton ranges, which in extreme cases means “all or nothing” for the PTV. The opposite scenario, of prolonged ranges, can become a threat in case the Bragg peak is shifted into OARs.

This planning study focused on IMPT and IMXT treatment plans of HNC patients that were not adapted "in time". Dosimetric alterations due to interfractional geometrical changes were analyzed by recalculating the initial plans on control images at different times during the treatment period.

4.2 Material and methods

4.2.1 Patient characteristics

The retrospective planning study was performed on data of five postoperative HNC patients (1 hypopharynx, 2 tonsil, 1 oral cavity, 1 larynx), previously treated by tomotherapy[1] at Klinikum rechts der Isar. Four of them underwent radiochemotherapy. The CTV was defined as the GTV delineated on pre-treatment CT and MRI, including the postoperative region, plus a safety margin of 10 mm. The elective nodal-CTV was defined according to Grégoire et al. and Chao et al. [51, 28]. A safety margin of 5 mm was applied from CTV to PTV. All patients featured similar PTV shapes with initial volumes ranging from 721.7 cm^3 to 1296.7 cm^3.
Patients were immobilized with a head and shoulder mask. Daily control megavoltage (MV) CTs were acquired and merged with the planning kilovoltage CT scan (kV-CT) before treatment. After registration by the bone and tissue registration algorithm provided by the tomotherapy unit, the automatic registration was manually corrected by a member of staff with regards to tumor coverage and spinal cord sparing. These images representing the actual treatment position served as a basis for the planning study. The merged image consisted of the MV-CT in the center and of small kV-CT parts to fill the area outside of the (smaller) field of view of the MV-CT (figure 4.3).

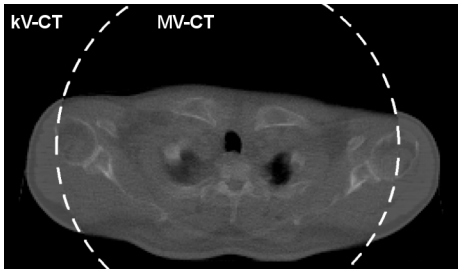

Figure 4.3: One slice of a merged CT consisting of a MV-image in the center and of small, initial kV-CT parts to fill the area outside of the (smaller) MV-CT's field of view.

For the contouring process on the MV-CTs, the images were imported into the Eclipse planning system[2]. In order to minimize bias, the contouring process was

[1] Accuray Inc., Madison, WI
[2] Varian Medical Systems Inc., Palo Alto, CA

done by the same physician for all CTs. The structures of the original PTV and organs at risk (OARs) of the kV-CT were copied to the merged images and manually adapted to the new anatomy (figure 4.4).
During the treatment period (approx. 6 weeks) all patients lost weight. The absolute amount varied during the treatment (e.g. by saline volume expansion during chemotherapy administration), and between patients from 2.0 kg to 12.8 kg. Similar fluctuations were observed for losses of PTV volumes. The mean PTV loss was 76.2 $\pm$ 50.3 cm^3 (corresponding to 7.0 $\pm$ 4.6% of the initial volume) and the greatest loss was 143.1 cm^3 (12.9%)(see tables A.10 - A.13).

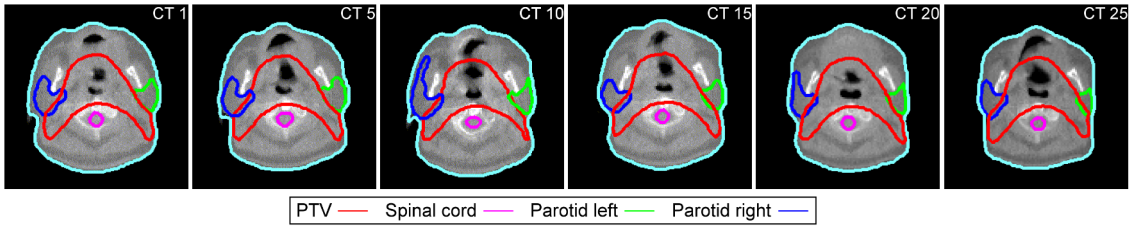

Figure 4.4: The course of patient geometry of one examplary patient in five fraction intervals.

4.2.2 Retrospective planning and evaluation criteria

One IMXT plan with seven equidistant fields and two different IMPT plans, with two fields (IMPT-2F) and three fields (IMPT-3F), were generated for each patient (IMRT theory see section 2.2). Both plans consisted of two lateral opposing fields (beam angles: 45° and 315°) and the latter of an additional posterior field (180°). This selected third field generally allows for a better sparing of the parotid glands. In some clinics, however, fields irradiated through the patient couch are avoided when utilizing additional immobilization equipment, such as masques or bite blocks. The edge of the board of these immobilization devices between patient and couch may generate a steep step in different materials within the field, which can cause differences in the proton range at slightly different patient set-ups.

The retrospective planning for both modalities was carried out in a research version of the KonRad planning system, developed at the German Cancer Research Center in Heidelberg [98].
Planning on MV-CTs required the adaption of look-up tables (LUT) to convert Hounsfield units into water equivalent depth/relative stopping power. The LUT data published by Newhauser [96] served as a basis for proton planning. For photon planning, the clinically used tomotherapy data was implemented. To avoid any Hounsfield unit calibration issues between kV- and MV-planning, and associated LUTs, all dose calculations were performed on MV-CTs, i.e. the first MV-CT was used as planning CT.

Proton plans were calculated using data of a virtual machine, providing particles of 160 MeV and a flexible range shifter for energy adaption, with a constant lateral beam width of 2.5 mm standard deviation (Gaussian beam profile) at the patient surface. For both plan types and all fields, the spot spacing was chosen to be $\Delta x = \Delta y = \Delta z = 0.3$ cm (within the PTV) (3D spot scanning technique [80]). The fields were optimized simultaneously assigning the weights to spots such that the combined dose distribution of all fields fulfilled the objectives defined in the optimizer as best as possible.
The IMXT plans (beam energy: 6 MV) were generated by simultaneous fluence optimization and direct translation into multileaf collimator (MLC) segments in step and shoot mode (leaf size: 0.5 mm). Complete blocking of kV-parts of the image was not possible. Since the geometry of the kV image was identical for each merged image and the influence of different LUTs for kV and MV on the photon dose is comparatively small, the relative error between CTs caused for IMXT planning can be neglected. For both IMPT and IMXT, the dose grid was 1.95 mm in x-/y-dimension and 3 mm in z-dimension.

The planning and evaluation processes were done on identical target structures for IMPT and IMXT. Typically, range uncertainties specific to IMPT can be addressed during the planning process by additional PTV margins adjusted to beam directions (see section 2.3). The definition of appropriate target structures for comparisons between IMPT and IMXT dose distributions is therefore difficult, and depends on the intention of the underlying study. Since the goal was to study the differences in dosimetric changes over the course of a treatment for each technique in any comparable target structure, the clinically used photon PTV served as the target volume here. The PTV accounts for setup errors, which - even with image guidance - can never be eliminated completely, and accounts for internal organ motion, which motivated the evaluation of the dose delivered to this volume (rather than e.g. to the CTV).

The initial plans were optimized by the same constraints (with individually adjusted penalty factors): first priority was given to PTV coverage, at least 95% of the PTV receiving 95% of the prescribed dose (50 Gy/50 Gy(RBE) for photons/protons, in 25 fractions). In the following, all dose values are given in Gy referring to absolute absorbed dose in case of photons and relative biological effect (RBE=1.1) weighted dose in case of protons. Second priority was given to the OARs, with the focus on the spinal cord (maximum dose $D_{max} < 45$ Gy, i.e. $D_{max} < 1.8$ Gy/fraction) and parotid glands (mean dose $D_{mean} < 26$ Gy, i.e. $D_{mean} < 1.04$ Gy/fraction). The former was achieved for all cases while the latter was not always possible. Sometimes objectives were given priority at the cost of the PTV.
The obtained plans, two IMPT plans and one IMXT plan for each patient, were recalculated on five MV-CTs (5th, 10th, 15th, 20th, 25th fraction) that were registered to the actual treatment position as described above (see figure 4.4).

The resulting dose distributions were analyzed in terms of DVHs and various indicators for the PTV and for OARs (see section 2.3.2). The PTV was investigated for coverage, conformity and homogeneity, with the indices CovI and ConI, and the standard deviation σ (PTV) (equations 2.9, 2.10, 2.11).
As to the OARs, the focus was on the spinal cord and parotid glands. Further organs such as the larynx and mandibula were considered, but without further conclusions. Maximum and mean dose were considered for the spinal cord and parotid glands respectively. Maximum and minimum doses were evaluated as the maximum and minimum received by at least 1 cm^3 of the structure.

4.3 Results

For both techniques, considerable differences in dose distributions were observed: on average the coverage of the PTV decreased and doses to the OARs increased during the course of treatment. In general, these effects were greater in IMPT plans and indicated more variations. Results depended strongly on the patient, with a more pronounced dependency for IMPT plans. The two IMPT geometries, i.e. IMPT-3F and -2F plans, differed mainly in the initial dose to the spinal cord and the parotids (figure 4.5) but yielded similar trends throughout the course of the treatment.

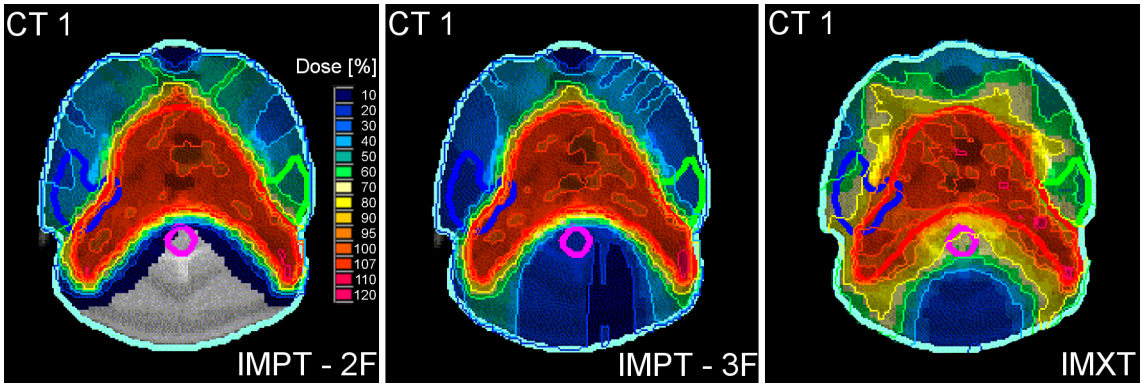

Figure 4.5: Dose distributions of all initial plans for one patient: both IMPT plan geometries (left, centre) and the IMXT plan (right)

Within the following, firstly the results of IMXT versus IMPT plans, by means of IMPT-3F plans, are presented by one exemplary patient case and a statistical evaluation of specific DVH criteria of the PTV and OARs over the collectivity of patients. Subsequently the two IMPT plan types are compared, i.e. IMPT-2F vs. IMPT-3F. Dose values are presented and discussed in dose per fraction (prescribed dose: 2 Gy).

4.3.1 Comparison of photon and proton plans: IMXT vs. IMPT-3F

Example patient

Figure 4.6 illustrates the resulting dose distributions in one CT slice and the corresponding DVHs for proton (top) and photon plans (center) of one representative patient over the treatment period.

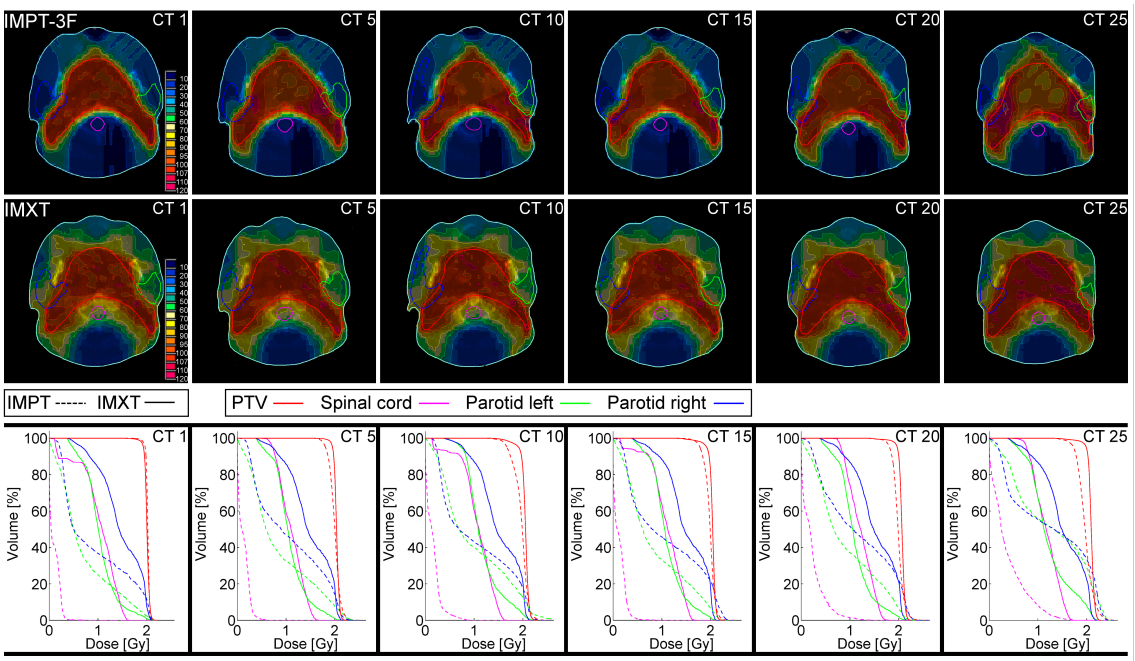

Figure 4.6: Dose distributions for IMPT (top row) and IMXT plans (second row) and corresponding DVHs (IMPT: dashed line, IMXT: solid line) of patient no. 1: Trends from initial plan (CT1, left) to recalculations of the last fraction (right). (Normalization: 100% = 2 Gy)

Dosimetric results are arranged from left demonstrating the initial plans, to right presenting the dose distributions at the last fraction. Geometrical changes of this patient are noticeable by comparing the contours of the patient in figure 4.4. The quantitative results, i.e. doses and indices, of the PTV and OARs for this patient, can be found in the first subplot of figures 4.8 - 4.11. While the PTV coverage was comparably satisfying, the dose distributions and DVHs indicated better target conformity and preservation of OARs in the initial IMPT plan as compared to the initial IMXT plan. Throughout the treatment the homogeneity and coverage of the PTV decreased and the areas of under- and overdosage increased for both plans. The resulted heterogeneity was far greater for proton than for photon plans (figure 4.6, 4.7). While IMPT plans revealed underdosed spots also in the central PTV (e.g. compare recalculations on 25th CT, figure 4.6), cold spots in IMXT plans were located at the outer PTV regions.

For both techniques the location of hot spots was not necessarily restricted to the PTV but were also found outside - e.g. within the parotid gland. The steepness of the DVH of the PTV degraded for both plan types. Compared to the IMPT plans, the IMXT plans changed moderately. The quality of the DVHs did not worsen monotonically but the plots of the 15th CT were superior to the 10th fraction for both types of plans.

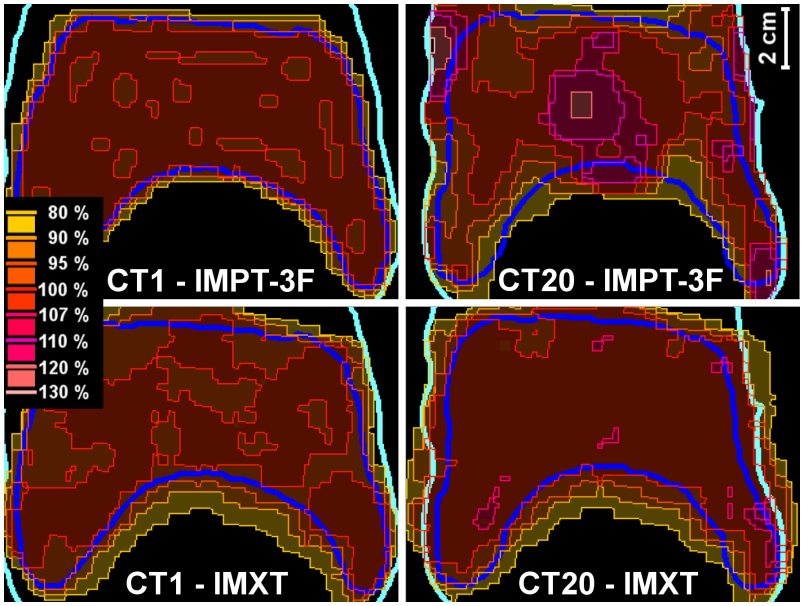

Figure 4.7: Dose distributions of the PTV area - initial plans (left) vs. recalculations (right) at 20th fraction for protons (top) and photons (bottom). (Normalization: 100% = 2 Gy; PTV contour: dark blue, patient contour: light blue)

PTV of all patients

The initial $D_{max}(1\ cm^3)$, $D_{min}(1\ cm^3)$ and D_{mean} of the PTV were similar for the five patients for IMPT and IMXT, except for $D_{min}(1\ cm^3)$ being slightly lower for photons (figure 4.8). The changes of doses during treatment were different though. The D_{mean} was almost constant at 2 Gy for both plans. The $D_{max}(1\ cm^3)$ increased and $D_{min}(1\ cm^3)$ decreased considerably for the IMPT plans, whereas this divergence was moderate for IMXT. Generally recalculated IMPT dose distributions showed extremer inhomogeneties (figure 4.6 and 4.7). In the IMPT plans spots of underdosage were located also in the centre of the PTV while in IMXT they restrained to the boundary area.

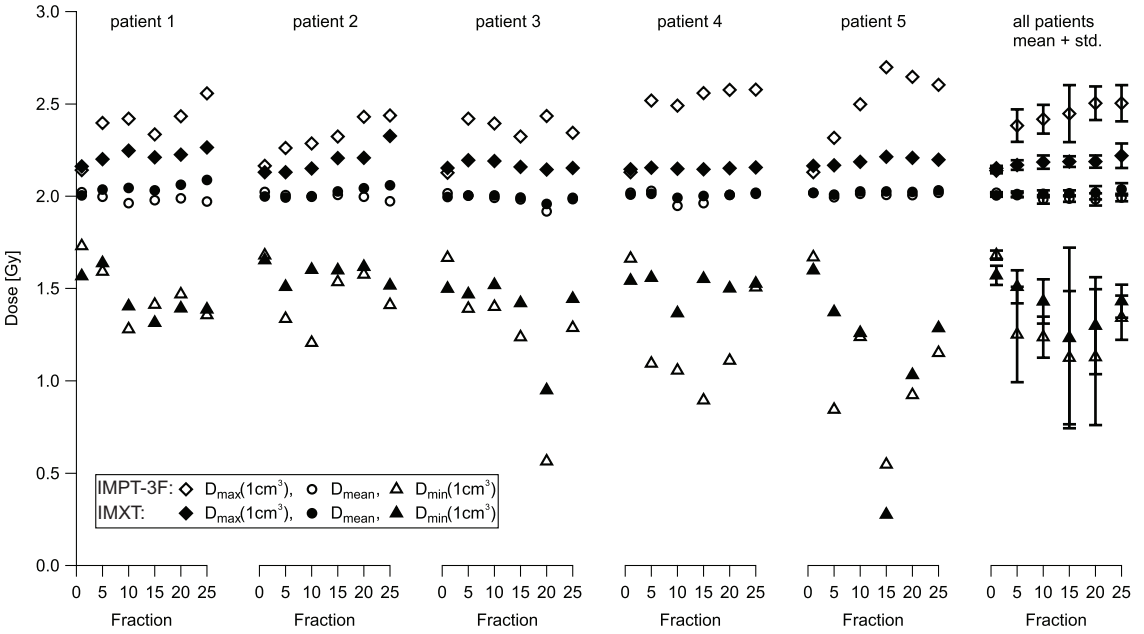

Figure 4.8: Dosimetric alterations within the PTV: $D_{max}(1\ cm^3)$, $D_{min}(1\ cm^3)$ and D_{mean} of five patients, corresponding mean values and standard deviation over all patients (right).

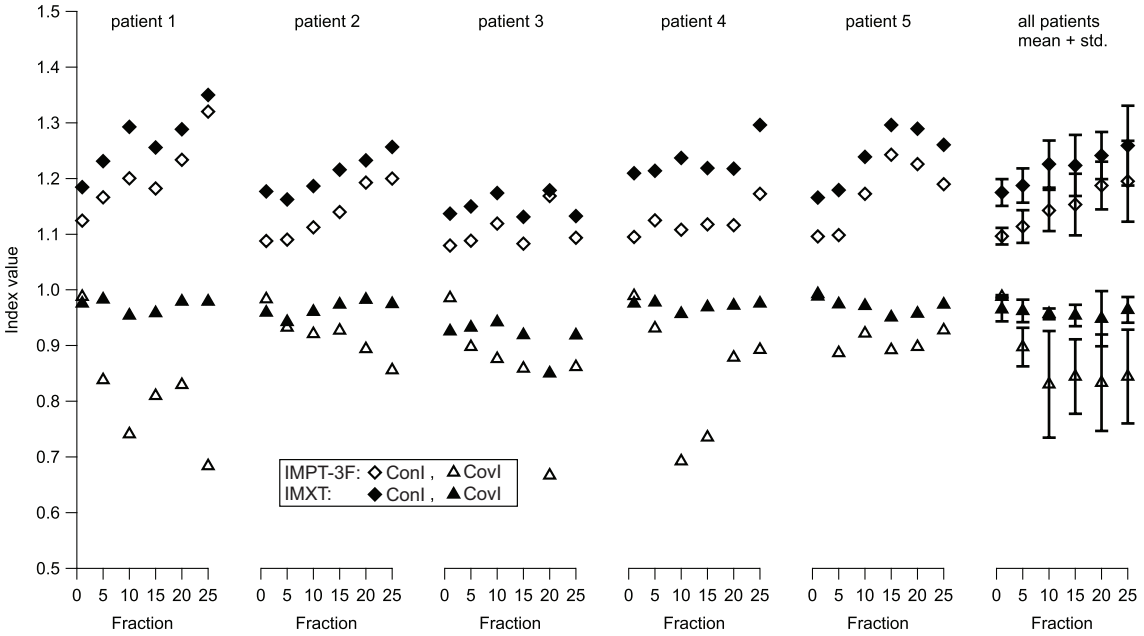

Figure 4.9: Trends of coverage (CovI) and conformity indices (ConI) for five patients, corresponding mean values and standard deviations (right).

The suggested decline in homogeneity and coverage was further supported by the increasing trend of ConI and decreasing trend of CovI (figure 4.9). An exception were the results of patient 5 in fraction 15: the $D_{min}(1\ cm^3)$ was smaller in the photon than in the proton plan - nonetheless the corresponding CovI was superior to the IMPT plan. Especially the assessed quantities of IMPT plans showed large standard deviations, i.e. great variations between patients (figure 4.8, 4.9). The general trends (e.g. decreasing coverage) were still seen in the individual patient graphs. Evaluated PTV criteria for all patients and fractions are presented in tables A.10 and A.11.

OARs of all patients

For both modalities an increasing trend of $D_{max}(1\ cm^3)$ to the spinal cord was observed, the absolute changes being greater for protons (figure 4.10). With $D_{max}(1\ cm^3)$ of the IMXT plans initiating at far higher values, no proton plan reached maxima in the range of the IMXT plans over the whole course.

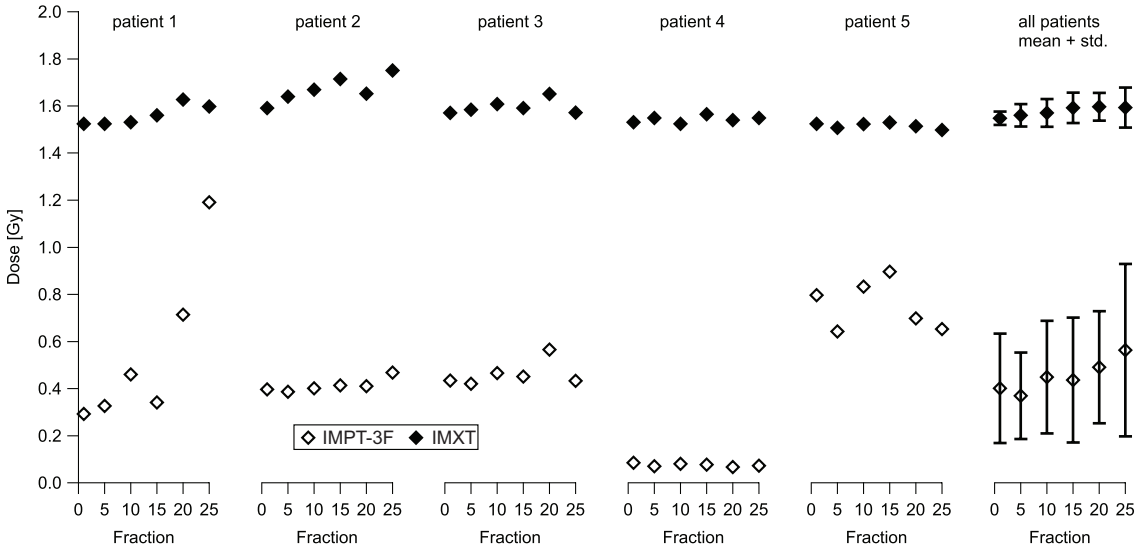

Figure 4.10: Trends of $D_{max}(1\ cm^3)$ to the spinal cord for five patients and corresponding mean values and standard deviations (right).

Parotid sparing was initially better in the IMPT plans (figure 4.11). Since the PTV was almost symmetrical there was no distinction between the ipsi- and contralateral parotid gland. Overall, both modalities had an increase in dose during treatment course, with smaller differences between the planned and recalculated doses for IMXT as compared to IMPT. Some cases showed a decreasing D_{mean} (e.g. left parotid of 3rd patient) for IMPT and IMXT, likely due to different positioning. These findings suggest that optimizing parotid doses as low as possible is reasonable: even if defined dose limits cannot be obtained, the sum of actual delivered doses might be below the first calculated doses.

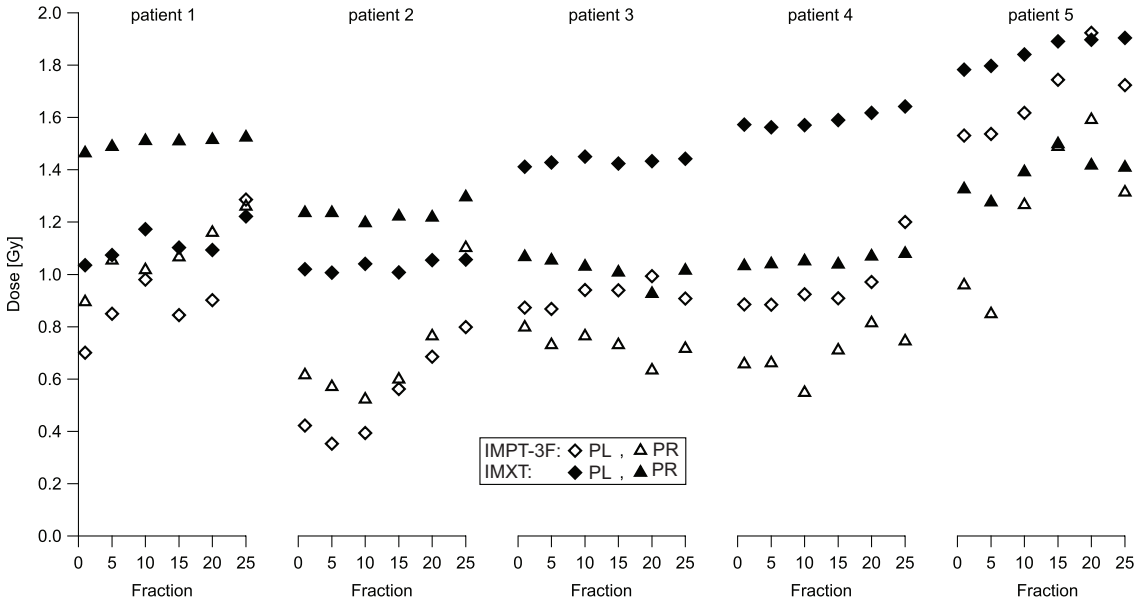

Figure 4.11: Trends of mean dose to left and right parotid glands (PL and PR) of five patients - each symbol represents one parotid and one modality.

Assessed DVH criteria of the spinal cord and parotid glands of all patients and fractions are presented in tables A.12 and A.13, respectively.

4.3.2 Comparison of proton plans: IMPT-2F vs. IMPT-3F

Example patient

The DVHs of the PTV (examplary patient of section 4.3.1) were almost concurrent (see figure 4.12) with minor differences being of observed in some specific DVH points (see table A.14).

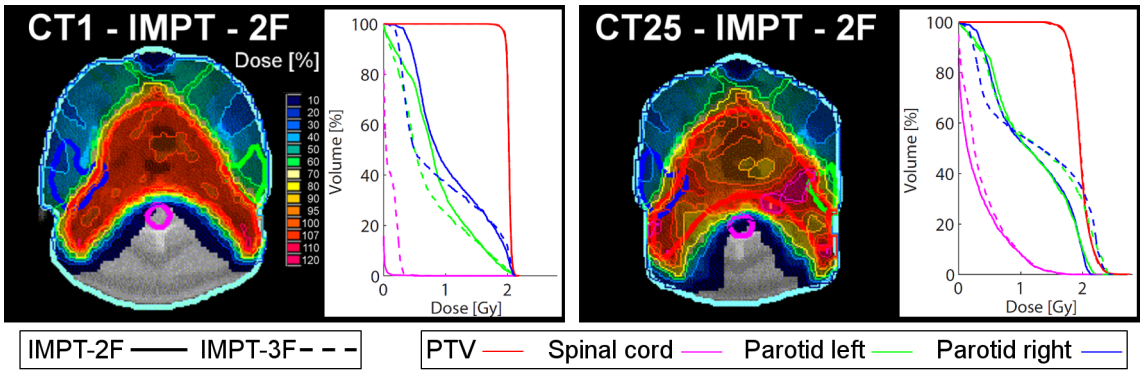

Figure 4.12: Dose distributions of the initial IMPT-2F plan and of the recalculated plan of the 25th fraction and corresponding DVHs compared to the associated results of IMPT-3F (dose distributions see figure 4.6).

The prescribed non-existing monotony in the degradation of the IMPT-3F plan was also found for the IMPT-2F plan. Similar to the IMPT-3F plan, PTV dose criteria were superior in the 15th than in the 10th fraction which obtained the lowest minimum dose over the treatment period. The initial doses of the spinal cord in IMPT-2F plans were almost zero for larger doses to the parotid glands, i.e. DVH curves were above the corresponding curves of IMPT-3F. Contrary to the IMPT-3F plan, the mean dose of the right parotid received larger doses than the critical value of 1.04 Gy. At the 25th fractions all parotid doses were increased and DVH curves of both plan types intersected.

PTV of all patients

Initial qualities of the dose distributions of the PTV were comparable. The average $D_{min}(1\ cm^3)$ and CovI was slightly lower in IMPT-2F than in IMPT-3F plans, an inevitable compromise caused by parotid sparing with two lateral fields (see figure 4.13, table A.14).

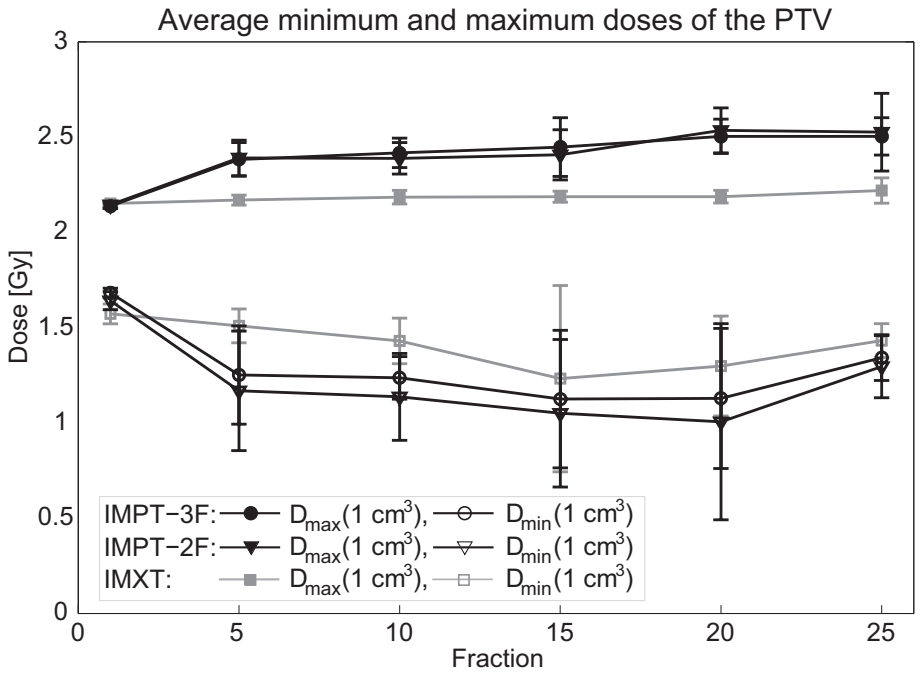

Figure 4.13: Average $D_{min}(1\ cm^3)$ and $D_{max}(1\ cm^3)$ of the PTV plus associated standard deviations over all patients of IMXT and both IMPT plans. Data points are connected by lines for a clearer presentation of the data sets; the course of doses in between two data points may well vary from this linear correlation and fluctuate.

Table A.14 summarizes the most relevant PTV criteria of both IMPT plans and compares corresponding deviations between the initially planned and recalculated quantities. During the course of treatment the standard deviation σ(PTV) increased

for both techniques, i.e. overdosed and underdosed regions appeared within the PTV, as prescribed above for IMPT-3F (see figure 4.12). The magnitude of the diverging effect was comparable for both plan types. The course of CovI and σ(PTV) was almost equal for all patients. The derived relative changes of CovI were identical in three out of five patients, for one patient IMPT-2F illustrated superior coverage, for one the IMPT-3F plan. The degree of impact on the minimum dose was not necessarily correlated to the coverage, i.e. the lowest minimum dose of a plan was not found in the plan of worst coverage. The lowest $D_{min}(1\ cm^3)$ and coverages were reached at the same fraction for both plan types. The fraction of the worst IMXT dose qualities was not concurrent with IMPT plans (tables A.10 and A.11).

OARs of all patients

The trends of larger absolute dose changes and fluctuations between patients and fractions compared to IMXT were also found in the IMPT-2F plan. The initial maximum doses to the spinal cord were almost zero for IMPT-2F plans and stayed mostly below the corresponding IMPT-3F values.
Figure 4.14 illustrates D_{mean} to the left and right parotid glands (PL and PR) of all plans and patients.

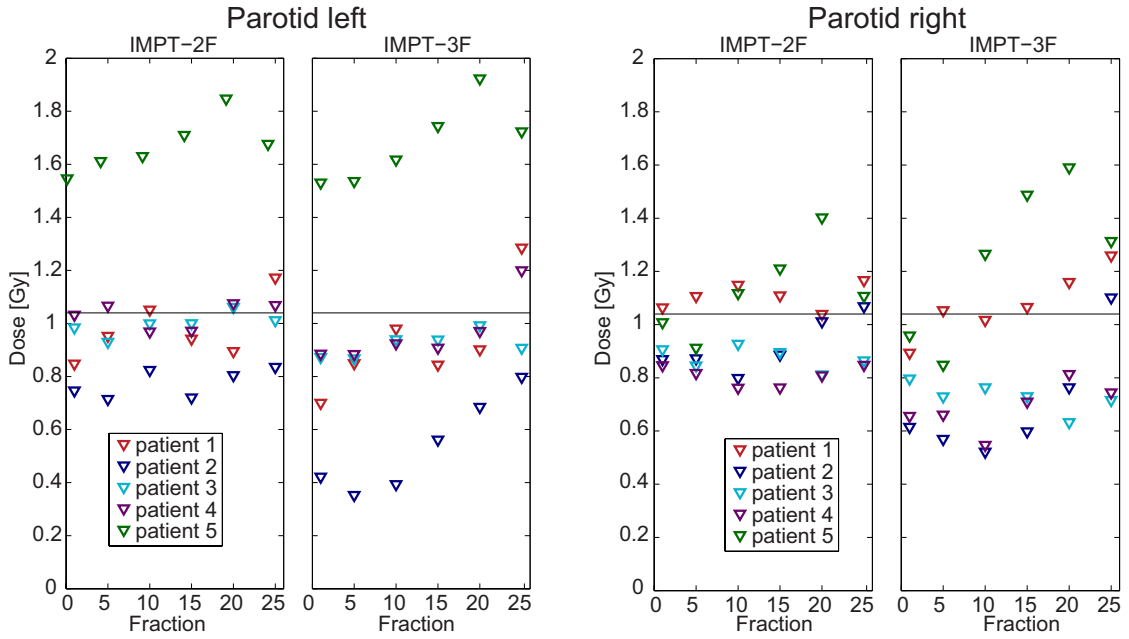

Figure 4.14: D_{mean} to the left and right parotid glands of all patients for IMPT-2F and IMPT-3F plans.

The clinical goal of $D_{mean} < 1.04$ Gy was initially reached for all but one parotid by IMPT-3F (PL, patient 5) and two parotids by IMPT-2F (PR, patient 1). Throughout the course of treatment the critical dose was exceeded more often in IMPT-2F than IMPT-3F plans. The trends of the individual patients were similar

for both techniques, e.g. the dose of the right parotid of patient 5 decreased from CT1 to CT5, increased up to fraction 20 and decreased again at the 25th fraction. Some parotids showed a considerable difference in the initial values but reached approximately the same value at the final fraction, the right parotid of patient 2 being an example. The initial D_{mean} (PR) of patient 5 was 0.96 Gy for IMPT-3F and 1.01 Gy for IMPT-2F and resulted in 1.41 Gy and 1.11 Gy, respectively, i.e. the 3F-plan ended up at a higher dose than the 2F-plan.

4.4 Discussion

Planning study results on interfractional changes in IMPT and IMXT

Recently a related study was published by Kraan et al. [71] analyzing the impact of clinical uncertainties to IMPT plans of oropharynx patients. A variety of scenarios of potential errors on the basis of two clinical CTs per patient (planning and one control CT) were simulated and the benefit of plan adaption was examined. Setup errors were simulated applying isocenter shifts and anatomical uncertainties were evaluated by recalculations on control CTs. The authors concluded that the combination of different errors can cause serious effects and recommended individual surveillance of anatomy, dose recalculations and plan adaptions. This recommendation is sustained by the here presented study analyzing several control CTs during the treatment course displaying the consequences of anatomical changes as well as patient positioning uncertainties on the dose distribution during fractionated radiotherapy. Observed dose changes varied between individual patients which is also consistent to the prescribed findings.
Simone II et al. [120] compared adaptive to non-adaptive planning with IMPT and IMXT for head and neck patients. One result was that adaptive IMPT offers the most favorable dose quality. The here presented results agree with that, assuming that the patient received the calculated dose.
In both above cited studies it was assumed that the anatomy remained identical up to the day of the control CT and then until treatment finalization. Since patients undergo continuous anatomical changes there is a certain risk that the dose was not delivered as planned until the fraction where the adaptation started. The results of the present study obtained by recalculations on the 5th and 10th control CT, indicated that adaption might already be relevant earlier during the treatment course. The performed investigations complement these studies with patient data that reflects the actual clinical situation in positioning and anatomy in frequent intervals.
In general results obtained in planning studies should be interpreted carefully. The delivered dose over the treatment period is always a superposition of the total number of fractions. Calculated doses do not supply the actual applied dose, i.e. do not contain every interfractional alteration and all intrafractional changes.

Specific results of the performed study

The resulting IMPT coverage values of as low as 66.7% lead to questions of clinical relevance and how this risk of underdosage should be dealt with. One has to note that this was a single fraction, and one has to take a closer look onto the calculated coverages over all fractions. Here only worst cases could be estimated, and mean coverages which were between 81% and 92% for IMPT. A more accurate statement would demand recalculations on daily control images and dose accumulation studies. Even though such extreme deviations like the above stated 66.7% were exceptions throughout the treatment period, they still show the need of accurate, high quality IGRT and frequent control CTs, especially in proton therapy.

Generally the doses to OARs were hardly reaching critical values, especially in IMPT plans. The prescriped dose of 50 Gy was comparably low: after receiving this dose patients commonly (often) undergo a consecutive second irradiation part to boost the tumor region leading to higher overall doses. In order to escalate doses for greater tumor control, the sparing of OARs has to be as good as possible. Extrapolating the study results to higher doses could be taken as an alert to be very precise and careful in positioning and to control the anatomical situation frequently as these large fluctuations can become a greater threat at higher dose levels.

When is the time to adapt a plan? - Finding an indicator to improve (planning) efficiency

Contrary to the possible assumption that anatomical changes and their dosimetric consequences worsen throughout the treatment, it was shown that the decrease in quality is not necessarily monotonic. Some assessed values "improved" again at the following control CT, acquired five fractions later. Nevertheless the general trend of DVH points indicated a decrease in quality towards the end of the treatment, i.e. dose quality indicators were worse at the last fraction than in the beginning.
The search for explanations of the non-existing monotony is challenging as well as the search of correlations between dose criteria and patient specific parameters (e.g.w̃eight loss) which could serve as more distinctive indicators for replanning.
Weights fluctuated considerably for the individual patients - due to side effects (weight loss) and saline volume expansion during chemotherapy (weight gain) and between patients. The plan recalculations for the patient with the most stable weight (overall loss: 2 kg) did however not lead to the most stable dose distributions for both techniques, judged by the evaluated dose criteria.
Another potential indicator could be found in changing volumes of specific structures (e.g. PTV): correlations to associated variations in dosimetric quantities were examined without leading to clear correlations. To give an example of the situation, in four out of five cases the tumor shrank over the RT course, mostly continuously. One patient however featured an almost constant PTV volume but was still subject to dose changes of similar magnitude as the other patients (see tables A.10).
The underlying number of patients of this study was furthermore not sufficient to

derive correlations to weight or structure volumes with statistical significance.
As a comparison of volumes (initial vs. current) demands prior contouring onto a new CT, patient weights or other indicators would be preferrable which require less assessment effort. Measures of the scope of specific body regions could be subject of future investigations. Due to the similarity to weight and the above and below discussed complexity between geometrical and dosimetric parameters it is however questionable whether this attempt would lead to promising results.

A general difficulty in the search for correlations between dose changes and anatomical changes is that the latter cannot be viewed separately from daily set-up variations which are likely to have a large impact on the dose distributions as well. In our study, the main part of set-up variations was corrected by IGRT (resulting in couch shifts) and had therefore no impact on the dose distributions, i.e. their absolute values (applied couch shifts) were not relevant for our analysis. Nevertheless as not all variations could be corrected there are remaining set-up errors influencing the delivered doses. In comparison to the degree of impact caused by anatomical changes and weight loss these are considered to have a rather small effect though. The impact of pure set-up uncertainties has been studied e.g. by Kraan et al. [71].

When to adapt a plan, i.e. to define the conditions for which a plan based on the current patient anatomy is no longer acceptable, will remain a question to be investigated in the future. Especially for IMPT the approach of this issue might be difficult, where impacts of misalignment are larger than in IMXT, as huge variations in dose between fractions implicated.

The potential benefit of plan adaption

Figure 4.8 shows steep gradients between the initial $D_{min}(1\ cm^3)$ and $D_{max}(1\ cm^3)$ of the PTV and the corresponding values at the 5th fraction while they remain more or less at the same level afterwards. This might be caused by greater geometrical changes between 1st and 5th fraction compared to the rest of the treatment period. A separation of anatomical changes and set-up variations is difficult (see above). Set-up varies statistically on a day-to-day basis while anatomical changes could occur continuously. Assuming a continuously changing anatomy into "one direction", i.e. continuously decreasing weight without fluctuations, the adaption of a plan after some fractions should lead to better dose distributions throughout the remaing treatment period. To follow that idea, an IMPT plan (three fields) was optimized on the 5th CT of patient 3 and recalculated on subsequent control CTs (adapted plans, figure 4.15). As expected the plan at the 5th fraction was of higher quality than the corresponding recalculations of the intial plan. Adapted plan recalculations resulted in similar plan quality degradations and partly worse PTV-DVHs than derived by the initial plan recalculations (table A.15).
From this perspective, one might question the reasonability of plan adaptions for IMPT in general and conclude that the day-to-day variations are larger than any

anatomical influences. Arguments against this extreme conclusion are given by an unfavorable conduction/ some weaknesses in this planning experiment though. The chosen patient hardly obliged to PTV changes, particularily not between 1st and 5th fraction, and the adapted plan quality (CT5) was not equally satisfying as the intial plan.

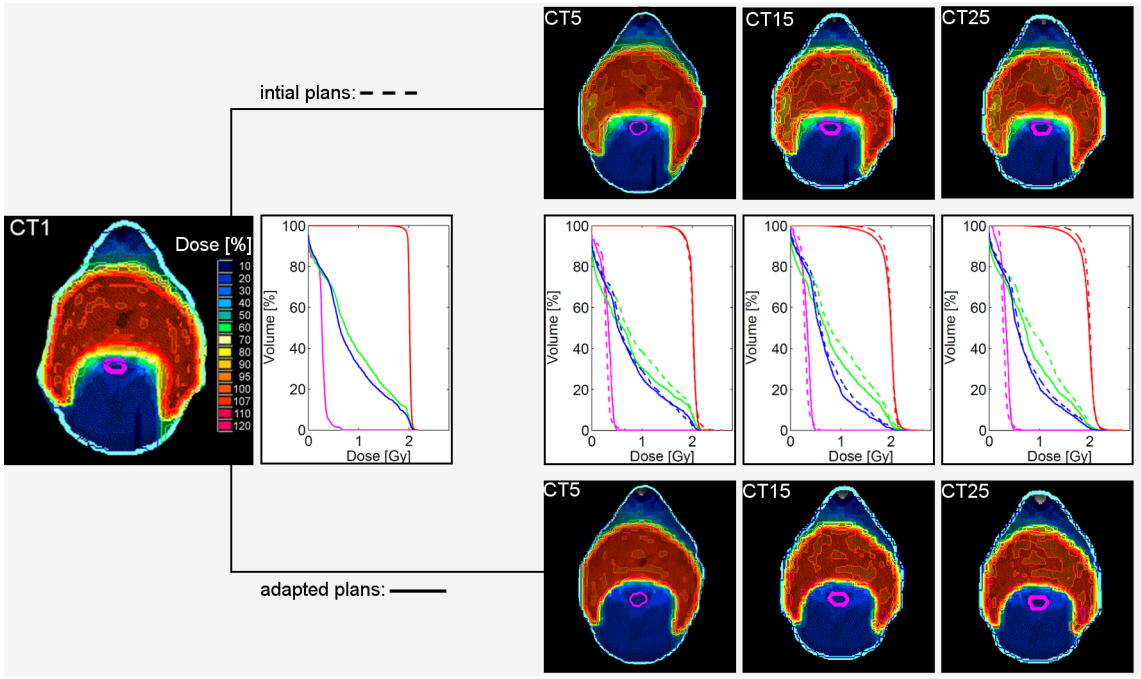

Figure 4.15: Dose distributions and DVHs of two possible treatment schemes: adaptive (at 5th fraction) vs. non-adaptive planning. The first plan is identical for both scenarios. The "adapted scenario" consists of a new plan at the 5th treatment which is then irradiated at each subsequent fraction; depicted are recalculations on the 15th and 25th CT.

Regardless of these, this analysis should not be left unmentioned as it presents a possible scenario of clinical practice and reveals issues for discussion. The initial plan quality might not always be achieved in the adapted plan, e.g. due to different anatomies and structures or/and shorter available planning times in case of "spontaneous" replanning. Moreover this simulation indicated that geometry changed in a similar magnitude between 1st and 5th fraction as between 5th and 10th such that the most recent adapted plan does not have to be considered to be superior for the remaining fractions of the treatment.
A possible solution of how to handle the latter, i.e. to assure that an adapted plan does not lead to degraded delivered dose quality, is by the application of the so-called "plan-of-the-day" approach [142]. This adaptive planning procedure was suggested for bladder cancer, where geometry varies considerably on a day-to-day basis [68, 127]. By supplying different plans of distinctive anatomical geometries for one patient the best suited plan to the current geometry is chosen out of a database

before every treatment. Concepts similar to this potentially improve the quality of treatment also in HNC treatments, e.g. by offering several plans for selection (initial plus all available adapted plans) at each treatment.

Field choice in IMPT: IMPT-2F and IMPT-3F

The number of fields in the IMPT plans did not make any difference regarding the overall conclusion compared to IMXT plans: both plan types showed larger absolute dose changes and greater variations between patients and fractions, of comparable magnitudes.
The initial difference of proton plans was found in the better parotid sparing by IMPT-3F plans - the additional field of 180° allowed for greater modulations in the relevant regions. With respect to the critical limit $D_{mean} < 1.04$ Gy/fraction this advantage made a difference for only one patient (right parotid, patient 1). Over the course of time, doses of both plan types exceeded the critical limit. Results indicated that less dose in the initial plan does not guarantee to result in a smaller overall dose over the whole treatment period. As absolute changes between fractions were of the same magnitude, the chances to stay below a certain level are higher with lower initial doses though.
The course of PTV and OARs dose criteria was similar for a number of cases, presumably due to the utilized identical lateral beam directions. Geometrical changes within those directions contributed to both dose distributions (with a more pronounced impact for IMPT-2F).
The quality of both plans was comparable and the magnitude of dose changes depended mainly on the patient and the day of treatment (CT number). The choice of fields is typically lead by factors as available validated gantry angles, confidence in patient set-up accuracy and measured data of introduced immobilization material, etc.. A fundamental part of IMPT planning includes robustness analysis consisting of the assessment of most stable beam directions as well as robust optimizations, which is discussed below.

Compensating IMPT range uncertainties

The dosimetric evaluation was performed for the PTV (as motivated in section 4.2.2) of which rather the inner part (i.e. the CTV) is of clinical relevance. Regarding the location of cold spots, dose inhomogeneities of IMPT recalculations were spread all over the target volume, i.e. within the CTV as well, while for IMXT underdosage was more pronounced in the peripheral regions of the PTV, outside of the CTV. This indicated that PTV-based plan optimization does not account sufficiently for all uncertainties in IMPT which was also shown elsewhere [128].
The introduction of a "PTV range", i.e. PTV plus additional safety margins within beam direction, as it is used in clinical practice, only compensates to some extent but does not improve the main weakness of the IMPT plans: the underdosage within the central PTV area.

Uncertainties in set-up and range are well-known issues for IMPT and can be reduced by so-called robust optimization [128, 79, 109, 29]. Different robust optimization algorithms and methods can improve the sensitivity of IMPT plans in terms of set-up errors and range uncertainties by incorporating uncertainty information into the planning process. Conducting the study with robust optimization might lead to different dosimetric results. However, for this study large differences in the dosimetric consequences were not expected and it can be presumed that the conclusion would be similar. The major impact on the dose distributions of this study was assumed to be caused by anatomical changes which are only partly taken into account in some of the algorithms by estimating the caused range uncertainties. For a detailed analysis, the study would have to be repeated on initial plans calculated using a robust optimization tool.

The accuracy of IMPT treatments and the associated proton range uncertainties feature an active field of research. Different proton range verification methods, e.g. in vivo imaging by PET [106] and prompt gamma ray spectroscopy [135, 134], and recently a technique based on acoustic signals [2], were suggested. Techniques like these will improve the accuracy of IMPT treatments in the future.

Origin of different impact on IMXT and IMPT dose distributions:

There are a number of potential sources for the great differences in the impact of geometrical changes between IMPT and IMXT plans. Explanations can be given by the **different physical properties of the particles**, i.e. the particular characteristics of dose depth curves, which were one of the motivations for the conduction of the study (see section 4.1), and corresponding distinctive intensity modulated treatment **plan features** (see subsection 2.2.2). The great advantage of the protons, its finite range and high spatial precision, is at the same time a well - known issue [84, 71, 86, 76, 81, 6, 128]. While changes of density and thickness of the traversed matter lead to a slight deviation in dose values for photons, the range of the protons is changed. Intensity modulated proton plans are known to be even less robust to density changes than single field optimized plans [112, 81]. Due to the applied intensity modulation and spot scanning technique each IMPT field consisted of spots of different weights and energies. The additional modulation in depth is one of the main features of IMPT compared to IMXT. While all photon segments are of the same energy, IMPT plans consist of spot layers of various energies. Density changes can cause shifts of single spots and lead to unfavorable dose accumulations from neighboring spots which are likely to be the most pronounced source of the larger changes in proton dose distributions. Spot scanning proton plans of only one field are also exposed to this scenario (see figure 4.16). The assigned intensities vary between spots (visualized by different colors) such that shifts of single spots may result in unfavorable superpositions.

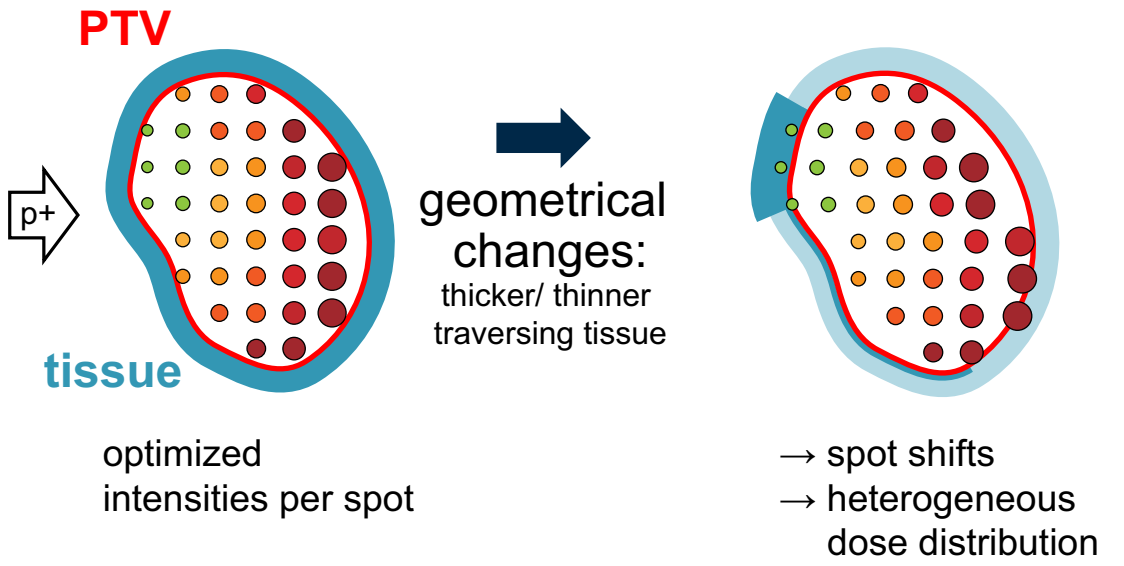

Figure 4.16: Schematic illustration of potential spot shifts of a single field IMPT plan (beam angle 270°). The introduction of more or less tissue (or material of different densities) can result in unfavorable superposition of neighboring spot weights; spot colors refer to different intensities.

The relevance of this "intrafield-shift-scenario" was investigated for the present study on one randomly picked patient example (patient 3). A single field proton plan of 45° (as utilized in both studied plans) was optimized to cover the PTV with 60 Gy, as homogeneous and conform as achievable, regardless of any OARs. Subsequent recalculations on control CTs showed remarkable differences in the dose distributions (see figure 4.17). The absolute maximum dose of the first plan increased from 60.44 Gy to 66.15 Gy at the 5th CT and to 65.87 Gy at the 25th CT. The utilization of more beams per plan allows additionally for interfield spot superpositions.

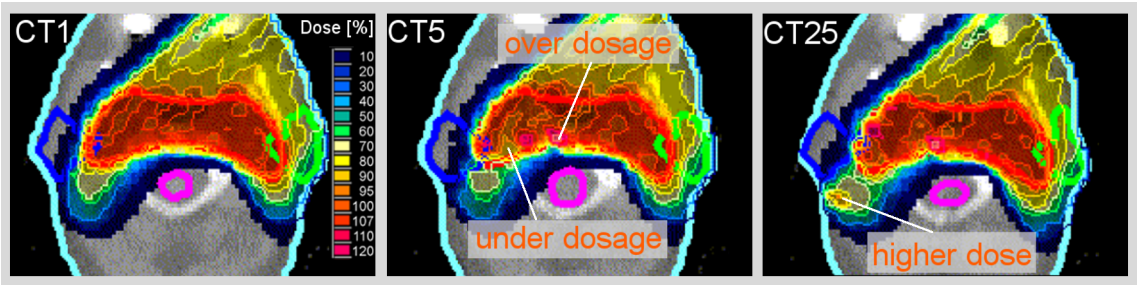

Figure 4.17: Dose distributions of a single field IMPT plan (beam angle: 45°), optimized on CT1 (left). The recalculated dose distributions on control CTs of the 5th and 25th fraction show remarkable differences (centre and right).

Furthermore the **degree of intensity modulation** (complexity of fluence patterns) or/and the **dose range** delivered by the individual fields presumably contributed to the larger changes in IMPT plans. The question if the delivered dose by one field of an IMPT plan (number of beams > 1) resulted in a more heterogene dose distribution within the PTV than one field of an IMXT plan was investigated. Additionally to the heterogeneity, measured by σ(PTV), the delivered dose interval between minimum and maximum dose to the PTV by one field was of interest.
The degree of modulation of one IMPT-field (gantry angle: 45°) and one IMXT-field (gantry angle: 0°) of the corresponding initial plans (proton: IMPT-3F) of patient three were compared by recalculating them seperately on the planning CT (CT1) (figure 4.18 and table 4.1).

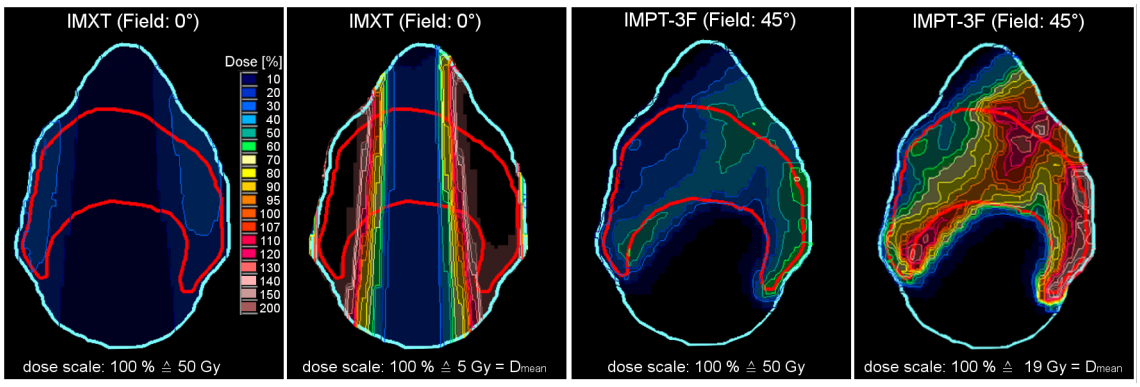

Figure 4.18: Dose distributions of one field of the IMXT plan (two left subfigures) and one field of the IMPT-3F plan of patient three (two right subfigures); each dose distribution was normalized to the prescribed dose of 50 Gy and to the mean dose contribution of the corresponding field.

Both, the dose interval and the absolute standard deviations within the PTV, were larger for the IMPT-field. The extreme dose differences within one field could become an issue in case of small spot displacements or when superimposed to the other fields of the plan, as described before.

RT technique	D_{min}(1 cm^3)	D_{max}(1 cm^3)	D_{mean}	σ(PTV)
IMXT (0°)	0.35 Gy	15.20 Gy	4.80 Gy	3.50 Gy
IMPT-3F (45°)	0.10 Gy	40.55 Gy	18.95 Gy	7.30 Gy

Table 4.1: DVH criteria of the PTV of the 45°-IMPT-field and 0°-IMXT-field of the corresponding intial plans of patient three.

Due to the smaller number of beam angles in the treatment plans, the mean dose of each field was also higher for IMPT which made the comparison of absolute σ(PTV) questionable with respect to a general statement on the degree of intensity

modulation in IMPT and IMXT. The normalization of dose distributions to D_{mean} of each field resulted in a (relative) standard deviation of σ(IMPT-3F)=0.39 and σ(IMXT)=0.73 which suggested the IMPT plans to be (even) less intensity modulated.

The analysis of the impact of geometrical changes on IMPT dose distributions by the plan properties and intensity modulations was only shortly touched and limited to a single patient case with one plan and one randomly selected field. For a more consolidated knowledge about the relevance and pronounciation of each of those effects, a more detailed analysis of more plans and fields is required.
The dosimetric consequences are likely to be an interplay of several effects and the role of each presumably varies from patient to patient or/and CT to CT.

4.5 Conclusion of planning study

The presented study investigated the impact of interfractional geometrical changes to dose distributions of IMPT and IMXT plans and demonstrated differences in the consequences of the two irradiation techniques. The two analyzed IMPT plan types, of two and three beams, showed similar trends of assessed dose values leading to similar conculsions.
Although the absolute variations of doses to OARs were larger for protons, the evaluated dose metrics for the OARs were lower than in the photon plans at all times. The PTV coverage and homogeneity turned out to be more stable in treatment with photons. For all assessed values the standard deviations were larger for IMPT compared to IMXT, indicating a stronger dependency on the individual patient. Moreover for both techniques, the variations between fractions were not always monotonic in time but assessed DVH points fluctuated between fractions, with a tendency to worsen at the end of the treatment.
For both modalities the data indicated the importance of frequent control imaging and recalculations of treatment plans on control CTs to recognize relevant anatomical changes. Plan adaptions triggered by these recalculations might reduce the underdosage of the tumor (most relevant for IMPT) and the overdosage of OARs (in IMXT).

4.6 Relevance for future clinical practice and efficiency

The obtained study results demonstrated the importance of IGRT and plan adaptions, to reduce set-up errors and account for anatomical changes, in HNC which represented a patient group who commonly undergo great anatomical changes.
Although the delivered dose of adapted plans will never be exactly as planned - due to variations in daily set-up (even with IGRT) and intrafractional motion - adaptive

planning is certainly a useful technique in order to improve dosimetric quality [119]. Adaptive planning however comes with an additional workload, as does IGRT. With respect to the workflow and required staff time, clear indicators could improve clinical efficiency. Identifying the patients and the time for whom and when replanning is reasonable would facilitate physicians' and physicists' work and hereby improve treatment quality and efficiency. Due to the complex correlations of different geometrical and dosimetric quantities (discussed in section 4.4) and an insufficient number of patient cases no indicator was found here. This will remain a future research task and for now the decission will be left to individual physicians' assessment. Recalculations of treatment plans on control CTs on a regular basis are recommended as a supportive and indespensive tool in order to prevent undesired dose depositions. Pure visual estimation is often not sufficient - at least not for protons.
Additionally to the work associated with the case identification, the current practice of plan adaptions is rather expensive as it comes along with a complex list of tasks, e.g. contouring, image registration, dose accumulation for an "exact" dose approximation over all fractions etc. (see also section 4.1).
Within the last years, steps of the adaptive planning workflow were continuously improved by progress in research and developments of specific software for adaptive planning[3]. Deformable image registration [48, 72], automatic contouring and planning [119, 77] are only some examples for ongoing research fields which promise to facilitate the workflow of adaptive planning further in the future.

The additional workload of adaptive planning may still require more staff. Previously various national and international studies were performed to identify required resources in radiotherapy [78, 137]. Distinctive associations and institutes give recommendations/guidelines on required staff capacities typically measured by patient load, number and types of machines, as well as utilized RT techniques (e.g. [60]). IGRT was partly covered in prior investigations - for the relatively novel and recently more and more established adaptive planning technique, data about the associated workload is lacking so far. QUIRO, a German study to measure the required resources in radiotherapy, found that times of room occupancy and staff involvement at the actual treatment varied strongly with the tumor entity, patient and treatment center [137]. The average overall involved working time of physicists, physicans and technicians at the first treatment (always with IGRT) was measured to be 74.9 minutes, a routine irradiation with imaging 39.7 min and without 22.9 min. Treatment room occupancy times were specified by 23.7 min at first treatment, 18.3 min and 10.6 min with and without IGRT, respectively. IGRT was applied in 73% of all HNC treatments, patients who were further identified to feature the longest treatment times compared to all other entities. With respect to the clinical work of treatment preparation, it was stated that the structure definition was the most time consuming process for physicians. Both delineation and planning was specified by

[3] e.g. www.brainlab.com/wp-content/uploads/2014/01/Flyer-iPlan-RT-Adaptive.pdf
or www.varian.com/sites/default/files/resource_attachments/VelocityCaseStudyCHUV.pdf

physicians and physicist, to be the most time consuming for HNC compared to other entities, demonstrating the cost of new plan generations - as for adaptive planning. Ongoing studies are currently performed in order to update prior study results to the current state of the art techniques of clinical practice.

From the perspective of the main clinical intention "to treat the patient with the best achievable dose distribution", it should however be worthwhile to do everything possible in order to achieve an applied dose in each fraction which is as close as possible to the desired planned dose - by taking the time for accurate positioning, for dose recalculations to estimate the current situation and for treatment plan adaptions if required.

5 Prioritized treatment planning to reduce IMPT delivery times

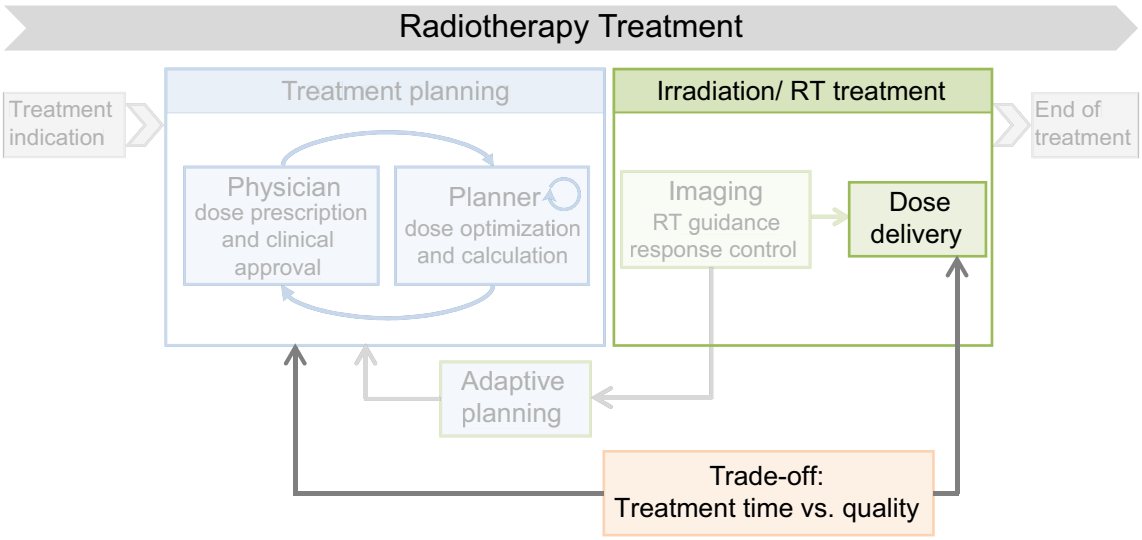

Figure 5.1: Efficiency and quality in radiotherapy, focusing on delivery efficiency.

Along with high dosimetric quality, short treatment times are a major concern in radiotherapy. The delivery time of a treatment plan and its dosimetric quality are however correlated (figure 5.1) which leads to inevitable trade-offs between both objectives (see section 2.3.3).

The following chapter suggests prioritized optimization [143] as a suitable method to reduce treatment times without compromising plan quality. The optimization routine, referred to as PrEfOpt (prioritized efficiency optimization), was developed for intensity modulated proton therapy. Its potential is demonstrated by two patient cases of different tumor sites.

5.1 Introduction to prioritized efficiency optimization

Short treatment times are important for various reasons in radiotherapy: faster plan deliveries increase patient comfort, cost-effectiveness and the patient capacities of clinics [130, 123]. Moreover shorter irradiation times potentially reduce intrafractional dose uncertainties, due to patient movement and organ deformation, and may additionally have a positive impact on biological response [91, 103, 11]. During the last years faster irradiation techniques were developed, volumetric arc [100] therapy being an example for an increasingly used modality due to its short treatment times. In intensity modulated radiotherapy with photons as well as with protons the degree of modulation often determines the plan quality and consequently the radiation time (RT time) (see section 2.3.3). The aim of greater efficiency is correlated to plan quality such that the major challenge when increasing delivery efficiency is not to compromise dosimetric quality. Treatment planning faces a trade-off problem, not only with respect to conflicting dosimetric goals, but also between plan quality and delivery efficiency [38, 22, 144, 91].
Multicriteria optimization is a well suitable method to investigate optimization tasks of interdependent objectives (MCO see section 2.3.1 and 3.2). MCO treatment planning is based on the creation of a database of optimal plans, the so-called Pareto front. It allows the user to search interactively by surface navigation for the plan of the best trade-off [37]. Craft et al. utilized this approach to study the complexity of IMXT plans as a measure for efficiency versus quality [38].
Previous studies on correlations between delivery efficiency and quality demonstrated that RT times of IMXT and IMPT plans can often be decreased without compromising plan quality [33, 38, 67, 91, 26, 130]. Sometimes plans are optimized to an unnecessary complexity [22]. The degeneracy of the solution space allows to generate similar dose distributions by different fluence maps or spot patterns [22, 26].

Different methods to decrease IMPT delivery times have been published before [67, 26, 130] and are partly realized in clinical practice - mostly focusing on the number of spots and energy layers (IMPT plans: see section 2.2.2). IMPT RT times can be reduced at different stages of the planning process: prior to optimization by selecting a large spot grid, via post-processing methods, e.g. by eliminating selective spots, or as a part of the optimization routine. The initial spot raster, given by the lateral spot distance Δx and Δy and the steps in depth Δz, defines the number of available spots. Larger grids typically reduce application times but concurrently decrease the number of degrees of freedom for the optimization. A trade-off strategy which keeps the number of spots at a minimum level but high enough to achieve adequate dosimetric qualities is required [54]. Non-uniform depth-scanning decreases the number of required energies, in particular for deep seated tumors [67]. Recent publications demonstrated remarkable reductions of IMPT times by eliminating energy layers, especially for facilities with large energy switch times [26, 130].
IMPT delivery times strongly depend on the individual facility and its characteris-

tics. Proton currents are frequently assumed to be constant or are not specifically addressed. The characteristic of variable currents, dependent on the optimized spot weight distribution, is crucial for some clinics: treatment currents determined by the lowest spot weight per energy layer often result in low currents and prolong treatment times. Particularly crucial are layers of large intensity differences between lowest and highest spot intensity. For different centers, dependent on their facility features, distinctive spot distributions may be more favorable than others with respect to an efficient delivery. In this context it should also be mentioned that proton facilities face a lowest spot intensity limit given by the monitor chamber which can lead to non deliverable spot patterns. Post-processing interactions such as manual elimination of the "responsible spots" can solve the issue but may degrade plan quality [58, 148].

From the background perspective that each facility has different technical characteristics and faces specific application difficulties, an optimization routine was developed which offers distinctive methods to increase delivery efficiency of IMPT plans. With the intention to control dosimetric quality during efficiency optimization, and to discuss potential trade-offs to plan quality, the algorithm was integrated into a prioritized optimization scheme [143]. Prioritized optimization prescribes a stepwise approach of implemented objectives which are translated into a mathematical optimization routine (see section 5.2.1). The here presented prioritized efficiency optimization routine (PrEfOpt) optimizes the plan quality first and allows to reduce treatment time via different alternative methods in the final step of the routine. The feasibility and potential of implemented efficiency optimization methods are demonstrated by applying it to a clinical astrocytoma case. The resulting treatment times were evaluated for two virtual facilities, i.e. with a constant and variable current.

5.2 The prioritized efficiency optimization algorithm

5.2.1 Prioritized treatment planning - the basis of PrEfOpt

Prioritized optimization prescribes a stepwise optimization routine of several consecutive optimization runs with different objective functions while the order refers to the clinical importance of each objective. Typically, and as initially suggested by Wilkens et al. for head and neck cancer patients [143], the target coverage is optimized in the first step under consideration of non-negotiable hard constraints to OARs (e.g. the maximum dose to the spinal cord). Subsequent steps reduce doses to OARs and helper structures of lower priorities or generally to all normal tissue. Achievements of each optimization run are turned into hard constraints for subsequent optimizations which can only be violated within a specified range: a so-called slip-factor (here: $\tilde{s}$) is introduced to enlarge the solution space by loosening previously derived hard constraints. This concept enables the user to control the

dosimetric trade-off between specified objectives, as illustrated in figure 5.2 by an astrocytoma patient case for two optimization steps: 1) the homogeneous PTV coverage with the prescribed dose of 60 Gy (step Ia) and 2) the reduction of the mean dose to brainstem and PTVwall, a ring shaped structure around the PTV (step Ib).

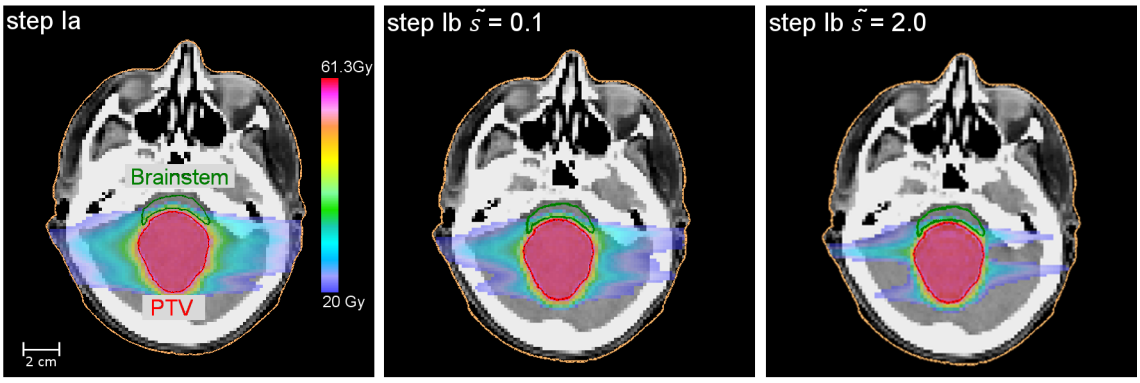

(a) Dose distributions of an astrocytoma patient case, optimized by step Ia and step Ib with $\tilde{s} = 0.1$ and $\tilde{s} = 2.0$; delineated structures: PTV (red) and brainstem (excluding PTV plus 2 mm) (green).

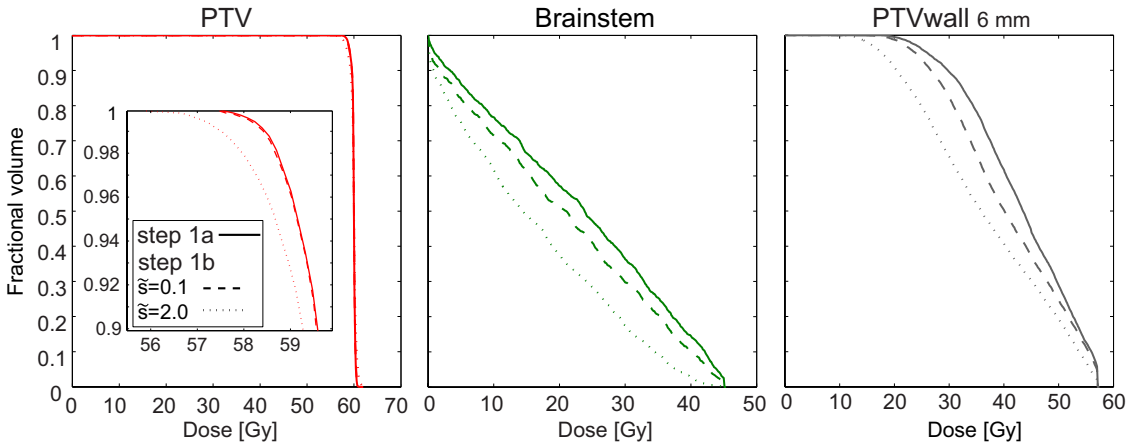

(b) Dose volume histograms of an astrocytoma patient case, optimized by step Ia (solid line) and step Ib with $\tilde{s} = 0.1$ (dashed line) and $\tilde{s} = 2.0$ (dotted line).

Figure 5.2: The slip factor concept illustrated by dose distributions and corresponding DVHs of an astrocytoma patient; results were derived by prioritized optimization step Ia and Ib.

5.2.2 Efficiency optimization methods of PrEfOpt

Similar to the original prioritized optimization routine (see above), the prioritized efficiency optimization algorithm (PrEfOpt) prescribes a stepwise optimization routine. PrEfOpt consists of two steps (figure 5.3). Step I comprises two consecutive sub-runs to optimize the dose distribution according to the clinical prescription: first

(step Ia) the homogeneous PTV coverage is optimized; second (step Ib) the mean dose of selective structures is reduced while considering prior achievements, which are introduced as constraints.

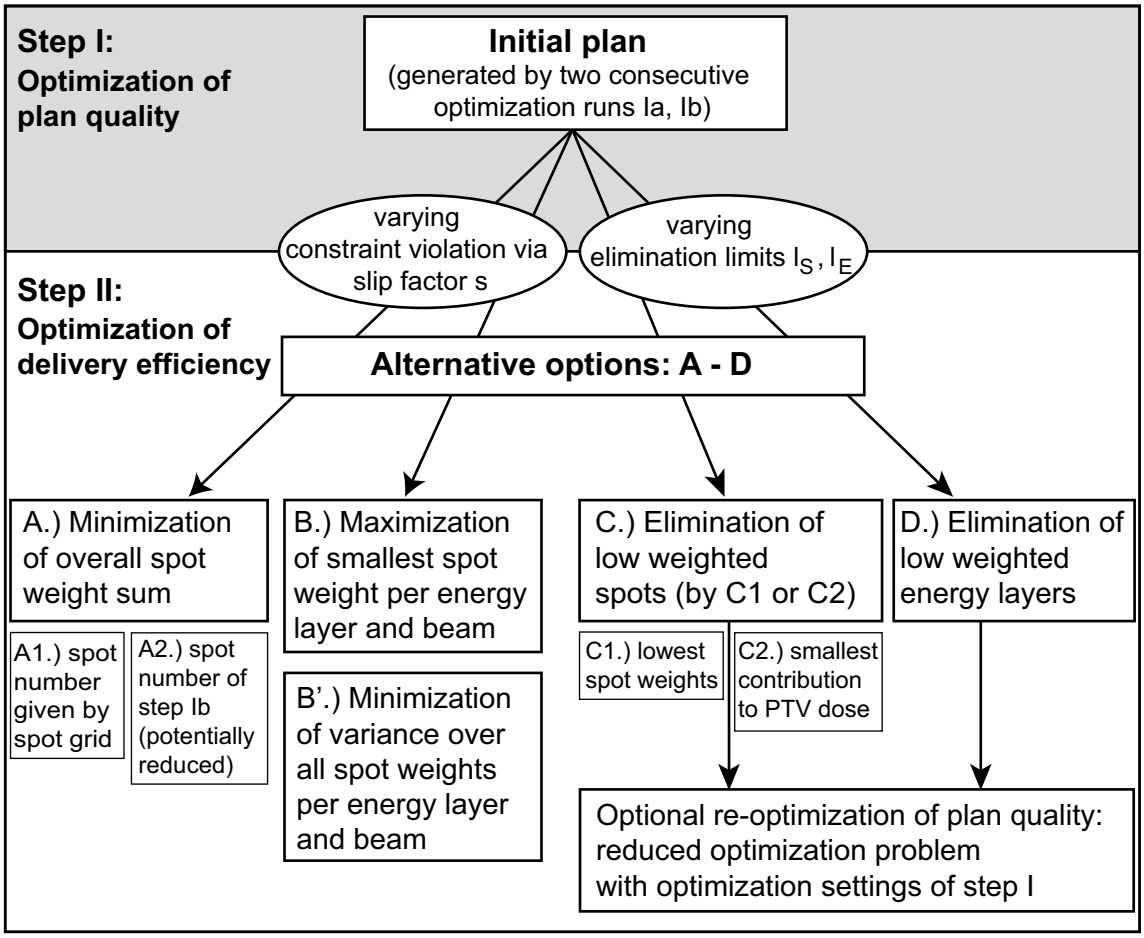

Figure 5.3: The optimization routine PrEfOpt: Plan quality is obtained in step I according to Wilkens et al. [143]; Step II offers four alternative methods to reduce the treatment time. The trade-off between plan quality (step I) and treatment time (step II) is controlled by option dependent "trade-off parameters". Method A1 and A2, as well as C1 and C2, are sub-versions of the associated methods. Option B' is an alternative to method B.

Delivery efficiency is optimized in step II by one of four alternative methods. Method A reduces the sum over all spot intensities; A1 and A2 are alternative sub-versions which differ in the number of available spots during the optimization. While method A1 places all spots of the initial spot grid at disposal, method A2 eliminates spots of zero weight after step Ib and consequently reduces the optimization problem. In case of no zero spot weights after step Ib, method A1 and A2 are identical. Method B maximizes the smallest spot intensity per energy and beam, and method B', an alternative to B, minimizes the spot weight variance within each energy layer. Both, method B and B', were developed with the intention to reduce times for facilities

with variable current. For method A and B prior dosimetric achievements are turned into hard constraints which may be violated within a small specified range given by the slip-factor s. Method C and D reduce the spot pattern by eliminating spots and energy layers, respectively. The number of eliminated spots (C) is defined by a variable limit l_S which is applied onto a limiting criterion (C1: the median spot weight, C2: the average PTV dose contribution of each spot). The number of eliminated energy layers per beam (D) is defined by the parameter l_E[1]: the l_E lowest weighted energy layers are deleted. For both methods, C and D, a successive re-optimization run of the plan quality using the remaining spots/layers and otherwise identical parameters of step I is optional.

5.2.3 Mathematical formulation of PrEfOpt

Each step of PrEfOpt comprises an objective function to optimize the vector $\underline{\omega}$ of n spot weights ω_j which multiplied by the influence matrix D_{ij} yields the dose $D_i(\underline{\omega})$ to the voxel i. OAR and PTV describe the set of voxels of the corresponding structure volumes (total number of voxels: N_{OAR} and N_{PTV}). Each spot weight w_j belongs to one beam and one energy layer.
The energies of each beam B (number of beams: N_B) are defined by:

$$E_k(B) \text{ with } k = \{1,...,M(B)\} \tag{5.1}$$

and energy layers by:

$$L(B,k) = \{j \in \{1,...n\} | j \text{ belongs to kth energy layer of beam } B\} \tag{5.2}$$

All optimization runs are subject to:

$$\omega_j \geq 0 \quad \forall\ j \in \{1,...n\} \tag{5.3}$$

and defined hard maximum dose constraints D^{max} to OARs:

$$D_i(\underline{\omega}) \leq D_i^{max} \quad \forall\ i \in OAR \tag{5.4}$$

Step I: Optimization of a homogeneous coverage of the PTV with the prescribed dose D^{prescr} by the standard quadratic objective function (Ia) and reduction of the mean dose D^{mean} to selective OARs (Ib) while the prior optimized PTV coverage is maintained by turning the achievements of step Ia into hard constraints. The introduction of $\tilde{s}$ allows for small deteriorations to enlarge the solution space. For the discussed case $\tilde{s} = 0.1$.

[1]The number l_E includes energy layers which consist exclusively of zero spot weights such that the final and the initial number of energy layers subtracted l_E energies times the number of beams may deviate; subsequent re-optimization may additionally lead to energy layers of zero weight which are then not taken into account in the final number of energy layers.

Step Ia:

$$F^{Ia}(\underline{\omega}^{Ia}) = \sum_{i \in PTV} (D_i(\underline{\omega}^{Ia}) - D^{prescr})^2 = min \tag{5.5}$$

Step Ib:

$$F^{Ib}(\underline{\omega}^{Ib}) = \frac{1}{N_{OAR}} \sum_{i \in OAR} D_i(\underline{\omega}^{Ib}) = min \tag{5.6}$$

subject to:

$$F^{Ia}(\underline{\omega}^{Ib}) = \sum_{i \in PTV} (D_i(\underline{\omega}^{Ib}) - D^{prescr})^2 \leq F^{Ia}(\underline{\omega}^{Ia})(1 + \tilde{s}) \tag{5.7}$$

Step II: Optimization of delivery efficiency by one of the presented alternative methods (A-D) and associated sub-versions.

Objective functions of case A and B are optimized with respect to previous achievements. A slip factor s ($s \geq \tilde{s} \geq 0$) is introduced to control the trade-off between plan quality (step I) and treatment time.
Case A: Minimization of the sum over all spot weights:
Case A1: All n spots of the initial spot grid are available for the optimization:

$$F^{II}(\underline{\omega}^{II}) = \sum_{j=1}^{n} \omega_j^{II} = min \tag{5.8}$$

subject to:

$$\sum_{i \in PTV} (D_i(\underline{\omega}^{II}) - D^{prescr})^2 \leq F^{Ia}(\underline{\omega}^{Ia})(1 + s)^2 \tag{5.9}$$

$$\frac{1}{N_{OAR}} \sum_{i \in OAR} D_i(\underline{\omega}^{II}) \leq F^{Ib}(\underline{\omega}^{Ib}) \tag{5.10}$$

Note that the slip factor is only applied to the PTV term, not to the achieved D^{mean} of the OAR.
Case A2: The available spot number is reduced by excluding spots which had zero weight in step Ib:

$$\omega_j^{II} = 0 \qquad \forall \quad j \quad \text{with} \quad \omega_j^{Ib} = 0 \tag{5.11}$$

Optimization of objective function 5.8 with a reduced number of spots, subject to equations 5.9 and 5.10.

For both methods B and B' spots of zero weight are eliminated prior to optimization according to equation 5.11.
Case B: Maximization of the smallest spot weight $t_{B,k} = min(\omega_j | j \in L(B,k))$:

$$F^{II}(\underline{t}) = \sum_{B} \sum_{k=1}^{M(B)} t_{B,k} = max \tag{5.12}$$

subject to equations 5.9 and 5.10 and:

$$\omega_j \; > \; t_{B,k}^{Ib} \qquad \forall \; j \in L(B,k) \tag{5.13}$$

Equation 5.13 guarantees that all spot weights ω_j of energy layer $L(B,k)$ are larger than the smallest spot weight $t_{B,k}^{Ib}$ of step Ib.
Case B': Minimization of the variance $V(\omega_j |\; j \; \in L(B,k))$:

$$F^{II}(\underline{\omega}^{II}) = \sum_{B} \sum_{k=1}^{M(B)} V(\omega_j | j \; \in L(B,k)) = min \tag{5.14}$$

subject to equations 5.9, 5.10 and 5.13.

Case C and D reduce the optimization problem by a defined number of spots (limit l_S) (C) or energy layers (limit l_E) (D).
Case C: Elimination of spot weights lower than a specified threshold:
Case C1: Spot elimination threshold given by the median spot weight $\tilde{\omega}_j^{Ib}$ and l_S:

$$\omega_j^{II} = 0 \qquad \forall \quad j \quad \text{with} \quad \omega_j^{II} \leq l_S \cdot \tilde{\omega}_j^{Ib} \quad \text{with} \; \; l_S \; \geq 0 \tag{5.15}$$

Case C2: Spot elimination threshold given by the average contribution of each spot to the integral PTV dose $\overline{d}(\underline{\omega}^{Ib})$ and l_S:

$$\omega_j^{II} = 0 \qquad \forall \; \; j \text{ with} \quad d_j(\omega_j^{Ib}) = \sum_{i \; \in \; PTV} D_{ij} \cdot \omega_j^{Ib} \leq l_S \cdot \overline{d}(\underline{\omega}^{Ib}) \tag{5.16}$$

and

$$\overline{d}(\underline{\omega}^{Ib}) = \frac{1}{n} \sum_{i \; \in \; PTV} D_i(\underline{\omega}^{Ib}) \quad \text{and} \quad l_S \; \geq 0 \tag{5.17}$$

Case D: Elimination of the l_E lowest weighted energy layers of each beam:

$$\omega_j^{II} = 0 \quad \forall \; j \in \{\text{the } l_E \text{ smallest } S(B,k) = \sum_{j \; \in \; L(B,k)} \omega_j^{II}\}, \; l_E \in \mathbb{N} \tag{5.18}$$

Case C and D: Optional re-optimization of the resulting optimization problem with the reduced number of spots and the optimization parameter used in step I.

5.2.4 Treatment time implementation

Treatment times were calculated as the sum over energy switch times t_E and the actual beam-on time t_S of a continuous scanning system, i.e. t_S included the scanning time. The minimum spot weight was defined as $\omega_{feasible}$=0.006 ($\omega_j = 1$ refers to 10^6 particles). All spot weights $\omega_j \leq \omega_{feasible}$ were set to zero after optimization. The default energy switch time was t_E= 1 s. Two virtual facilities with different proton current characteristics were simulated (figure 5.4).

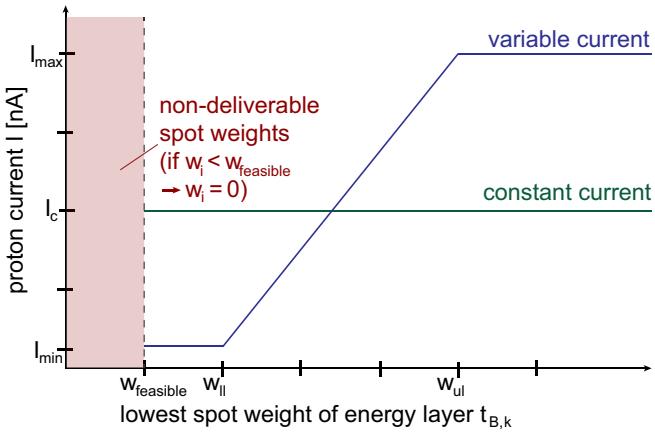

Figure 5.4: Proton current implementation in PrEfOpt simulating two facility types, i.e. of variable and constant proton current.

Facility type 1: constant proton current $I_c = 1\ nA$.
Facility type 2: variable proton current $I_v(\underline{\omega}) = [I_{min}, I_{max}]$, dependent on the lowest spot intensity of each energy layer and beam $t_{B,k}$. $I_v(\underline{\omega})$ was implemented by a linear function between a lower and upper weight limit, ω_{ll} and ω_{ul}:

$$\begin{aligned} t_{B,k} \leq \omega_{ll} = 0.06 \quad &\rightarrow \quad I_v = I_{min} = 0.1\ nA \\ t_{B,k} \geq \omega_{ul} = 150 \quad &\rightarrow \quad I_v = I_{max} = 2.0\ nA \end{aligned} \tag{5.19}$$

5.3 Application of PrEfOpt: methods

Implementation into a treatment planning system

The algorithm was implemented into a research planning system for 3D spot scanning protons [80, 98] in the computational environment of CERR (MATLAB) [41, 116]. All runs were optimized with the commercial toolbox Mosek (www.mosek.com). Dose calculations were based on dose depth curves which were previously generated by Monte Carlo simulations [65].

5.3.1 Patient cases and evaluation criteria

PrEfOpt was applied to an astrocytoma and a prostate case (figure 5.5), both previously treated with photon therapy at Klinkum rechts der Isar. Clinical contours and prescriptions were utilized for retrospective planning. Prescribed doses to the PTVs were 60 Gy for the astrocytoma and 74 Gy for the prostate patient. In order to achieve greater dose conformity, supportive ring shaped helper structures were generated around the PTV with different radiuses, referred to as "PTVwall".

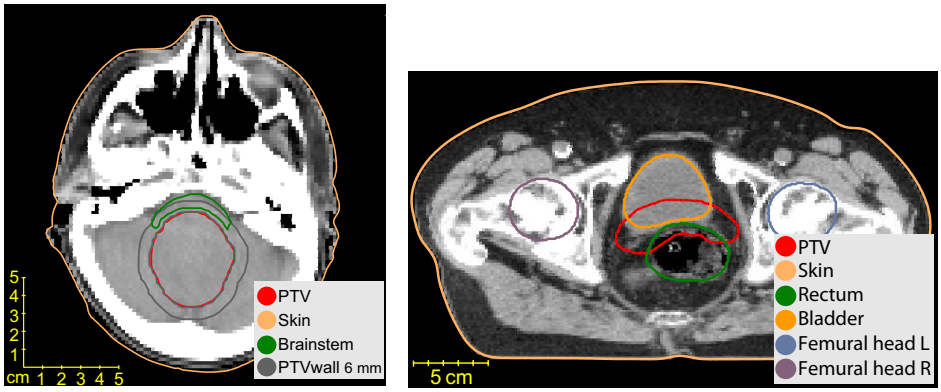

(a) Astrocytoma patient (b) Prostate patient

Figure 5.5: Astrocytoma and prostate patient: CT images and delineated contours.

Evaluation criteria

Dosimetric quality was assessed by various DVH indicators of the PTV and OARs (see section 2.3.2). PTVs were analyzed by $D_{min}(1\ cm^3)$, $D_{max}(1\ cm^3)$ and D_{mean}, as well as by coverage, conformity and homogeneity (indices and σ(PTV), see equations 2.9, 2.10, 2.11). $D_{max}(1\ cm^3)$ and D_{mean} of case specific relevant OARs were evaluated, i.e. of the brainstem (excluding the PTV plus 2 mm) for the astrocytoma patient, and of the rectum and bladder (excluding the CTV) for the prostate case. Due to the formulation of the algorithm the maximum dose to OARs was not worsened in step II. In order to compare the potential of each efficiency optimization method an automatic script was applied. The plan of the shortest delivery time was determined for each facility which maintained the initial dosimetric criteria up to a maximum change of $\Delta D = \pm 1\%$ and $\pm 2\%$ in $D_{min}(1\ cm^3)$(PTV) and $D_{max}(1\ cm^3)$(PTV) (referred to as evaluation criteria D1 and D2). The derived relative delivery time reductions $\Delta t_{RT}/t_{RT}$(initial) for facilities with constant current (delivery time: RT time 1) and variable current (RT time 2) were analyzed for all methods.

5.3.2 Treatment planning with PrEfOpt

Geometrical settings and plan quality optimization

For both cases, plans of three different geometries and optimization settings were calculated, referred to as "ASTRO G1/G2/G3" and "PRO G1/G2/G3" (settings see tables A.16 and A.17). All plans featured two opposed beams (90° and 270°, except for ASTRO G3) which were simultaneously optimized. The spot patterns varied by the volume within the spots were placed (PTV plus variable margin) and by the spot distances, i.e. the lateral spacing $\Delta x = \Delta y$ and non-uniform depth scanning $\Delta z = PWM \cdot w_{80}$ (with a variable "peak width multiplier" (PWM) and the width w_{80} at the 80% intensity level of the Bragg peak) (table A.16). Available energies ranged from 50 MeV to 250 MeV in steps of 1 MeV. The beam featured a constant width of $FWHM = 2 \cdot \Delta x$ at the patient surface (FWHM: full width half maximum of a Gaussian profile).
The initial plans, referring to the results after optimization of step Ib, were optimized with a slip-factor of $\tilde{s}$=0.1 in step Ib for all cases. Plan quality and efficiency indicators of the initial plans which were the baseline comparison results for all subsequent efficiency optimized plan results are presented in table A.18.

Trade-off exploration of delivery time and plan quality

Case dependent "trade-off parameters" allowed to control and steer the compromise between plan quality and treatment time for each optimization method (table 5.1).

	Method A and B	Method C	Method D
Trade-off parameter	slip factor s, $s > \tilde{s} > 0$ utilized $s \in [0.1, ..., 4.8]$	elimination limit l_S, $l_S > 0$ utilized $l_S \in [0.01, ..., 1]$	elimination limit l_E, $l_E \in \mathbb{N}$ utilized $l_E \in [1, .., 15]$
Functionality	controls the degree of constraint violation	determines the number of eliminated spots (indirectly)	determines the number of eliminated energy layers per beam

Table 5.1: Overview of implemented method dependent trade-off parameters; the utilized values refer to the performed planning study.

5.4 Application of PrEfOpt: results

Each initial plan was optimized by all alternative efficiency optimization methods (figure 5.3) with varying associated trade-off parameters s, l_S and l_E.
In the following, first, the results of selective method-facility combinations for the astrocytoma patient are presented; prostate results follow by demonstrating similiarities and differences to the astrocytoma results. The demonstrated method-facility combinations restrict to one alternative of each sub-methods. A comparison of sub-versions is presented afterwards. Finally the impact of energy switch times

is analyzed. As some methods were specifically developed for one facility type, e.g. method A for constant and B for variable currents, selective demonstrations may focus more specifically on the "intended" method-facility constellations.

5.4.1 Trade-off results for an astrocytoma patient

Illustration of the slip-factor concept in efficiency optimization

DVH results of the initial and two efficiency optimized plans (with "the minimization of the total spot weight sum", $s = 0.4$ and $s = 1.2$) are depicted in figure 5.6. The larger slip factor permitted greater deviations from the initially achieved PTV coverage (step I) and enabled hereby superior optimization of the underlying objective function which resulted in shorter treatment times. The calculated RT times for a constant current were reduced from 191.6 s to 155.2 s for $s = 0.4$ and to 141.0 s for $s = 1.2$. Compromises were found in slightly decreasing minimum doses: $D_{min}(1\ cm^3)(initial) = 58.6$ Gy, $D_{min}(1\ cm^3)(s = 0.4) = 58.2$ Gy and $D_{min}(1\ cm^3)(s = 1.2) = 57.2$ Gy. The PTV coverage with the 95%-isodose of initially 100% was maintained for $s = 0.4$ and reduced to 98.7% for $s = 1.2$. Due to the defined hard constraints on D_{max} for all runs and on the achieved D_{mean} of step Ib, brainstem doses of both efficiency optimized plans were equally good or lower than in the initial plan.

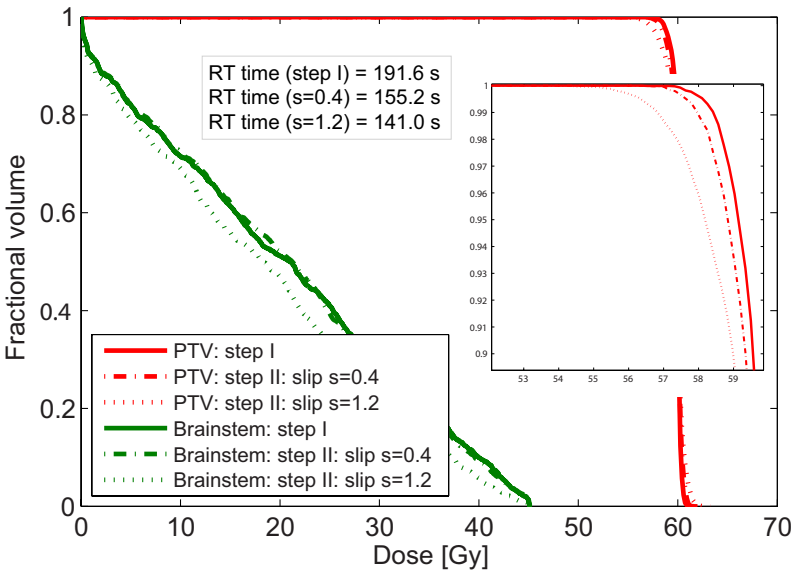

Figure 5.6: The impact of the slip factor s on efficiency-optimization: Dose volume histograms of the initial plan (solid line) and two plans after optimizing the plan via "minimization of the overall spot weight sums" (method A) with slip $s = 0.4$ (dashed line) and $s = 1.2$ (dotted line).

Trade-off results for facilities with a constant current

The largest time reduction was achieved by minimizing the total spot weight sum (A) which is visualized in the corresponding trade-off plot by a gap in treatment time between step I and the first plan of step II ($s = 0.4$) at similar doses (figure 5.7, left; and DVH figure 5.6). The least time was saved by eliminating spots without re-optimization. The efficacy of this method was improved by re-optimizing the problem as it enabled the elimination of a larger number of spots (figure 5.14, left). Dose distributions derived by eliminating energy layers were qualitatively not comparable to the initial plan but required subsequent re-optimization of plan quality (figure 5.7, right). The hereby derived time reductions were comparable to the gain achieved by method A. The presented trade-off plots showed a trend of diverging $D_{min}(1\ cm^3)$ and $D_{max}(1\ cm^3)$ of the PTV and decreasing $D_{max}(1\ cm^3)$ of the brainstem with shorter treatment times.

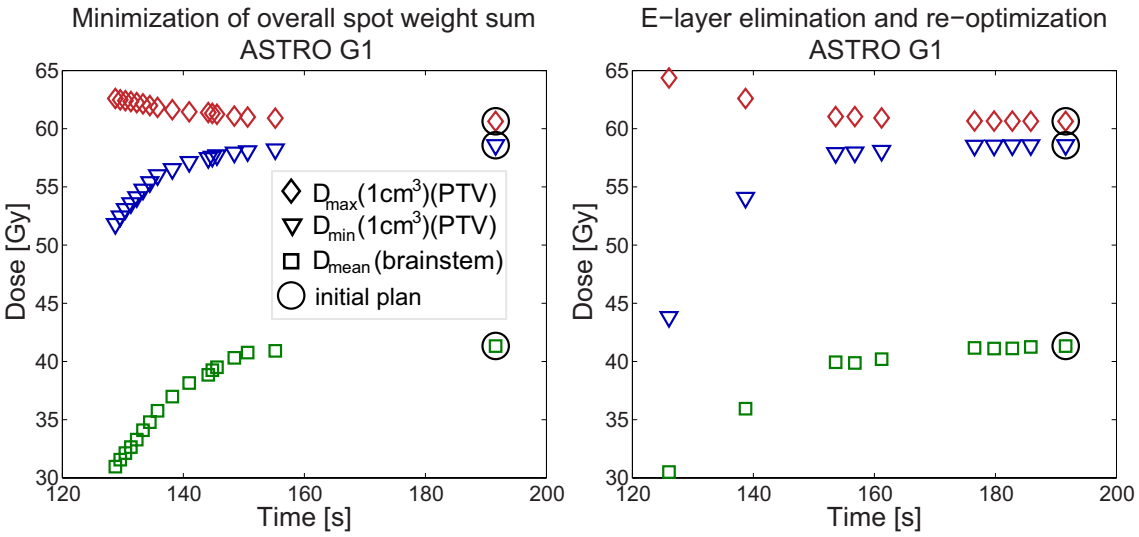

Figure 5.7: Trade-off between plan quality and delivery time for an astrocytoma case with a constant treatment current. Each subplot illustrates the plan results optimized by the specified method. Each plan is represented by three DVH points; initial plan results (without efficiency optimization) are encircled.

Trade-off results for facilities with a variable current

By maximizing the smallest spot weight of each energy layer (figure 5.8, left) times were reduced by e.g. $\Delta t_{RT}(I_v) = 76.9\%$ at a constant D95-coverage of 100% and a decrease in $\Delta\ D_{min}(1\ cm^3) < 0.2\%$. Similar results were achieved by deleting small spot weights (C) (figure 5.8, right).

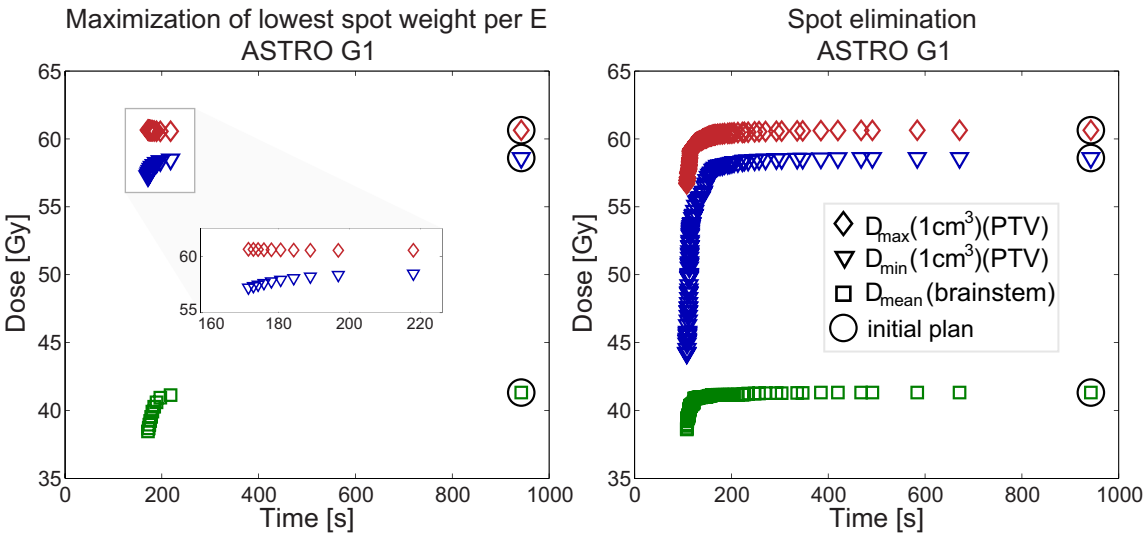

Figure 5.8: Trade-off between plan quality and delivery time for an astrocytoma case with a variable treatment current. Each subplot illustrates the plan results optimized by the specified method. Each plan is represented by three DVH points; initial plan results (without efficiency optimization) are encircled.

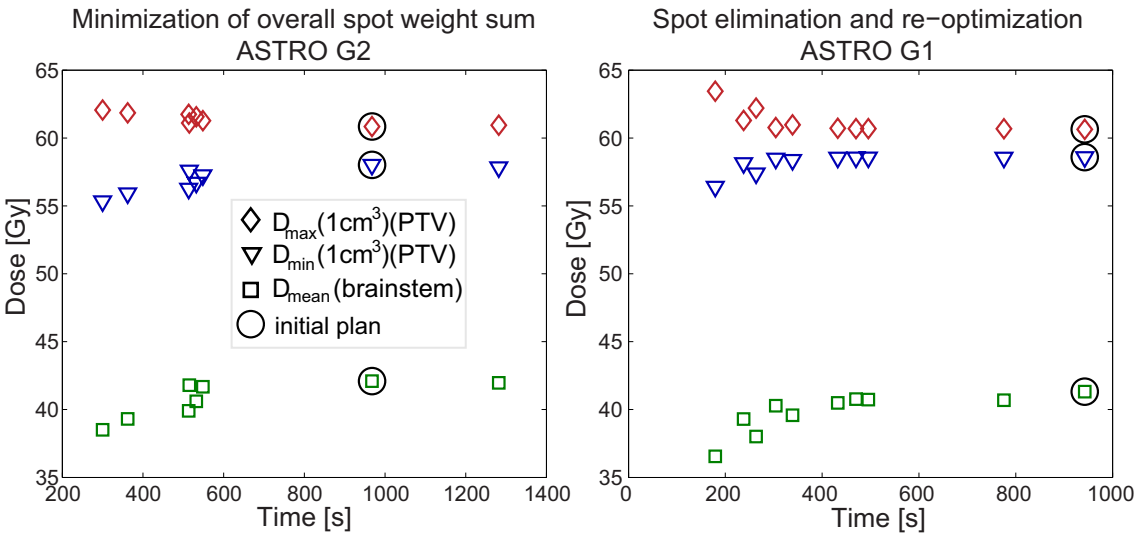

Figure 5.9: Trade-off between plan quality and delivery time for astrocytoma cases derived by less suitable methods for variable treatment current facilities.

A larger number of spots was eliminated by method C with consecutive re-optimization, which also lead to time reductions compared to the initial plan - but less than without re-optimization (figure 5.9, right). "Minimizing the total spot weight sum" resulted in larger and shorter delivery times with varying plan qualities (figure 5.9, left). Similar results were obtained by eliminating energy layers with re-optimization. Both re-optimization runs (of method C and D) as well as method A did not result in strictly montonic correlations between the obtained delivery times and quality indicators, i.e. decreasing delivery times did not lead to simultaneously strictly diverging $D_{min}(1\ cm^3)$ and $D_{max}(1\ cm^3)$ of the PTV. The results of both re-optimization runs, after spot and energy elimination, indicated that less spots or energy layers do not necessarily result in shorter treatment times.

Results of all optimization method-facility-combinations

Achieved time savings for all optimization variants and two current implementations, derived by the above suggested evaluation criteria D1 and D2, of one examplary astrocytoma patient are presented in table 5.2. The obtained delivery time reductions of all astrocytoma geometries and facility-method combinations can be found in table A.19. Corresponding plan properties, i.e. dosimetric criteria and efficiency determining parameters, are presented in tables A.21 - A.26.

Proton	Eval.	**Method A**		**Method B**		**Method C1**		**Method C2**		**Method D**	
current	criteria	A1	A2	B	B'	NR	R	NR	R	NR	R
constant	D1	21.4	13.4	4.1	0.0	1.4	4.9	1.9	4.4	0.0	15.9
	D2	24.5	16.5	6.3	0.0	1.7	5.9	3.2	11.2	1.9	19.8
variable	D1	29.5	36.6	80.5	34.9	81.8	67.7	66.4	44.3	0.0	15.0
	D2	46.1	47.0	81.5	34.9	83.3	74.8	69.8	53.5	0.6	30.7

Table 5.2: Achieved time savings [%] for one astrocytoma geometry (ASTRO G1); the evaluation criteria D1 and D2 refer to 1% and 2% deviations in $D_{min}(1\ cm^3)$ and $D_{max}\ (1\ cm^3)$ within the PTV.

5.4.2 Trade-off results for a prostate patient

The prostate results obtained by methods A, C and D were similar to the trends derived for the astrocytoma patient - relative time reductions differed though (figures 5.10 and 5.11, left). Contrary to the astrocytoma patient, method B ("maximization of lowest spot intensity") did not reduce RT times within the defined evaluation criteria but for dose changes larger than 2% in $D_{min}(1\ cm^3)$ and $D_{max}(1\ cm^3)$ of the PTV (figure 5.11, right).
Achieved time reductions of all prostate geometries and facility-method combinations can be found in table A.20. Corresponding plan properties, dosimetric criteria and efficiency determining parameters, are presented in tables A.27 - A.32.

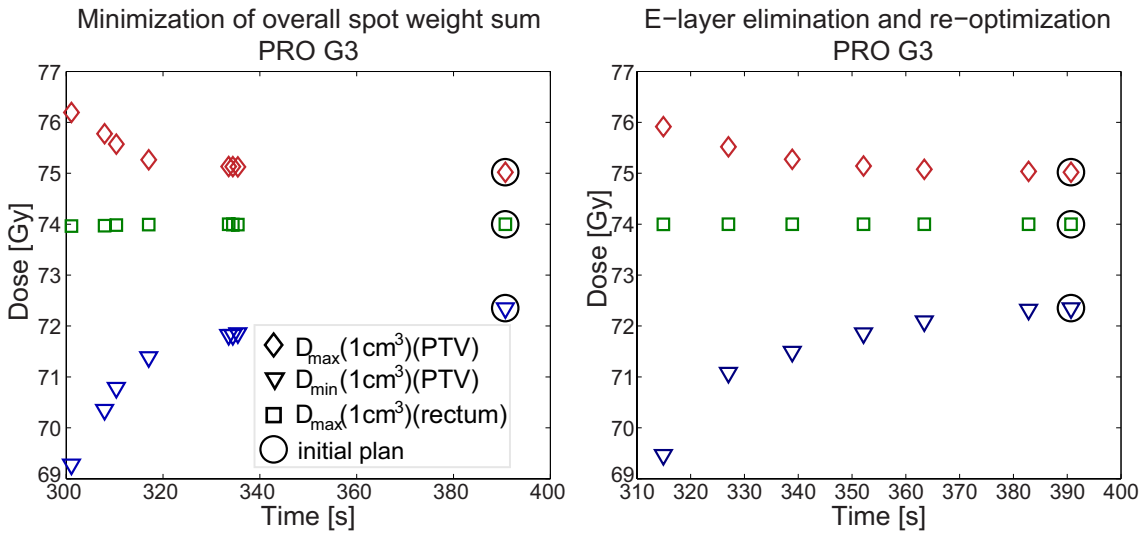

Figure 5.10: Trade-off between plan quality and delivery time for a prostate case and a facility with a constant current. Each subplot illustrates the results optimized by the optional methods given in the title of subfigure. Plans are represented by three DVH points. The plan results of step I are encircled.

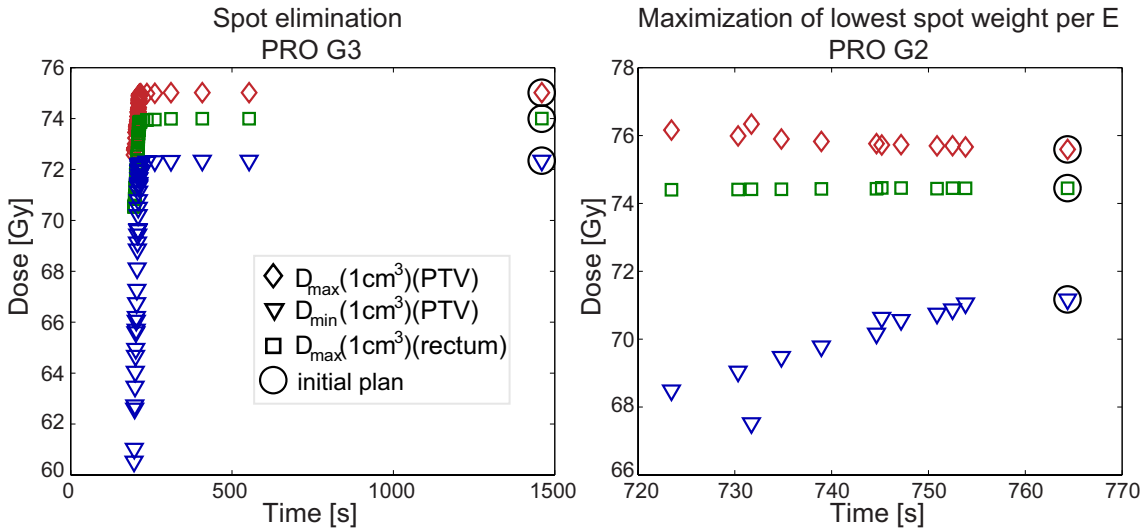

Figure 5.11: Trade-off between plan quality and delivery time for prostate cases and a facility with a variable current. Elimination of spots resulted in shorter delivery times (left); method B did not lead to reduced times within specified quality criteria (right).

5.4.3 Additional sub-method alternatives

Minimization of spot weight variance

Minimizing the variance of spot weights within each energy layer resulted in shorter RT times for $I = I_v$ for both patients - for the prostate case however not within specified limiting dose criteria. Time reductions of 60% were achievable however for minimum doses below the selected 2% evaluation limit (figure 5.12, right).
The plan quality, represented by DVH points of the PTV, did not strictly decrease with delivery times (figure 5.12, left). Relative time savings were smaller compared to the results derived by the "maximization of the smallest spot weight" (method B, presented above).

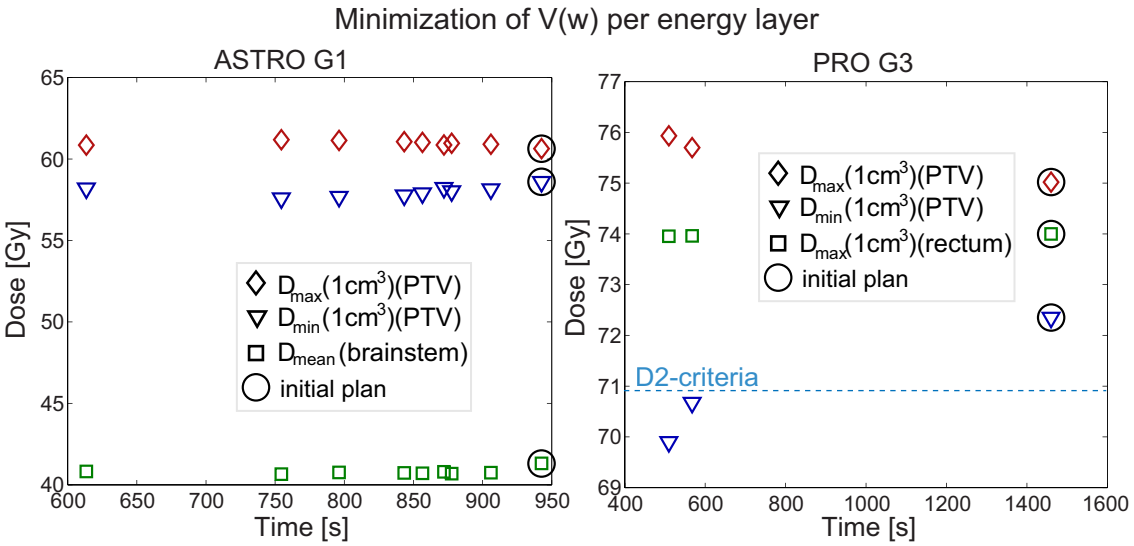

Figure 5.12: Trade-off results derived by "minimization of the spot weight variance within each energy layer" with $I = I_v$. Within the given evaluation criteria of 2% changes in $D_{min}(1\ cm^3)$ (dashed line) no time reductions were obtained for the prostate (right).

Minimization of overall spot weight sum - a comparison of A1 and A2

The "minimization of the overall spot weight sum" of both available sub-versions, A1 and A2, resulted in shorter treatment times for all plans (for $I = I_c$). Shorter delivery times at similar plan qualities were achieved by A1, i.e. for the larger number of available spots within the optimization (figure 5.13). Contrary results were noted for facilities of variable currents, for which A2 achieved shorter delivery times[2] (see tables A.19 and A.20).

[2]with one exception: PRO G1;

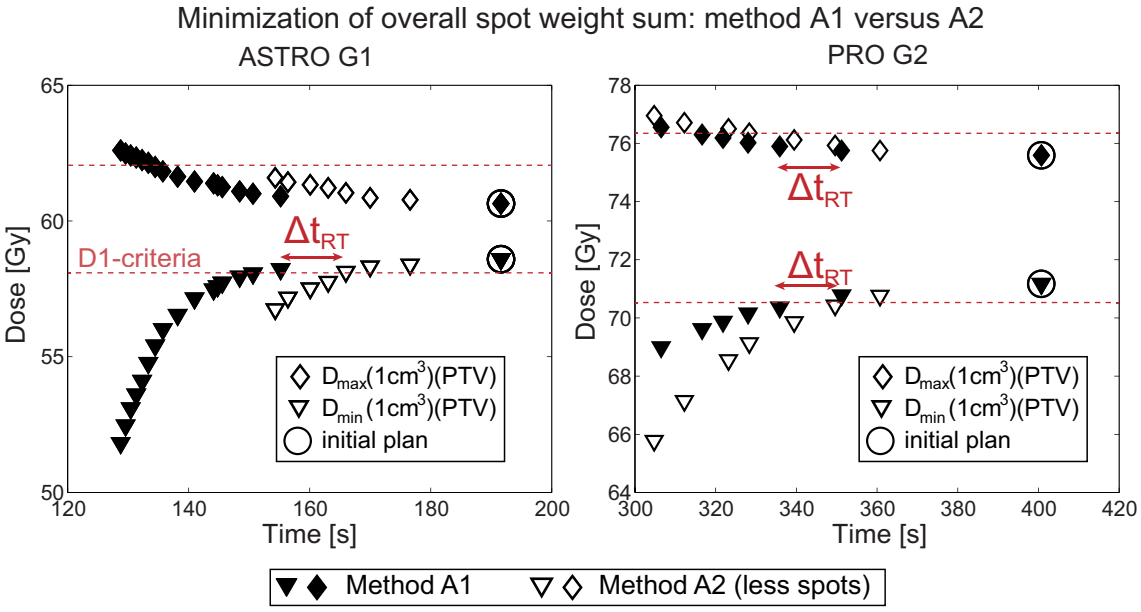

Figure 5.13: Results obtained by "minimization of the overall spot weight sum" with the initial number of spots (method A1) and a reduced spot number (A2) with $I = I_c$. The dashed line depicts the evaluation criteria D1 (1% dose deviation in $D_{min}(1\ cm^3)$ and $D_{max}(1\ cm^3)$ of the PTV).

Spot eliminiation - a comparison of C1 and C2

For both spot elimination methods facilities with variable current showed greater time savings without re-optimization of plan quality, while for facilities with constant current consecutive re-optimization lead to shorter treatment times. The deleted spots by method C1 and C2 are mostly overlapping. Identical values of l_s, which determine the eliminated spots, lead to a larger number of deleted spots by variant C2. A comparison of the derived trade-off results, and intrapolations between plan data points, by both methods with re-optimization and $I = I_c$ indicated greater savings for method C2, i.e. the elimination threshold measured by the average spot contribution (figure 5.14). For facilities of $I = I_v$ and without re-optimization, C1 (threshold given by the median spot weight) resulted in shorter delivery times. This trend was consistent for all plans of both patients and underlined by the results of evaluation criteria D2 (see tables A.19 and A.20). Time savings obtained by the D1 criteria are in contrast to the suggested efficacy difference which is a result due to the limited number of plans and thus different plan qualities of both methods (see discussion, section 5.5).

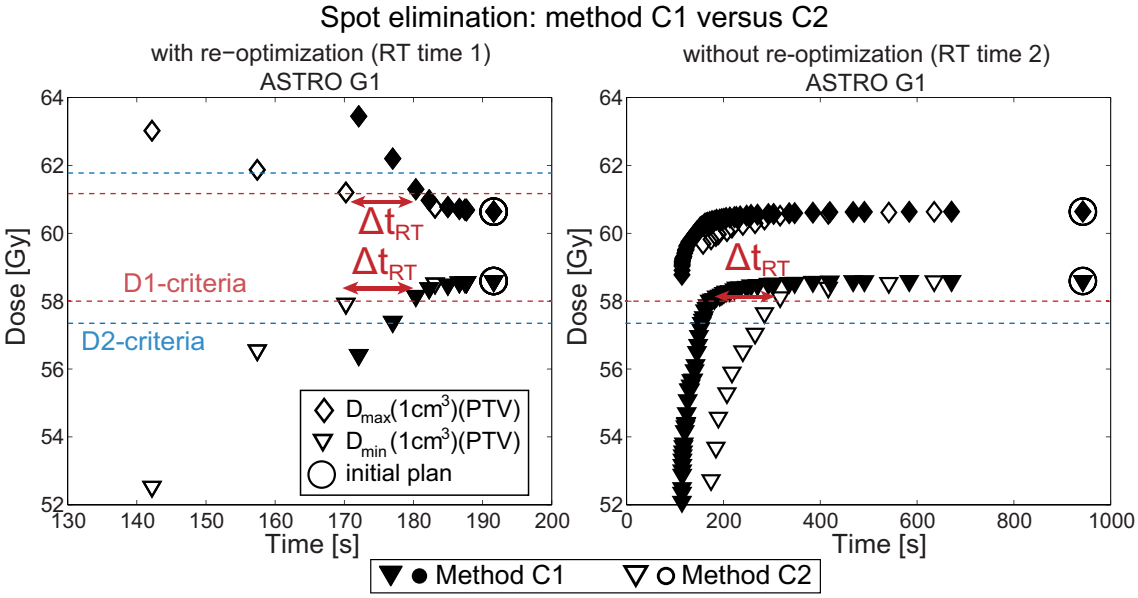

Figure 5.14: Comparison of method C1 and C2 for an astrocytoma case, with re-optimization at $I = I_c$ (RT time 1) and without re-optimization at $I = I_v$ (RT time 2). The dashed line depicts the evaluation criteria D1 and D2 (referring to 1% and 2% dose deviation in $D_{min}(1\ cm^3)$ and $D_{max}(1\ cm^3)$ of the PTV).

5.4.4 The impact of energy switch times

In order to investigate the impact of energy switch times, delivery times were additionally calculated with energy switch times of t_E=5 s (table A.33). Relative time reductions were compared to the prior presented results for t_E=1 s. The impact of an increasing t_E varied with the optimization method, and for method A additionally between tumor sites and initial plans. The "elimination of energy layers" lead to larger time reductions[3] for greater energy switch times while the "maximization of the smallest spot weights per energy" and "elimination of small spot weights" resulted in smaller time reductions, with and without re-optimization, for all plans. Figure 5.15 presents trade-off comparisons between two different energy switch time implementations of selective patients and methods for a facility with constant current.

[3]One exception was found for RT time 2 and criteria D2 (PRO G3).

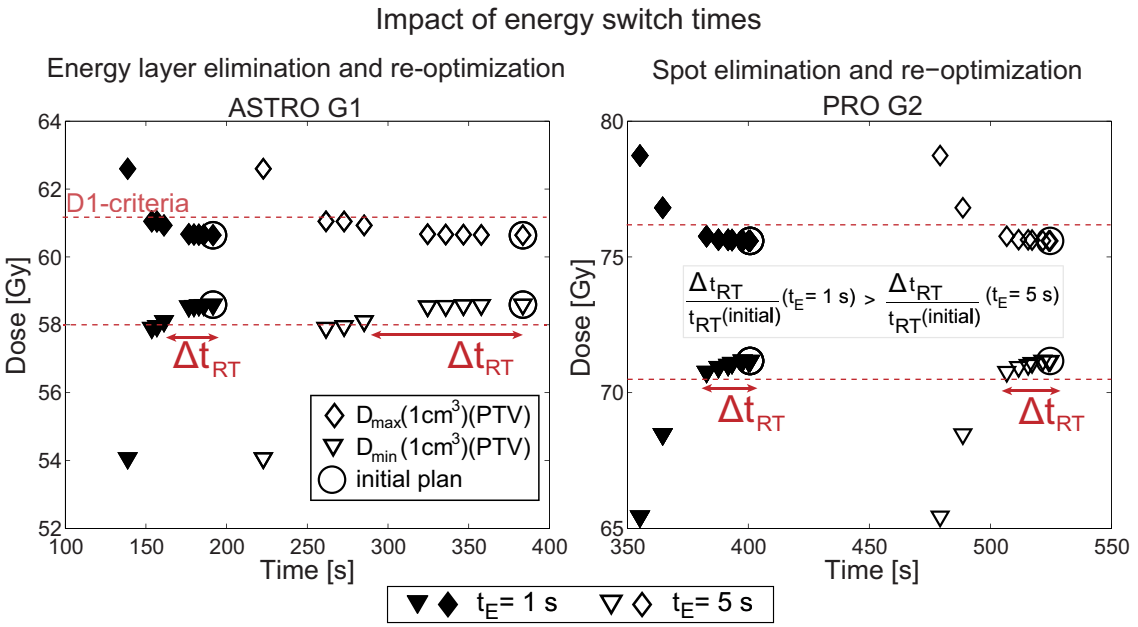

Figure 5.15: Impact of energy switch times for a facility with a constant current. Eliminating energy layers resulted in larger relative time reductions for greater t_E (left) while spot eliminations lead to comparably less time savings (right).

5.5 Discussion

Analysis of obtained PrEfOpt results and variations between facility types

The treatment planning algorithm PrEfOpt was developed as a two step routine, to optimize IMPT plans dosimetrically and to reduce treatment times while controlling plan quality. PrEfOpt offers different methods to increase delivery efficiency which were applied to an astrocytoma and prostate patient case. For both simulated treatment centers, radiation time reductions were achievable without major compromises in plan quality - however by different methods.
By varying the allowed deteriorations in plan quality, various plans of different trade-offs in quality and delivery time were calculated. Trade-off plots depicted fronts similar to Pareto surfaces for most applied methods (e.g. figures 5.7, 5.8, 5.10). The trade-off plots with $I = I_v$ which were derived by methods A and method C/ D with re-optimization differed from this "Pareto surface appearences" (e.g. figure 5.9). While the pure elimination of low weighted spots (C) resulted in extreme time savings, subsequent re-optimization lead to reappearing small spot intensities at different positions which consequently reduced the current and lowered the gain in RT time. Spot intensities do not oblige to any restrictions in "regular" dose optimization formulations (as in step I) which is also the origin of the varying RT time results derived by method A and method D with re-optimization. Energy layer

eliminiation (D) reduces the degrees of freedom for the re-optimization process which may degrade plan quality; simultaneously lower intensities than in the intial plan can be assigned; consequently plans of lower plan qualities but greater treatment times may be generated. Similar behaviour is observed by "the minimization of the overall spot weight sum" (A) which cannot guarantee to improve RT times for facilities with variable current as long as small spot weights are not controlled simultaneously in the optimization.

Analysis of results by selective (sub-)methods

Method A1 and A2 differ in the number of available spots to minimize the total spot weight sum. Larger spot numbers (A1) imply more degrees of freedom in the optimization, and enable hereby larger time reductions at constant treatment currents - the facility type for which method A was developed for. Fluctuating RT time results proved this method to be problematic at $I = I_v$ (see above); here A2 achieved better results than A1 due to the reduced available spot positions for the ascription of low intensities.
Method B and B' were developed to reduce RT times for facilities with variable current by increasing the proton current or decreasing fluctuations of extremly large and small spot intensities. Both lead to remarkable time savings for the astrocytoma patient - with preferable results for method B. For the prostate case none of the methods resulted in notable delivery time reductions which fulfilled the specified evaluation criteria (D1 and D2). Optimization processes resulted in conflicts between infeasible problem formulations at low slip factor values and great quality compromises at larger slip factor values (see separate discussion below). While method B' achieved time reductions for slightly lower $D_{min}(1\ cm^3)$ (PTV) than the specified 2% limit, method B did not lead to shorter delivery times even at remarkable quality compromises. Explanations for the not achieved time reductions - even at raised treatment currents - are given by simultaneous influences on other efficiency determining quantities such as increasing spot weight variances (see e.g. table A.31). Method B and B' did not necessarily result in monotonic correlations between worsening quality and decreasing delivery times which is also ascribed to the impact of additional efficiency determining parameters on delivery times.
The comparison of **method C1 and C2** found C1 (threshold: median spot weight) without re-optimization to be preferable for variable current and C2 (threshold: average spot contribution) with re-optimization to be favorable for constant current facilities. C1 eliminates, per definition, particulary small spot weights which are responsible for long RT times 2 ($I = I_v$). The exclusively on the absolute spot number dependent RT times 1 ($I = I_c$) benefit from re-optimizations; superior results were obtained by C2 which may be favorable for re-optimization runs as it deletes the least important spots to the PTV-coverage, and focuses therefore on the most relevant spot positions in subsequent quality optimizations.

Identification of the "most effective" optimization method

A generally valid declaration of “the most effective” optimization method is not possible. Delivery times strongly vary with the implemented values for the treatment time calculations (see section 5.2.4). The initial treatment times of facility 1 were smaller than of facility 2 such that absolute times are not comparable amongst both virtual facility types. The simulated treatment times serve to measure the potential of distinctive methods for each facility type separately.

The selection of the most suitable time reduction method for a certain facility type does not only depend on the current implementation and actual current values but also on the energy switch times. Obviously the larger the energy switch time, the more impact is given to the “energy layer elimination”-method. The great potential of reducing energy layers for a decrease in treatment times was published recently [130, 26]. Van de Water [130] presented an iterative optimization routine to reduce energy layers (and spots) in robust IMPT treatment planning in a multicriteria optimization system. The routine consisted of a prior minimization of the logarithm over the total spot weight sum per energy layer and the reduction of low weighted spots. Based on prioritized optimization the algorithm assured the plan quality by introducing dose constraints. The published time savings for energy switch times of 1 s and 5 s are consistent with the obtained results for a constant current (method D with re-opt.). Both, [26] and [130], concluded that due to the degenaracy of IMPT plans, times can be reduced without affecting dosimetric plan quality. The here presented findings, by the application of PrEfOpt, underline this conclusion and complement their research by discussing different facility types for which different efficiency-optimization methods may be of greater potential.

In order to compare the methods towards efficacy the plans of the shortest calculated application times were selected which still fulfilled certain DVH criteria. As the number of calculated plans was limited and varied between methods the proximity of the chosen plan to the exclusion criteria, and thus corresponding qualities, differed slightly. The suggested system allowed to find the shortest feasible treatment time and revealed the “first plan” violating the criteria; the “true” feasible irradiation time lies somewhere in between. Derived RT times indicated method A and D to be superior for $I = I_c$, method B (with limitations) and C may be more suitable for $I = I_v$.
Method B achieved promising results for the astrocytoma case while delivery times of the prostate case were hardly (if at all) decreased (as discussed above). The problem formulation does not guarantee shorter RT times even though - as intended - the current was raised in all cases. Specific adjustments of the algorithm could make this method more reliable in the optimization of efficiency for centers with variable currents. The present implementation allowed simultaneous influences on distinctive efficiency determining parameters, as the overall weight sum and spot weight variance, which may “work against” the intended shorter RT times.

The introduction of additional constraints could solve this situation; additional constraints might however influence the feasibility of the problem (see separate discussion below).

It should be noted that the implemented efficiency-optimization methods in PrEfOpt are not complete; more variants may exist and combinations of optimization methods could also be of great potential.

Dependencies on initial geometry and optimization settings

Plans of different initial spot patterns, as well as optimization parameters, were analyzed, presenting an exposal of various possible constellations; changes in the intial settings may influence the results obtained by efficiency-optimization.
The selected **spot spacing** determines the dosimetric quality of the intial plan: generally larger spot numbers, i.e. denser spot grids, achieve better plan qualities due to more degrees of freedom in the optimization [54] - exceptions may occur though. Simulations, prior to the study to determine a suitable spacing in depth, indicated that for certain geometrical circumstances larger spot distances achieve superior dose distributions; some plans showed comparably higher doses to the spinal cord at denser spot grids due to the unfavorable proximity of spots to the structure. Along with the impact on dosimetric quality, the selection of the intial spot grid influences the achievable relative time savings; especially for method C/D, the initial spot and energy layer number are the basis for subsequent eliminations.
The utilized **optimization parameters** in step I steered the initial plan quality; different dosimetric results were achieved for both patients upon which efficiency investigations were performed. As the evaluation method was based on relative dose changes of the initial DVH values, the absolute quality was hardly (for most methods) of relevance for the obtained time reductions: independent of different initial plan qualities similar trends were noted for several "method-case-facility" combinations (e.g. method A for $I = I_c$, method C without re-opt. for $I = I_v$). The choice of optimization parameters however play a fundamental role with respect to the feasibilty of the optimization problem (see below).

Feasibility of optimization problems

The objective function formulations of method B and B' ("maximization of smallest spot weight" and "minimization of spot weight variance") lead to optimization complications for the prostate patient - such as slowly converging objective functions and feasibility problems (also discussed above). These complications were mainly attributed to the definition of too many and/ or non-achievable dose constraints which was motivated by the following observations: case specific lower slip factor boundaries were determined, above which optimizations were feasible. Moreover

optimization difficulties were eliminated by the selection of greater sampling rates[4], for which optimizations yielded solutions to the formulated objectives. The exclusion of multiple voxels allows the optimization of hot spots into structures which oblige to constraints without notification. The definition of intial maximum dose constraints to OARs or helper structures requires some considerations: a comparably high D_{max} to the "PTVwall" leads to good coverage and low objective function values $F_{Ia}(\underline{\omega})$, and sets hereby the level for the constraint in step II which may in the following not be achievable for small slip factor values. Constraints of smaller maximum doses lead to comparably worse coverage and larger objective function values $F_{Ia}(\underline{\omega})$ but the defined D_{max} may become problematic for subsequent optimizations. These issues could partly be solvable by warm-start optimizations, i.e. by providing the previous optimization result as starting point for the consecutive run; this was however not realizable for the underlying objective functions and utilized optimizer (interior point method, for details see e.g. [111] and www.mosek.com). The optimizer was also considered to be a source for some optimization difficulties but this was not analyzed in detail. Moreover, specific to method B and B', the objective function formulations may not be convex, and the (highly) multidimensional obtimization problem might not converge, and yield several minima (solutions) or a very broad extremum (degeneracy).

Potential for further improvements of the TPS and its application

The plan quality in the here presented analysis was exclusively evaluated by DVH points of the dose distributions. In IMPT, range uncertainties are of great concern which are reduced by robust planning or incorporated by robust optimization [128, 109, 129]. No robustness analysis was performed here which should be considered in clinical settings. Along with dosimetric quality the maintenance of plan robustness has to be assured.
Further limitation of the treatment planning might be found in the objective functions of step I: the minimization of the mean dose (step Ib) may not lead to the most optimal plan quality for every tumor case. Step I is however merely an example and can be replaced by different objective functions.

Designed for IMPT, PrEfOpt could further be adapted to IMXT. One option to optimize plan efficiency in regular IMXT was implemented in the original work by Wilkens et al. [143]. By smoothing the fluence map in the final step the complexity of IMXT plans can be reduced. More methods like the reduction of monitor units or intensity levels in the sequencer could be implemented as alternatives in a potential PrEfOpt-IMXT version (for methods see e.g. [38, 91]).

[4]Sampling rates larger than one unify several voxels which is realized by excluding all but one voxel; the optimization problem is hereby reduced.

Selecting the best trade-off - ethical concerns

Provided that a plan was efficiency-optimized (by any method), a method to decide for the best trade-off is required. What degree of plan degradation is still acceptable and is it acceptable to influence the plan quality at all with the pure intention to save time? These are difficult questions, partly enrolling ethical issues, which should not remain unmentioned in this context. The question whether any person should (have to) make the crucial decision on the trade-off between efficiency and quality was earlier arisen by Bortfeld and Webb [22] who stated that "it should be worth to wait a minute longer for a better plan" - which should certainly be followed. There may be patients however for whom the benefit of shorter treatment times might be larger than the impact of minor compromises in the calculated dose distributions. Moreover our work and prior publications indicated that large time savings do not necessarily mean to give up in quality [33, 38, 67, 91, 26, 130].

Selecting the best trade-off: realization of PrEfOpt in a MCO setting

One method to select the treatment plans of best trade-off is by execution of an automatic script. Similar to the above suggested system to compare efficacy of different optimization options, the shortest plan which still fulfills specific DVH criteria can be selected. This method will always pick the worst plan within the defined interval of the acceptable DVH values and may not necessarily result in the same choice as if selected in person. Some cases achieved large time reductions for minor dose changes and comparably small time improvements were achieved at further plan degradation. Method B and C at variable currents (figure 5.8) present typical examples of the issue: a large decrease in time was achieved between the intial and the efficiency-optimized plan with the best quality. The latter would most likely be the "trade-off choice" made in person. Moreover instead of comparing the actual dose distributions an automated plan selection takes exclusively DVH points into account.
The best trade-off choice presumably differs between patients. Decisions may vary with the derived dose distributions and patient background, i.e. the intention of the treatment and physical conditions defining how long the patient can stay on the treatment couch without extensive pain.
The creation of a plan database similar to MCO treatment planning could be a useful application to realize efficiency improving algorithms in clinical practice. PrEfOpt could generate multiple plans of different compromises to fill the database. By providing a slider on the planning interface which represents the treatment time, along with the sliders to control dosimetric objectives, the trade-off between time and quality could be steered interactively by the user. MCO would give the trade-off control to the planner or/and responsible physician rather than hard-coded in a planning system.

5.6 Conclusion: realization of shorter delivery times in clinical practice

This work demonstrated the potential of efficiency optimization in IMPT planning via different optimization methods. By prioritizing objectives, PrEfOpt achieved remarkable time reductions while maintaining the prior obtained dosimetric quality. Unevitable trade-offs between quality and delivery time were detected indicating a limit of achievable reasonable time reductions. A possible clinical application of PrEfOpt is the generation of multiple plans with different trade-offs for a multicriteria optimization setting. Then, the planner could select the preferred compromise between treatment time and quality for every individual patient.

Investigations of distinctive efficiency-optimization methods demonstrated the feasibility of more efficient plan deliveries in spot scanning proton therapy without major plan quality degradation before [67, 26, 130]. Similar promising results were previously found for IMXT plans [33, 38, 91]. Regarding the benefits of shorter treatment times, algorithms to improve efficiency are of great potential for clinical settings. Even though their applications do not generally guarantee to decrease RT times, the implementation of an efficiency-optimization step into the optimization process of clinical TPSs is considered to be reasonable. If a plan cannot be improved towards shorter RT times at a similar plan quality, the initial plan may still be selected for treatment. However if treatment planning systems which allow RT time reductions are introduced in clinical practice, it has to be assured - by the optimization algorithm and by staff (e.g. in guidelines/clinically guiding rules) - that the individual treatment quality is maintained and no compromises to quality are based on pure economical interest.

6 Improving efficiency and dosimetric quality in IMRT planning: summary and outlook

6.1 Summary and conclusion

This thesis investigated methods to improve the interdependent objectives efficiency and dosimetric quality in IMRT. Diverse components of radiotherapy treatment and of the associated clinical workflow were considered, and different aspects of efficiency and its correlation to quality were addressed. IMRT planning is the core process of this work as it determines the dosimetric quality and influences efficiency, in terms of planning time and delivery time.

Summary

The generation of RT treatment plans was investigated by two main components, the actual optimization process and the clinical planning procedure, which are both frequently inefficient and do not necessarily lead to the best plan result for the individual patient.
The trial-and-error process in regular IMRT plan optimization of selecting suitable penalty factors, which steer the dose distribution into the intended directions, is often time consuming. It is typically terminated as the plan fulfills the dosimetric demands (formulated in the prescription), as the planner runs out of time or/and believes that no further improvements are obtainable. The planner is never fully aware whether further adaption of optimization parameters will lead to superior results. Multicriteria optimization eliminates this trial-and-error process by a more intuitive approach of optimization goals (see section 3.2), and guarantees optimality in defined objectives [37]. The superiority of MCO in planning time and dosimetric quality (by reduced doses to OARs) was demonstrated by a comparison between MCO and non-MCO planning for NSCLC (see section 3.3). MCO further showed advantages with respect to the general concerns of inconsistent planning between planners and strong dependencies on planners' experiences. While the search and implementation of class solutions [145] are difficult in regular IMRT planning, due to variations between patients' geometries and individual desired dose trade-offs, template based planning in MCO was demonstrated to be feasible by the physician driven planning study (see section 3.4): the calculation of a plan database of a wide range of dosimetric options accounts for interpatient differences, and the subsequent final plan navigation adds the individual component to the planning process. This concept moreover enables less experienced planner [69] and physicians

to generate high quality treatment plans, while the latter was shown for brain and prostate cases in the physician driven planning study. This alternated planning procedure gave the control over the final dose trade-offs into the hands of physicians instead of having dosimetrists translate their "plan desires". Physicians chose their preferences by experiencing the interdependence of different objectives and weighing their importances. Physicians' generated plans were of high quality and clinically acceptable, which demonstrated the feasibility of the proposed workflow; the benefit in dosimetric quality and efficiency compared to dosimetrists' plans was not clearly proven. As planning capability of physicians increased during the study conduction, it is assumed that a similar study at a later stage of physicians' MCO training, may lead to the clinical evidence in preferable dose distributions and shorter planning times.

For accurate dose deliveries patients' set-ups are corrected by IGRT, and severe anatomical changes throughout the RT period are accounted for by adaptive planning. The relevance of these techniques was analyzed by a retrospective treatment planning study for head and neck cancer patients. Based on clinical control CT images, acquired at different RT fractions in the actual treatment positions, the impact of variations in patients' geometry on IMXT and IMPT dose distributions were evaluated (see chapter 4). Dosimetric influences varied between IMXT and IMPT, due to the different physical properties and plan features. Larger absolute dose changes were observed in IMPT plans. Starting at higher initial dose values, however, doses to OARs were more critical for IMXT plans. While PTV-coverages of IMXT plans were almost stable, IMPT plans resulted in heterogeneous dose distributions, even in the central PTV, and revealed extreme underdosage for some patients and fractions. The quality of DVHs did not worsen monotonically for both types of plans, and the amount of dosimetric changes differed largely between the individual patients, in particular for IMPT plans. Due to the complexity of different influences, i.e. set-up and anatomy, on dose changes, and a limitted number of patients, no obvious indicator (as weight loss) for re-planning was found. The meaning of this study is found in the illustration of dosimetric consequences in case plans are not adapted in time. Results demonstrated the importance of frequent image controls and dose recalculations, and should be interpreted as an alert to clinical practice. Even though accompanied by increased workloads, adaptive planning should be performed, in order to assure the application of the planned dose distribution.

The final project of this work addressed efficiency and plan quality in terms of dose delivery in IMPT (see chapter 5). Treatment times are a major concern not only for economical but also for quality reasons, since shorter treatment times reduce intrafractional uncertainties in the dose application and moreover improve patient comfort. Delivery efficiency is, amongst others, determined by plan parameters, which are assigned during plan optimization. The interdependence of both objectives makes RT time reduction a challenge without compromising dosimetric quality.

Within this work an algorithm was developed, which offers alternative efficiency optimization methods, specifically addressed to different existing facility types (constant and variable proton current). The routine was implemented as a two step routine, based on prioritized optimization: first treatment quality is optimized, and in a second step delivery efficiency is increased, while prior achievements are controlled by method dependent trade-off parameters. The algorithm was applied to an astrocytoma and a prostate case. Plans of varying trade-offs between RT times and dosimetric quality were generated. Trade-off plots similar to Pareto fronts were derived, which emphasized the inevitable compromise between both objectives. Remarkable time reductions at similar plan qualities were achieved and preferable methods were identified, dependent on the treatment current. Already rather simple methods, as pure spot elimination for facilities with variable current, reduced times considerably without noteable plan degradations. Therefore efficiency optimization is of great potential in clinical practice, if the maintenance of quality is assured by the TPS, e.g. by hard constraints, similar to the here presented algorithm. For plan selections, MCO was suggested: by presenting the inevitable trade-offs, MCO plan navigation would support physicians and/or physicists in the search of the best compromise between time and dose quality. Developed for IMPT, the routines could further be adapted to IMXT, by implementing methods specifically to corresponding efficiency determining parameters.

Conclusion

This thesis demonstrated the feasibility of improving both main objectives of RT, efficiency and dosimetric quality. With respect to the planning process, the utilization of a treatment planning system based on MCO certainly facilitates the planning process and increases planning efficiency as well as plan quality. The benefit of an alteration of the current clinical planning workflow towards a greater physician involvement, based on MCO, is not (yet) assured. Personally, I believe, that the suggested routine, with physician driven trade-off decisions by MCO, is of great potential, and the demonstration of evidence lacks only slightly more planning practice of physicians.
Adaptive planning is a time consuming, costly procedure. Here no indicator, which could identify the cases for whom plan adaption is beneficial, was found. Plan recalculations, however, emphasized the importance of both, IGRT and adaptive planning. The additional work and expenses should be worth the benefit in dosimetric quality.
The integration of a delivery efficiency optimizing step after the “regular” plan quality optimizationis is certainly reasonable in clinical practice. Generally time reductions are obtainable at similar plan qualities and even if no time reduction is achievable, the original plan can always be selected for treatment. Efficient delivery is not only of economical interest but can also improve the quality of the actual applied patient dose, e.g. by reduced motion. Moreover compromises in dose criteria do not necessarily correlate to treatment quality degradation, but for some cases the

gain of reduced RT times may be a greater than a slight compromise in the dose distribution, e.g. in case of severe pain when lying on the treatment couch. For the trade-off each individual situation has to be considered. The search for the best compromise could be realized by plan navigation as performed by MCO planning.
To conclude, efficiency and dosimetric quality are improvable by diverse methods at different stages of IMRT planning. The presented options are not complete and further improvable components presumably exist. Not all considered processes may be realizable in every institute, and its potential may vary amongst suggested methods, between patient cases and clinics. Each presented optimization approach of efficiency and quality comprises these interdependent objectives. The most critical point, when optimizing efficiency, is to clearly identify these correlations and contradictions and weigh its importances individually. Obtaining high plan quality should always be the main focus when improving efficiency.

6.2 Outlook: challenges of future RT

The progress in RT throughout the last decades was impressive. For clinical staff, who started their careers within the last years, it is unimaginable how RT worked only few decades ago, e.g. without CT based planning. Even though it seems like the biggest advancements in RT were already achieved, there is room for improvements in IMXT and IMPT techniques and in their clinical applications. RT, as well as other cancer treatments, will remain an active field of reasearch in the future.
Developments of novel technologies are ongoing, and will further improve radiotherapy treatments, but may simultaneously be accompanied by even more expenses. To achieve treatments of high dosimetric quality at each RT session, while being as efficient as possible, will therefore remain a challenge of RT practice in the future.
Evolving investigations range from improvements in computational planning to progresses in RT delivery accuracy. During the last decades, TPSs were steadily developed towards greater support of clinical personnel in specific tasks of the planning process: e.g. by elastic image registration, automatic segmentation and planning, and increasingly implemented MCO techniques [48, 72, 136, 77, 94].
With respect to dose delivery, gating and tracking techniques are frequently more applied, and studies are ongoing to evaluate their clinical benefits [99, 13, 31]. Within this work, the difficulty of range uncertainties in proton therapy was addressed. Diverse range verification methods are currently under investigation to decrease these and to give definite information on the delivered region [134, 2], which will remarkably improve accuracy of proton treatments. The generally preferable physical properties, compared to photon therapy, could then be fully made use of in the future. If along with the progress in delivery precission, sizes of machines and costs are reduced, the utilization of proton therapy could and should further emerge in the future.
Generally the implementation of novel techniques needs clinical experience and practice in order to establish efficient workflows, and to identify the patient cases

who benefit from those techniques. Every institute may have to consider their practices, find suitable procedures and maybe even compromises between efficiency and quality.
Not all of the invented techniques or applications may be reasonable or beneficial for every patient or tumor entity; each technique requires critical investigations and analysis with respect to their relevance and real clinical benefit. Advancements in RT, whose clinical evidence is assured, such as IGRT and adaptive planning, may however demand more staff. Studies are performed to investigate workloads, associated with the application of state of the art RT techniques, in order to supply clinics not only with technologies, but also with a recommendation for an adequate size of staff [137]. No technique or development improves treatment quality without sufficient, well trained staff who know how to utilize the techniques to achieve the best results.
Now and in the future, we need to make use of the achieved technical advancements in optimal manner, efficiency- and qualitywise, identify reasonable techniques and the patients who benefit from them.

A Appendix

A.1 Tabular data of physician driven planning study

Prostate	Constraints		Objectives	
	PTV	Min Dose: 59.9 Gy Max Dose: 76.6 Gy	PTV	Min Dose: 66.6 Gy Max Dose: 66.6 Gy
	CTV	Min DVH: 66.6 Gy to 95 % volume	CTV	Min Dose: 66.6 Gy
	Rectum	Max Dose: 69.9 Gy	Rectum	Dose-Fall off: 66.6 Gy to 0 Gy in 1 cm
	Bladder excluding CTV	Max Dose: 69.9 Gy	Bladder excluding CTV	Dose-Fall off: 66.6 Gy to 0 Gy in 1 cm
	PTVwall (1cm ring around PTV)	Max Dose: 68.6 Gy	Normal tissue	Dose-Fall off: 66.6 Gy to 0 Gy in 1 cm
	Normal tissue*	Max Dose: 66.6 Gy	Femurs	EUD, a=2
Brain tumors	Constraints		Objectives	
	PTV	Min Dose: 51.0 Gy, Max Dose: 67.0 Gy Min DVH: 60.0 Gy to 80 % volume	PTV	Min Dose: 60.0 Gy Max Dose: 60.0 Gy
	PTV excluding OARs	Min DVH: 60.0 Gy to 95 % volume	GTV**	Min Dose: 60.0 Gy
	Brainstem (BS) excluding PTV Inner BS Outer BS	Max DVH: 59.9 Gy to 5 % volume Max Dose: 62.0 Gy Max DVH: 58.8 Gy to 5 % volume Max DVH: 63.0 Gy to 1 % volume	Brainstem	EUD, a=4
	Chiasm	Max Dose: 54.0 Gy	Chiasm	EUD, a=2
	Optic nerve L and R	Max Dose: 54.0 Gy	Optic nerve L and R	EUD, a=2
	Lens L and R	Max Dose: 10.0 Gy	Lens L and R	EUD, a=2
	Eye L and R	Max Dose: 45.0 Gy	Eye L and R	EUD, a=2
			Cochlea L and R	EUD, a=2
			Lacrimal L and R	EUD, a=1
	Normal tissue	Max Dose: 62.0 Gy	Normal tissue	Dose Fall-off: 50.0 Gy to 0 Gy in 1 cm

Table A.1: Typical MCO-problem formulations for prostate (prescription: 66.6 Gy) and CNS (prescription 60.0 Gy, for different prescriptions parameters have been scaled); L: left, R: right, EUD: equivalent uniform dose [97], *excluding PTV wall, ** deviation for CNS: if the GTV was far from any OARs, a minimum dose was defined as hard constraint to the GTV instead of the objective.

Patient	Volume [cm³]	D99 [Gy]		D98 [Gy]		D95 [Gy]		D_{mean} [Gy]		D2 [Gy]		D1 [Gy]		V65 [%]	
		Clinical	Physician	Clinical	Physician	Clinical	Physician	Clinical	Physician	Clinical	Physician	Clinical	Physician	Clinical	Physician
PRO1	272.44	58.73	62.29	61.83	62.98	64.65	64.03	68.15	67.83	71.47	71.72	71.79	72.25	93.84	89.25
PRO2	320.81	34.93	62.55	38.72	63.11	48.19	64.25	66.55	67.70	72.05	71.45	72.54	71.97	86.19	90.67
PRO3	286.16	65.16	63.42	65.70	64.01	66.35	64.93	67.72	68.14	69.87	72.13	70.16	72.93	99.07	94.07
PRO4	220.88	62.22	63.25	63.51	64.10	65.26	65.19	67.95	68.02	70.45	70.79	70.85	71.15	95.40	95.30
PRO5	265.84	65.20	63.54	65.80	64.21	66.61	65.09	68.26	67.82	70.33	70.24	70.63	70.62	99.08	94.86
PRO6	268.80	65.27	62.41	65.94	63.18	66.58	64.31	67.80	68.09	69.61	72.24	70.11	72.96	99.11	91.57
PRO7	295.52	63.17	62.51	64.44	63.24	65.58	64.29	67.63	67.77	70.75	71.43	71.40	71.90	96.65	90.74
PRO8	326.79	64.61	62.53	65.44	63.46	66.60	64.71	68.98	67.80	72.44	70.64	72.80	70.95	98.45	93.15
PRO9	198.70	65.14	62.66	65.82	63.56	66.62	64.82	67.82	67.72	69.83	70.92	70.16	71.46	99.03	93.73
PRO10	229.14	66.15	63.71	66.45	64.41	66.72	65.24	67.77	67.48	71.37	70.10	71.97	70.55	99.72	95.63

Table A.2: Selective DVH points of the PTV of physician and clinical prostate plans.

Patient	Volume [cm³]	D99 [Gy]		D98 [Gy]		D95 [Gy]		D_{mean} [Gy]		D2 [Gy]		D1 [Gy]	
		Clinical	Physician	Clinical	Physician	Clinical	Physician	Clinical	Physician	Clinical	Physician	Clinical	Physician
PRO1	117.33	66.47	65.79	66.74	66.08	67.09	66.66	68.69	68.86	71.21	71.86	71.50	72.35
PRO2	140.69	54.08	66.07	57.40	66.35	63.90	66.76	68.46	68.73	72.14	71.68	72.60	72.12
PRO3	113.72	66.45	66.45	66.56	66.67	66.73	67.06	67.66	69.12	69.53	72.50	69.88	73.24
PRO4	93.65	66.54	66.47	66.77	66.72	67.15	67.05	68.39	68.62	70.37	70.81	70.67	71.07
PRO5	106.20	66.84	66.76	67.01	67.01	67.26	67.35	68.41	68.71	70.25	70.68	70.54	71.11
PRO6	116.85	66.55	66.52	66.71	66.68	66.92	66.98	67.79	69.08	69.29	72.30	69.49	72.88
PRO7	110.44	65.81	66.22	65.98	66.48	66.27	66.84	67.71	68.76	70.75	71.84	72.33	72.29
PRO8	146.50	67.07	66.01	67.20	66.28	67.43	66.64	69.02	68.50	72.25	70.64	72.66	70.89
PRO9	83.85	66.74	66.71	66.84	66.83	66.97	67.02	67.71	68.43	69.22	71.05	69.63	71.60
PRO10	99.32	66.56	66.31	66.67	66.52	66.84	66.82	67.52	67.93	69.18	69.93	69.75	70.25

Table A.3: Selective DVH points of the CTV of physician and clinical prostate plans.

Patient	Rectum									Bladder							
	Volume [cm³]	D_{mean} [Gy]		D1 [Gy]		V65 [%]		V40 [%]		Volume [cm³]	D_{mean} [Gy]		D1 [Gy]		V65 [%]		V40 [%]	
		Clinical	Physician	Clinical	Physician	Clinical	Physician	Clinical	Physician		Clinical	Physician	Clinical	Physician	Clinical	Physician	Clinical	Physician
PRO1	99.97	40.02	42.00	68.64	68.00	10.00	11.38	55.43	55.24	105.53	46.13	45.78	71.59	68.94	31.97	23.62	63.04	61.76
PRO2	160.56	43.48	44.94	69.94	67.66	16.62	9.19	51.78	57.96	63.68	63.58	58.87	72.27	69.27	60.77	42.82	98.03	91.45
PRO3	145.05	43.16	42.53	67.89	68.21	17.40	11.73	50.38	50.60	160.18	46.21	46.78	69.21	68.93	26.50	21.33	62.83	64.62
PRO4	76.84	29.27	36.23	68.17	67.71	5.23	6.47	33.96	51.64	62.94	43.12	43.46	69.66	70.15	26.49	26.83	57.41	58.46
PRO5	154.94	39.60	41.70	68.04	67.30	9.09	8.06	47.69	51.69	503.39	22.55	21.22	68.94	68.18	8.89	6.21	26.80	23.68
PRO6	149.21	38.43	36.47	67.71	67.14	10.78	8.00	44.34	40.33	76.02	46.46	45.60	69.07	69.01	26.79	20.63	61.77	59.69
PRO7	117.85	42.63	42.52	69.23	68.57	23.60	18.62	54.28	55.27	98.61	45.58	49.05	69.97	69.58	30.11	23.44	59.51	68.29
PRO8	154.31	35.50	37.47	68.90	66.98	7.25	4.81	38.27	41.27	209.09	33.73	36.23	71.21	68.67	15.80	13.40	37.75	44.90
PRO9	118.71	35.68	33.00	68.77	67.52	10.98	7.17	41.75	36.22	80.08	47.60	42.98	69.34	69.48	36.17	27.45	66.84	58.08
PRO10	133.97	38.90	29.92	67.85	67.30	13.66	7.14	47.50	26.39	67.54	55.41	47.51	71.57	69.08	43.68	29.12	80.67	63.48

Table A.4: Selective DVH points of rectum and bladder of physician and clinical prostate plans.

Patient	Femur L							Femur R						
	Volume [cm³]	D_{mean} [Gy]		D1 [Gy]		V45 [%]		Volume [cm³]	D_{mean} [Gy]		D1 [Gy]		V45 [%]	
		Clinical	Physician	Clinical	Physician	Clinical	Physician		Clinical	Physician	Clinical	Physician	Clinical	Physician
PRO1	185.48	20.20	21.47	44.90	49.64	1.07	3.08	187.90	20.51	20.62	48.76	46.20	3.50	1.74
PRO2	183.60	17.77	20.17	41.52	43.14	0.09	0.23	180.95	17.51	20.31	43.01	47.02	0.22	3.09
PRO3	157.23	19.62	14.91	38.21	38.59	0.00	0.10	156.46	15.10	15.21	35.53	42.99	0.00	0.57
PRO4	152.12	19.23	16.20	47.44	46.80	2.15	1.72	169.54	17.75	14.61	43.22	40.23	0.54	0.05
PRO5	159.39	18.91	16.94	38.16	44.15	0.03	0.82	153.62	18.72	18.02	39.63	44.23	0.11	0.87
PRO6	236.72	16.93	12.18	37.29	28.83	0.00	0.00	234.99	18.25	14.40	39.59	32.84	0.00	0.00
PRO7	237.52	13.50	17.34	42.78	39.87	0.33	0.01	227.71	15.08	17.11	41.05	39.81	0.14	0.04
PRO8	122.19	19.70	17.89	46.98	47.33	1.75	1.51	126.71	17.33	15.42	42.17	38.55	0.29	0.05
PRO9	210.79	15.48	17.08	40.71	40.97	0.33	0.32	221.96	14.02	17.03	41.36	40.58	0.12	0.01
PRO10	175.95	21.60	21.50	45.13	41.81	1.23	0.01	174.08	21.38	23.62	45.03	44.24	1.17	0.70

Table A.5: Selective DVH points of left (L) and right (R) femural heads of physician and clinical prostate plans.

Patient	prescribed Dose [Gy]	Volume [cm³]	D99 [Gy]		D98 [Gy]		D95 [Gy]		D_{mean} [Gy]		D2 [Gy]		D1 [Gy]	
			Clinical	Physician	Clinical	Physician	Clinical	Physician	Clinical	Physician	Clinical	Physician	Clinical	Physician
CNS1	60	611.95	55.42	56.65	57.04	58.05	58.64	59.47	61.41	60.82	63.45	62.62	63.60	62.96
CNS2	60	454.51	59.34	58.79	60.01	59.46	60.66	60.22	61.36	61.87	62.49	63.53	62.72	63.77
CNS3	54	8.27	50.32	50.54	51.14	51.42	52.31	52.67	55.01	55.25	56.81	56.94	56.96	57.16
CNS4	59.4	243.45	54.34	55.58	56.72	57.10	59.09	58.93	61.24	61.36	63.33	63.51	63.65	63.95
CNS5	60	385.62	51.91	54.51	53.69	56.29	57.06	58.55	61.32	61.73	64.42	65.31	64.81	65.75
CNS6	59.4	194.67	49.10	53.80	50.16	55.02	51.17	56.69	59.05	59.70	63.36	61.02	63.66	61.18
CNS7	60	479.88	58.88	57.10	59.55	58.10	60.10	59.16	60.86	60.25	62.39	61.30	62.77	61.46
CNS8	60	426.47	55.07	55.84	56.96	57.58	59.36	59.55	60.91	62.22	63.05	65.59	63.58	66.06
CNS9	50.4	3.52	49.45	49.01	49.77	49.28	50.26	49.52	51.09	50.91	51.96	52.91	52.05	53.07
CNS10	36	14.72	34.43	33.35	34.83	33.97	35.40	35.18	36.77	36.85	38.12	38.43	38.29	38.59
CNS11	40.05	399.38	38.98	37.90	39.51	38.66	40.04	39.94	40.63	41.54	41.41	42.89	41.69	42.99
CNS12	40.05	456.07	39.17	37.49	39.59	38.43	39.93	39.78	40.51	41.65	41.42	43.80	41.63	44.04

Table A.6: Selective DVH points of the PTV of physician and clinical CNS plans.

Patient	D_{prescr}[Gy]	Volume [cm³]	D99 [Gy]		D98 [Gy]		D95 [Gy]		D_{mean} [Gy]		D2 [Gy]		D1 [Gy]	
			Clinical	Physician	Clinical	Physician	Clinical	Physician	Clinical	Physician	Clinical	Physician	Clinical	Physician
CNS1	60	479.47	58.73	59.46	59.60	59.82	60.40	60.08	61.84	61.00	63.49	62.67	63.64	63.01
CNS2	60	360.94	60.44	60.61	60.66	60.85	60.87	61.14	61.42	62.17	62.46	63.61	62.69	63.89
CNS3	54	4.00	52.44	53.55	52.92	54.05	53.71	54.73	55.40	55.88	56.92	57.08	57.10	57.22
CNS4	59.4	177.36	58.74	59.68	59.67	60.20	60.35	60.62	61.54	61.85	63.34	63.60	63.65	64.08
CNS5	60	296.35	57.11	57.23	58.68	58.87	59.92	60.16	61.84	62.17	64.42	65.43	64.78	65.84
CNS6	59.4	140.05	50.08	55.44	50.60	56.22	51.37	57.42	59.35	59.88	63.41	60.99	63.72	61.12
CNS7	60	379.05	60.20	59.52	60.27	59.65	60.37	59.82	60.96	60.42	62.38	61.32	62.71	61.48
CNS8	60	330.70	57.81	60.11	59.22	60.63	60.12	61.04	61.08	62.71	63.08	65.75	63.59	66.19
CNS9	50.4	0.87	50.54	49.29	50.55	49.33	50.61	49.47	51.26	50.77	51.91	52.91	51.97	53.04
CNS10	36	5.94	35.87	36.42	35.97	36.49	36.11	36.59	37.03	37.39	38.31	38.64	38.44	38.75
CNS11	40.05	315.56	39.85	40.33	40.05	40.52	40.25	40.73	40.67	41.83	41.32	42.93	41.58	43.02
CNS12	40.05	355.92	39.85	39.90	39.94	40.53	40.08	40.96	40.56	42.00	41.41	43.90	41.62	44.12

Table A.7: Selective DVH points of the CTV of physician and clinical CNS plans.

Patient	D_{prescr}[Gy]	Brainstem					Chiasm		Lacrimal L		LacrimalR	
		Volume [cm³]	D5 [Gy]		D1 [Gy]		D1 [Gy]		D_{mean} [Gy]		D_{mean} [Gy]	
			Clinical	Physician	Clinical	Physician	Clinical	Physician	Clinical	Physician	Clinical	Physician
CNS1	60.00	31.02	56.41	59.00	58.25	61.21	52.04	54.67	6.58	3.87	20.57	13.79
CNS2	60.00	31.61	56.66	54.55	58.94	59.09	39.24	35.41	12.06	12.55	1.51	1.60
CNS3	54.00	34.97	49.41	46.74	52.97	53.03	47.76	47.13	0.00	0.00	0.00	0.00
CNS4	59.40	28.66	53.96	55.95	58.70	59.24	52.50	56.02	5.31	5.18	2.96	3.14
CNS5	60.00	25.30	56.66	56.67	58.76	59.62	54.36	55.35	23.00	13.01	7.59	5.25
CNS6	59.40	31.83	53.76	59.80	55.53	60.36	33.01	39.26	3.71	3.79	11.14	8.52
CNS7	60.00	26.72	23.09	26.35	36.52	39.64	40.21	44.11	9.19	7.73	12.82	10.27
CNS8	60.00	26.33	48.32	49.16	51.32	55.99	52.78	54.20	11.09	7.72	9.41	8.19
CNS9	50.40	0.00	0.00	0.00	0.00	0.00	19.39	14.68	4.73	6.82	11.47	4.79
CNS10	36.00	24.96	35.09	34.77	36.07	36.59	24.17	24.13	0.52	0.47	0.40	0.38
CNS11	40.05	27.63	29.23	29.13	36.52	35.57	39.93	38.22	7.61	7.23	5.26	6.70
CNS12	40.05	30.92	39.01	38.27	40.32	40.64	39.99	38.96	4.41	2.85	11.21	16.05

Table A.8: DVH points of selective OARs of physician and clinical CNS plans.

Patient	D_{prescr}[Gy]	Eyes L		Eyes R		Lens L		Lens R		OpticNerve L		OpticNerve R	
		Clinical	Physician	Clinical	Physician	Clinical	Physician	Clinical	Physician	Clinical	Physician	Clinical	Physician
CNS1	60.00	22.73	16.89	36.88	24.98	6.81	4.15	8.50	5.23	32.40	36.53	50.99	54.32
CNS2	60.00	11.31	12.08	3.67	4.45	9.69	10.41	1.76	1.92	14.65	15.71	11.32	12.44
CNS3	54.00	0.00	0.00	0.00	0.00	0.00	0.00	0.00	0.00	20.26	15.32	16.99	12.40
CNS4	59.40	9.09	10.56	4.23	5.37	4.45	4.36	3.25	3.34	53.10	54.55	35.59	39.34
CNS5	60.00	23.12	19.46	15.79	11.51	10.08	7.11	8.19	6.09	53.35	54.95	53.94	55.33
CNS6	59.40	4.42	4.80	14.69	11.92	2.80	2.63	6.14	5.93	24.95	28.27	22.82	24.30
CNS7	60.00	15.62	13.19	18.99	19.61	6.72	6.00	5.87	5.99	19.48	13.35	25.88	18.31
CNS8	60.00	30.98	31.86	19.40	20.93	6.60	6.41	8.89	8.02	53.25	55.03	50.17	52.06
CNS9	50.40	6.85	9.32	15.39	14.51	1.59	1.73	2.08	2.07	18.00	19.03	51.12	51.01
CNS10	36.00	0.66	0.61	0.50	0.48	0.40	0.37	0.29	0.28	14.98	16.74	14.24	13.62
CNS11	40.05	14.55	11.13	18.50	17.13	3.85	3.53	3.41	3.43	39.77	39.32	40.00	39.48
CNS12	40.05	15.63	6.80	19.93	27.26	4.11	3.16	3.96	7.73	28.38	17.93	39.65	38.32

Table A.9: Maximum doses D1 [Gy] of selective OARs of physician and clinical CNS plans.

A.2 Tabular data of impact of interfractional changes study

PTV	DVH criteria	RT technique	CT 1	CT 5	CT 10	CT 15	CT 20	CT 25
patient 1	$D_{min}(1\ cm^3)$ [Gy]	IMPT-2F	1.71	1.54	1.34	1.38	1.52	1.42
		IMPT-3F	1.73	1.59	1.28	1.41	1.47	1.36
		IMXT	1.57	1.64	1.40	1.31	1.39	1.39
	$D_{max}(1\ cm^3)$ [Gy]	IMPT-2F	2.15	2.36	2.39	2.35	2.46	2.53
		IMPT-3F	2.14	2.40	2.42	2.33	2.43	2.56
		IMXT	2.16	2.20	2.25	2.21	2.23	2.26
	D_{mean} [Gy]	IMPT-2F	2.02	1.99	1.95	1.98	1.99	1.97
		IMPT-3F	2.02	2.00	1.96	1.98	1.99	1.97
		IMXT	2.00	2.04	2.04	2.03	2.06	2.09
	σ [Gy]	IMPT-2F	0.04	0.11	0.15	0.11	0.12	0.16
		IMPT-3F	0.04	0.11	0.15	0.11	0.11	0.16
		IMXT	0.05	0.05	0.09	0.09	0.07	0.08
	CovI	IMPT-2F	0.98	0.84	0.72	0.80	0.82	0.69
		IMPT-3F	0.99	0.84	0.74	0.81	0.83	0.68
		IMXT	0.98	0.98	0.95	0.96	0.98	0.98
	ConI	IMPT-2F	1.13	1.17	1.20	1.17	1.21	1.28
		IMPT-3F	1.12	1.17	1.20	1.18	1.23	1.32
		IMXT	1.18	1.23	1.29	1.26	1.29	1.35
	volume [cm^3]		1034.12	966.76	966.14	975.22	962.85	933.00
patient 2	$D_{min}(1\ cm^3)$ [Gy]	IMPT-2F	1.68	1.38	1.27	1.51	1.54	1.46
		IMPT-3F	1.68	1.34	1.21	1.53	1.58	1.41
		IMXT	1.65	1.51	1.60	1.60	1.62	1.52
	$D_{max}(1\ cm^3)$ [Gy]	IMPT-2F	2.17	2.26	2.31	2.32	2.46	2.32
		IMPT-3F	2.16	2.26	2.29	2.32	2.43	2.44
		IMXT	2.13	2.13	2.15	2.21	2.21	2.33
	D_{mean} [Gy]	IMPT-2F	2.02	2.01	2.00	2.00	1.99	1.97
		IMPT-3F	2.02	2.01	2.00	2.01	2.00	1.97
		IMXT	2.00	1.99	2.00	2.03	2.04	2.06
	σ [Gy]	IMPT-2F	0.05	0.08	0.09	0.08	0.09	0.09
		IMPT-3F	0.04	0.09	0.09	0.08	0.09	0.10
		IMXT	0.05	0.06	0.05	0.06	0.06	0.08
	CovI	IMPT-2F	0.98	0.94	0.92	0.92	0.87	0.86
		IMPT-3F	0.98	0.93	0.92	0.93	0.89	0.86
		IMXT	0.96	0.94	0.96	0.97	0.98	0.97
	ConI	IMPT-2F	1.10	1.10	1.12	1.13	1.18	1.16
		IMPT-3F	1.09	1.09	1.11	1.14	1.19	1.20
		IMXT	1.18	1.16	1.19	1.22	1.23	1.26
	volume [cm^3]		1296.65	1322.93	1271.27	1302.00	1271.93	1234.81
patient 3	$D_{min}(1\ cm^3)$ [Gy]	IMPT-2F	1.60	1.30	1.25	1.12	0.15	1.18
		IMPT-3F	1.67	1.39	1.40	1.24	0.56	1.29
		IMXT	1.50	1.47	1.52	1.42	0.95	1.44
	$D_{max}(1\ cm^3)$ [Gy]	IMPT-2F	2.14	2.39	2.28	2.25	2.40	2.27
		IMPT-3F	2.13	2.42	2.39	2.32	2.43	2.34
		IMXT	2.15	2.19	2.19	2.16	2.14	2.15
	D_{mean} [Gy]	IMPT-2F	2.00	1.98	1.97	1.97	1.92	1.96
		IMPT-3F	2.02	2.00	1.99	1.98	1.92	1.98
		IMXT	2.00	2.00	2.00	1.99	1.96	1.99
	σ [Gy]	IMPT-2F	0.05	0.11	0.11	0.13	0.25	0.13
		IMPT-3F	0.04	0.10	0.11	0.12	0.23	0.12
		IMXT	0.07	0.08	0.07	0.08	0.13	0.08
	CovI	IMPT-2F	0.97	0.86	0.84	0.84	0.73	0.83
		IMPT-3F	0.99	0.90	0.88	0.86	0.67	0.86
		IMXT	0.93	0.93	0.94	0.92	0.85	0.92
	ConI	IMPT-2F	1.08	1.10	1.12	1.09	1.16	1.09
		IMPT-3F	1.08	1.09	1.12	1.08	1.17	1.09
		IMXT	1.14	1.15	1.17	1.13	1.18	1.13
	volume [cm^3]		721.70	717.39	699.87	732.40	728.12	730.89

Table A.10: DVH criteria of the PTV of patients 1-3.

PTV	DVH criteria	RT technique	CT 1	CT 5	CT 10	CT 15	CT 20	CT 25
patient 4	D_{min}(1 cm^3) [Gy]	IMPT-2F	1.60	0.94	0.70	0.79	0.99	1.39
		IMPT-3F	1.66	1.09	1.06	0.89	1.11	1.51
		IMXT	1.54	1.56	1.37	1.55	1.50	1.53
	D_{max}(1 cm^3) [Gy]	IMPT-2F	2.12	2.55	2.50	2.51	2.71	2.77
		IMPT-3F	2.13	2.52	2.49	2.56	2.58	2.58
		IMXT	2.15	2.15	2.15	2.15	2.15	2.16
	D_{mean} [Gy]	IMPT-2F	2.01	2.00	1.95	1.96	2.00	2.01
		IMPT-3F	2.02	2.03	1.95	1.96	2.01	2.01
		IMXT	2.01	2.01	1.99	2.00	2.01	2.02
	σ [Gy]	IMPT-2F	0.04	0.12	0.20	0.18	0.13	0.13
		IMPT-3F	0.04	0.12	0.16	0.17	0.13	0.11
		IMXT	0.05	0.05	0.07	0.06	0.06	0.06
	CovI	IMPT-2F	0.98	0.90	0.74	0.77	0.88	0.88
		IMPT-3F	0.99	0.93	0.69	0.74	0.88	0.89
		IMXT	0.98	0.98	0.96	0.97	0.97	0.98
	ConI	IMPT-2F	1.09	1.12	1.09	1.10	1.11	1.18
		IMPT-3F	1.10	1.12	1.11	1.12	1.12	1.17
		IMXT	1.21	1.21	1.24	1.22	1.22	1.30
	volume [cm^3]		1106.05	1076.82	1056.41	1053.07	1039.99	962.97
patient 5	D_{min}(1 cm^3) [Gy]	IMPT-2F	1.61	0.68	1.13	0.45	0.82	1.03
		IMPT-3F	1.67	0.84	1.24	0.55	0.92	1.15
		IMXT	1.60	1.37	1.26	0.28	1.03	1.29
	D_{max}(1 cm^3) [Gy]	IMPT-2F	2.15	2.40	2.46	2.61	2.64	2.73
		IMPT-3F	2.13	2.32	2.50	2.70	2.65	2.60
		IMXT	2.16	2.17	2.19	2.21	2.21	2.20
	D_{mean} [Gy]	IMPT-2F	2.02	1.99	2.01	1.99	1.99	2.00
		IMPT-3F	2.02	1.99	2.01	2.01	2.01	2.02
		IMXT	2.02	2.01	2.03	2.03	2.02	2.03
	σ [Gy]	IMPT-2F	0.04	0.13	0.11	0.17	0.14	0.13
		IMPT-3F	0.03	0.13	0.11	0.16	0.13	0.12
		IMXT	0.04	0.06	0.07	0.13	0.10	0.07
	CovI	IMPT-2F	0.99	0.90	0.91	0.86	0.87	0.90
		IMPT-3F	0.99	0.89	0.92	0.89	0.90	0.93
		IMXT	0.99	0.97	0.97	0.95	0.96	0.97
	ConI	IMPT-2F	1.10	1.11	1.18	1.25	1.23	1.20
		IMPT-3F	1.10	1.10	1.17	1.24	1.23	1.19
		IMXT	1.17	1.18	1.24	1.30	1.29	1.26
	volume [cm^3]		1270.70	1286.34	1214.22	1178.06	1169.34	1186.56
mean ± std	D_{min}(1 cm^3) [Gy]	IMPT-2F	1.64 ± 0.05	1.17 ± 0.31	1.14 ± 0.23	1.05 ± 0.39	1.01 ± 0.51	1.30 ± 0.16
		IMPT-3F	1.68 ± 0.03	1.25 ± 0.26	1.24 ± 0.11	1.13 ± 0.36	1.13 ± 0.37	1.34 ± 0.12
		IMXT	1.57 ± 0.05	1.51 ± 0.09	1.43 ± 0.12	1.23 ± 0.49	1.3 ± 0.26	1.43 ± 0.09
	D_{max}(1 cm^3) [Gy]	IMPT-2F	2.14 ± 0.02	2.39 ± 0.09	2.39 ± 0.08	2.41 ± 0.13	2.53 ± 0.12	2.53 ± 0.2
		IMPT-3F	2.14 ± 0.01	2.38 ± 0.09	2.42 ± 0.08	2.45 ± 0.15	2.50 ± 0.09	2.50 ± 0.1
		IMXT	2.15 ± 0.01	2.17 ± 0.03	2.18 ± 0.04	2.19 ± 0.03	2.19 ± 0.03	2.22 ± 0.07
	D_{mean} [Gy]	IMPT-2F	2.01 ± 0.01	1.99 ± 0.01	1.98 ± 0.02	1.98 ± 0.01	1.98 ± 0.03	1.98 ± 0.02
		IMPT-3F	2.02 ± 0	2.01 ± 0.01	1.98 ± 0.02	1.99 ± 0.02	1.98 ± 0.03	1.99 ± 0.02
		IMXT	2.00 ± 0.01	2.01 ± 0.01	2.01 ± 0.02	2.02 ± 0.02	2.02 ± 0.04	2.04 ± 0.03
	σ [Gy]	IMPT-2F	0.04 ± 0.0	0.11 ± 0.02	0.13 ± 0.04	0.13 ± 0.04	0.15 ± 0.06	0.13 ± 0.02
		IMPT-3F	0.04 ± 0	0.11 ± 0.01	0.12 ± 0.03	0.13 ± 0.03	0.14 ± 0.05	0.12 ± 0.02
		IMXT	0.05 ± 0.01	0.06 ± 0.01	0.07 ± 0.01	0.08 ± 0.03	0.08 ± 0.03	0.07 ± 0.01
	CovI	IMPT-2F	0.98 ± 0.01	0.89 ± 0.04	0.83 ± 0.08	0.84 ± 0.05	0.83 ± 0.06	0.83 ± 0.08
		IMPT-3F	0.99 ± 0	0.90 ± 0.03	0.82 ± 0.10	0.84 ± 0.07	0.83 ± 0.09	0.84 ± 0.08
		IMXT	0.96 ± 0.02	0.96 ± 0.02	0.96 ± 0.01	0.95 ± 0.02	0.95 ± 0.05	0.96 ± 0.02
	ConI	IMPT-2F	1.10 ± 0.02	1.12 ± 0.03	1.14 ± 0.04	1.15 ± 0.06	1.18 ± 0.04	1.18 ± 0.06
		IMPT-3F	1.10 ± 0.02	1.11 ± 0.03	1.14 ± 0.04	1.15 ± 0.06	1.19 ± 0.04	1.2 ± 0.07
		IMXT	1.17 ± 0.02	1.19 ± 0.03	1.23 ± 0.04	1.22 ± 0.05	1.24 ± 0.04	1.26 ± 0.07
	volume [cm^3]		1085.84 ± 207.02	1074.05 om 221.69	1041.58 ± 202.6	1048.15 ± 193.06	1034.45 ± 186.33	1009.65 ± 183.17

Table A.11: DVH criteria of the PTV of patients 4-5 and mean and standard deviations (std.) over all patients (1-5).

spinal cord	DVH criteria	RT technique	CT 1	CT 5	CT 10	CT 15	CT 20	CT 25
patient 1	D_{max}(1 cm^3) [Gy]	IMPT-2F	0.02	0.17	0.45	0.19	0.59	1.16
		IMPT-3F	0.29	0.33	0.46	0.34	0.71	1.19
		IMXT	1.52	1.52	1.53	1.56	1.63	1.60
	volume [cm^3]		26.63	25.13	24.75	24.56	23.39	24.22
patient 2	D_{max}(1 cm^3) [Gy]	IMPT-2F	0.02	0.05	0.04	0.13	0.30	0.28
		IMPT-3F	0.40	0.39	0.40	0.41	0.41	0.47
		IMXT	1.59	1.64	1.67	1.71	1.65	1.75
	volume [cm^3]		36.63	34.06	29.15	26.64	26.26	32.74
patient 3	D_{max}(1 cm^3) [Gy]	IMPT-2F	0.31	0.30	0.38	0.34	0.44	0.34
		IMPT-3F	0.43	0.42	0.47	0.45	0.56	0.43
		IMXT	1.57	1.58	1.61	1.59	1.65	1.57
	volume [cm^3]		24.32	25.41	29.89	26.52	29.32	23.21
patient 4	D_{max}(1 cm^3) [Gy]	IMPT-2F	0.02	0.02	0.02	0.04	0.02	0.02
		IMPT-3F	0.08	0.07	0.08	0.08	0.07	0.07
		IMXT	1.53	1.55	1.52	1.56	1.54	1.55
	volume [cm^3]		32.79	27.37	26.05	25.34	23.76	26.18
patient 5	D_{max}(1 cm^3) [Gy]	IMPT-2F	0.89	0.66	0.87	0.82	0.71	0.67
		IMPT-3F	0.80	0.64	0.83	0.90	0.70	0.65
		IMXT	1.52	1.51	1.52	1.53	1.51	1.50
	volume [cm^3]		27.41	21.13	21.22	21.62	21.67	21.13
mean ± std.	D_{max}(1 cm^3) [Gy]	IMPT-2F	0.25± 0.34	0.24± 0.23	0.35± 0.31	0.30± 0.28	0.41 ± 0.24	0.49± 0.39
		IMPT-3F	0.40 ± 0.23	0.37± 0.18	0.45± 0.24	0.44± 0.26	0.49± 0.24	0.56 ± 0.37
		IMXT	1.55± 0.03	1.56± 0.05	1.57 ± 0.06	1.59± 0.06	1.60 ± 0.06	1.59± 0.09
	volume [cm^3]		29.55 ± 4.5	26.62± 4.24	26.21 ± 3.14	24.93 ± 1.83	24.88± 2.66	25.49 ± 3.97

Table A.12: DVH criteria of the spinal cord of all patients. Mean and standard deviation (std.) over all patients are given.

Parotids	DVH criteria	RT technique	Structure	CT 1	CT 5	CT 10	CT 15	CT 20	CT 25
patient 1	D_{mean} [Gy]	IMPT-2F	PL	0.85	0.95	1.05	0.94	0.90	1.17
			PR	1.06	1.11	1.15	1.11	1.04	1.17
		IMPT-3F	PL	0.70	0.85	0.98	0.84	0.90	1.29
			PR	0.89	1.05	1.02	1.07	1.16	1.26
		IMXT	PL	1.03	1.07	1.17	1.10	1.09	1.22
			PR	1.46	1.49	1.51	1.51	1.51	1.52
	volume [cm^3]		PL	37.51	35.72	30.41	30.74	29.28	26.22
			PR	37.51	33.87	34.51	33.24	31.28	32.33
patient 2	D_{mean} [Gy]	IMPT-2F	PL	0.75	0.72	0.82	0.72	0.80	0.84
			PR	0.87	0.87	0.80	0.89	1.01	1.07
		IMPT-3F	PL	0.42	0.35	0.39	0.56	0.69	0.80
			PR	0.61	0.57	0.52	0.60	0.76	1.10
		IMXT	PL	1.02	1.01	1.04	1.01	1.06	1.06
			PR	1.24	1.23	1.20	1.22	1.22	1.30
	volume [cm^3]		PL	30.01	29.94	31.26	32.58	31.77	28.41
			PR	29.55	29.85	22.51	30.99	32.81	30.83
patient 3	D_{mean} [Gy]	IMPT-2F	PL	0.98	0.93	1.00	1.00	1.06	1.01
			PR	0.91	0.85	0.93	0.90	0.81	0.87
		IMPT-3F	PL	0.87	0.87	0.94	0.94	0.99	0.91
			PR	0.80	0.73	0.76	0.73	0.63	0.72
		IMXT	PL	1.41	1.43	1.45	1.42	1.43	1.44
			PR	1.07	1.05	1.03	1.01	0.93	1.01
	volume [cm^3]		PL	31.02	27.97	29.01	26.21	30.41	26.05
			PR	31.56	33.21	28.66	26.82	24.10	26.41
patient 4	D_{mean} [Gy]	IMPT-2F	PL	1.03	1.07	0.97	0.97	1.08	1.07
			PR	0.85	0.82	0.76	0.76	0.81	0.85
		IMPT-3F	PL	0.89	0.88	0.92	0.91	0.97	1.20
			PR	0.66	0.66	0.55	0.71	0.81	0.74
		IMXT	PL	1.57	1.56	1.57	1.59	1.62	1.64
			PR	1.03	1.04	1.05	1.04	1.07	1.08
	volume [cm^3]		PL	30.83	27.57	25.10	24.60	23.57	24.63
			PR	31.33	29.73	26.88	24.99	23.06	28.00
patient 5	D_{mean} [Gy]	IMPT-2F	PL	1.55	1.61	1.63	1.71	1.85	1.68
			PR	1.01	0.91	1.12	1.21	1.40	1.11
		IMPT-3F	PL	1.53	1.54	1.62	1.74	1.92	1.72
			PR	0.96	0.85	1.27	1.49	1.59	1.31
		IMXT	PL	1.78	1.80	1.84	1.89	1.90	1.90
			PR	1.33	1.28	1.39	1.50	1.42	1.41
	volume [cm^3]		PL	23.78	22.34	19.01	15.86	17.18	17.89
			PR	17.60	19.39	17.66	13.63	15.70	14.45

Table A.13: DVH criteria of the parotid glands (PL: left parotid, PR: right parotid).

		Initial values		Mean values: CT 1-25		relative deviation mean/ planned value	
	DVH criteria	IMPT-2F	IMPT-3F	IMPT-2F	IMPT-3F	IMPT-2F	IMPT-3F
patient 1	D_{min}(1 cm^3) [Gy]	1.71	1.73	1.49	1.47	**0.87**	0.85
	D_{max}(1 cm^3) [Gy]	2.15	2.14	2.37	2.38	1.11	1.11
	σ [Gy]	0.04	0.04	0.11	0.11	**2.73**	2.95
	CovI	0.98	0.99	0.81	0.81	0.82	0.82
patient 2	D_{min}(1 cm^3) [Gy]	1.68	1.68	1.47	1.46	**0.88**	0.87
	D_{max}(1 cm^3) [Gy]	2.17	2.16	2.31	2.32	**1.06**	1.07
	σ [Gy]	0.05	0.04	0.08	0.08	**1.72**	1.84
	CovI	0.98	0.98	0.92	0.92	0.93	0.93
patient 3	D_{min}(1 cm^3) [Gy]	1.60	1.67	1.10	1.26	0.69	**0.75**
	D_{max}(1 cm^3) [Gy]	2.14	2.13	2.29	2.34	**1.07**	1.10
	σ [Gy]	0.05	0.04	0.13	0.12	**2.67**	3.05
	CovI	0.97	0.99	0.85	0.86	0.87	0.87
patient 4	D_{min}(1 cm^3) [Gy]	1.60	1.66	1.07	1.22	0.67	**0.73**
	D_{max}(1 cm^3) [Gy]	2.12	2.13	2.53	2.48	1.19	**1.16**
	σ [Gy]	0.04	0.04	0.13	0.12	3.48	**3.40**
	CovI	0.98	0.99	0.86	0.85	**0.87**	0.86
patient 5	D_{min}(1 cm^3) [Gy]	1.61	1.67	0.95	1.06	0.59	**0.64**
	D_{max}(1 cm^3) [Gy]	2.15	2.13	2.50	2.48	**1.16**	1.17
	σ [Gy]	0.04	0.03	0.12	0.11	**3.38**	3.66
	CovI	0.99	0.99	0.90	0.92	0.91	**0.93**

Table A.14: Initial PTV dose criteria of IMPT-2F and -3F plans of all patients and the average value over all CTs (CT 1, 5, 10, 15, 20, 25). Mean values are compared to the initially planned values (last columns). In bold print the superior results are marked.

CT fraction	plan (planning CT)	D_{min}(cm^3) [Gy]	D_{max}(cm^3) [Gy]	σ [Gy]	CovI
CT 1	initial (CT 1)	1.67	2.08	0.98	98.54
CT 5	initial (CT 1)	1.39	2.21	2.58	89.77
CT 5	adapted (CT 5)	1.41	2.13	2.21	91.47
CT 15	initial (CT 1)	1.24	2.16	2.95	85.89
CT 15	adapted (CT 5)	0.74	2.19	4.57	79.73
CT 25	initial (CT 1)	1.29	2.17	3.01	86.19
CT 25	adapted (CT 5)	0.79	2.19	4.45	76.47

Table A.15: Comparison of adapted to non-adapted planning: dosimetric results of the PTV of plan recalulations of the initial IMPT-3F plan, optimized on CT 1, and of the adapted plan, optimized on CT 5, of patient 3.

A.3 Tabular data of PrEfOpt study

	Beam angles [°]	Spot spacing Δ x/y [cm]	Spot spacing Δ z	PTV margin [cm] for spot placement
ASTRO G1	90/270	0.4	$1.2 \cdot w_{80}$	0.5
ASTRO G2	90/270	0.5	$1.3 \cdot w_{80}$	0.5
ASTRO G3	120/275	0.5	$1.2 \cdot w_{80}$	0.2
PRO G1	90/270	0.5	$1.3 \cdot w_{80}$	0
PRO G2	90/270	0.6	$1.3 \cdot w_{80}$	0.2
PRO G3	90/270	0.6	$1.2 \cdot w_{80}$	0.5

Table A.16: Spot spacing and beam angles of astrocytoma and prostate plans; w_{80} refers to the width at the 80% intensity level of the Bragg peak.

Geometry	Contour	D_{prescr} [Gy]	Step Ia Constraint D_{max} [Gy]	Step Ib Penalties[a]
ASTRO (G1, G2, G3)	PTV	60.0	-	-
	PTVwall (1 cm)	-	57.0	-
	PTVwall (6 mm)	-	-	1.0
	Brainstem	-	45.0	1.0
PRO G1	PTV	74.0	-	-
	PTVwall (1 cm)	-	65.0	-
	PTVwall (6 mm)	-	74.5	0.8
	Rectum	-	74.5	1.5
	Bladder	-	74.5	1.2
PRO G2	PTV	74.0	-	-
	PTVwall (1 cm)	-	70.0	
	PTVwall (6 mm)	-	75.0	0.8
	Rectum	-	74.5	1.5
	Bladder	-	74.5	1.2
PRO G3	PTV	74.0	-	-
	PTVwall (1 cm)	-	-	-
	PTVwall (6 mm)	-	73.0	1
	Rectum	-	74.0	-

Table A.17: Optimization parameters of step I for distinctive astrocytoma and prostate geometries (table A.16); the slip-factor in step Ib was $\tilde{s} = 0.1$ for all plans.

[a] penalty factors determine the relative importance to reduce the mean dose of each structure.

	ASTRO G1	ASTRO G2	ASTRO G3	PRO G1	PRO G2	PRO G3
RT time 1 ($I = I_c$) [s]	191.6	191.4	197.0	360.1	400.7	390.7
RT time 2 ($I = I_v$) [s]	942.6	967.5	727.2	1827.8	764.4	1460.1
Number of energy layers	48	41	47	30	31	36
Number of spots	2071	1370	1587	698	791	1046
Total spot weight sum	$9.0 \cdot 10^5$	$9.4 \cdot 10^5$	$9.4 \cdot 10^5$	$2.1 \cdot 10^6$	$2.3 \cdot 10^6$	$2.2 \cdot 10^6$
Average minimum weight $t_{B,k}$	54.0	43.8	72.3	508.6	277.6	576.9
Average variance $V(\omega(E_k,B))$	$1.3 \cdot 10^5$	$3.1 \cdot 10^5$	$3.3 \cdot 10^5$	$1.1 \cdot 10^7$	$9.8 \cdot 10^6$	$6.2 \cdot 10^6$
Coverage index CovI	1.0	1.0	1.0	1.0	1.0	1.0
D_{min}(1 cm^3) (PTV) [Gy]	58.6	58.0	57.9	67.2	71.2	72.3
D_{max}(1 cm^3) (PTV) [Gy]	60.6	60.8	61.1	77.5	75.6	75.0
σ (PTV) [Gy]	0.4	0.6	0.6	1.5	0.7	0.5
D_{mean} (PTV) [Gy]	59.9	59.9	59.9	73.7	73.9	73.9
Conformity index ConI	1.0	1.0	1.0	1.1	1.1	1.2
D_{max}(1 cm^3) (brainstem) [Gy]	41.3	42.1	39.7	-	-	-
D_{mean} (brainstem) [Gy]	20.8	23.3	19.7	-	-	-
D_{mean} (PTVwall 6 mm) [Gy]	40.6	42.1	41.5	55.6	61.0	62.2
D_{max}(1 cm^3) (bladder) [Gy]	-	-	-	74.2	74.3	74.6
D_{mean} (bladder) [Gy]	-	-	-	28.3	32.1	34.0
D_{max}(1 cm^3) (rectum) [Gy]	-	-	-	74.5	74.4	74.0
D_{mean} (rectum) [Gy]	-	-	-	23.2	27.1	30.8

Table A.18: Initial plan quality indicators and efficiency determining quantities (after step Ib) of distinctive astrocytoma and prostate settings.

Astrocytoma geometry	Proton current	Eval. criteria	**Method A** A1 [a]	A2 [b]	**Method B** B [c]	B' [d]	**Method C1** NR [e]	R [f]	**Method C2** NR	R	**Method D** NR	R
ASTRO G1	const.	D1	21.4	13.4	4.1	0.0	1.4	4.9	1.9	4.4	0.0	15.9
		D2	24.5	16.5	6.3	0.0	1.7	5.9	3.2	11.2	1.9	19.8
	var.	D1	29.5	36.6	80.5	34.9	81.8	67.7	66.4	44.3	0.0	15.0
		D2	46.1	47.0	81.5	34.9	83.3	74.8	69.8	53.5	0.6	30.7
ASTRO G2	const.	D1	15.7	10.3	5.2	0.0	0.9	4.3	0.8	2.3	1.3	14.0
		D2	21.4	13.1	7.4	0.0	1.8	5.4	2.2	8.3	1.3	18.8
	var.	D1	46.8	48.5	82.5	54.5	86.6	81.0	73.8	48.3	0.6	40.0
		D2	46.8	54.4	82.8	69.3	88.0	81.0	77.8	55.1	0.6	40.0
ASTRO G3	const.	D1	11.8	10.7	5.5	0.0	0.8	5.3	1.8	2.7	1.1	12.0
		D2	14.6	13.5	7.7	0.0	1.4	5.3	3.0	10.9	2.8	14.3
	var.	D1	22.5	47.1	76.3	0.0	79.8	59.7	61.3	40.3	0.3	3.7
		D2	40.1	49.4	76.9	47.7	82.2	59.7	71.5	43.5	1.2	30.4
Mean over all geometries	const.	D1	16.3	11.5	4.9	0.0	1.0	4.8	1.5	3.1	0.8	13.9
		D2	20.1	14.4	7.1	0.0	1.6	5.5	2.8	10.1	2.0	17.7
	var.	D1	32.9	44.0	79.7	29.8	82.7	69.5	67.2	44.3	0.3	19.6
		D2	44.3	50.3	80.4	50.6	84.5	71.8	73.0	50.7	0.8	33.7
Std. over all geometries	const.	D1	4.0	1.4	0.6	0.0	0.3	0.4	0.5	0.9	0.6	1.6
		D2	4.1	1.5	0.6	0.0	0.2	0.3	0.4	1.3	0.6	2.4
	var.	D1	10.2	5.3	2.6	22.5	2.9	8.8	5.2	3.3	0.2	15.2
		D2	3.0	3.1	2.5	14.2	2.5	8.9	3.5	5.1	0.3	4.5

Table A.19: Achieved time savings [%] for different astrocytoma geometries; the evaluation criteria D1 and D2 refer to 1% and 2% deviations in $D_{min}(1\ cm^3)$ and $D_{max}\ (1\ cm^3)$ within the PTV.

[a] A1: minimization over total spot weight sum with all spots
[b] A2: minimization over total spot weight sum with potentially reduced spot number
[c] B: maximization of smallest spot weight per energy and beam
[d] B': minimization of variance
[e] NR: no consecutive re-optimization
[f] R: consecutive re-optimization

Prostate geometry	Proton current	Eval. criteria	**Method A** A1 [a]	A2 [b]	**Method B** B [c]	B' [d]	**Method C1** NR [e]	R [f]	**Method C2** NR	R	**Method D** NR	R
PRO G1	const.	D1	9.4	8.3	0.1	0.0	1.9	2.3	0.7	3.3	0.0	4.3
		D2	9.4	8.3	1.0	0.0	2.1	2.3	1.5	6.1	0.0	7.7
	var.	D1	68.6	64.4	0.0	0.0	89.5	85.4	89.!	88.0	0.0	7.3
		D2	68.6	64.4	1.0	0.0	89.5	85.4	89.5	88.0	0.0	7.3
PRO G2	const.	D1	12.4	10.0	0.0	-	1.3	4.5	0.8	5.3	0.0	4.5
		D2	19.7	15.3	0.0	-	1.9	4.5	1.2	5.3	0.0	9.2
	var.	D1	0.0	0.0	2.5	-	72.1	71.4	69.6	54.2	0.0	0.0
		D2	34.9	44.7	3.3	-	72.3	71.4	71.6	54.2	0.0	0.0
PRO G3	const.	D1	14.6	13.0	0.0	0.0	1.0	5.2	0.8	5.0	0.0	9.9
		D2	18.9	16.0	0.2	0.0	1.5	9.9	2.4	13.3	0.0	16.3
	var.	D1	0.0	56.6	0.7	0.0	85.5	68.1	82.3	0.0	0.0	35.7
		D2	26.2	72.3	0.7	0.0	85.6	85.0	84.0	45.9	0.0	35.7
Mean over all geometries	const.	D1	12.1	10.4	0.0	0.0	1.4	4.0	0.8	4.6	0.0	6.2
		D2	16.0	13.2	0.4	0.0	1.9	5.6	1.7	8.2	0.0	11.1
	var.	D1	22.9	40.3	1.1	0.0	82.4	75.0	80.3	47.4	0.0	14.3
		D2	43.2	60.5	1.7	0.0	82.5	80.6	81.7	62.7	0.0	14.3
Std. over all geometries	const.	D1	2.1	1.9	0.0	0.0	0.4	1.2	0.0	0.9	0.0	2.6
		D2	4.7	3.4	0.4	0.0	0.2	3.2	0.5	3.6	0.0	3.8
	var.	D1	32.3	28.7	1.1	0.0	7.5	7.5	8.1	36.2	0.0	15.4
		D2	18.3	11.6	1.2	0.0	7.4	6.5	7.5	18.2	0.0	15.4

Table A.20: Achieved time savings [%] for different prostate geometries; the evaluation criteria D1 and D2 refer to 1% and 2% deviations in $D_{min}(1\ cm^3)$ and D_{max} $(1\ cm^3)$ within the PTV.

[a] A1: minimization over total spot weight sum with all spots
[b] A2: minimization over total spot weight sum with potentially reduced spot number
[c] B: maximization of smallest spot weight per energy and beam
[d] B': minimization of variance
[e] NR: no consecutive re-optimization
[f] R: consecutive re-optimization

	Initial plan	Method A						Method B					
		Method A1			Method A2			Method B		Method B'			
Evaluation criteria D1/D2		D1	D2		D1	D2		D1	D2	D1		D2	
Shortest RT time for facility type		RT1/2	RT1	RT2	RT1/2	RT1	RT2	RT1/2	RT1/2	RT1	RT2	RT1	RT2
Trade-off factor s/ l_S, l_E	-	0.5	1.0	0.8	0.5	1.0	0.8	0.4	0.8	-	0.1	-	0.1
RT time 1 ($I = I_c$) [s]	191.6	150.6	144.1	145.5	166.0	160.1	163.0	183.8	179.6		195.1		195.1
RT time 2 ($I = I_v$) [s]	942.6	664.6	682.5	507.9	598.1	532.1	500.1	184.3	174.2		613.5		613.5
Number of energy layers	48	35	33	33	44	44	45	48	48		48		48
Number of spots	2071	1286	1105	1173	1178	997	1061	2071	2071		2071		2071
Total spot weight sum	$9.0{\cdot}10^5$	$7.2{\cdot}10^5$	$6.9{\cdot}10^5$	$7.0{\cdot}10^5$	$7.6{\cdot}10^5$	$7.3{\cdot}10^5$	$7.4{\cdot}10^5$	$8.5{\cdot}10^5$	$8.2{\cdot}10^5$		$9.2{\cdot}10^5$		$9.2{\cdot}10^5$
Average minimum $t_{B,k}$	54.0	31.3	50.2	52.5	97.9	138.9	151.6	132.6	137.8		87.4		87.4
Average $V(\omega(E_k,B))$	$1.3{\cdot}10^5$	$1.9{\cdot}10^5$	$2.2{\cdot}10^5$	$1.9{\cdot}10^5$	$3.1{\cdot}10^5$	$2.9{\cdot}10^5$	$3.0{\cdot}10^5$	$1.0{\cdot}10^5$	$1.0{\cdot}10^5$		$4.2{\cdot}10^4$		$4.2{\cdot}10^4$
Coverage index CovI	1.0	1.0	1.0	1.0	1.0	1.0	1.0	1.0	1.0		1.0		1.0
D_{min}(1 cm^3) (PTV) [Gy]	58.6	58.1	57.5	57.7	58.1	57.5	57.8	58.1	57.5		58.2		58.2
D_{max}(1 cm^3) (PTV) [Gy]	60.6	61.0	61.4	61.2	61.0	61.3	61.2	60.6	60.6		60.9		60.9
σ (PTV) [Gy]	0.4	0.6	0.8	0.7	0.6	0.8	0.7	0.5	0.7		0.5		0.5
D_{mean} (PTV) [Gy]	59.9	59.9	59.9	59.9	59.9	59.9	59.9	59.8	59.8		59.9		59.9
Conformity index ConI	1.0	1.0	1.0	1.0	1.0	1.0	1.0	1.0	1.0		1.0		1.0
D_{max}(1 cm^3) (brainstem) [Gy]	41.3	40.8	38.8	39.5	40.0	38.7	39.3	40.3	38.9		40.8		40.8
D_{mean} (brainstem) [Gy]	20.8	20.7	19.1	19.7	20.1	19.3	19.6	20.2	19.4		20.7		20.7
D_{mean} (PTVwall 6 mm) [Gy]	40.6	37.5	35.6	36.3	37.4	35.9	36.4	38.8	37.6		40.5		40.5
$Sum(\omega(B_1))$/ $Sum(\omega(B_2))$	0.9	1.0	1.0	1.0	0.8	0.8	0.8	0.9	0.9		0.9		0.9

Table A.21: Obtained plan quality indicators and efficiency determining quantities by efficiency-optimization with methods A and B of ASTRO G1; presented are the plan results of the shortest RT times for each facility type with maximal dose changes of 1% and 2% in D_{min}(1 cm^3) and D_{max}(1 cm^3) of the PTV.

	Initial plan	Method C1					Method C2				Method D				
		NR		R			NR		R		NR	R			
Evaluation criteria D1/D2		D1	D2	D1		D2	D1	D2	D1	D2	D2	D1		D2	
Shortest RT time for facility type		RT1/2	RT1/2	RT1	RT2	RT1/2	RT1/2	RT1/2	RT1/2	RT1/2	RT1/2	RT1	RT2	RT1	RT2
Trade-off factor s/ l_S, l_E	-	0.3	0.3	0.8	0.6	1.0	0.1	0.1	0.1	0.3	7.0	14.0	8.0	16.0	15.0
RT time 1 ($I = I_c$) [s]	191.6	189.0	188.4	182.3	185.0	180.4	187.9	185.5	183.1	170.2	187.9	161.2	185.8	153.6	156.8
RT time 2 ($I = I_v$) [s]	942.6	171.7	157.8	338.8	304.1	237.9	317.2	284.8	525.5	438.3	937.1	852.5	801.1	885.0	653.0
Number of energy layers	48	47	47	46	47	46	46	45	44	42	45	31	43	27	29
Number of spots	2071	1748	1701	1082	1277	931	1857	1794	1556	1074	2049	1498	1997	1402	1409
Total spot weight sum	$9.0{\cdot}10^5$	$8.9{\cdot}10^5$	$8.8{\cdot}10^5$	$8.5{\cdot}10^5$	$8.6{\cdot}10^5$	$8.4{\cdot}10^5$	$8.9{\cdot}10^5$	$8.8{\cdot}10^5$	$8.7{\cdot}10^5$	$8.0{\cdot}10^5$	$8.9{\cdot}10^5$	$8.1{\cdot}10^5$	$8.9{\cdot}10^5$	$7.9{\cdot}10^5$	$8.0{\cdot}10^5$
Average minimum $t_{B,k}$	54.0	110.2	116.6	133.9	100.9	191.1	86.1	91.6	83.9	142.6	53.2	36.5	72.0	21.2	34.2
Average $V(\omega(E_k,B))$	$1.3{\cdot}10^5$	$1.31{\cdot}10^5$	$1.3{\cdot}10^5$	$2.4{\cdot}10^5$	$1.9{\cdot}10^5$	$2.7{\cdot}10^5$	$1.3{\cdot}10^5$	$1.3{\cdot}10^5$	$1.9{\cdot}10^5$	$2.8{\cdot}10^5$	$1.3{\cdot}10^5$	$2.2{\cdot}10^5$	$1.5{\cdot}10^5$	$2.1{\cdot}10^5$	$2.1{\cdot}10^5$
Coverage index CovI	1.0	1.0	1.0	1.0	1.0	1.0	1.0	1.0	1.0	1.0	1.0	1.0	1.0	1.0	1.0
D_{min}(1 cm^3) (PTV) [Gy]	58.6	58.0	57.5	58.4	58.5	58.2	58.1	57.6	58.5	57.9	57.6	58.1	58.6	57.9	58.0
D_{max}(1 cm^3) (PTV) [Gy]	60.6	60.3	60.2	61.0	60.8	61.3	60.5	60.4	60.8	61.2	60.6	60.9	60.6	61.0	61.0
σ (PTV) [Gy]	0.4	0.5	0.6	0.6	0.5	0.7	0.5	0.6	0.4	0.7	0.6	0.6	0.4	0.7	0.7
D_{mean} (PTV) [Gy]	59.9	59.2	58.9	59.9	59.9	59.9	59.8	59.7	59.9	59.9	59.8	59.9	59.9	59.9	59.9
Conformity index ConI	1.0	1.0	1.0	1.0	1.0	1.0	1.0	1.0	1.0	1.0	1.0	1.0	1.0	1.0	1.0
D_{max}(1 cm^3) (brainstem) [Gy]	41.3	41.2	41.1	39.6	40.3	39.3	41.2	41.0	40.3	38.7	41.3	40.2	41.2	39.9	39.9
D_{mean} (brainstem) [Gy]	20.8	20.7	20.6	19.7	20.0	19.5	20.6	20.5	20.0	19.1	20.7	20.1	20.7	19.8	19.9
D_{mean} (PTVwall 6 mm) [Gy]	40.6	40.2	40.1	39.4	39.7	39.0	40.1	39.8	39.8	37.9	40.4	39.6	40.5	39.2	39.3
$Sum(\omega(B_1))$/ $Sum(\omega(B_2))$	0.9	0.9	0.9	1.0	1.0	0.9	0.9	0.9	0.9	1.0	0.9	1.0	0.9	0.9	0.9

Table A.22: Obtained plan quality indicators and efficiency determining quantities by efficiency-optimization with methods C and D of ASTRO G1; presented are the plan results of the shortest RT times for each facility type with maximal dose changes of 1% and 2% in D_{min}(1 cm^3) and D_{max}(1 cm^3) of the PTV.

	Initial plan	Method A					Method B							
		Method A1			Method A2		Method B				Method B'			
Evaluation criteria D1/D2		D1	D2		D1	D2	D1		D2		D1		D2	
Shortest RT time for facility type		RT1/2	RT1	RT2	RT1/2	RT1/2	RT1	RT2	RT1	RT2	RT1	RT2	RT1	RT2
Trade-off factor s/ l_S, l_E	-	0.3	0.5	0.3	0.3	0.5	0.3	0.2	0.5	0.4	-	0.3	-	0.8
RT time 1 ($I = I_c$) [s]	191.4	161.4	150.5	161.4	171.8	166.2	181.5	184.4	177.2	179.5		196.9		196.2
RT time 2 ($I = I_v$) [s]	967.5	514.8	548.6	514.8	498.2	440.9	169.7	168.2	167.4	166.1		440.1		297.3
Number of energy layers	41	36	29	36	40	39	41	41	41	41		41		41
Number of spots	1370	943	855	943	839	745	1370	1370	1370	1370		1370		1370
Total spot weight sum	$9.4{\cdot}10^5$	$7.8{\cdot}10^5$	$7.6{\cdot}10^5$	$7.8{\cdot}10^5$	$8.2{\cdot}10^5$	$7.9{\cdot}10^5$	$8.8{\cdot}10^5$	$8.9{\cdot}10^5$	$8.5{\cdot}10^5$	$8.6{\cdot}10^5$		$9.7{\cdot}10^5$		$9.7{\cdot}10^5$
Average minimum $t_{B,k}$	43.8	99.7	83.2	99.7	162.5	150.4	118.3	117.9	120.9	121.3		108.7		136.1
Average $V(\omega(E_k,B))$	$3.1{\cdot}10^5$	$3.3{\cdot}10^5$	$4.7{\cdot}10^5$	$3.3{\cdot}10^5$	$4.5{\cdot}10^5$	$5.1{\cdot}10^5$	$2.7{\cdot}10^5$	$2.6{\cdot}10^5$	$2.8{\cdot}10^5$	$2.7{\cdot}10^5$		$8.7{\cdot}10^4$		$6.0{\cdot}10^4$
Coverage index CovI	1.0	1.0	1.0	1.0	1.0	1.0	1.0	1.0	1.0	1.0		1.0		1.0
D_{min}(1 cm^3) (PTV) [Gy]	58.0	57.6	57.3	57.6	57.7	57.3	57.6	57.7	57.2	57.4		57.6		56.9
D_{max}(1 cm^3) (PTV) [Gy]	60.8	61.1	61.3	61.1	61.1	61.3	60.9	60.8	61.0	60.9		61.1		61.4
σ (PTV) [Gy]	0.6	0.7	0.8	0.7	0.7	0.8	0.7	0.6	0.8	0.7		0.7		1.0
D_{mean} (PTV) [Gy]	59.9	59.9	59.8	59.9	59.9	59.9	59.8	59.9	59.8	59.8		59.9		59.8
Conformity index ConI	1.0	1.0	1.0	1.0	1.0	1.0	1.0	1.0	1.0	1.0		1.0		1.0
D_{max}(1 cm^3) (brainstem) [Gy]	42.1	41.8	41.7	41.8	41.9	41.4	41.4	41.7	40.5	41.0		41.5		41.3
D_{mean} (brainstem) [Gy]	23.3	23.3	23.3	23.3	23.3	22.8	22.9	23.3	22.2	22.6		23.3		23.1
D_{mean} (PTVwall 6 mm) [Gy]	42.1	40.5	39.3	40.5	40.0	39.2	40.2	40.8	39.3	39.8		42.3		41.8
Sum($\omega(B_1)$)/ Sum($\omega(B_2)$)	0.8	0.8	0.9	0.8	0.8	0.9	0.9	0.9	0.9	0.9		0.9		0.9

Table A.23: Obtained plan quality indicators and efficiency determining quantities by efficiency-optimization with method A and B of ASTRO G2; presented are the plan results of the shortest RT times for each facility type with maximal dose changes of 1% and 2% in D_{min}(1 cm^3) and D_{max}(1 cm^3) of the PTV.

	Initial plan	Method C1					Method C2				Method D				
		NR		R			NR		R		NR		R		
Evaluation criteria D1/D2		D1	D2	D1	D2		D1	D2	D1	D2	D1	D2	D1	D2	
Shortest RT time for facility type		RT1/2	RT1/2	RT1/2	RT1	RT2	RT1/2	RT1/2	RT1/2	RT1/2	RT1/2	RT1/2	RT1/2	RT1	RT2
Trade-off factor s/ l_S, l_E	-	0.2	0.3	0.8	1.0	0.8	0.1	0.1	0.1	0.3	8.0	8.0	14.0	15.0	14.0
RT time 1 ($I = I_c$) [s]	191.4	189.8	187.9	183.2	181.0	183.2	189.8	187.3	187.1	175.5	188.8	188.8	164.7	155.4	164.7
RT time 2 ($I = I_v$) [s]	967.5	129.8	116.3	183.8	231.8	183.8	253.2	214.7	499.9	434.6	961.8	961.8	580.3	721.6	580.3
Number of energy layers	41	41	40	40	40	40	41	41	41	38	39	39	27	24	27
Number of spots	1370	1161	1118	730	635	730	1241	1158	1048	710	1356	1356	1031	898	1031
Total spot weight sum	$9.4{\cdot}10^5$	$9.3{\cdot}10^5$	$9.2{\cdot}10^5$	$8.9{\cdot}10^5$	$8.8{\cdot}10^5$	$8.9{\cdot}10^5$	$9.3{\cdot}10^5$	$9.1{\cdot}10^5$	$9.1{\cdot}10^5$	$8.5{\cdot}10^5$	$9.4{\cdot}10^5$	$9.4{\cdot}10^5$	$8.6{\cdot}10^5$	$8.2{\cdot}10^5$	$8.6{\cdot}10^5$
Average minimum $t_{B,k}$	43.8	146.0	195.1	241.5	267.6	241.5	159.4	172.9	147.8	232.4	41.6	41.6	35.9	57.3	35.9
Average $V(\omega(E_k,B))$	$3.1{\cdot}10^5$	$3.1{\cdot}10^5$	$2.7{\cdot}10^5$	$4.0{\cdot}10^5$	$4.8{\cdot}10^5$	$4.0{\cdot}10^5$	$2.7{\cdot}10^5$	$2.8{\cdot}10^5$	$3.6{\cdot}10^5$	$5.8{\cdot}10^5$	$3.1{\cdot}10^5$	$3.1{\cdot}10^5$	$3.7{\cdot}10^5$	$3.6{\cdot}10^5$	$3.7{\cdot}10^5$
Coverage index CovI	1.0	1.0	1.0	1.0	1.0	1.0	1.0	1.0	1.0	1.0	1.0	1.0	1.0	1.0	1.0
D_{min}(1 cm^3) (PTV) [Gy]	58.0	57.5	57.1	57.8	57.5	57.8	57.7	57.1	57.9	57.3	57.6	57.6	57.6	56.9	57.6
D_{max}(1 cm^3) (PTV) [Gy]	60.8	60.6	60.4	61.1	61.5	61.1	60.8	60.6	61.0	61.4	60.8	60.8	61.2	61.6	61.2
σ (PTV) [Gy]	0.6	0.6	0.7	0.7	0.9	0.7	0.6	0.8	0.6	0.9	0.7	0.7	0.7	1.0	0.7
D_{mean} (PTV) [Gy]	59.9	59.2	58.9	59.9	59.9	59.9	59.8	59.5	59.9	59.9	59.8	59.8	59.9	59.8	59.9
Conformity index ConI	1.0	1.0	1.0	1.0	1.0	1.0	1.0	1.0	1.0	1.0	1.0	1.0	1.0	1.0	1.0
D_{max}(1 cm^3) (brainstem) [Gy]	42.1	42.0	41.8	40.9	40.3	40.9	42.0	41.7	41.6	40.0	42.1	42.1	41.6	40.6	41.6
D_{mean} (brainstem) [Gy]	23.3	23.1	23.1	21.9	21.5	21.9	23.1	22.9	22.3	21.2	23.3	23.3	23.0	22.2	23.0
D_{mean} (PTVwall 6 mm) [Gy]	42.1	41.7	41.5	41.1	40.7	41.1	41.7	41.0	41.5	39.8	41.9	41.9	41.2	40.6	41.2
Sum($\omega(B_1)$)/ Sum($\omega(B_2)$)	0.8	0.8	0.8	0.9	0.9	0.9	0.8	0.8	0.8	0.8	0.8	0.8	0.9	0.8	0.9

Table A.24: Obtained plan quality indicators and efficiency determining quantities by efficiency-optimization with method C and D of ASTRO G2; presented are the plan results of the shortest RT times for each facility type with maximal dose changes of 1% and 2% in D_{min}(1 cm^3) and D_{max}(1 cm^3) of the PTV.

	Initial plan	Method A				Method B			
		Method A1		Method A2		Method B		Method B'	
Evaluation criteria D1/D2		D1	D2	D1	D2	D1	D2	D2	
Shortest RT time for facility type		RT1/2	RT1/2	RT1/2	RT1/2	RT1/2	RT1/2	RT1	RT2
Trade-off factor s/ l_S, l_E	-	0.3	0.5	0.3	0.5	0.3	0.5	-	0.5
RT time 1 ($I = I_c$) [s]	197.0	173.8	168.3	175.9	170.5	186.1	181.9		201.3
RT time 2 ($I = I_v$) [s]	727.2	563.6	435.8	384.9	367.7	172.6	167.7		380.7
Number of energy layers	47	46	46	45	45	47	47		47
Number of spots	1587	1059	909	996	866	1587	1587		1587
Total spot weight sum	$9.4{\cdot}10^5$	$8.0{\cdot}10^5$	$7.6{\cdot}10^5$	$8.2{\cdot}10^5$	$7.8{\cdot}10^5$	$8.7{\cdot}10^5$	$8.4{\cdot}10^5$		$9.6{\cdot}10^5$
Average minimum $t_{B,k}$	72.3	121.8	137.3	80.0	108.3	150.3	148.1		154.8
Average $V(\omega(E_k,B))$	$3.3{\cdot}10^5$	$4.5{\cdot}10^5$	$5.3{\cdot}10^5$	$5.0{\cdot}10^5$	$5.7{\cdot}10^5$	$3.0{\cdot}10^5$	$3.0{\cdot}10^5$		$8.1{\cdot}10^4$
Coverage index CovI	1.0	1.0	1.0	1.0	1.0	1.0	1.0		1.0
$D_{min}(1\ cm^3)$ (PTV) [Gy]	57.9	57.5	57.1	57.5	57.1	57.4	57.0		57.2
$D_{max}(1\ cm^3)$ (PTV) [Gy]	61.1	61.3	61.5	61.3	61.5	61.2	61.2		61.5
σ (PTV) [Gy]	0.6	0.8	0.9	0.8	0.9	0.8	0.9		0.9
D_{mean} (PTV) [Gy]	59.9	59.9	59.9	59.9	59.9	59.9	59.8		59.9
Conformity index ConI	1.0	1.0	1.0	1.0	1.0	1.0	1.0		1.0
$D_{max}(1\ cm^3)$ (brainstem) [Gy]	39.7	39.6	39.0	39.4	38.7	38.5	37.6		38.4
D_{mean} (brainstem) [Gy]	19.7	19.7	19.1	19.4	18.7	19.2	18.5		19.7
D_{mean} (PTVwall 6 mm) [Gy]	41.5	39.1	38.2	39.2	38.2	39.5	38.5		41.3
$Sum(\omega(B_1))/$ $Sum(\omega(B_2))$	0.9	1.0	1.0	1.0	1.0	1.0	1.0		0.9

Table A.25: Obtained plan quality indicators and efficiency determining quantities by efficiency-optimization with methods A and B of ASTRO G3; presented are the plan results of the shortest RT times for each facility type with maximal dose changes of 1% and 2% in $D_{min}(1\ cm^3)$ and $D_{max}(1\ cm^3)$ of the PTV.

	Initial plan	Method C1				Method C2				Method D				
		NR		R		NR		R		NR		R		
Evaluation criteria D1/D2		D1	D2	D1	D2	D1	D2	D1	D2	D1	D2	D1		D2
Shortest RT time for facility type		RT1/2	RT1/2	RT1/2	RT1/2	RT1/2	RT1/2	RT1/2	RT1/2	RT1/2	RT1/2	RT1	RT2	RT1/2
Trade-off factor s/ l_S, l_E	-	0.2	0.3	0.8	0.8	0.1	0.1	0.1	0.3	3.0	4.0	8.0	2.0	9.0
RT time 1 ($I = I_c$) [s]	197.0	195.5	194.3	186.6	186.6	193.4	191.1	191.7	175.6	194.8	191.4	173.4	196.0	168.8
RT time 2 ($I = I_v$) [s]	727.2	147.2	129.3	293.0	293.0	281.1	207.6	433.9	410.7	725.1	718.4	753.4	700.2	506.2
Number of energy layers	47	47	47	45	45	45	45	45	40	45	43	35	46	33
Number of spots	1587	1374	1302	848	848	1449	1369	1297	871	1582	1551	1180	1585	1048
Total spot weight sum	$9.4{\cdot}10^5$	$9.3{\cdot}10^5$	$9.2{\cdot}10^5$	$8.8{\cdot}10^5$	$8.8{\cdot}10^5$	$9.3{\cdot}10^5$	$9.1{\cdot}10^5$	$9.2{\cdot}10^5$	$8.5{\cdot}10^5$	$9.4{\cdot}10^5$	$9.3{\cdot}10^5$	$8.6{\cdot}10^5$	$9.4{\cdot}10^5$	$8.5{\cdot}10^5$
Average minimum $t_{B,k}$	72.3	142.9	183.9	174.4	174.4	97.1	120.9	114.2	137.3	65.6	64.2	69.4	70.0	48.0
Average $V(\omega(E_k,B))$	$3.3{\cdot}10^5$	$3.3{\cdot}10^5$	$3.2{\cdot}10^5$	$4.5{\cdot}10^5$	$4.5{\cdot}10^5$	$3.3{\cdot}10^5$	$3.3{\cdot}10^5$	$3.7{\cdot}10^5$	$5.7{\cdot}10^5$	$3.3{\cdot}10^5$	$3.3{\cdot}10^5$	$3.7{\cdot}10^5$	$3.3{\cdot}10^5$	$4.1{\cdot}10^5$
Coverage index CovI	1.0	1.0	1.0	1.0	1.0	1.0	1.0	1.0	1.0	1.0	1.0	1.0	1.0	1.0
$D_{min}(1\ cm^3)$ (PTV) [Gy]	57.9	57.5	56.8	57.6	57.6	57.5	56.9	57.8	57.2	57.9	57.0	57.4	57.9	57.0
$D_{max}(1\ cm^3)$ (PTV) [Gy]	61.1	60.8	60.7	61.4	61.4	61.0	60.9	61.1	61.6	61.1	61.1	61.5	61.1	61.7
σ (PTV) [Gy]	0.6	0.7	0.9	0.8	0.8	0.7	0.9	0.7	0.9	0.6	0.8	0.8	0.6	0.9
D_{mean} (PTV) [Gy]	59.9	59.3	58.7	59.9	59.9	59.8	59.5	59.9	59.9	59.9	59.8	59.9	59.9	59.9
Conformity index ConI	1.0	1.0	1.0	1.0	1.0	1.0	1.0	1.0	1.0	1.0	1.0	1.0	1.0	1.0
$D_{max}(1\ cm^3)$ (brainstem) [Gy]	39.7	39.7	39.6	38.3	38.3	39.7	39.7	39.0	38.1	39.7	39.7	38.7	39.7	38.2
D_{mean} (brainstem) [Gy]	19.7	19.6	19.6	18.3	18.3	19.7	19.6	18.9	18.0	19.7	19.7	18.7	19.7	18.1
D_{mean} (PTVwall 6 mm) [Gy]	41.5	41.2	40.9	40.3	40.3	41.1	40.5	40.9	39.3	41.5	41.1	40.0	41.5	39.4
$Sum(\omega(B_1))/$ $Sum(\omega(B_2))$	0.9	0.9	0.9	1.0	1.0	1.0	1.0	0.9	0.9	0.9	0.9	0.8	0.9	0.6

Table A.26: Obtained plan quality indicators and efficiency determining quantities by efficiency-optimization with methods C and D of ASTRO G3; presented are the plan results of the shortest RT times for each facility type with maximal dose changes of 1% and 2% in $D_{min}(1\ cm^3)$ and $D_{max}(1\ cm^3)$ of the PTV.

	Initial plan	Method A		Method B		
		Method A1	Method A2			
Evaluation criteria D1/D2		D1/2	D1/2	D1		D2
Shortest RT time for facility type		RT1/2	RT1/2	RT1	RT2	RT1/2
Trade-off factor s/ l_S, l_E	-	0.1	0.1	0.1	-	0.3
RT time 1 ($I = I_c$) [s]	360.1	326.2	330.0	359.7		356.4
RT time 2 ($I = I_v$) [s]	1827.8	574.9	650.2	1829.0		1810.4
Number of energies	30	31	30	30		30
Number of spots	698	590	540	698		698
Total spot weight sum	$2.1{\cdot}10^6$	$1.8{\cdot}10^6$	$1.9{\cdot}10^6$	$2.1{\cdot}10^6$		$2.0{\cdot}10^6$
Average minimum $t_k(E_k,B)$	508.6	696.6	764.4	1509.4		1921.9
Average $V(\omega(E_k,B))$	$1.1{\cdot}10^7$	$1.3{\cdot}10^7$	$1.6{\cdot}10^7$	$1.0{\cdot}10^7$		$1.4{\cdot}10^7$
Coverage index CovI	1.0	1.0	1.0	1.0		1.0
D_{min}(1 cm^3) (PTV) [Gy]	67.2	66.7	66.8	66.8		65.9
D_{max}(1 cm^3) (PTV) [Gy]	77.5	77.6	77.6	77.6		78.2
σ (PTV)	1.5	1.6	1.6	1.6		1.8
D_{mean} (PTV) [Gy]	73.7	73.7	73.7	73.7		73.6
Conformity index ConI	1.1	1.1	1.1	1.1		1.1
D_{max}(1 cm^3) (bladder) [Gy]	74.2	74.2	74.2	74.2		74.2
D_{mean} (bladder) [Gy]	28.3	28.3	28.3	28.3		28.3
D_{max}(1 cm^3) (rectum) [Gy]	74.5	74.4	74.5	74.5		74.5
D_{mean} (rectum) [Gy]	23.2	23.2	23.2	23.2		23.2
D_{mean} (PTVwall 6 mm) [Gy]	55.6	54.7	54.7	55.6		55.2
$Sum(\omega(B_1))/Sum(\omega(B_2))$	1.5	1.6	1.7	1.7		1.7

Table A.27: Obtained plan quality indicators and efficiency determining quantities by efficiency-optimization with methods A and B of PRO G1; presented are the plan results of the shortest RT times for each facility type with maximal dose changes of 1% and 2% in D_{min}(1 cm^3) and D_{max}(1 cm^3) of the PTV.

	Initial plan	Method C1			Method C2					Method D		
		NR		R	NR		R			R		
Evaluation criteria D1/D2		D1	D2	D1/2	D1	D2	D1	D2		D1	D2	
Shortest RT time for facility type		RT1/2	RT1/2	RT1/2	RT1/2	RT1/2	RT1/2	RT1	RT2	RT1/2	RT1	RT2
Trade-off factor s/ l_S, l_E	-	0.4	0.4	0.5	0.1	0.1	0.2	0.3	0.2	2.0	3.0	2.0
RT time 1 ($I = I_c$) [s]	360.1	353.2	352.5	351.6	357.5	354.7	348.1	338.3	348.1	344.4	332.4	344.4
RT time 2 ($I = I_v$) [s]	1827.8	191.6	191.3	266.3	198.3	192.3	219.2	303.4	219.2	1693.7	2134.9	1693.7
Number of energies	30	30	30	30	30	30	30	29	30	28	26	28
Number of spots	698	558	552	483	625	598	507	408	507	631	603	631
Total spot weight sum	$2.1{\cdot}10^6$	$2.0{\cdot}10^6$	$2.0{\cdot}10^6$	$2.0{\cdot}10^6$	$2.0{\cdot}10^6$	$2.0{\cdot}10^6$	$2.0{\cdot}10^6$	$1.9{\cdot}10^6$	$2.0{\cdot}10^6$	$2.0{\cdot}10^6$	$1.9{\cdot}10^6$	$2.0{\cdot}10^6$
Average minimum $t_{B,k}$	508.6	1093.1	1113.4	1069.0	881.0	1177.7	1205.6	1358.2	1205.6	555.4	288.4	555.4
Average $V(\omega(E_k,B))$	$1.1{\cdot}10^7$	$1.2{\cdot}10^7$	$1.1{\cdot}10^7$	$1.3{\cdot}10^7$	$1.1{\cdot}10^7$	$1.1{\cdot}10^7$	$1.4{\cdot}10^7$	$1.8{\cdot}10^7$	$1.4{\cdot}10^7$	$1.1{\cdot}10^7$	$1.1{\cdot}10^7$	$1.1{\cdot}10^7$
Coverage index CovI	1.0	0.8	0.8	1.0	1.0	0.9	1.0	0.9	1.0	1.0	1.0	1.0
D_{min}(1 cm^3) (PTV) [Gy]	67.2	66.6	66.1	67.1	67.1	66.3	66.9	66.0	66.9	66.6	66.5	66.6
D_{max}(1 cm^3) (PTV) [Gy]	77.5	76.9	76.9	77.6	77.4	77.3	77.6	77.9	77.6	77.6	77.7	77.6
σ (PTV)	1.5	1.9	2.1	1.6	1.5	1.7	1.6	1.9	1.6	1.6	1.7	1.6
D_{mean} (PTV) [Gy]	73.7	72.1	71.9	73.7	73.5	73.2	73.7	73.5	73.7	73.7	73.6	73.7
Conformity index ConI	1.1	1.0	1.0	1.1	1.1	1.0	1.1	1.1	1.1	1.1	1.1	1.1
D_{max}(1 cm^3) (bladder) [Gy]	74.2	73.5	73.5	74.1	74.0	73.8	74.2	74.0	74.2	74.2	74.2	74.2
D_{mean} (bladder) [Gy]	28.3	27.9	27.9	27.8	28.2	28.1	27.8	27.2	27.8	27.7	27.5	27.7
D_{max}(1 cm^3) (rectum) [Gy]	74.5	73.4	73.2	74.5	74.4	74.3	74.5	74.5	74.5	74.5	74.5	74.5
D_{mean} (rectum) [Gy]	23.2	22.7	22.7	22.9	23.2	23.1	22.9	22.7	22.9	23.4	23.3	23.4
D_{mean} (PTVwall 6 mm) [Gy]	55.6	54.6	54.6	55.1	55.2	54.9	54.9	54.2	54.9	54.8	54.3	54.8
$Sum(\omega(B_1))/Sum(\omega(B_2))$	1.5	1.5	1.5	1.5	1.5	1.5	1.5	1.5	1.5	1.3	1.4	1.3

Table A.28: Obtained plan quality indicators and efficiency determining quantities by efficiency-optimization with methods C and D of PRO G1; presented are the plan results of the shortest RT times for each facility type with maximal dose changes of 1% and 2% in D_{min}(1 cm^3) and D_{max}(1 cm^3) of the PTV.

	Initial plan	Method A							Method B			
		Method A1				Method A2						
Evaluation criteria D1/D2		D1		D2		D1		D2	D1		D2	
Shortest RT time for facility type		RT1	RT2	RT1	RT2	RT1	RT2	RT1/2	RT1	RT2	RT1	RT2
Trade-off factor s/ l_S, l_E	-	0.1	-	0.5	0.3	0.1	-	0.5	-	0.2	-	0.4
RT time 1 ($I = I_c$) [s]	400.7	351.2		321.8	335.9	360.7		339.4		405.5		405.3
RT time 2 ($I = I_v$) [s]	764.4	2689.0		673.2	497.3	2163.3		422.6		745.2		738.9
Number of energy layers	31	33		31	31	31		31		31		31
Number of spots	791	1558		520	559	791		448		791		791
Total spot weight sum	$2.3{\cdot}10^6$	$2.0{\cdot}10^6$		$1.8{\cdot}10^6$	$1.9{\cdot}10^6$	$2.1{\cdot}10^6$		$1.9{\cdot}10^6$		$2.3{\cdot}10^6$		$2.3{\cdot}10^6$
Average minimum $t_{B,k}$	277.6	33.7		592.4	624.6	182.5		891.5		531.3		564.9
Average $V(\omega(E_k,B))$	$9.8{\cdot}10^6$	$1.1{\cdot}10^7$		$1.4{\cdot}10^7$	$1.4{\cdot}10^7$	$1.6{\cdot}10^7$		$2.2{\cdot}10^7$		$1.0{\cdot}10^7$		$1.1{\cdot}10^7$
Coverage index CovI	1.0	1.0		1.0	1.0	1.0		1.0		1.0		1.0
D_{min}(1 cm^3) (PTV) [Gy]	71.2	70.8		69.9	70.4	70.8		69.9		70.6		69.8
D_{max}(1 cm^3) (PTV) [Gy]	75.6	75.8		76.2	75.9	75.8		76.1		75.7		75.8
σ (PTV) [Gy]	0.7	0.8		1.0	0.8	0.8		1.0		0.8		0.9
D_{mean} (PTV) [Gy]	73.9	73.9		73.8	73.8	73.9		73.8		73.9		73.8
Conformity index ConI	1.1	1.1		1.1	1.1	1.1		1.1		1.1		1.1
D_{max}(1 cm^3) (bladder) [Gy]	74.3	74.3		74.3	74.3	74.3		74.3		74.3		74.3
D_{mean} (bladder) [Gy]	32.1	32.1		32.1	32.1	32.1		31.8		32.1		32.1
D_{max}(1 cm^3) (rectum) [Gy]	74.4	74.4		74.5	74.4	74.4		74.4		74.5		74.4
D_{mean} (rectum) [Gy]	27.1	27.1		27.1	27.1	27.1		27.1		27.1		27.1
D_{mean} (PTVwall 6 mm) [Gy]	61.0	60.0		58.6	59.4	60.2		59.0		61.0		60.8
Sum($\omega(B_1)$)/ Sum($\omega(B_2)$)	1.1	1.2	-	1.2	1.2	1.2		1.3		1.2		1.2

Table A.29: Obtained plan quality indicators and efficiency determining quantities by efficiency-optimization with methods A and B of PRO G2; presented are the plan results of the shortest RT times for each facility type with maximal dose changes of 1% and 2% in D_{min}(1 cm^3) and D_{max}(1 cm^3) of the PTV.

	Initial plan	Method C1						Method C2						Method D			
		NR		R				NR		R				R			
Evaluation criteria D1/D2		D1	D2	D1		D2		D1	D2	D1		D2		D1		D2	
Shortest RT time for facility type		RT1/2	RT1/2	RT1	RT2	RT1	RT2	RT1/2	RT1/2	RT1	RT2	RT1	RT2	RT1	RT2	RT1	RT2
Trade-off factor s/ l_S, l_E	-	0.3	0.3	0.8	0.1	0.8	0.1	0.1	0.1	0.2	0.1	0.2	0.1	3.0	-	4.0	-
RT time 1 ($I = I_c$) [s]	400.7	395.7	393.0	382.8	400.2	382.8	400.2	397.7	395.8	379.4	394.0	379.4	394.0	382.7		364.0	
RT time 2 ($I = I_v$) [s]	764.4	213.4	212.0	250.6	218.6	250.6	218.6	232.1	217.0	622.1	350.2	622.1	350.2	1018.3		1233.7	
Number of energy layers	31	31	31	31	31	31	31	31	31	30	31	30	31	27		25	
Number of spots	791	664	634	435	738	435	738	727	705	546	666	546	666	708		635	
Total spot weight sum	$2.3{\cdot}10^6$	$2.3{\cdot}10^6$	$2.3{\cdot}10^6$	$2.2{\cdot}10^6$	$2.3{\cdot}10^6$	$2.2{\cdot}10^6$	$2.3{\cdot}10^6$	$2.3{\cdot}10^6$	$2.3{\cdot}10^6$	$2.2{\cdot}10^6$	$2.3{\cdot}10^6$	$2.2{\cdot}10^6$	$2.3{\cdot}10^6$	$2.2{\cdot}10^6$		$2.1{\cdot}10^6$	
Average minimum $t_{B,k}$	277.6	921.0	1024.9	944.9	453.1	944.9	453.1	659.6	706.5	771.1	794.5	771.1	794.5	467.4		352.9	
Average $V(\omega(E_k,B))$	$9.8{\cdot}10^6$	$9.5{\cdot}10^6$	$9.5{\cdot}10^6$	$1.4{\cdot}10^7$	$1.0{\cdot}10^7$	$1.4{\cdot}10^7$	$1.0{\cdot}10^7$	$9.5{\cdot}10^6$	$9.6{\cdot}10^6$	$1.4{\cdot}10^7$	$1.0{\cdot}10^7$	$1.4{\cdot}10^7$	$1.0{\cdot}10^7$	$1.1{\cdot}10^7$		$1.2{\cdot}10^7$	
Coverage index CovI	1.0	1.0	1.0	1.0	1.0	1.0	1.0	1.0	1.0	1.0	1.0	1.0	1.0	1.0		1.0	
D_{min}(1 cm^3) (PTV) [Gy]	71.2	70.5	69.8	70.8	71.2	70.8	71.2	70.7	70.3	70.5	71.1	70.5	71.1	70.8		70.4	
D_{max}(1 cm^3) (PTV) [Gy]	75.6	75.1	74.8	75.8	75.6	75.8	75.6	75.5	75.4	75.9	75.6	75.9	75.6	75.8		76.0	
σ (PTV) [Gy]	0.7	0.9	1.0	0.8	0.7	0.8	0.7	0.7	0.8	0.8	0.7	0.8	0.7	0.8		0.9	
D_{mean} (PTV) [Gy]	73.9	72.7	72.1	73.8	73.9	73.8	73.9	73.7	73.6	73.9	73.9	73.9	73.9	73.9		73.8	
Conformity index ConI	1.1	1.1	1.1	1.1	1.1	1.1	1.1	1.1	1.1	1.1	1.1	1.1	1.1	1.1		1.1	
D_{max}(1 cm^3) (bladder) [Gy]	74.3	73.8	73.4	74.3	74.3	74.3	74.3	74.1	74.1	74.3	74.3	74.3	74.3	74.3		74.3	
D_{mean} (bladder) [Gy]	32.1	31.9	31.7	31.7	32.0	31.7	32.0	32.0	32.0	31.6	31.9	31.6	31.9	31.8		31.4	
D_{max}(1 cm^3) (rectum) [Gy]	74.4	73.7	73.6	74.4	74.4	74.4	74.4	74.4	74.4	74.5	74.5	74.5	74.5	74.4		74.4	
D_{mean} (rectum) [Gy]	27.1	26.9	26.8	26.5	27.0	26.5	27.0	27.1	27.1	26.5	26.9	26.5	26.9	27.2		26.9	
D_{mean} (PTVwall 6 mm) [Gy]	61.0	60.4	60.1	60.4	61.0	60.4	61.0	60.7	60.5	60.4	60.8	60.4	60.8	60.6		59.8	
Sum($\omega(B_1)$)/ Sum($\omega(B_2)$)	1.1	1.1	1.1	1.0	1.1	1.0	1.1	1.1	1.1	1.0	1.1	1.0	1.1	1.3		1.3	

Table A.30: Obtained plan quality indicators and efficiency determining quantities by efficiency-optimization with methods C and D of PRO G2; presented are the plan results of the shortest RT times for each facility type with maximal dose changes of 1% and 2% in D_{min}(1 cm^3) and D_{max}(1 cm^3) of the PTV.

	Initial plan	Method A					Method B			
		Method A1			Method A2					
Evaluation criteria D1/D2		D1		D2	D1	D2	D1		D2	
Shortest RT time for facility type		RT1	RT2	RT1/2	RT1/2	RT1/2	RT1	RT2	RT1	RT2
Trade-off factor s/ l_S, l_E	-	0.3	-	0.5	0.3	0.5	-	0.5	0.8	0.5
RT time 1 ($I = I_c$) [s]	390.7	333.6		317.0	340.1	328.4		391.1	390.1	391.1
RT time 2 ($I = I_v$) [s]	1460.1	3005.5		1077.6	633.8	404.3		1449.6	1456.7	1449.6
Number of energy layers	36	38		29	34	32		36	36	36
Number of spots	1046	2128		605	610	525		1046	1046	1046
Total spot weight sum	$2.2{\cdot}10^6$	$1.8{\cdot}10^6$		$1.8{\cdot}10^6$	$1.9{\cdot}10^6$	$1.8{\cdot}10^6$		$2.2{\cdot}10^6$	$2.2{\cdot}10^6$	$2.2{\cdot}10^6$
Average minimum $t_{B,k}$	576.9	0.03		285.2	994.3	874.7		1022.1	1079.5	1022.1
Average $V(\omega(E_k,B))$	$6.2{\cdot}10^6$	$5.5{\cdot}10^6$		$8.5{\cdot}10^6$	$8.7{\cdot}10^6$	$1.0{\cdot}10^7$		$7.7{\cdot}10^6$	$8.3{\cdot}10^6$	$7.7{\cdot}10^6$
Coverage index CovI	1.0	1.0		1.0	1.0	1.0		1.0	1.0	1.0
D_{min}(1 cm^3) (PTV) [Gy]	72.3	71.8		71.4	71.9	71.4		72.0	71.6	72.0
D_{max}(1 cm^3) (PTV) [Gy]	75.0	75.1		75.3	75.2	75.3		75.1	75.2	75.1
σ (PTV) [Gy]	0.5	0.6		0.6	0.6	0.6		0.7	0.8	0.7
D_{mean} (PTV) [Gy]	73.9	73.8		73.8	73.8	73.8		73.8	73.8	73.8
Conformity index ConI	1.2	1.2		1.1	1.2	1.1		1.2	1.2	1.2
D_{max}(1 cm^3) (rectum) [Gy]	74.0	74.0		74.0	74.0	74.0		74.0	74.0	74.0
D_{mean} (rectum) [Gy]	30.8	30.4		29.3	30.5	29.9		31.7	31.7	31.7
D_{mean} (PTVwall 6 mm) [Gy]	62.2	61.8		60.6	61.2	60.5		62.2	62.2	62.2
$Sum(\omega(B_1))$/ $Sum(\omega(B_2))$	1.1	1.3		1.2	1.2	1.2		1.2	1.3	1.2

Table A.31: Obtained plan quality indicators and efficiency determining quantities by efficiency-optimization with methods A and B of PRO G3; presented are the plan results of the shortest RT times for each facility type with maximal dose changes of 1% and 2% in D_{min}(1 cm^3) and D_{max}(1 cm^3) of the PTV.

	Initial plan	Method C1					Method C2					Method D			
		NR		R			NR		R			R			
Evaluation criteria D1/D2		D1	D2	D1		D2	D1	D2	D1		D2	D1		D2	
Shortest RT time for facility type		RT1/2	RT1/2	RT1	RT2	RT1/2	RT1/2	RT1/2	RT1	RT2	RT1/2	RT1	RT2	RT1	RT2
Trade-off factor s/ l_S, l_E	-	0.3	0.3	0.8	0.3	1.2	0.0	0.1	0.1	-	0.3	5.0	4.0	7.0	4.0
RT time 1 ($I = I_c$) [s]	390.7	386.9	384.7	370.4	383.1	352.1	387.5	381.4	371.1		338.7	352.1	363.4	327.0	363.4
RT time 2 ($I = I_v$) [s]	1460.1	211.5	210.4	712.1	466.2	218.5	258.4	233.4	1525.2		789.9	2044.7	939.2	2057.5	939.2
Number of energy layers	36	36	36	36	36	36	36	35	35		30	27	30	22	30
Number of spots	1046	888	852	553	861	388	957	922	785		509	830	865	684	865
Total spot weight sum	$2.2{\cdot}10^6$	$2.2{\cdot}10^6$	$2.2{\cdot}10^6$	$2.1{\cdot}10^6$	$2.2{\cdot}10^6$	$2.0{\cdot}10^6$	$2.2{\cdot}10^6$	$2.2{\cdot}10^6$	$2.1{\cdot}10^6$		$1.9{\cdot}10^6$	$2.0{\cdot}10^6$	$2.1{\cdot}10^6$	$1.9{\cdot}10^6$	$2.1{\cdot}10^6$
Average minimum $t_{B,k}$	576.9	849.3	937.0	666.0	629.3	1306.9	705.3	645.8	817.3		1008.4	414.7	329.8	406.0	329.8
Average $V(\omega(E_k,B))$	$6.2{\cdot}10^6$	$6.2{\cdot}10^6$	$6.2{\cdot}10^6$	$8.9{\cdot}10^6$	$7.2{\cdot}10^6$	$1.1{\cdot}10^7$	$6.2{\cdot}10^6$	$6.2{\cdot}10^6$	$7.4{\cdot}10^6$		$9.9{\cdot}10^6$	$7.4{\cdot}10^6$	$7.2{\cdot}10^6$	$8.6{\cdot}10^6$	$7.2{\cdot}10^6$
Coverage index CovI	1.0	1.0	1.0	1.0	1.0	1.0	1.0	1.0	1.0		1.0	1.0	1.0	1.0	1.0
D_{min}(1 cm^3) (PTV) [Gy]	72.3	71.7	71.1	71.9	72.3	71.0	72.0	71.0	72.2		71.2	71.9	72.1	71.1	72.1
D_{max}(1 cm^3) (PTV) [Gy]	75.0	74.7	74.4	75.2	75.0	76.0	74.9	74.9	75.1		75.3	75.1	75.1	75.5	75.1
σ (PTV) [Gy]	0.5	0.6	0.6	0.6	0.5	1.0	0.5	0.6	0.5		0.7	0.5	0.5	0.8	0.5
D_{mean} (PTV) [Gy]	73.9	73.1	72.6	73.8	73.9	73.7	73.8	73.6	73.9		73.8	73.8	73.9	73.8	73.9
Conformity index ConI	1.2	1.1	1.1	1.1	1.2	1.1	1.2	1.1	1.1		1.1	1.2	1.2	1.1	1.2
D_{max}(1 cm^3) (rectum) [Gy]	74.0	73.7	73.4	74.0	74.0	73.9	74.0	74.0	74.0		74.0	74.0	74.0	74.0	74.0
D_{mean} (rectum) [Gy]	30.8	30.7	30.6	30.1	30.5	29.9	30.8	30.8	30.2		30.3	30.8	31.0	29.9	31.0
D_{mean} (PTVwall 6 mm) [Gy]	62.2	61.7	61.4	61.2	61.8	60.5	61.9	61.4	61.4		60.5	61.6	61.9	60.7	61.9
$Sum(\omega(B_1))$/ $Sum(\omega(B_2))$	1.1	1.1	1.1	1.1	1.0	1.1	1.1	1.1	1.0		1.1	1.2	1.2	1.3	1.2

Table A.32: Obtained plan quality indicators and efficiency determining quantities by efficiency-optimization with methods C and D of PRO G3; presented are the plan results of the shortest RT times for each facility type with maximal dose changes of 1% and 2% in D_{min}(1 cm^3) and D_{max}(1 cm^3) of the PTV.

Case Geometries	Proton current	limitting PTV DVH Criteria	**Method A1**		**Method B**		**Method C1** NR		**Method C1** R		**Method D** R	
			$t_E = 1s$	$t_E = 5s$	$t_E = 1s$	$t_E = 5s$	$t_E = 1s$	$t_E = 5s$	$t_E = 1s$	$t_E = 5s$	$t_E = 1s$	$t_E = 5s$
ASTRO Geo 1	const.	D1	**21.4**	**24.2**	4.1	2.0	1.4	1.7	**4.9**	**4.5**	**15.9**	**25.7**
		D2	**24.5**	**28.0**	6.3	3.1	1.7	1.9	**5.9**	**5.0**	**19.8**	**31.8**
	var.	D1	29.5	29.1	**80.5**	**66.8**	**81.8**	**68.3**	67.7	56.6	15.0	14.2
		D2	46.1	43.6	**81.5**	**67.7**	**83.3**	**69.5**	74.8	62.8	30.7	33.2
ASTRO Geo 2	const.	D1	**15.7**	**14.1**	5.2	3.3	0.9	0.5	**4.3**	**3.4**	**14.0**	**53.7**
		D2	**21.4**	**25.0**	7.4	5.1	1.8	2.1	**5.4**	**4.0**	**18.8**	**56.3**
	var.	D1	46.8	41.7	**82.5**	**70.8**	**86.6**	**74.0**	81.0	69.6	40.0	48.7
		D2	46.8	41.7	**82.8**	**71.1**	**88.0**	**75.6**	81.0	69.6	40.0	48.7
ASTRO Geo 3	const.	D1	**11.8**	**7.0**	5.5	2.8	0.8	0.4	**5.3**	**4.8**	**12.0**	**55.0**
		D2	**14.6**	**8.5**	7.7	3.9	1.4	0.7	**5.3**	**4.8**	**14.3**	**56.2**
	var.	D1	22.5	18.3	**76.3**	**60.6**	**79.8**	**63.4**	59.7	48.3	3.7	3.4
		D2	40.1	32.3	**76.9**	**61.1**	**82.2**	**65.3**	59.7	48.3	30.4	44.7
Pro Geo 1	const.	D1	**9.4**	**6.2**	0.1	0.0	1.9	1.4	**2.3**	**1.8**	**4.3**	**4.9**
		D2	**9.4**	**6.2**	1.0	0.8	2.1	1.6	**2.3**	**1.8**	**7.7**	**9.1**
	var.	D1	68.6	64.1	**0.0**	**0.0**	**89.5**	**84.0**	85.4	80.2	7.3	7.3
		D2	68.6	64.1	**1.0**	**0.9**	**89.5**	**84.0**	85.4	80.2	7.3	7.3
Pro Geo 2	const.	D1	**12.4**	**7.9**	0.0	0.0	1.3	1.0	**4.5**	**3.4**	**4.5**	**6.5**
		D2	**19.7**	**15.0**	0.0	0.0	1.9	1.4	**4.5**	**3.4**	**9.2**	**11.6**
	var.	D1	0.0	0.0	**2.5**	**2.2**	**72.1**	**62.0**	71.4	61.4	0.0	0.0
		D2	34.9	30.1	**3.3**	**2.9**	**72.3**	**62.2**	71.4	61.4	0.0	0.0
Pro Geo 3	const.	D1	**14.6**	**9.2**	0.0	0.0	1.0	0.7	**5.2**	**3.8**	**9.9**	**14.0**
		D2	**18.9**	**19.0**	0.2	0.1	1.5	1.1	**9.9**	**7.2**	**16.3**	**22.4**
	var.	D1	0.0	0.0	**0.7**	**0.6**	**85.5**	**77.8**	68.1	62.0	35.7	34.0
		D2	26.2	25.6	**0.7**	**0.6**	**85.6**	**77.9**	85.0	77.4	35.7	34.0

Table A.33: Comparison of time savings [%] for energy switch times of $t_E = 1s$ and $t_E = 5s$ for different astrocytoma and prostate geometries of selective optimization methods.

Acronyms

3D-CRT	3D conformal radiotherapy
CE	Contralateral esophagus
ConI	Conformity index
CovI	Coverage index
CT	Computed tomography image
CTV	Clinical target volume
DNA	Deoxyribonucleic acid
DVH	Dose volume histogram
EUD	Equivalent uniform dose
GTV	Gross tumor volume
HNC	Head and neck cancer
HU	Hounsfield units
IGRT	Image guided radiotherapy
IMPT	Intensity modulated proton therapy
IMPT-2F	IMPT plan of two fields/ beam angles
IMPT-3F	IMPT plan of three fields/ beam angles
IMRT	Intensity modulated radiotherapy
IMXT	Intensity modulated photon therapy
Linac	Linear accelerator
LUT	Look-up table
MCO	Multicriteria optimization
MLC	Multileaf collimator
MRI	Magnetic resonance imaging

MU	Monitor unit
NSCLC	Non-small cell lung cancer
OAR	Organ at risk
OF	Objective function
p-CT	Planning computed tomography
PET	Positron emission tomography
PrEfOpt	Prioritized efficiency optimization
PTV	Planning target volume
RBE	Relative biological effectiveness
RT	Radiotherapy
SFUD	Single field uniform dose
TPS	Treatment planning system
VMAT	Volumetric modulated arc therapy
VOI	Volume of interest

List of Figures

List of Tables

Bibliography

[1] N. J. Aherne, L. C. Benjamin, P. J. Horsley, T. Silva, S. Wilcox, J. Amalaseelan, P. Dwyer, A. M. R. Tahir, J. Hill, A. Last, C. Hansen, C. S. McLachlan, Y. L. Lee, M. J. McKay, and T. P. Shakespeare. Improved Outcomes with Intensity Modulated Radiation Therapy Combined with Temozolomide for Newly Diagnosed Glioblastoma Multiforme. *Neurology Research International*, 2014:945620, 2014.

[2] M. Ahmad, L. Xiang, S. Yousefi, and L. Xing. Theoretical detection threshold of the proton-acoustic range verification technique. *Medical Physics*, 42(10):5735–44, 2015.

[3] A. Ahnesjö and M. M. Aspradakis. Dose calculations for external photon beams in radiotherapy. *Physics in Medicine and Biology*, 44(11):R99–155, 1999.

[4] H. Al-Halabi, P. Paetzold, G. C. Sharp, C. Olsen, and H. Willers. A Contralateral Esophagus-Sparing Technique to Limit Severe Esophagitis Associated With Concurrent High-Dose Radiation and Chemotherapy in Patients With Thoracic Malignancies. *International Journal of Radiation Oncology, Biology, Physics*, 92(4):803–10, 2015.

[5] M. Alber, G. Meedt, F. Nüsslin, and R. Reemtsen. On the degeneracy of the IMRT optimization problem. *Medical Physics*, 29(11):2584–9, 2002.

[6] F. Albertini, A. Bolsi, A. J. Lomax, H. P. Rutz, B. Timmerman, and G. Goitein. Sensitivity of intensity modulated proton therapy plans to changes in patient weight. *Radiotherapy and Oncology*, 86(2):187–94, 2008.

[7] P. Andreo. Monte Carlo techniques in medical radiation physics. *Physics in Medicine and Biology*, 36(7):861–920, 1991.

[8] M. Bamberg, M. Molls, and H. Sack, editors. *Radioonkologie Band 2: Klinik*. W. Zuckschwerdt Verlag GmbH, 2009.

[9] J. Belderbos, W. Heemsbergen, M. Hoogeman, K. Pengel, M. Rossi, and J. Lebesque. Acute esophageal toxicity in non-small cell lung cancer patients after high dose conformal radiotherapy. *Radiotherapy and Oncology*, 75(2):157–64, 2005.

[10] D. Bertsimas, V. Cacchiani, D. Craft, and O. Nohadani. A hybrid approach to beam angle optimization in intensity-modulated radiation therapy. *Computers and Operations Research*, 40(9):2187–97, 2013.

[11] J. M. Bewes, N. Suchowerska, M. Jackson, M. Zhang, and D. R. McKenzie. The radiobiological effect of intra-fraction dose-rate modulation in intensity modulated radiation therapy (IMRT). *Physics in Medicine and Biology*, 53(13):3567–78, 2008.

[12] R. Bokrantz. *Multicriteria optimization for managing tradeoffs in radiation therapy treatment planning*. PhD thesis, KTH Royal Institute of Technology, 2013.

[13] J. Booth, J. Ng, R. O'Brien, P. Keall, P. Poulsen, V. Calliet, P. Juneja, T. Eade, and A. Kneebone. TH-AB-303-09: Gated Prostate Radiotherapy: Accuracy and Dosimetric Results From First Clinical Study with Kilovoltage Intrafraction Monitoring. *Medical Physics*, 42(6):3712–3, 2015.

[14] T. Bortfeld. Optimized planning using physical objectives and constraints. *Seminars in Radiation Oncology*, 9(1):20–34, 1999.

[15] T. Bortfeld. IMRT: a review and preview. *Physics in Medicine and Biology*, 51(13):R363–79, 2006.

[16] T. Bortfeld. The number of beams in IMRT - theoretical investigations and implications for single-arc IMRT. *Physics in Medicine and Biology*, 55(1):83–97, 2010.

[17] T. Bortfeld, A. L. Boyer, W. Schlegel, D. L. Kahler, and T. J. Waldron. Realization and verification of three-dimensional conformal radiotherapy with modulated fields. *International Journal of Radiation Oncology, Biology, Physics*, 30(4):899–908, 1994.

[18] T. Bortfeld, J. Bürkelbach, R. Boesecke, and W. Schlegel. Methods of image reconstruction from projections applied to conformation radiotherapy. *Physics in Medicine and Biology*, 35(10):1423–34, 1990.

[19] T. Bortfeld and R. Jeraj. The physical basis and future of radiation therapy. *British Journal of Radiology*, 84(1002):485–98, 2011.

[20] T. Bortfeld, W. Schlegel, and B. Rhein. Decomposition of pencil beam kernels for fast dose calculations in three-dimensional treatment planning. *Medical Physics*, 20(2):311–8, 1993.

[21] T. Bortfeld, R. Schmidt-Ullrich, W. De Neve, and D. E. Wazer, editors. *Image-Guided IMRT*. Springer, 2006.

[22] T. Bortfeld and S. Webb. Single-Arc IMRT? *Physics in Medicine and Biology*, 54(1):N9–20, 2009.

[23] A. Brahme. Optimization of stationary and moving beam radiation therapy techniques. *Radiotherapy and Oncology*, 12(2):129–40, 1988.

[24] W. Budach, E. Bölke, R. Fietkau, A. Buchali, T. G. Wendt, W. Popp, C. Matuschek, and H. Sack. Evaluation of Time, Attendance of Medical Staff, and Resources During Radiotherapy for Head and Neck Cancer Patients. *Strahlentherapie und Onkologie*, 187(8):449–60, 2011.

[25] Statistisches Bundesamt. Todesursachen in Deutschland - Fachserie 12 Reihe 4 - 2014, 2016.

[26] W. Cao, G. Lim, L. Liao, Y. Li, S. Jiang, X. Li, H. Li, K. Suzuki, X. R. A. Zhu, D. Gomez, and X. Zhang. Proton energy optimization and reduction for intensity-modulated proton therapy. *Physics in Medicine and Biology*, 59(21):6341–54, 2014.

[27] A. W. Chan and N. J. Liebsch. Proton radiation therapy for head and neck cancer. *Journal of Surgical Oncology*, 97(8):697–700, 2008.

[28] K. S. C. Chao, F. J. Wippold II, G. Ozyigit, B. N. Tran, and J. F. Dempsey. Determination and delineation of nodal target volumes for head-and-neck cancer based on patterns of failure in patients receiving definitive and postoperative IMRT. *International Journal of Radiation Oncology, Biology, Physics*, 53(5):1174–84, 2002.

[29] W. Chen, J. Unkelbach, A. Trofimov, T. Madden, H. Kooy, T. Bortfeld, and D. Craft. Including robustness in multi-criteria optimization for intensity-modulated proton therapy. *Physics in Medicine and Biology*, 57(3):591–608, 2012.

[30] C. S. Chung, T. I. Yock, K. Nelson, Y. Xu, N. L. Keating, and N. J. Tarbell. Incidence of Second Malignancies Among Patients Treated With Proton Versus Photon Radiation. *International Journal of Radiation Oncology, Biology, Physics*, 87(1):46–52, 2013.

[31] E. Colvill, J. Booth, S. Nill, M. Fast, J. Bedford, U. Oelfke, M. Nakamura, P. Poulsen, E. Worm, R. Hansen, T. Ravkilde, J. S. Rydhög, T. Pommer, P. M. af Rosenschold, S. Lang, M. Guckenberger, C. Groh, C. Herrmann, D. Verellen, K. Poels, L. Wang, M. Hadsell, T. Sothmann, O. Blanck, and P. Keall. A dosimetric comparison of real-time adaptive and non-adaptive radiotherapy: A multi-institutional study encompassing robotic, gimbaled, multileaf collimator and couch tracking. *Radiotherapy and Oncology*, in press, 2016. http://dx.doi.org/10.1016/j.radonc.2016.03.006.

[32] D. J. Convery and M. E. Rosenbloom. The generation of intensity-modulated fields for conformal radiotherapy by dynamic collimation. *Physics in Medicine and Biology*, 37(6):1359–74, 1992.

[33] M. M. Coselmon, J. M. Moran, J. D. Radawski, and B. A. Fraass. Improving IMRT delivery efficiency using intensity limits during inverse planning. *Medical Physics*, 32(5):1234–45, 2005.

[34] L. Cozzi, A. Fogliata, A. Lomax, and A. Bolsi. A treatment planning comparison of 3D conformal therapy, intensity modulated photon therapy and proton therapy for treatment of advanced head and neck tumours. *Radiotherapy and Oncology*, 61(3):287–97, 2001.

[35] D. Craft. Calculating and controlling the error of discrete representations of Pareto surfaces in convex multi-criteria optimization. *Physica Medica*, 26:184–91, 2010.

[36] D. Craft and T. Bortfeld. How many plans are needed in an IMRT multi-objective plan database? *Physics in Medicine and Biology*, 53(11):2785–96, 2008.

[37] D. Craft, T. Halabi, and T. Bortfeld. Exploration of tradeoffs in intensity-modulated radiotherapy. *Physics in Medicine and Biology*, 50(24):5857–68, 2005.

[38] D. Craft, P. Süss, and T. Bortfeld. The Tradeoff Between Treatment Plan Quality and Required Number of Monitor Units in Intensity-modulated Radiotherapy. *International Journal of Radiation Oncology, Biology, Physics*, 67(5):1596–605, 2007.

[39] D. L. Craft, T. S. Hong, H. A. Shih, and T. R. Bortfeld. Improved planning time and plan quality through multicriteria optimization for intensity-modulated radiotherapy. *International Journal of Radiation Oncology, Biology, Physics*, 82(1):e83–90, 2012.

[40] S. M. Crooks, L. F. McAven, D. F. Robinson, and L. Xing. Minimizing delivery time and monitor units in static IMRT by leaf-sequencing. *Physics in Medicine and Biology*, 47(17):3105–16, 2002.

[41] J. O. Deasy, A. I. Blanco, and V. H. Clark. CERR: A computational environment for radiotherapy research. *Medical Physics*, 30(5):979–85, 2003.

[42] J. Dineley. Treatment images highlight dose changes, 2015. http://medicalphysicsweb.org/cws/article/research/60912.

[43] R. E. Drzymala, R. Mohan, L. Brewster, J. Chu, M. Goitein, W. Harms, and M. Urie. Dose-volume histograms. *International Journal of Radiation Oncology, Biology, Physics*, 21(1):71–8, 1991.

[44] M. N. Duma, S. Kampfer, J. J. Wilkens, T. Schuster, M. Molls, and H. Geinitz. Comparative analysis of an image-guided versus a non-image-guided setup approach in terms of delivered dose to the parotid glands in head-and-neck cancer IMRT. *International Journal of Radiation Oncology, Biology, Physics*, 77(4):1266–73, 2010.

[45] B. Emami, J. Lyman, A. Brown, L. Cola, M. Goitein, J. E. Munzenrider, B. Shank, L. J. Solin, and M. Wesson. Tolerance of normal tissue to therapeutic irradiation. *International Journal of Radiation Oncology, Biology, Physics*, 21(1):109–22, 1991.

[46] K. Epstein. Is spending on proton beam therapy for cancer going too far, too fast? *British Medical Journal*, 344(7583):20–1, 2012.

[47] A. Fredriksson and R. Bokrantz. Deliverable navigation for multicriteria IMRT treatment planning by combining shared and individual apertures. *Physics in Medicine and Biology*, 58(21):7683–97, 2013.

[48] A. Godley, E. Ahunbay, C. Peng, and X. A. Li. Automated registration of large deformations for adaptive radiation therapy of prostate cancer. *Medical Physics*, 36(4):1433–41, 2009.

[49] M. Goitein. *Radiation Oncology: A Physicist's-Eye View*. Springer, 2008.

[50] M. Gotein, A. J. Lomax, and E. S. Pedroni. Treating cancer with protons. *Physics Today*, 55(9):45–50, 2002.

[51] V. Grégoire, A. Eisbruch, M. Hamoir, and P. Levendag. Proposal for the delineation of the nodal CTV in the node-positive and the post-operative neck. *Radiotherapy and Oncology*, 79(1):15–20, 2006.

[52] A. Grzadziel, A. Grosu, and P. Kneschaurek. Three-dimensional conformal versus intensity-modulated radiotherapy dose planning in stereotactic radiotherapy: Application of standard quality parameters for plan evaluation. *International Journal of Radiation Oncology, Biology, Physics*, 66(4, Suppl.):S87–94, 2006.

[53] E. K. Hansen, M. K. Bucci, J. M. Quivey, V. Weinberg, and P. Xia. Repeat CT imaging and replanning during the course of IMRT for head-and-neck cancer. *International Journal of Radiation Oncology, Biology, Physics*, 64(2):355–62, 2006.

[54] M. Hillbrand and D. Georg. Assessing a set of optimal user interface parameters for intensity-modulated proton therapy planning. *Journal of Applied Clinical Medical Physics*, 11(4):93–104, 2010.

[55] K. F. Ho, T. Marchant, C. Moore, G. Webster, C. Rowbottom, H. Penington, L. Lee, B. Yap, A. Sykes, and N. Slevin. Monitoring Dosimetric Impact of Weight Loss With Kilovoltage (KV) Cone Beam CT (CBCT) During Parotid-Sparing IMRT and Concurrent Chemotherapy. *International Journal of Radiation Oncology, Biology, Physics*, 82(3):e375–82, 2012.

[56] K. M. Hofmann, U. Masood, J. Pawelke, and J. J. Wilkens. A treatment planning study to assess the feasibility of laser-driven proton therapy using a compact gantry design. *Medical Physics*, 42(9):5120–9, 2015.

[57] B. S. Hoppe, J. M. Michalski, N. P. Mendenhall, C. G. Morris, R. H. Henderson, R. C. Nichols, W. M. Mendenhall, Christopher R. Williams, M. M. Regan, J. J. Chipman, C. M. Crociani, H. M. Sandler, M. G. Sanda, and D. A. Hamstra. Comparative effectiveness study of patient-reported outcomes after proton therapy or intensity-modulated radiotherapy for prostate cancer. *Cancer*, 120(7):1076–82, 2014.

[58] M. Howard, C. Beltran, C. S. Mayo, and M. G. Herman. Effects of minimum monitor unit threshold on spot scanning proton plan quality. *Medical Physics*, 41(9):091703, 2014.

[59] ICRU. ICRU Report 62: Prescribing, Recording and Reporting Photon Beam Therapy (Supplement to ICRU Report 50). *International Commission on Radiation Units and Measurements*, 1999.

[60] IPEM. IPEM Recommendations for the Provision of a Physics Service to Radiotherapy. *Institute of Physics and Engineering in Medicine*, 2009.

[61] A. Jemal, F. Bray, M. M. Center, J. Ferlay, E. Ward, and D. Forman. Global cancer statistics. *CA: A Cancer Journal for Clinicians*, 61(2):69–90, 2011.

[62] A. D. Jensen, S. Nill, P. E. Huber, R. Bendl, J. Debus, and M. W. Münter. A clinical concept for interfractional adaptive radiation therapy in the treatment of head and neck cancer. *International Journal of Radiation Oncology, Biology, Physics*, 82(2):590–6, 2012.

[63] Z.-Q. Jiang, K. Yang, R. Komaki, X. Wei, S. L. Tucker, Y. Zhuang, M. K. Martel, S. Vedam, P. Balter, G. Zhu, D. Gomez, C. Lu, R. Mohan, J. D. Cox, and Z. Liao. Long-term clinical outcome of intensity-modulated radiotherapy for inoperable non-small cell lung cancer: the MD Anderson experience. *International Journal of Radiation Oncology, Biology, Physics*, 83(1):332–9, 2012.

[64] D. Jolly, D. Alahakone, and J. Meyer. A RapidArc planning strategy for prostate with simultaneous integrated boost. *Journal of Applied Clinical Medical Physics*, 12(1):35–49, 2010.

[65] F. Kamp. Comparison of the Lateral Dose Fall-Off for Proton and Ion Beams in Radiation Therapy. Master's thesis, Technische Universität München, 2011.

[66] S. C. Kamran, B. S. Mueller, P. Paetzold, J. Dunlap, A. Niemierko, T. Bortfeld, H. Willers, and D. Craft. Multi-criteria optimization achieves superior normal tissue sparing in a planning study of intensity-modulated

radiation therapy for RTOG 1308-eligible non-small cell lung cancer patients. *Radiotherapy and Oncology*, 118(3):515–20, 2016.

[67] J. H. Kang, J. J. Wilkens, and U. Oelfke. Non-uniform depth scanning for proton therapy systems employing active energy variation. *Physics in Medicine and Biology*, 53(9):N149–55, 2008.

[68] A. Z. Kibrom and K. A. Knight. Adaptive radiation therapy for bladder cancer: a review of adaptive techniques used in clinical practice. *Journal of Medical Radiation Sciences*, 62(4):277–85, 2015.

[69] R. G. J. Kierkels, R. Visser, H. P. Bijl, J. A. Langendijk, A. A. van't Veld, R. J. H. M. Steenbakkers, and E. W. Korevaar. Multicriteria optimization enables less experienced planners to efficiently produce high quality treatment plans in head and neck cancer radiotherapy. *Radiation Oncology*, 10(1):87, 2015.

[70] P. Källman, A. Ågren, and A. Brahme. Tumour and Normal Tissue Responses to Fractionated Non-uniform Dose Delivery. *International Journal of Radiation Biology*, 62(2):249–62, 1992.

[71] A. C. Kraan, S. van de Water, D. N. Teguh, A. Al-Mamgani, T. Madden, H. M. Kooy, B. J. M. Heijmen, and M. S. Hoogeman. Dose Uncertainties in IMPT for Oropharyngeal Cancer in the Presence of Anatomical, Range, and Setup Errors. *International Journal of Radiation Oncology, Biology, Physics*, 87(5):888–96, 2013.

[72] A. Kumarasiri, F. Siddiqui, C. Liu, R. Yechieli, M. Shah, D. Pradhan, H. Zhong, I. J. Chetty, and J. Kim. Deformable image registration based automatic CT-to-CT contour propagation for head and neck adaptive radiotherapy in the routine clinical setting. *Medical Physics*, 41(12), 2014.

[73] M. Kwint, W. Uyterlinde, J. Nijkamp, C. Chen, J. de Bois, J. Sonke, M. van den Heuvel, J. Knegjens, M. van Herk, and J. Belderbos. Acute Esophagus Toxicity in Lung Cancer Patients After Intensity Modulated Radiation Therapy and Concurrent Chemotherapy. *International Journal of Radiation Oncology, Biology, Physics*, 84(2):e223–8, 2012.

[74] J. A. Langendijk, P. Lambin, D. D. Ruyssche, J. Widder, M. Bos, and M. Verheij. Selection of patients for radiotherapy with protons aiming at reduction of side effects: The model-based approach. *Radiotherapy and Oncology*, 107(3):267–73, 2013.

[75] M. Langer, V. Thai, and L. Papiez. Improved leaf sequencing reduces segments or monitor units needed to deliver IMRT using multileaf collimators. *Medical Physics*, 28(12):2450–58, 2001.

[76] Y. Lassen-Ramshad, A. Vestergaard, L. P. Muren, M. Hoyer, and J. B. B. Petersen. Plan robustness in proton beam therapy of a childhood brain tumour. *Acta Oncologica*, 50(6):791–96, 2011.

[77] N. Li, M. Zarepisheh, A. Uribe-Sanchez, K. Moore, Z. Tian, X. Zhen, Y. Graves Jiang, Q. Gautier, L. Mell, L. Zhou, X. Jia, and S. Jiang. Automatic treatment plan re-optimization for adaptive radiotherapy guided with the initial plan DVHs. *Physics in Medicine and Biology*, 58(24):8725–38, 2013.

[78] Y. Lievens, N. Defourny, M. Coffey, J. P. Borras, P. Dunscombe, B. Slotman, J. Malicki, M. Bogusz, C. Gasparotto, C. Grau, A. Kokobobo, F. Sedlmayer, E. Slobina, P. Coucke, R. Gabrovski, M. Vosmik, J. G. Eriksen, J. Jaal, C. Dejean, C. Polgar, J. Johannsson, M. Cunningham, V. Atkocius, C. Back, M. Pirotta, V. Karadjinovic, S. Levernes, B. Maciejewski, M. L. Trigo, B. Šegedin, A. Palacios, B. Pastoors, C. Beardmore, S. Erridge, G. Smyth, and R.C. Soler. Radiotherapy staffing in the European countries: Final results from the ESTRO-HERO survey. *Radiotherapy and Oncology*, 112(2):178–86, 2014.

[79] W. Liu, S. J. Frank, X. Li, Y. Li, R. X. Zhu, and R. Mohan. PTV-based IMPT optimization incorporating planning risk volumes vs robust optimization. *Medical Physics*, 40(2):3089–101, 2013.

[80] A. J. Lomax. Intensity modulation methods for proton radiotherapy. *Physics in Medicine and Biology*, 44(1):185–205, 1999.

[81] A. J. Lomax. Intensity modulated proton therapy and its sensitivity to treatment uncertainties 2: the potential effects of inter-fraction and inter-field motions. *Physics in Medicine and Biology*, 53(4):1043–56, 2008.

[82] A. J. Lomax, T. Bortfeld, G. Goitein, J. Debus, C. Dykstra, P. Tercier, P. A. Coucke, and R. O. Mirimanoff. A treatment planning inter-comparison of proton and intensity modulated photon radiotherapy. *Radiotherapy and Oncology*, 51(3):257–71, 1999.

[83] N. J. Lomax and S. G. Scheib. Quantifying the degree of conformity in radiosurgery treatment planning. *International Journal of Radiation Oncology, Biology, Physics*, 55(5):1409–19, 2003.

[84] T. Lomax. Towards daily adapted proton therapy. *Physica Medica*, 30(Suppl. 1):e3, 2014.

[85] J. Lundkvist, M. Ekman, S. R. Ericsson, B. Jönsson, and B. Glimelius. Proton therapy of cancer: Potential clinical advantages and cost-effectiveness. *Acta Oncologica*, 44(8):850–61, 2005.

[86] S. E. McGowan, N. G. Burnet, and A. J. Lomax. Treatment planning optimisation in proton therapy. *British Journal of Radiology*, 86(1021), 2013.

[87] T. McNutt, B. Wu, J. Moore, S. Petit, M. Kazhdan, and R. Taylor. TH-E-BRCD-02: Automated Treatment Planning Using a Database of Prior Patient Treatment Plans. *Medical Physics*, 39(6):4008, 2012.

[88] N. P. Mendenhall, R. S. Malyapa, Z. SU, D. Yeung, W. M. Mendenhall, and Z. LI. Proton therapy for head and neck cancer: Rationale, potential indications, practical considerations, and current clinical evidence. *Acta Oncologica*, 50(6):763–71, 2011.

[89] R. C. Miller, M. Lodge, M. H. Murad, and B. Jones. Controversies in clinical trials in proton radiotherapy: the present and the future. *Seminars in Radiation Oncology*, 23(2):127–33, 2013.

[90] R. Miralbell, A. Lomax, L. Cella, and U. Schneider. Potential reduction of the incidence of radiation-induced second cancers by using proton beams in the treatment of pediatric tumors. *International Journal of Radiation Oncology, Biology, Physics*, 54(3):824–9, 2002.

[91] K. Mittauer, B. Lu, G. Yan, D. Kahler, A. Gopal, R. Amdur, and C. Liu. A study of IMRT planning parameters on planning efficiency, delivery efficiency, and plan quality. *Medical Physics*, 40(6):061704, 2013.

[92] R. Mohan, M. Arnfield, S. Tong, Q. Wu, and J. Siebers. The impact of fluctuations in intensity patterns on the number of monitor units and the quality and accuracy of intensity modulated radiotherapy. *Medical Physics*, 27(6):1226–37, 2000.

[93] J. Moore, W. Yang, E. T. Kimberly, J. F. Juan, J. M. Herman, and T. R. McNutt. Clinical Deployment of Automatic Treatment Planning for Pancreas SBRT Patients. *International Journal of Radiation Oncology, Biology, Physics*, 87(2, Suppl.):S136–37, 2013.

[94] J. A. Moore, K. Evans, W. Yang, J. Herman, and T. McNutt. Automatic treatment planning implementation using a database of previously treated patients. *Journal of Physics: Conference Series*, 489(1):010901, 2014.

[95] B. S. Müller, M. N. Duma, S. Kampfer, S. Nill, U. Oelfke, H. Geinitz, and J. J. Wilkens. Impact of interfractional changes in head and neck cancer patients on the delivered dose in intensity modulated radiotherapy with protons and photons. *Physica Medica*, 31(3):266–72, 2015.

[96] W. D. Newhauser, A. Giebeler, K. M. Langen, D. Mirkovic, and R. Mohan. Can megavoltage computed tomography reduce proton range uncertainties in treatment plans for patients with large metal implants? *Physics in Medicine and Biology*, 53(9):2327–44, 2008.

[97] A. Niemierko. A generalized concept of equivalent uniform dose (EUD). *Medical Physics*, 26:1100(abstract), 1999.

[98] S. Nill, T. Bortfeld, and U. Oelfke. Inverse planning of intensity modulated proton therapy. *Zeitschrift für Medizinische Physik*, 14:35–40, 2004.

[99] M. Oechsner, J. Berndt, J.J. Wilkens, and M.N. Duma. Respiratory-Gated Lung Stereotactic Body Radiation Therapy: A Planning Study of 3D-CRT Versus VMAT. *International Journal of Radiation Oncology, Biology, Physics*, 90(1, Suppl.):S904, 2014.

[100] K. Otto. Volumetric Modulated Arc Therapy: IMRT in a single arc? *Medical Physics*, 35(1):310–17, 2008.

[101] K. Otto. Letter to the Editor on 'Single-Arc IMRT?'. *Physics in Medicine and Biology*, 54(8):L37–41, 2009.

[102] K. Otto. Real-time interactive treatment planning. *Physics in Medicine and Biology*, 59(17):4845–59, 2014.

[103] H. Paganetti. Changes in tumor cell response due to prolonged dose delivery times in fractionated radiation therapy. *International Journal of Radiation Oncology, Biology, Physics*, 63(3):892–900, 2005.

[104] H. Paganetti. Range uncertainties in proton therapy and the role of Monte Carlo simulations. *Physics in Medicine and Biology*, 57(11):R99–117, 2012.

[105] R. R. Parikh, M. L. Grossbard, L. B. Harrison, and J. Yahalom. Association of intensity-modulated radiation therapy on overall survival for patients with Hodgkin lymphoma. *Radiotherapy and Oncology*, 118(1):52–9, 2016.

[106] K. Parodi, H. Paganetti, H. A. Shih, S. Michaud, J. S. Loeffler, T. F. DeLaney, N. J. Liebsch, J. E. Munzenrider, A. J. Fischman, A. Knopf, and T. Bortfeld. Patient study of in vivo verification of beam delivery and range, using positron emission tomography and computed tomography imaging after proton therapy. *International Journal of Radiation Oncology, Biology Physics*, 68(3):920–34, 2007.

[107] A. Peeters, J. P. C. Grutters, M. Pijls-Johannesma, S. Reimoser, D. D. Ruysscher, J. L. Severens, M. A. Joore, and P. Lambin. How costly is particle therapy? Cost analysis of external beam radiotherapy with carbon-ions, protons and photons. *Radiotherapy and Oncology*, 95(1):45–53, 2010.

[108] L. Perrier, M. Morelle, P. Pommier, J. Lagrange, A. Laplanche, P. Dudouet, S. Supiot, B. Chauvet, T. Nguyen, G. Crehange, V. Beckendorf, F. Pene, X. Muracciole, J. Bachaud, E. Le Prisé, and R. de Crevoisier. Cost of prostate image-guided radiation therapy: Results of a randomized trial. *Radiotherapy and Oncology*, 106(1):50–8, 2013.

[109] D. Pflugfelder, J. J. Wilkens, and U. Oelfke. Worst case optimization: a method to account for uncertainties in the optimization of intensity modulated proton therapy. *Physics in Medicine and Biology*, 53(6):1689–1700, 2008.

[110] E. B. Podgorsak, editor. *Radiation oncology physics: a handbook for teachers and students*. International atomic energy agency, 2005.

[111] F. A. Potra and S. J. Wright. Interior-point methods. *Journal of Computational and Applied Mathematics*, 124(1-2):281–302, 2000.

[112] E. M. Quan, W. Liu, R. Wu, Y. Li, S. J. Frank, X. Zhang, X. R. Zhu, and R. Mohan. Preliminary evaluation of multifield and single-field optimization for the treatment planning of spot-scanning proton therapy of head and neck cancer. *Medical Physics*, 40(8):081709, 2013.

[113] B. L. T. Ramaekers, J. P. C. Grutters, M. Pijls-Johannesma, P. Lambin, M. A. Joore, and J. A. Langendijk. Protons in Head-and-Neck Cancer: Bridging the Gap of Evidence. *International Journal of Radiation Oncology, Biology, Physics*, 85(5):1282–88, 2013.

[114] D. D. Ruysscher, M. M. Lodge, B. Jones, M. Brada, A. Munro, T. Jefferson, and M. Pijls-Johannesma. Charged particles in radiotherapy: A 5-year update of a systematic review. *Radiotherapy and Oncology*, 103(1):5–7, 2012.

[115] B. Schaffner and E. Pedroni. The precision of proton range calculations in proton radiotherapy treatment planning: experimental verification of the relation between CT-HU and proton stopping power. *Physics in Medicine and Biology*, 43(6):1579–92, 1998.

[116] S. Schell and J.J. Wilkens. Advanced treatment planning methods for efficient radiation therapy with laser accelerated proton and ion beams. *Medical Physics*, 37(10):5330–40, 2010.

[117] W. Schlegel, T. Bortfeld, and A. Grosu, editors. *New Technologies in Radiation Oncology*. Springer, 2006.

[118] U. Schneider, E. Pedroni, and A. Lomax. The calibration of CT Hounsfield units for radiotherapy treatment planning. *Physics in Medicine and Biology*, 41(1):111–24, 1996.

[119] D. L. Schwartz, A. S. Garden, J. Thomas, Y. Chen, Y. Zhang, J. Lewin, M. S. Chambers, and L. Dong. Adaptive Radiotherapy for Head-and-Neck Cancer: Initial Clinical Outcomes From a Prospective Trial. *International Journal of Radiation Oncology, Biology, Physics*, 83(3):986–93, 2012.

[120] C. B. Simone II, D. Ly, T. D. Dan, J. Ondos, H. Ning, A. Belard, J. O' Connell, R. W. Miller, and N. L. Simone. Comparison of intensity-modulated radiotherapy, adaptive radiotherapy, proton radiotherapy, and

adaptive proton radiotherapy for treatment of locally advanced head and neck cancer. *Radiotherapy and Oncology*, 101(3):376–82, 2011.

[121] J. Stein, T. Bortfeld, B. Dörschel, and W. Schlegel. Dynamic X-ray compensation for conformal radiotherapy by means of multi-leaf collimation. *Radiotherapy and Oncology*, 32(2):163–73, 1994.

[122] M. Steneker, A. Lomax, and U. Schneider. Intensity modulated photon and proton therapy for the treatment of head and neck tumors. *Radiotherapy and Oncology*, 80(2):263–67, 2006.

[123] K. Suzuki, M. T. Gillin, N. Sahoo, X. R. Zhu, A. K. Lee, and D. Lippy. Quantitative analysis of beam delivery parameters and treatment process time for proton beam therapy. *Medical Physics*, 38(7):4329–37, 2011.

[124] Z. Taheri-Kadkhoda, T. Björk-Eriksson, S. Nill, J. J. Wilkens, U. Oelfke, K.-A. Johansson, P. E. Huber, and M. W. Münter. Intensity-modulated radiotherapy of nasopharyngeal carcinoma: a comparative treatment planning study of photons and protons. *Radiation Oncology*, 3:4, 2008.

[125] C. Thieke, K. H. Kuefer, M. Monz, A. Scherrer, F. Alonso, S. Nill, C. Thilmann, and T. Bortfeld. Beyond weight factors: new concepts for defining and analysing dose optimisation. *Radiotherapy and Oncology*, 73 (Suppl. 1):S75, 2004.

[126] S. Tribius and C. Bergelt. Intensity-modulated radiotherapy versus conventional and 3D conformal radiotherapy in patients with head and neck cancer: Is there a worthwhile quality of life gain? *Cancer Treatment Reviews*, 37(7):511–9, 2011.

[127] L. Tuomikoski, J. Korhonen, J. Collan, J. Keyriläinen, H. Visapää, J. Sairanen, K. Saarilahti, and M. Tenhunen. Implementation of adaptive radiation therapy for urinary bladder carcinoma: Imaging, planning and image guidance. *Acta Oncologica*, 52(7):1451–7, 2013.

[128] J. Unkelbach, T. Bortfeld, B. C. Martin, and M. Soukup. Reducing the sensitivity of IMPT treatment plans to setup errors and range uncertainties via probabilistic treatment planning. *Medical Physics*, 36(1):149–63, 2009.

[129] J. Unkelbach, T. C. Y. Chan, and T. Bortfeld. Accounting for range uncertainties in the optimization of intensity modulated proton therapy. *Physics in Medicine and Biology*, 52(10):2755–73, 2007.

[130] S. van de Water, Hanne M. Kooy, B. J. M. Heijmen, and M. S. Hoogeman. Shortening delivery times of intensity modulated proton therapy by reducing proton energy layers during treatment plan optimization. *International Journal of Radiation Oncology, Biology, Physics*, 92(2):460–8, 2015.

[131] S. van de Water, A. C. Kraan, S. Breedveld, W. Schillemans, D. N. Teguh, H. M. Kooy, T. M. Madden, B. J. M. Heijmen, and M. S. Hoogeman. Improved efficiency of multi-criteria IMPT treatment planning using iterative resampling of randomly placed pencil beams. *Physics in Medicine and Biology*, 58(19):6969–83, 2013.

[132] E. Van de Werf, Y. Lievens, J. Verstraete, K. Pauwels, and W. Van den Bogaert. Time and motion study of radiotherapy delivery: Economic burden of increased quality assurance and MRT. *Radiotherapy and Oncology*, 93(1):137–40, 2009.

[133] E. Van de Werf, J. Verstraete, and Y. Lievens. The cost of radiotherapy in a decade of technology evolution. *Radiotherapy and Oncology*, 102(1):148–53, 2012.

[134] J. M. Verburg and J. Seco. Proton range verification through prompt gamma-ray spectroscopy. *Physics in Medicine and Biology*, 59(23):7089–106, 2014.

[135] J. M. Verburg, H. A. Shih, and J. Seco. Simulation of prompt gamma-ray emission during proton radiotherapy. *Physics in Medicine and Biology*, 57(17):5459–72, 2012.

[136] P. W. J. Voet, M. L. P. Dirkx, S. Breedveld, D. Fransen, P. C. Levendag, and B. J. M. Heijmen. Toward Fully Automated Multicriterial Plan Generation: A Prospective Clinical Study. *International Journal of Radiation Oncology, Biology, Physics*, 85(3):866–72, 2013.

[137] H. Vorwerk, K. Zink, R. Schiller, V. Budach, D. Böhmer, S. Kampfer, W. Popp, H. Sack, and R. Engenhart-Cabillic. Protection of quality and innovation in radiation oncology: The prospective multicenter trial the German Society of Radiation Oncology (DEGRO-QUIRO study). *Strahlentherapie und Onkologie*, 190(5):433–43, 2014.

[138] J. Wala, D. Craft, J. Paly, A. Zietman, and J. Efstathiou. Maximizing dosimetric benefits of IMRT in the treatment of localized prostate cancer through multicriteria optimization planning. *Medical Dosimetry*, 38(3):298–303, 2013.

[139] D. Wang. A critical appraisal of the clinical utility of proton therapy in oncology. *Medical Devices: Evidence and Research*, 8:439–46, 2015.

[140] S. Webb. Optimisation of conformal radiotherapy dose distribution by simulated annealing. *Physics in Medicine and Biology*, 34(10):1349–70, 1989.

[141] S. Webb. The physical basis of IMRT and inverse planning. *The British Journal of Radiology*, 76(910):678–89, 2003.

[142] G. J. Webster, J. Stratford, J. Rodgers, J. E. Livsey, D. Macintosh, and A. Choudhury. Comparison of adaptive radiotherapy techniques for the treatment of bladder cancer. *The British Journal of Radiology*, 86(1021):20120433, 2013.

[143] J. J. Wilkens, J. R. Alaly, K. Zakarian, W. L. Thorstad, and J. O. Deasy. IMRT treatment planning based on prioritizing prescription goals. *Physics in Medicine and Biology*, 52(6):1675–92, 2007.

[144] J. R. Wilkie, M. M. Matuszak, M. Feng, J. M. Moran, and B. A. Fraass. Use of plan quality degradation to evaluate tradeoffs in delivery efficiency and clinical plan metrics arising from IMRT optimizer and sequencer compromises. *Medical Physics*, 40(7):071708, 2013.

[145] I. Xhaferllari, E. Wong, K. Bzdusek, M. Lock, and J. Chen. Automated IMRT planning with regional optimization using planning scripts. *Journal of Applied Clinical Medical Physics*, 14(1):176–91, 2013.

[146] L. Yuan, Q. J. Wu, Y. Sheng, J. Liu, A. Benitez, F. Yin, and Y. Ge. SU-E-T-537: Local Multi-Criteria Optimization for Clinical Tradeoff Decision Guidance in RT Planning. *Medical Physics*, 42(6):3459, 2015.

[147] M. J. Zelefsky, Z. Fuks, L. Happersett, H. J. Lee, C. C. Ling, C. M. Burman, M. Hunt, T. Wolfe, E. S. Venkatraman, A. Jackson, M. Skwarchuk, and S. A. Leibel. Clinical experience with intensity modulated radiation therapy (IMRT) in prostate cancer. *Radiotherapy and Oncology*, 55(3):241–9, 2000.

[148] X. R. Zhu, N. Sahoo, X. Zhang, D. Robertson, H. Li, S. Choi, A. K. Lee, and M. T. Gillin. Intensity modulated proton therapy treatment planning using single-field optimization: The impact of monitor unit constraints on plan quality. *Medical Physics*, 37(3):1210–19, 2010.

Publications

Papers in journals

First author

- B. S. Müller, J. J. Wilkens: "Prioritized efficiency optimization for intensity modulated proton therapy", submitted to Physics in Medicine and Biology.

- B. S. Müller, H. A. Shih, J. Efstathiou, T. Bortfeld, D. Craft: "Multi-criteria plan optimization in the hands of physicians: a pilot study in prostate cancer and brain tumors.", Practical Radiation Oncology, in revision.

- B. S. Müller, M. N. Duma, S. Kampfer, S. Nill, U. Oelfke, H. Geinitz, J. J. Wilkens: "Impact of interfractional changes in head and cancer patients on the delivered dose in intensity modulated radiotherapy with protons and photons", Physica Medica, 31(3), 266–272, 2015.

Coauthor

- S. C. Kamran, B. S. Mueller, P. Paetzold, J. Dunlap, A. Niemierko, T. Bortfeld, D. Craft, H. Willers: "Multi-criteria optimization achieves superior normal tissue sparing in a planning study of intensity-modulated radiation therapy for RTOG 1308-eligible non-small cell lung cancer patients", Radiotherapy and Oncology, 118 (3), 515–20, 2016.

Papers in books and conference proceedings

First author

- B. S. Müller and J. J. Wilkens: "Optimierung der Bestrahlungseffizienz intensitätsmodulierter Protontherapiepläne durch priorisierte Optimierung", in: Abstractband, 22. Jahrestagung der Deutschen Gesellschaft für Radioonkologie, 2016 (poster).

- B. S. Müller and J. J. Wilkens: "Optimisation of plan delivery efficiency of intensity modulated proton plans with prioritised optimizsation", in: Abstractband, 46. Jahrestagung der Deutschen Gesellschaft für Medizinische Physik (DGMP: Marburg), ISBN 978-3-9816508-8-4, p. 155, 2015 (oral presentation).

- B. S. Müller and J. J. Wilkens: "Improving plan delivery efficiency of intensity modulated proton plans with prioritized optimization", Medical Physics, 42(6), p. 3527, 2015 (oral presentation).
- B. S. Müller, T. Bortfeld, J. Efstathiou, H. A. Shih, D. Craft: "Involving physicians in IMRT planning by interactive plan navigation", Radiotherapy and Oncology, 115[Suppl.1]:S713, 2015 (electronic poster).
- B. S. Müller, M. N. Duma, S. Kampfer, H. Geinitz, J. J. Wilkens: "Impact of interfractional anatomical changes in intensity modulated photon and proton therapy of head & neck cancer", Radiotherapy and Oncology, 111[Suppl.1]:S91-2, 2014 (poster presentation).
- B. S. Müller, M. N. Duma, S. Kampfer, H. Geinitz, J. J. Wilkens: "Impact of interfractional anatomical changes and relevance of adaptive planning for intensity modulated radiotherapy – a comparison of proton and photon plans for head and neck cancer patients", in: H. Treuer (ed.) Medizinische Physik 2013, 44. Jahrestagung der Deutschen Gesellschaft für Medizinische Physik (DGMP: Köln), ISBN 978-3-9816002-1-6, pp. 208-10, 2013 (oral presentation).

Coauthor

- M. Devecka, M. N. Duma, S. Kampfer, C. Hugo, K. M. Hofmann, B. S. Müller, C. Heinrich, J. J. Wilkens, S.E. Combs: "Is there a "best technique" available for reducing acute toxicities in craniospinal irradiation?", Radiotherapy and Oncology, 119[Suppl.1]:S410, 2016.
- S. C. Kamran, B. S. Mueller, P. Paetzold, J. Dunlap, T. Bortfeld, H. Willers, D. Craft: "Multicriteria Optimization (MCO) Achieves Superior Normal Tissue Sparing By Intensity Modulated Radiation Therapy (IMRT) in Lung Cancer Patients Using RTOG 1308 Guidelines", International Journal of Radiation Oncology*Biology*Physics, 93(3)[Suppl.]:E556-7, 2015.
- T. Domke, C. Skalsky, G. Datzmann, B. Müller, M. Hillbrand, J. Hauffe: "Long-term stability of a scanned proton pencil beam - a roadmap to Intensity Modulated Proton Therapy", in: Abstractband, Dreiländertagung der ÖGMP, DGMP und SGSMP: 2011 - Medizinische Physik, ISBN: 3-925218-89-0, p.45, 2011.

Acknowledgments

I would like to express my gratidude to a number of people who contributed to this work. Without their support this work would not have been possible.

First and foremost, I thank Prof. Dr. Jan J. Wilkens, my supervisor and first examiner, for giving me the opportunity to join his research group Advanced Technologies in Radiation Therapy and to work on this multifaceted project. Thank you for always having been available for advice and discussions, for your enthusiasm and ideas which essentially shaped this work. Thank you, Jan, for all your support throughout the last years! It was a pleasure to work with you, as well as being part of ATRT and the clinical physics group.
I am also very grateful to Prof. Dr. Franz Pfeiffer for being my second examiner.

I appreciate the funding of my PhD position and of my participation at several conferences by Munich-Centre for Advanced Photonics (MAP), German Research Foundation (DFG).

Parts of this work were realized at Massachusetts General Hospital, Boston. I am particularly grateful to Prof. Dr. Thomas Bortfeld for giving me the opportunity to work with him and his colleagues, and to experience this great research environment. Special thanks are directed to Dr. David Craft for supervising my work at MGH, for enlightening discussions, MCO explanations and his continuous support. Dr. Helen Shih and Dr. Jason Efstathiou, thank you very much for performing physician sliding and for enthusiastically supporting this project. I am grateful for having cooperated with Dr. Sophia Kamran, Peter Paetzold, Joseph Dunlap and Dr. Henning Willers on the MCO-non-MCO study. Moreover, I appreciate the warm welcome and helpful working environment provided by the MGH staff and the Harvard garden researchers, who enriched this research stay - apart from work - by several joint events. In this context, I would like to acknowledge the financial support of this research stay by the TUM Graduate School and the Department Graduate Center Physics.

I am thankful to a number of researchers and colleagues for the productive cooperation on the impact of interfractional changes planning study: Dr. Marciana N. Duma for performing the clinical parts, for sharing her clinical experience and the fruitful discussions; Severin Kampfer, in particular for the support on Tomotherapy related difficulties; Prof. Dr. Hans Geinitz for the constructive suggestions and valuable input on the project; Prof. Dr. Uwe Oelfke, Dr. Simeon Nill and the KonRad developer team (DKFZ), as well as Dr. Rolf Bendl and the VIRTUOS developer team (DKFZ), for supplying their softwares KonRad and VIRTUOS.

During parts of my PhD phase, I worked in the clinical environment of the radiation oncology department. For giving me this opportunity, I would like to thank Prof. Dr. M. Molls and Prof. Dr. Jan J. Wilkens. Morerover I thank the all medical physicists and the clinical staff of the department for the friendly and supportive working environment.

I would like to thank my ATRT colleagues, including all former and current group members, for having made the time as a PhD student so enjoyable. Thank you very much for the friendly and productive atmosphere, for several discussions, for adhering strictly to the cake rules and the good times we shared! Especially, I would like to thank Dr. Nicole Humble for carefully proofreading my thesis, as well as Dr. Stefan Schell, Dr. Florian Kamp and Dr. Kerstin Hofmann for their support on LapCerr.

Last but not least, I want to thank my family and close friends for their continuous support and encouragement. I am particularly grateful to my parents and my brother Jochen for being there for me at any time, for the input and interest in my work, and for supporting me in so many ways getting to this point. Finally, I would like to thank Daniel for his patience, the intensive proofreading and valuable ideas, specifically on schematic illustrations. Thank you for being my calm anchor, for motivating and supporting me - regardless of what I am doing. I consider myself most fortunate to have this family and such good friends in my life!